Synthesis and characterization of multiphase copolymers

By

Wael K. S. Elhrari

Dissertation presented for the degree of Doctor of Science in the Faculty of Science

at

Stellenbosch University

Promoter: Prof. P.E. Mallon

Department of Chemistry and Polymer Science

December 2011

Declaration

By submitting this dissertation electronically, I declare that the entirety of the work contained therein is my own, original work, that I am the sole author thereof (save to the extent explicitly otherwise stated), that reproduction and publication thereof by Stellenbosch University will not infringe any third party rights and that I have not previously in its entirety or in part submitted it for obtaining any qualification.

Signature: …… Date: ……

Abstract

Multiphase copolymers generally consist of copolymers where the disparate natures of each of the segments results in complex phase-segregated morphologies in the solid state. The outstanding properties and wide range of applications of multiphase copolymers has led to the need for more sophisticated synthesis methods to produce copolymers with controlled structures. Associated with developments in synthetic methods is the need to develop suitable techniques to characterize these materials in order to obtain a better understanding of their structure–property relationships.

The synthesis of multiphase copolymers presents many challenges. These are related to the nature of the molecular requirements, were the monomers of each of the different components may not be polymerized by all available polymerization techniques. This has led to the need to combine different polymerization techniques to overcome such limitations.

The focus of this study is the combination of living controlled polymerization techniques, namely anionic polymerization and RAFT polymerization, with hydroboration/autoxidation, to produce non-polyolefin block and graft copolymers. Block copolymers were synthesized by coupling anionic polymerization and hydroboration/autoxidation reactions. The first block segment was prepared via anionic polymerization, and then end-functionalized with a suitable functional group (e.g. an allyl group). A hydroboration/autoxidation reaction was then used to initiate the polymerization of the second block by the slow addition of oxygen at room temperature.

Graft copolymers were synthesized using the 'grafting from' technique, by coupling RAFT copolymerization with hydroboration/autoxidation reactions. The backbone polymer was synthesized via RAFT copolymerization of symmetric and asymmetric monomer, after which a hydroboration/autoxidation reaction was carried out to produce graft copolymers.

The hydroboration/hydroxylation reaction could also be used to modify an unsaturated polymer chain. The EPDM rubber chain was modified by transforming the double bond into an hydroxyl group, which could undergo an esterification reaction with an acid chloride RAFT agent to produce the multifunctional RAFT polymer. This was used for the controlled living free radical polymerization of the graft chains. Significant amounts of homopolymerization in addition to graft formation were obtained.

Solid state NMR (SS NMR) and positron annihilation lifetime spectroscopy were used to determine the compositional phase segregation point in the graft copolymers. The spin diffusion data from the SS NMR provided insight into the seemingly anomalous positron data at the phase segregation point. It is demonstrated how these two techniques can provide complimentary data on the solid state morphology of these multiphase materials.

Opsomming

In die algemeen bestaan multifase kopolimere uit segmente van verskillende aard wat komplekse fase-geskeide-morfologie in die vastetoestand tot gevolg het. Die uitstekende eienskappe en wye reeks toepassings van multifase kopolimere het daartoe gelei dat meer gesofistikeerde sintesemetodes vir die bereiding van kopolimere met gekontrolleerde strukture nodig was. Gepaardgaande met verwante ontwikkelings op die gebied van sintesemetodes was dit nodig om gepaste analitiese tegnieke te ontwikkel vir die karakterisering van hierdie verbindings, ten einde die struktuur–eienskap verwantskap van hierdie materiale beter te verstaan.

Daar is egter baie uitdagings m.b.t. die sintese van hierdie multifase kopolimere. Dit is afhanklik van die aard van die molekulêre vereistes waar die monomere van elk van die verskillende komponente nie deur alle beskikbare polimerisasietegnieke gepolimeriseer kan word nie. Dit het daartoe gelei dat verskillende polimerasietegnieke gekombineer is ten einde hierdie beperkinge te oorbrug.

Die fokus van hierdie studie is die kombinering van lewende vry-radikaal gekontrolleerde polimerisasietegnieke, naamlik anioniese polimerisasie en RAFT-polimerisasie, met hidroborering/outoksidasie, om nie-olefiniese blok- en entkopolimere te berei. Blok-kopolimere is berei deur die koppeling van anioniese polimerisasie en hidroborering/outoksidasie reaksies. Die eerste bloksegment is berei via anioniese polimerisasie en daarna is endfunksionering met 'n geskikte funksionele groep (bv. 'n allielgroep) bewerkstellig. Daarna is 'n hidroborering/outoksidasie reaksie gebruik om die polimerisasie van die tweede blok te inisieer d.m.v. die stadige toevoeging van suurstof by kamertemperatuur.

Entkopolimere is berei deur gebruik te maak van die 'ent-vanaf' tegniek, d.m.v. die koppeling van RAFT-kopolimerisasie met hidroborering/outoksidasie reaksies. Die rugraatpolimeer is berei d.m.v. kopolimerisasie van simmetriese en nie-simmetriese monomere waarna die hidroborering/outoksidasie reaksie uitgevoer is om sodoende entkopolimere te vorm.

Die hidroborering/hidroksilasie reaksie kon ook gebruik word om 'n onversadigde polimeerketting te wysig. Die EPDM rubberketting is gewysig deur die omskakeling van die dubbelbinding in 'n hidroksielgroep, wat dan 'n esterifikasie reaskie kon ondergaan met 'n suurchloried-RAFT verbinding, om sodoende die multifunksionele RAFT-polimeer te vorm. Dit is gebruik vir die gekontrolleerde lewende vry-radikaalpolimerisasie van die entkettings. Behalwe entvorming is 'n hoë mate van homopolimerisasie waargeneem.

Vastetoestand KMR (VS KMR) en positronvernietigingsleeftydspektroskopie is gebruik om die saamgestelde faseskeidingspunt in die entkopolimere te bepaal. Die spindifffusie data van VS KMR het insig verleen aan die oënskynlik onreëlmatige

positrondata by die faseskeidingspunt. In die studie is bewys hoe hierdie twee tegnieke komplimentêre data kan lewer m.b.t. die vastetoestandmorfologie van hierdie multifase materiale.

Acknowledgments

All praise and thanks are due to (Allah), the one and only, the Indivisible Creator and Sustainer of the World. To Him we belong, and to Him we shall return. I wish to thank Him for all that He has bestowed on us, although He can never be praised or thanked enough. Also, I express my loving gratitude to my parents for their guidance and unwavering support throughout my life. They were behind me at every step in my life, even when I didn't really know where I was going, and helped me always to find my direction. I can only hope to show them the same kind of dedication and love.

I also extend my deep gratitude to my wife, Samia, and daughters, Fatima and Buthaina for their love, patience, and support. My brothers, Jassem and Suhaib, my sisters, Maysoon and Marwa, thank you so much.

Also, I would like to express my sincerest gratitude to the following people and institutions for their contribution towards this study:

Prof. P. E. Mallon, who has been a determined guide and consultant throughout my study.

The Libyan International Center for Macromolecular Chemistry and Technology Tripoli for their constant financial support and giving me the opportunity to study in this field.

The Institute of Polymer Science at the University of Stellenbosch, who welcomed me and provided me with the opportunity to further my studies. I feel very fortunate to have attended lectures and conferences with this extraordinary department.

My colleagues in Lab 134 with whom I spent my hours: Abduelmaged, Aimme, Elana, Gareth, and Sweed.

My friends and colleagues in the department for their support and encouragement. Especially Abdalah, Abduelmaged, Omar, Osama, and Walid for their support and encouraging words.

I would like to express my profound regards to Jeanette and Uhan Groenewald for their warm hospitality.

Table of Contents

List of Abbreviations i
List of Schemes v
List of Figures vi
List of Tables x
CHAPTER 1 1
INTRODUCTION AND OBJECTIVES 1
1.1 Introduction 1
1.2 Objectives 3
1.3 Layout of the thesis 4
1.4 References 5
CHAPTER 2 10
LITERATURE REVIEW AND BACKGROUND 10
2.1 Boron chemistry 10
2.1.1 Hydroboration-oxidation reaction 10
2.1.2 Autoxidation reaction 11
2.2 Living anionic polymerization 13
2.3 Controlled radical polymerization 15
2.3.1 Reversible addition-fragmentation chain transfer polymerization 18
2.4 Mulitphase copolymers 21
2.4.1 Random and gradient copolymers 22
2.4.2 Block copolymer 23
2.4.3 Graft copolymer 23
2.5 Combining various synthesis techniques 25
2.5.1 Combination of living anionic polymerization and autoxidation of 9-BBN 26
2.5.2 Combination of controlled radical polymerization and autoxidation of 9-BBN 26
2.6 Free volume and glass transition temperature 26
2.6.1 Glass transition temperature 26
2.6.2 Free volume 27
2.7 Solid state nuclear magnetic resonance (NMR) 31
2.8 Chromatographic analysis 31
2.9 References 33
CHAPTER 3 44
SYNTHESIS AND CHARACTERIZATION OF PS-b-PMMA 44
3.1 Introduction 44
3.2 Experimental 46
3.2.1 Materials 46
3.2.2 Synthesis of the styrene macromonomer 47
3.2.3 Hydroboration reaction 47
3.2.4 Extraction of unreacted PS homopolymer 49
3.3 Characterization 49
3.3.1 Size-exclusion chromatography (SEC) 49
3.3.2 Liquid chromatography under critical conditions (LCCC) 49
3.3.3 Two-dimensional liquid chromatography 49
3.3.4 Nuclear magnetic resonance (NMR) spectroscopy 50
3.4 Results and discussion 50
3.4.1 Hydroboration-hydroxylation of 1-decene to 1-decanol 50
3.4.2 Optimising the hydroboration-autoxidation reaction using methyl methacrylate monomer 51
3.4.3 Synthesis of styrene macromonmers 52
3.4.4 Copolymerization reaction via hydroboration-autoxidation 54
3.4.5 Chromatographic analysis at the critical point of adsorption of styrene 58
3.4.6 Chromatographic analysis at the critical point of adsorption of methyl methacrylate 61
3.5 Conclusions 63
3.6 References 64
CHAPTER 4 67
A new approach to the preparation of graft copolymers by a combination of RAFT and the borane approach 67
4.1 Introduction 67
4.2 Experimental 68
4.2.1 Materials 68
4.2.2 Synthesis of 2-cyanoprop-2-yl dithiobenzoate 69
4.2.3 RAFT-mediated allyl methacrylate polymerizations 70

4.2.4	RAFT-mediated copolymerization of styrene and allyl methacrylate	70
4.2.5	RAFT-mediated copolymerization of methyl methacrylate and allyl methacrylate	71
4.2.6	RAFT-mediated copolymerization of butyl acrylate and allyl methacrylate	71
4.2.7	Functionalization and autoxidation of the copolymer by 9-BBN	72
4.3	Characterization	72
4.3.1	Size exclusion chromatography	72
4.3.2	Gradient chromatography	73
4.3.3	Nuclear magnetic resonance (NMR) spectroscopy	73
4.4	Results and discussion	73
4.4.1	RAFT-mediated AM polymerizations	73
4.4.2	RAFT-mediated copolymerization of PS-co-AM	76
4.4.3	RAFT-mediated copolymerization of PMMA-co-AM	88
4.4.4	RAFT-mediated copolymerization of PBA-co-AM	94
4.5	Conclusions	96
4.6	References	98
CHAPTER 5		100
GRAFTED EPDM RUBBER		100
5.1	Introduction	100
5.2	Experimental	102
5.2.1	Materials	102
5.2.2	Hydroboration and hydroxylation of EPDM	102
5.2.3	Synthesis of S-1-dodecyl-S'-(isobutyric acid) trithiocarbonate (DIBTC)	103
5.2.4	Esterification of EPDM-OH with DIBTC-Cl	104
5.2.5	RAFT-mediated copolymerization of EPDM-g-PS	105
5.2.6	Soxhlet extraction of insoluble polymer fractions from its homopolymer	106
5.3	Characterization	107
5.3.1	IR	107
5.3.2	SEC	107
5.3.3	NMR	108
5.3.4	HPLC	108
5.4	Results and discussion	108
5.4.1	Immobilisation of DIBTC onto EPDM rubber	108
5.4.2	RAFT-mediated copolymerization of EPDM-g-PS in solution	112
5.4.3	HPLC gradient analysis	117
5.5	Conclusions	121
5.6	References	122
CHAPTER 6		124
MICROPHASE STRUCTURE OF MULTIPHASE POLYMER VIA POSITRON ANNIHILATION LIFETIME TECHNIQUE AND SOLID STATE NMR		124
6.1	Introduction	124
6.2	Experimental	125
6.2.1	Positron annihilation lifetime spectroscopy	125
6.2.2	Positron lifetime data analysis	126
6.2.3	Solid State NMR	127
6.3	Results and discussion	127
6.3.1	Microstructure of (PS-co-AM)-g-PMMA	127
6.3.2	Microstructure of PMMA-g-PS	134
6.4	Conclusion	141
6.5	References	142
CHAPTER 7		143
CONCLUSIONS		143
7.1	Combination of hydroboration and living anionic polymerization to produce block-copolymers	143
7.2	Combination of hydroboration and living free RAFT radical polymerization for the production of graft copolymers	144
7.3	Synthesis and characterization of the EPDM-g-PS	144
7.4	Microphase structure	145
7.5	Recommendations	146

List of Abbreviations

ABS	Acrylonitrile-butadiene-styrene
ACN	Acetonitrile
AFM	Atomic force microscopy
AIBN	2,2`Azobisisobutyronitrile
AM	Allyl methacrylate
ARGET ATRP	Activators generated by election transfer
ATRP	Atom transfer radical polymerization
ATRPP	Atom transfer radical precipitation polymerization
BA	Butyl acrylate
9-BBN	Bis(9-borabicyclo[3.3.1]nonane)
Bpy	2,2`-Bipyridine
BDB	Benzyl dithiobenzoate
BHT	2,6-Di-tert-butyl-4-methylphenol
CCD	Chemical composition distribution
CDB	Cumyl dithiobezoate
CP	Cross-polarization
CPDB	2-cyanoprop-2-yl dithiobenzoate
CRP	Living controlled free radical polymerization
CSIRO	Australian Commonweath Scientific and Research Organization
CTA	Chain transfer agent
D	Diffusion coefficient
DCC	N,N` Dicyclohexylcarbodiimide
DCPD	Dicyclopentadiene
DIBTC	S-1-dodecyl-S`-(isobutyric acid) trithiocarbonate
DIBTC-Cl	Acid chloride functionality (DIBTC-Cl)
DMA	Dynamic mechanical analysis
DMAP	4(Dimethylamino)pyridine
DMSO	Dimethyl sulfoxide
DSC	Differential scanning calorimetry
ELSD	Evaporative Light Scattering Detector
ENB	Ethylidene norbornene
EP	Ethylene propylene
EPDM	Ethylene-propylene-diene-monomer
EPR	Ethylene-propylene rubbers
FWHM	Full width of half maximum

GEC	Gradient elution chromatography
GMA	Glycidyl methacrylate
GPC	Gel permeation chromatography
HBPS	Hyperbranched polysiloxysilane
HCl	Hydrochloric acid
HIPS	High-impact polystyrene
HPLC	High-performance liquid chromatography
IUPAC	International Union of Pure and Applied Chemistry
$I^{\cdot}$	Initiator fragment
I_3	Intensity of the ortho-positronium formation
IR	Infrared
i-PP-b-PMMA	Isotactic polypropylene-b-poly(methyl methacrylate)
R_o	Infinite spherical potential radius
$<fv(\tau_3)>$	Mean hole volume
L	Ligand
L	Maximum spin diffusive path length
LAC	Liquid adsorption chromatography
LC	Liquid chromatography
LCCC	Liquid chromatography under critical conditions
LiCl	Lithium chloride
[M]	Concentration of the monomer
MA	Methyl acrylate
MAS	Magic-angle-spinning
MADIX	Macromolecular design via the interchange of xanthates
MMA	Methyl methacrylate
MMD	Molecular mass distribution
Mt	Metal
M_n	Number average molar mass
M_w	Weight average molar mass
nBA	n-Butyl acrylate
NMP	Nitroxide mediated polymerization
NMR	Nuclear magnetic resonance spectroscopy
PAN	Polyacrylonitrile
o-Ps	Ortho-positronium
PALS	Positron annihilation lifetime spectroscopy
PAM	Poly(allyl methacrylate)
PBA-co-AM	Poly(butyl acrylate)-co-(allyl methacrylate)
PBA	Poly(butyl actylate)

PBd	Polybutadiene
PC	Polycarbonate
PDI	Polydispersity
PE	Polyethylene
PI	Polyisoprene
PMMA	Poly(methyl methacrylate)
PMMA-co-AM	Poly(methyl methacrylate)-co-(allyl methacrylate)
(PMMA-co-AM)-g-BA	(Poly(methyl methacrylate)-co-(allyl methacrylate))-g-(butyl acrylate)
PMMA-g-PDMS	Poly(methyl methacrylate)-g-poly(dimethylsiloxane)
PP	Polypropylene
PP-MA	Polypropylene-co-methylacrylate
PP-b-PMMA	Polypropylene-b-polymethyl methactylate
PP-b-PVA	Polypropylene-b-polyvinyl acetate
PP-b-PS	Polypropylene-b-polystyrene
p-Ps	Para- positronium
PS	Polystyrene
Ps	Positronium
PS-b-PMMA	Polystyrene-block-poly(methyl methacrylate)
PS-co-AM	Polystyrene-co-(allyl methacrylate)
PS-co-MMA	Polystyrene-co-(methyl methacrylate)
(PS-co-AM)-g-PMMA	(Polystyrene-co-(allyl methacrylate))-graft- (methyl methacrylate)
PTFEA	Poly(trifluoroethyl acrylate)
PVC	Poly(vinyl chloride)
QTRP	Quinone transfer radical polymerization
RAFT	Reversible addition−fragmentation chain transfer polymerization
RI	Refractive index
ROMP	Ring-opening metathesis polymerization
R	Radius of the free volume holes
S=C(Z)S-R	Thiocarbonylthio compounds
SBRP	Organostibene mediated radical polymerization
SEC	Size exclusion chromatography
SEM	Scanning electron microscopy
SFRP	Stable free radical polymerization
SSNMR	Solid state nuclear magnetic resonance spectroscopy
SLM	Standard liters per minute
STM	Scanning tunneling microscopy
T	Temperatures

tBA	Tert-butyl acrylate
TEM	Transmission electron microscopy
TEMPO	2,2,6,6-Tetramethylpiperidine-N-oxide
TERP	Tellurium mediated radical polymerization
T_g	Glass transition
$T_{1\rho}$	Spin-lattice relaxation time rotating frame
THF	Tetrahydrofuran
TMS	Tetramethylsilane
UV	Ultraviolet
VAc	Vinyl acetate
VCT	Variable contact time
2VN	2-vinyl naphthalene
fv	Average free volume holes size
*f*fv	Fractional free volume
WLF	Williams, Landel, and Ferry in their equation
η	Viscosity
τ	Relaxation time
τ_1	Lifetime of para positronium
τ_2	Lifetime of self-annihilation of positron
τ_3	Lifetime of ortho positronium

List of Schemes

Chapter 2

Scheme 2.1: Mechanism of hydroboration, showing the formation of a four-centered transition state……10

Scheme 2.2: Hydroboration of chain-end unsaturated linear polymer, oxidation, and subsequent free radical chain end extension MMA. ……..12

Scheme 2.3: Nitroxide-mediated polymerization (NMR) using TEMPO (nitroxide) as capping agent……17

Scheme 2.4: Schematic representation of the ATRP process. Mt represents a transition metal, L represents the ligands complexed to the transition metal, and RX is an alkyl (pseudo)halide……17

Scheme 2.5: General structures of common RAFT agents……18

Scheme 2.6: Mechanism of RAFT process ……20

Scheme 2.7: Different type of multiphase polymer structures……22

Chapter 3

Scheme 3.1: Anionic polymerization of styrene in toluene, using n-BuLi as initiator, terminated via allylchlorodimethylsilane……52

Scheme 3.2: Hydroboration and subsequent autoxidation of styrene macromonomer based on scheme by Chung et al……55

Chapter 5

Scheme 5.1: Structure of EPDM containing ENB……..100

Scheme 5.2: Hydroboration and hydroxylation of EPDM followed by immobilization of DIBTC RAFT agent……..103

Scheme 5.3: RAFT-mediated copolymerization of EPDM-DIBTC……106

Scheme 5.4: Schematic representation of the extraction process used for the EPDM-g-PS……...107

Scheme 5.5: Illustration of the four steps in the initiation and RAFT-mediated polymerization of EPDM-DIBTC……..113

List of Figures

Chapter 3

Figure 3.1: ^{1}H-NMR spectrum of the product of the reaction of 1-decene with 9-BBN. (Solvent: $CDCl_3$)……51

Figure 3.2: Conversion vs. time, and M_n, of autoxidation polymerization of MMA with 9-BBN……52

Figure 3.3: ^{1}H-NMR of PS macromonomer end-capped with allyldimethylsilane, showing the allyl functional end group to be used in further reactions (solvent: $CDCl_3$)……53

Figure 3.4: SEC traces of conversion reaction of block formation PS_{ally2}-b-PMMA showing molar mass distributions with increasing conversion……56

Figure 3.5: SEC traces of the product of three copolymerization reactions to yield: $PS_{allyl}1$, $PS_{allyl}2$, and $PS_{allyl}3$……57

Figure 3.6: Monomer conversion versus time for the block copolymer reaction of $PS_{allyl}2$-b-PMMA via hydroboration-autoxidation……57

Figure 3.7 SEC traces of $PS_{allyl}2$-b-PMMA after solvent extraction (heptane/Cyclohexane)……58

Figure 3.8: Molar mass versus elution volume of narrow PS standards using ACN/THF as eluent, in different ratios: 52.2, 51.7, 51.4, and 51.3 vol%. Experimental: columns symmetry C18 5 micro and Nucleosil C18. of ACN. Sample solvent was 50/50 eluent. Flow rate of 0.5mL/min, injection volume 20 mL, and polymer concentration was 5.0 mg/mL. The critical condition was at elution mixture 51.7…..59

Figure 3.9: Separation to the block copolymer PS-b-PMMA under the critical conditions for styrene……60

Figure 3.10: 2D-LC contour plots of the block copolymer $PS_{allyl}2$-b-PMMA showing separation of the block copolymer and the unreacted styrene macromonomer. First dimension: critical conditions for PS, flow rate 0.05 mL/min; second dimension: SEC, flow rate 4 mL/min. (Experimental conditions as described in the text.)……61

Figure 3.11: Molar mass versus elution volume of narrow PMMA standards using MEK/Cyclohexane as eluent, in different ratios: 70, 75, 77 and 79 vol% of MEK. [Exp: column Nucleosil Si 300. Sample solvent was 70/30 eluent. Flow rate of 0.5mL/min, injection volume 20 mL, and polymer concentration was 2.0 mg/mL. The critical condition was at elution mixture 77]……62

Figure 3.12: Example of separation of the block copolymer $PS_{allyl}2$-b-PMMA under the critical conditions for MMA……63

Chapter 4

Figure 4.1: Conversion versus M_n and kinetic plot of the polymerization of AM in the presence of CPDB……74

Figure 4.2: SEC of the RAFT mediated radical polymerization of PAM homopolymer as a function of reaction time. [Exp: the temperature was 70^{o} C, the polymerization condition was as follows: [M]/[CPDB]/[AIBN] = 800:1:0.1]……..75

Figure 4.3: Molar mass distributions curves of the RAFT mediated radical copolymerization of (PS-co-AM as function of time.[Exp: the temperature was 70 ^{o}C, the copolymerization condition was as follows: [M]/[CPDB]/[AIBN] = 800:1:0.1]……...77

Figure 4.4: Conversion and kinetic plots of the copolymerization of PS-co-AM 5, 10 and 20% AM in the presence of CPDB……78

Figure 4.5: ^{1}H-NMR spectra in $CDCl_3$ of PS-co-AM copolymers (5, 10, and 20 mol% AM) in the feed obtained from RAFT mediated polymerization at 70^{o} C before the gelation reaction take place at 25% conversion……79

Figure 4.6: Copolymer composition (F_{AM}) obtained from ^{1}H-NMR, as a function of conversion for the 20% AM PS-co-AM copolymer……..80

Figure 4.7: Proton decoupled ^{13}C-NMR spectra in $CDCl_3$ of copolymer PS-co-AM 5, 10 and 20% AM in the feed obtained from RAFT mediated polymerization at 70^{o} C before the gelation reaction take place at 25% conversion……..…81

Figure 4.8: Proton decoupled ^{13}C-NMR spectra of PAM and corresponding copolymers PS-co-AM (5, 10, and 20% AM) at 25% conversion……..82

Figure 4.9: SEC elution of the borane autoxidation radical copolymerization of (PS-co-AM)-g-PMMA, a) 5% AM b) 10% AM, and c) 20% AM……..84

Figure 4.10: Gradient HPLC separation of the grafts copolymers,[Exp: stationary phase: Silce 300, mobile phase: 100% ACN for 2 min then 10 min linear gradient ACN-THF 100 to 0% ACN, flow rate: 1 mL/min, detection: ELSD]……85

Figure 4.11: ^{1}H-NMR in $CDCl_3$ the graft copolymers (PS-co-AM)-g-PMMA 20% AM shows the presence of the allyl functional group in the graft copolymer……..…87

Figure 4.12: SEC elution of the RAFT mediated radical copolymerization of PMMA-co-AM (20% AM). [Exp: the temperature was 70^{o} C, the copolymerization condition was as follows: [M]/[CPDB]/[AIBN] = 800:1:0.1]……..89

Figure 4.13: Conversion and kinetic plot of copolymerization of PMMA-co-AM in the presence of CPDB……90

Figure 4.14: ^{1}H-NMR spectra in $CDCl_3$ of PMMA-co-AM copolymers (5, 10, and 20 mol% AM) at 15% conversion shows the assignment of the functional group of each copolymer……90

Figure 4.15: SEC elution of the borane autoxidation radical copolymerization of (PMMA-co-AM)-g-PBA……92

Figure 4.16: ^{1}H-NMR in $CDCl_3$ the graft copolymers (PMMA-co-AM)-g-PBA show the assignment of the signal of each component……..……..92

Figure 4.17: Gradient HPLC separation of the corresponding homopolymers BA and (MMA-co-AM) the graft copolymer, stationary phase: Silice100, mobile phase: 100% n-Hept for 1 min then 10 min linear gradient n-hept-THF 100 to 0% n-hept, flow rate: 0.5 mL/min, detection: ELSD……..…….93

Figure 4.18: SEC traces of RAFT mediated polymerization of the PBA-co-AM, at 70^{o} C in tolune solution, a) 5, b) 10, and c) 20% AM……..…….95

Figure 4.19: ^{1}H-NMR spectra in $CDCl_3$ of PBA-co-AM copolymers (5, 10, and 20 mol% AM)……..……..96

Chapter 5

Figure 5.1: Typical example of ^{1}H-NMR spectrum of EPDM rubber ($CDCl_3$)…...…109

Figure 5.2: ^{1}H-NMR spectra of EPDM (a) and EPDM-OH (b) ($CDCl_3$)……...110

Figure 5.3: FTIR spectra of thin films of EPDM and EPDM-OH……..……..110

Figure 5.4: ^{1}H-NMR spectrum of EPDM-DIBTC ($CDCl_3$)……..111

Figure 5.5: FTIR spectra of a thin film of EPDM, a KBr disc DIBTC, and a thin film of EPDM-DIBTC ……..……112

Figure 5.6: FTIR spectra of thin films of EPDM, and EPDM-g-PS……..113

Figure 5.7: SEC traces of RAFT-mediated copolymerization of EPDM-g-PS…...…114

Figure 5.8: ^{1}H-NMR spectra of extracted EPDM and EPDM-g-PS graft copolymer ($CDCl_3$)…….....115

Figure 5.9: SEC traces of RAFT-mediated copolymerization of EPDM-DIBTC in presence of free DIBTC in solution ……..……..116

Figure 5.10: ^{1}H-NMR of extracted EPDM and EPDM-g-PS graft copolymer……...117

Figure 5.11: Gradient HPLC separation of the homopolymers a) EPDM and b) PS.
[Exp: stationary phase, CN 100 Á; mobile phase, 90% i-oct for 2 min then 10 min linear gradient i-oct-THF 100-0% flow rate, 1 mL/min, detection: ELSD.]……...118

Figure 5.12: Gradient HPLC separation of the EPDM-g-PS grafts from the EPDM-DIBTC and PS.
[Exp: stationary phase, CN 100 Á; mobile phase, 90% i-oct for 2 min then 10 min linear gradient i-oct-THF 100-0% flow rate, 1 mL/min, detection: ELSD.]
……119

Figure 5.13: Gradient HPLC separation of the EPDM-g-PS grafts from the EPDM-DIBTC and PS in presence of free DIBTC in solution
[Exp: stationary phase, CN 100 Á; mobile phase, 90% i-oct for 2 min then 10 min linear gradient i-oct-THF 100-0% flow rate, 1 mL/min, detection: ELSD.]……..119

Chapter 6

Figure 6.1: Standard positron lifetime set-up: PM TUBE, photomultiplier tube, CF DIFF DISC, constant fraction differential discriminator, DELAY, delay box fixed length of 50 Ω cable, TAC, time-to-amplitude converter, MCA, multichannel analyzer……..126

Figure 6.2: A typical positron lifetime spectra PALS of synthesized graft copolymer (PS-co-AM)-g-PMMA with three different decays decomposing Ps lifetimes fitted using PATFIT……..…….127

Figure 6.3: *o*-Ps lifetime τ_3 in PS-co-AM (5, 10, and 20%) copolymer and the graft copolymers as a function of comonomer composition and graft composition……129

Figure 6.4: *o*-Ps intensity I_3 in PS-co-AM (5, 10, and 20%) copolymer graft copolymers as a functions of comonomer composition and graft composition…....129

Figure 6.5: ^{13}C CP/MAS spectrum of graft copolymer (PS-co-AM)-g-PMMA and PMMA homopolymer (*) peaks indicate spinning side bands……..……131

Figure 6.6: Values of $\ln(I/I_{max})$ versus contact time for graft copolymer (PS-co-AM)-g-PMMA, the $T_{1\rho}$ values determined from the negative inverse of the slope of the decay part of the curve. ……132

Figure 6.7: DSC curves of the PS-co-AM with different comonomer content (5, 10, 20 AM%), the heat rate 10^{o} C/min. ……133

Figure 6.8: *o*-Ps lifetime τ_3 in graft copolymer PMMA-g-PS_{VB} as function of macromonomer content (wt %) and radius of free volume holes……136

Figure 6.9: *o*-Ps intensity I_3 in graft copolymer PMMA-g-PS_{VB} as function of macromonomer content (wt %)……..……..137

Figure 6.10: Relationship between T_g with o-Ps lifetime τ_3 of PMMA-g-PS_{VB}. (Note: values indicated in brackets are for second detected T_g.) ……..138

Figure 6.11:^{13}C CPMAS spectrum of graft copolymer PMMA-g-PS_{VB}. ……139

Figure 6.12: Relationship between macromonomer contents with T_g, τ_3, and $T_{1\rho}$ of the graft copolymers PMMA-g-PS_{VB}……140

List of Tables

Chapter 3

Table 3.1: Compositions and characteristics, M_n, M_w, and PDI, of the styrene macromonomers terminated by an allyl functional group……..53

Table 3.2: 2D data of M_n and M_w of the block copolymers, obtained using PMMA calibration standards……61

Chapter 4

Table 4.1: Compositions and characteristics of PS-co-AM prepared via free radical polymerization in the presence of RAFT agent CPDB……..…71

Table 4.2: Compositions and characteristics of PMMA-co-AM prepared via free radical polymerization in presence of RAFT agent CPDB……..71

Table 4.3: Compositions and characteristics of PBA-co-AM prepared via free radical polymerization in presence of RAFT agent CPDB……..……..……72

Table 4.4: Gradient profile for reversed phase separation of the (PS-co-AM)-g-PMMA ……..……..……73

Table 4.5: Gradient profile for reversed phase separation of the (PMMA-co-AM)-g-BA ……..……73

Table 4.6: SEC data of soluble fraction of PAM homopolymer……..74

Table 4.7: Copolymer composition data obtained from ^{1}H-NMR of the (PS-co-AM) copolymer at 20% conversion……80

Table 4.8: Experimentally observed (^{13}C-NMR) α-methyl resonances of AM centered sequences for various PS-co-AM copolymers prepared by RAFT-mediated polymerization with different monomer feed compositions ……..83

Table 4.9: Estimation of component amounts for graft copolymers as determined by gradient HPLC analysis……..86

Table 4.10: Grafting efficiency via hydroboration reaction for the 5, 10, and 20% AM copolymers……..87

Table 4.11: ^{1}H-NMR analysis of the collect graft copolymer from HPLC……88

Table 4.12: Copolymer composition at 15% conversion obtained from ^{1}H-NMR of the PMMA-co-AM copolymer……91

Table 4.13: Estimate of component amounts for graft copolymers as determined by gradient analysis……..……94

Table 4.14: Copolymer composition data of the PBA-co-AM copolymer (at high conversion)……96

Chapter 5

Table 5.1: Hydroxylation and esterification reactions conditions ……..105

Table 5.2: Gradient profile of THF used for the reversed phase separation of EPDM-g-PS……..118

Table 5.3: Relative peak areas of EPDM-g-PS and cross-linked material in the reaction mixture calculated from gradient HPLC……120

Chapter 6

Table 6.1: Positron data of PS-co-AM and (PS-co-AM)-g-PMMA copolymers, lifetime (τ_3) relative intensity (I_3) radius of free volume hole (R) free volume (fv) fractional free volume (*f*fv)……..128

Table 6.2: $T_{1\rho}$ data obtained from the VCT experiment of the backbone copolymer and graft copolymers……133

Table 6.3: Glass transition temperatures and free volume fraction of PS-co-AM copolymer with different comonomer content 5, 10, and 20%AM ……..134

Table 6.4: Formulation and characterization of graft copolymers, number average molar mass and weight average molar mass of the graft copolymers obtained via SEC, and chemical compositions of graft copolymers PMMA-g-PS_{VB} determined using ^{1}H-NMR……..135

Table 6.5: Positron data, lifetime (τ_3) relative intensity (I_3) radius of free volume hole (R) free volume (fv) fractional free volume (*f*fv) ……135

Table 6.6: $T_{1\rho}$ data obtained from the VCT experiment of homopolymers PS and PMMA and graft copolymers PMMA-g-PS……139

Table 6.7: Microphase structure of the graft copolymer (PS-co-AM)-g-PMMA and PMMA-g-PS_{VB}……..141

CHAPTER 1

INTRODUCTION AND OBJECTIVES

1.1 Introduction

Interest in the synthesis and characterization of multiphase copolymers has increased significantly over the past few years, particularly because of their properties and potential applications in various fields.[1-12] Multiphase copolymers can be used as templates (soft or hard) for polymer synthesis,[13] in energy storage,[14] as polymer-stabilized quantum dots,[15] as compatibilizers in blends systems,[16] as polymeric films in transparent packaging,[17] and in drug delivery.[18,19]

Multiphase copolymers are copolymer materials in which dissimilar (and therefore incompatible) segments are covalently bonded in one polymer molecule. Typically, this means that these materials form complicated phase separated morphologies in the solid state. Most often, multiphase copolymers consist of block (di- or multi-) or graft copolymer structures, although it is also possible to get phase separated morphologies with other types of copolymer structures.

The potential outstanding properties and wide range of applications of multiphase copolymers has led to the need for more sophisticated synthesis methods to produce copolymers with controlled structures. Associated with related developments in synthetic methods is the need to develop suitable techniques to characterize these polymers in order to obtain a better understanding of the structure–property relationships of the materials.[20-35]

There are, however, many challenges facing scientists during the synthesis of these types of polymer materials. The nature of the molecular requirements for multiphase materials means that it is often challenging to synthesize these copolymers because not all monomers can be polymerized by all available polymerization techniques. This has lead to the need to combine different polymerization techniques to overcome such limitations.[36-38]

The characterization of multiphase copolymers can also be very complicated and challenging. For example, the materials most often have heterogeneity in terms of their chemical composition and molar mass distribution. The heterogeneity in the solid state (SS) microstructure of the polymers is a further obstacle.

The synthesis of block and graft copolymers via living polymerization has been shown to be an excellent technique to synthesis copolymers with well defined structures.[39,40] Historically, the living polymerization technique used has been anionic polymerization. While this provides excellent control over the molar mass and structure, it does have limitations, as not all monomers can be polymerized using the anionic technique. For example, the non-ideal behavior of the alkyl (meth)acrylate monomers during polymerization has made the process of preparing block copolymers containing acrylate monomers rather challenging.

One of the challenges is to reduce the nucleophilicity of the chain-end to allow the acrylic monomer to react with carbanions, either by introducing a sterically hindered initiator or reducing the temperature (below zero), together with a good choice of solvent and ligands.[41-43] There are many papers and reviews describing the synthesis of block and graft copolymers via the anionic technique.[43-47] Hadjichristidis et al.[40] have presented an excellent review on the use of living anionic polymerization to produce complex architectures – from simple block copolymers to complex cyclic polymers.

Living free radical polymerization is widely used to synthesize block and graft copolymers,[10,48,49] due to it is compatibility with various monomers. Some limitations[50] occur with the different living radical techniques for example nitroxide-mediated radical polymerization (NMP) is limited to styrene and styrene derivatives. Atom Transfer Radical Polymerization (ATRP) also has limitations[50] with monomers or initiators containing acid functionality and certain ionic groups and in addition provides products contaminated with metal ions. Reversible addition-fragmentation chain transfer (RAFT) polymerization is among the most successful living free radical polymerization processes, largely due to its applicability to a wide range of monomers.[51-55] It also has some limitations however:[50] monomers containing primary or secondary amines cannot be polymerized, and some monomers are limited to low monomer conversion.[56] A number of these limitations can nonetheless be overcome by the appropriate selection of the monomers, reagents, and reaction conditions.

Hydroboration reactions have become a very important tool and attracted wide application in organic synthesis and functionalization.[57-65] The trialkylborane moiety can be used to introduce free radicals by selective oxidation,[66] which can then facilitate polymerization under favorable conditions. Chung et al.[67-70] were the first to introduce a novel method for the synthesis of polyolefin block or graft copolymers via the hydroboration/autoxidation reaction. Only polyolefins containing boron as an end or side functional group are used to initiate free radical polymerisation to produce block or graft copolymers of polyolefins with another vinyl monomers such as maleic anhydride, methyl methacrylate, and styrene.

The combination of different polymerization techniques is an alternative approach that can be used to overcome the limitations of the individual techniques and produce well defined copolymers. Use of such a combination of techniques to prepare block and graft copolymers has been widely reported,[36-38,71-80] most frequently for the purpose of overcoming the limitations of monomer selection.

Combining hydroboration with metallocene catalyst polymerization has been reported.[67,70] However, the combination of hydroboration–autoxidation with other living

polymerization techniques, such as anionic or living free radical polymerization, is a novel process and presents new challenges, which have not yet been published.

The characterization of synthetic polymers is most often complicated and time consuming, due to their complex structures and the heterogeneous nature of the synthesized polymers. The heterogeneity of the polymer is multidimensional: molar mass, end group, chemical composition and architecture. In the case of copolymers, the heterogeneity is even more complicated; it can vary from chain to chain and along each chain. This heterogeneity has an effect on the polymer properties, which vary from polymer to polymer depending on the heterogeneity.

Therefore, polymer characterization techniques must cover both the chemical and physical heterogeneity. Spectroscopy techniques, nuclear magnetic resonance (NMR), and infrared (IR) generally yield information on the average chemical composition and functionality of unfractionated polymers. Chromatographic techniques, on the other hand, characterize the polymer via separation of the polymer, and provide information on the chemical composition, molar mass, and end group distribution. Gradient elution chromatography (GEC) and liquid chromatography under critical conditions (LCCC) are considered the most successful techniques to determine the chemical composition distribution of copolymers.[33,34,81-85]

The determination of structure and understanding structure-property relationships of polymers are important areas of research and require analysis of the structure and macroscopic properties. Solid state NMR (SSNMR) contributes to this analysis through the dependence of the NMR parameters on the local structure. Application of SSNMR to determine the structure and function of synthetic polymers has been investigated by many scientists. Segment motions in polymers and copolymers have been reviewed.[86,87] Using proton relaxation times and spin-diffusion measurements, information on the minimum domain size of copolymers and mobility can be obtained,[88-91] as well as information on microphase separation.[27,92,93] These studies have, however, so far been limited to examining relatively simple block copolymers. Beside the SSNMR, positron annihilation lifetime spectroscopy (PALS) and free volume studies of the polymers provide a good understanding of the structure-property relationships in view of the fact that the free volume has a significant effect on the property of the polymer.

1.2 Objectives

The specific objectives of this study are the following:

1 Synthesis of multiphase block copolymers by combining borane chemistry (hydroboration–autoxidation reactions) with living anionic polymerization.

- Synthesis of block copolymers polystyrene-block-polymethyl methacrylate (PS-b-PMMA) via a combination of living anionic polymerization and hydroboration-autoxidation reactions of styrene as the functional end group.
    - Synthesis of styrene macroinitiators of different molar masses via living anionic polymerization and termination via allylchlorodimethylsilana.
    - Hydroboration-autoxidation reactions of the functional end group in the presence of (MMA) monomer.

2 Synthesis of multiphase graft copolymers via the "grafting from" technique. This was to be done by first synthesizing the backbone to contain unsaturated allyl functional groups as the active sites, which allows the 9-BBN to initiate polymerization of the branches via the hydroboration-autoxidation reaction.

- Synthesis of random copolymers (PS-co-AM), (PMMA-co-AM), and (PBA-co-AM) via living controlled free radical polymerization (RAFT) to have different comonomer contents.
- Synthesis of graft copolymers (polystyrene-co-(allyl methacrylate))-graft-poly(methyl methacrylate) (PS-co-AM)-g-PMMA and (poly(methyl methacrylate)-co-(allyl methacrylate))-graft-poly(butyl acrylate) (PMMA-co-AM)-g-PBA via hydroboration-autoxidation reactions of the functional groups on the side chains.

3 Synthesis of multiphase graft copolymers using ethylene propylene diene monomer (EPDM) rubber via two-step reactions.

- Hydroxylation of the double bond of the EPDM rubber using the hydroboration agent (9-BBN).
- Esterification reaction of hydroxyl group with an acid chloride RAFT agent.
- Graft copolymerization, carried out in solution in the presence of styrene monomer.

4 Study of the microphase structure of synthesized multiphase copolymers via positron annihilation lifetime spectroscopy (PALS) and SSNMR.

1.3 Layout of the thesis

Chapter 1 provides a brief introduction to the study and lists the objectives.

Chapter 2 presents an historical review; theoretical background to several polymerization techniques considered in this study, including, living anionic polymerization, living free radical polymerization, hydroboration, and oxidation reactions; the use of different combined polymerization techniques to synthesize multiphase copolymers; and an overview of chromatographic analyses used to characterize copolymers.

Chapter 3 describes the synthesis and characterization of the block copolymer PS-b-PMMA.

Chapter 4 describes the synthesis and characterization of the graft copolymers [(PS-co-AM)-g-PMMA] and [(PMMA-co-AM)-g-BA].

Chapter 5 describes the synthesis of the graft copolymer ethylene propylene diene monomer -graft-polystyrene (EPDM-g-PS) using two-step reactions. Chapter 6 presents the study of the microphase of the multiphase copolymer using PALS, and SSNMR.

Chapter 7 presents the conclusions and offers some recommendations for future research.

1.4 References

1. Hadjichristidis, N.; Pispas, S. *Advances in Polymer Science* **2006,** 200, 37-55.
2. Liu, G.; Qiao, L.; Guo, A. *Macromolecules* **1996,** 29, 5508-5510.
3. Hamley, I. W. *Advances in Polymer Science* **1999,** 148, 113-137.
4. Xie, H.-Q.; Xie, D. *Progress in Polymer Science* **1999,** 24, 275-313.
5. Jiang, R.; Jin, Q.; Li, B.; Ding, D.; Wickham, R. A.; Shi, A.-C. *Macromolecules* **2008,** 41, 5457-5465.
6. Abetz, V.; Simon, P. F. W. *Advances in Polymer Science* **2005,** 189, 125-212.
7. Oh, H.; Green, P. F. *Macromolecules* **2008,** 41, 2561-2566.
8. Ding, J.; Carver, T. J.; Windle, A. H. *Computational and Theoretical Polymer Science* **2001,** 11, 483-490.
9. Ishizu, K.; Uchida, S. *Progress in Polymer Science* **1999,** 24, 1439-1480.
10. Hadjichristidis, N.; Pitsikalis, M.; Iatrou, H. *Advances in Polymer Science* **2005,** 189, 1-124.
11. Dong, J.-Y.; Hu, Y. *Coordination Chemistry Reviews* **2006,** 250, 47-65.
12. Pitsikalis, M.; Pispas, S.; W.Mays, J.; Hadjichristidis, N. *Advances in Polymer Science* **1998,** 135, 1-129.
13. Sohn, B.-H.; Choi, J.-M.; Yoo, S. I.; Yun, S.-H.; Zin, W.-C.; Jung, J. C.; Kanehara, M.; Hirata, T.; Teranishi, T. *Journal of the American Chemical Society* **2003,** 125, 6368-6369.
14. Pan, L.; Qiu, H.; Dou, C.; Li, Y.; Pu, L.; Xu, J.; Shi, Y. *International Journal of Molecular Sciences* **2010,** 11, 2636-2657.
15. Wang, C.-W.; Oskooei, A.; Sinton, D.; Moffitt, M. G. *Langmuir* **2010,** 26, 716-723.
16. Bourland, L. G.; Braunstein, D. M. *Journal of Applied Polymer Science* **2003,** 32, 6131-6149.
17. Adhikari, R.; Michler, G. H. *Progress in Polymer Science* **2004,** 29, 949-986.
18. Nishiyama, N.; Kataoka, K. *Advances in Polymer Science* **2006,** 193, 67-101.
19. Bo, J.; Ming, X. *European Polymer Journal* **1992,** 28, 827-830.
20. Heffner, S. A.; Bovey, F. A.; Verge, L. M.; Mirau, P. A.; Tonelli, A. E. *Macromolecules* **1986,** 19, 1628-1634.
21. Aerdts, A. M.; Haan, J. W. D.; German, A. L.; Velden, G. P. M. V. d. *Macromolecules* **1991,** 24, 1473-1479.

22. Brar, A. S.; Yadav, A. *Journal of Molecular Structure* **2002,** 602-603, 29-39.

23. Nakashima, K.; Bahadur, P. *Advances in Colloid and Interface Science* **2006,** 123-126, 75-96.

24. Schlaad, H.; Kilz, P. *Analytical Chemistry* **2003,** 75, 1548-1551.

25. Meng, H.; Liu, L.; Yang, W. *Journal of Macromolecular Science Part A: Pure and Applied Chemistry* **2009,** 46, 921-927.

26. Cho, G.; Natansohn, A.; Ho, T.; Wynne, K. J. *Macromolecules* **1996,** 29, 2563-2569.

27. Wang, L.; Fang, P.; Ye, C.; Feng, J. *Journal of Polymer Science: Part B: Polymer Physics* **2006,** 44, 2864-2879.

28. Garcia, H.; Barros, A. S.; Goncalves, C.; Gama, F. M.; Gil, A. M. *European Polymer Journal* **2008,** 44, 2318-2329.

29. Feldermann, A.; Toy, A. A.; Plan, H.; Stenzel, M. H.; DAvis, T. P.; Barner-Kowollik, C. *Polymer* **2004,** 45, 3997-4007.

30. Hiller, W.; Sinha, P.; Pasch, H. *Macromolecular Chemistry and Physics* **2007,** 208, 1965-1978.

31. Im, K.; Park, H.-W.; Kim, Y.; Chung, B.; Ree, M.; Chang, T. *Analytical Chemistry* **2007,** 79, 1067-1072.

32. Adrian, J.; Esser, E.; Hellmann, G.; Pasch, H. *Polymer* **2000,** 41, 2439-2449.

33. Olesik, S. V. *Analytical and Bioanalytical Chemistry* **2004,** 378, 43-45.

34. Pasch, H.; Brinkmann, C.; Gallot, Y. *Polymer* **1993,** 34, 4100-4104.

35. Pasch, H. *Polymer* **1993,** 34, 4095-4099.

36. Tsoukatos, T.; Pispas, S.; Hadjichristidis, N. *Macromolecules* **2000,** 33, 9504-9511.

37. Lutz, J. F.; Borner, H. G.; Weichenhan, K. *Macromolecules* **2006,** 39, 6376-6383.

38. Kobatake, S.; Harwood, H. J.; Quirk, R. P.; Priddy, D. B. *Macromolecules* **1998,** 31, 3735-3739.

39. Davis, K. A.; Matyjaszewski, K. *Advances in Polymer Science* **2002,** 159, 1-156.

40. Hadjichristids, N.; Pitsikalis, M.; Pispas, S.; Latrou, H. *Chemical Reviews* **2001,** 101, 3747-3792.

41. Zundel, T.; Zune, C.; Teyssie, P.; Jerome, R. *Macromolecules* **1998,** 31, 4089-4092.

42. Fayt, R.; Forte, R.; Jacobs, C.; Jerome, R.; Ouhadi, T.; Teyssie, P.; Varshney, S. K. *Macromolecules* **1987,** 20, 1442-1444.

43. Baskaran, D.; Muller, A. H. E. *Progress in Polymer Science* **2007,** 32, 173-219.

44. Zeng, F.; Yang, M.; Zhang, J.; Varshney, S. K. *Journal of Polymer Science: Part A: Polymer Chemistry* **2002,** 40, 4387-4397.

45. Chung, T. C.; Lu, H. L.; Ding, R. D. *Macromolecules* **1997,** 30, 1272-1278.

46. Matsumoto, K.; Deguchi, M.; Nakano, M.; Yamaoka, H. *Journal of Polymer Science: Part A: Polymer Chemistry* **1998,** 36, 2699-2706.

47. Koutalas, G.; Lohes, D. J.; Hadjichristidis, N. *Journal of Polymer Science: Part A: Polymer Chemistry* **2005,** 43, 4040-4049.

48. Wong, K. H.; Davis, T. P.; Barner-Kowollik, C.; Stenzel, M. H. *Polymer* **2007,** 48, 4950-4965.

49. Zhao, Y.; Perrier, S. *Macromolecules* **2006,** 39, 8603-8608.

50. Hansen, N. M. L.; Jankova, K.; Hvilsted, S. *European Polymer Journal* **2007,** 43, 255-293.

51. Barsbay, M.; Guven, O.; Davis, T. P.; Barner-Kowollik, C.; Barner, L. *Polymer* **2009,** 50, 973-982.

52. Ray, B.; Isobe, Y.; Matsumoto, K.; Habaue, S.; Okamoto, Y.; Kamigaito, M.; Sawamoto, M. *Macromolecules* **2004,** 37, 1702-1710.

53. Tang, C.; Kowalewski, T.; Matyjaszewski, K. *Macromolecules* **2003,** 36, 8587-8589.

54. Zhang, Z.; Zhu, J.; Cheng, Z.; Zhu, X. *Polymer* **2007,** 48, 4393-4400.

55. Chong, Y. K.; Moad, G.; Rizzardo, E.; Skidmore, M. A.; Thang, S. H. *Macromolecules* **2007,** 40, 9262-9271.

56. David, G.; Asri, Z. E.; Rich, S.; Castignolles, P.; Guillaneuf, Y.; Lacroix-Desmazes, P.; Boutevin, B. *Macromolecular Chemistry and Physics* **2009,** 210, 631-639.

57. Huang, S.-W.; Peng, W.-L.; Shan, Z.-X.; Zhao, D.-J. *New Journal of Chemistry* **2001,** 25, 869-871.

58. MacKay, B. A.; Johnson, S. A.; Patrick, B. O.; Fryzuk, M. D. *Canadian Journal of Chemistry* **2005,** 83, 315-323.

59. Duin, M. v.; Leemans, L.; Neilen, M. *Polymer* **1999,** 40, 1001-1009.

60. Hewes, J. D.; Kreimendahl, C. W.; Marder, T. B.; Hawthorne, M. F. *Journal of the American Chemical Society* **1984,** 106, 5757-5759.

61. Wynberg, N. A.; Leger, L. J.; Conrad, M. L.; Vogels, C. M.; Decken, A.; Duffy, S. J.; Westcott, S. A. *Canadian Journal of Chemistry* **2005,** 83, 661-667.

62. Zhang, Z.-C.; Wang, Z.; Chung, T. C. M. *Macromolecules* **2007,** 40, 5235-5240.

63. Ilich, P. P.; Rickertsen, L. S.; Becker, E. *Journal of Chemical Education* **2006,** 83, 1681-1685.

64. Brinkman, J. A.; Nguyen, T. T.; Sowa, J. R. *Organic Letters* **2000,** 2, 981-983.

65. Hanson, J. R. *Journal of Chemical Research* **2004**, 1-5.

66. Chung, T. C.; Janvikul, W.; Lu, H. L. *Journal of the American Chemical Society* **1996,** 118, 705-706.

67. Chung, T. C.; Rhubright, D.; Jiang, G. J. *Macromolecules* **1993,** 26, 3467-3471.

68. Chung, T. C.; Janvikul, W.; Bernard, R.; Jiang, G. J. *Macromolecules* **1994,** 27, 26-31.

69. Chung, T. C.; Janvikul, W.; Bernard, R.; Hu, R. *Polymer* **1995,** 36, 3565-3574.

70. Chung, T. C.; Lu, H. L.; Janvikul, W. *Polymer* **1997,** 38, 1495-1502.

71. Korczagin, I.; Hempenius, M. A.; Vancso, G. J. *Macromolecules* **2004,** 37, 1686-1690.

72. Acar, M. H.; Matyjaszewski, K. *Macromolecular Chemistry and Physics* **1999,** 200, 1094-1100.

73. Binder, W. H.; Kluger, C. *Macromolecules* **2004,** 37, 9321-9330.

74. Favier, A.; Luneau, B.; Vinas, J.; Laissaoui, N.; Gigmes, D.; Bertin, D. *Macromolecules* **2009,** 42, 5953-5964.

75. Grubbs, R. B. *Macromolecular Chemistry and Physics* **2005,** 206, 625-627.

76. Zhu, Y.; Storey, R. F. *Macromolecules* **2010,** 43, 7048-7055.

77. Venkatesh, R.; Yajjou, L.; Koning, C. E.; Klumperman, B. *Macromolecular Chemistry and Physics* **2004,** 205, 2161-2168.

78. Mahajan, S.; Renker, S.; Simon, P. F. W.; Gutmann, J. S.; Jain, A.; Gruner, S. M.; Fetters, L. J.; Coates, G. W.; Wiesner, U. *Macromolecular Chemistry and Physics* **2003,** 204, 1047-1055.

79. Kaneyoshi, H.; Inoue, Y.; Matyjaszewski, K. *Macromolecules* **2005,** 38, 5425-5435.

80. Wang, W. P.; You, Y. Z.; Hong, C. Y.; Xu, J.; Pan, C. Y. *Polymer* **2005,** 46, 9489-9494.

81. Mori, S.; Naito, M. *Journal of Chromatography A* **1993,** 655, 185-190.

82. Sato, H.; Mitstani, K.; Shimizu, I.; Tanaka, Y. *Journal of Chromatography* **1988,** 447, 387-391.

83. Philipsen, H. J. A. *Journal of Chromatography A* **2004,** 1037, 329-350.

84. Glockner, G.; Berg, J. H. M. V. D. *Journal of Chromatography* **1987,** 384, 135-144.

85. Chang, T.; Lee, H. C.; Lee, W.; Park, S.; Ko, C. *Macromolecular Chemistry and Physics* **1999,** 200, 2188-2204.

86. Saxena, S.; Cizmeciyan, D.; Kornfield, J. A. *Solid State Nuclear Magnetic Resonance* **1998,** 12, 165-181.

87. Gandhi, S.; Melian, C.; Demco, D. E.; Brar, A. S.; Blumich, B. *Macromolecular Chemistry and Physics* **2008,** 209, 1576-1585.

88. Geppi, M.; Ciardelli, F.; Veraeini, C. A.; Forte, C.; Cecchin, G.; Ferrari, P. *Polymer* **1997,** 38, 5713-5723.

89. Abis, L.; Floridi, G.; Merlo, E.; Po, R.; Zannoni, C. *Journal of Polymer Science: Part B: Polymer Physics* **1998,** 36, 1557-1566.

90. Gentzler, M.; Reimer, J. A. *Macromolecules* **1997,** 30, 8365-8374.

91. Jack, K. S.; Natansohn, A.; Wang, J.; Favis, B. D.; Cigana, P. *Chemistry of Materials* **1998,** 10, 1301-1308.

92. Li, M.; Li, C.; Zhang, B.; Huang, W.; Men, A.; He, B. *European Polymer Journal* **1998,** 34, 515-521.

93. Heinen, W.; Wenzel, C. B.; Rosenmoller, C. H.; Mulder, F. M.; Jan Boender, G.; Lugtenburg, J.; de Groot, H. J. M.; van Duin, M.; Klumperman, B. *Macromolecules* **1998,** 31, 7404-7412.

CHAPTER 2

LITERATURE REVIEW AND BACKGROUND

Boron chemistry is reviewed in this chapter, especially the hydroboration and autoxidation reactions and their use in chemical modification, as well as the role of bis(9-borabicyclo[3.3.1]nonane) (9-BBN) in the synthesis of multiphase copolymers. The following topics are also addressed: anionic and free radical polymerization, controlled living free radical polymerization, and the combination of different polymerization techniques and their use in the synthesis of multiphase copolymers. The applications of chromatographic analysis and free volume analysis to the study of multiphase copolymers are included.

2.1 Boron chemistry

In the early 1950s, H. C. Brown of Purdue University discovered that diborane (B_2H_6) adds to the double bond of an alkene to form a product called an organoborane. The simple addition of a boron-hydrogen bond to carbon-carbon multiple bonds of unsaturated organic derivatives makes the organoboranes very useful in organic synthesis.

2.1.1 Hydroboration-oxidation reaction

Hydroboration is the most important method for the preparation of organoboranes and has been applied to a wide variety of alkenes. The most common and useful application of the hydroboration reaction of alkenes is to form alcohols by anti-Markovnikov addition by oxidation of the organoborane with hydrogen peroxide or sodium perborate.[1]

The mechanism of hydroboration[2-4] is show in Scheme 2.1. The addition of boron in a simple reaction of propene and BH_3 is believed to involve the addition of a monomeric borane to a carbon-carbon double bond via a four-centered transition state.[5-7]

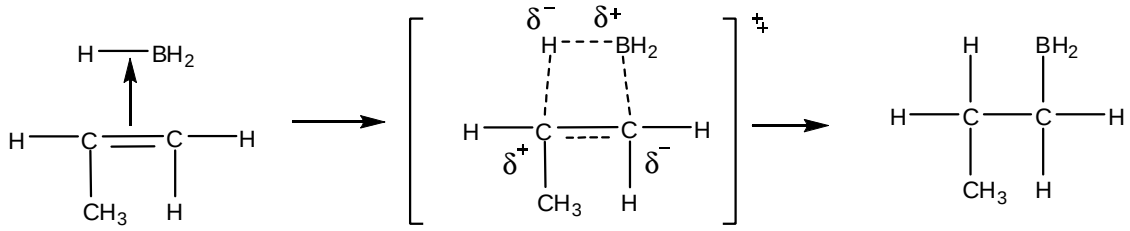

Scheme 2.1: Mechanism of hydroboration, showing the formation of a four-centered transition state.

The first step is the attack of the alkene on BH_3, which results in the formation a four-member ring intermediate of partial bonds and, subsequently, the anti-Markovnikov product. Since the boron atom is highly electrophilic, due to its empty *p*-orbital, there is slight bonding interaction with the π bond. The electron density from the double bond is more inclined

towards the boron atom, and therefore the carbon opposite the boron is slightly electron deficient with a slightly positive charge. The electron deficiency would be stabilized by more highly substituted carbons, so the carbon opposite the boron tends to be the most highly substituted. Once the transition state breaks down, BH_2 attaches to the least substituted carbon.

The hydroboration reaction applies to various organic compounds, including alkenes containing two, three or four alkyl substituents on the double bond,[8] cyclic and/or bicyclic olefins, and even a number of steroids[9] with highly hindered double-bonds. The hydroboration reaction of diborane with a carbon-carbon double bond is very fast, even faster than the reaction of diborane with many functional groups.[10] Because borane compounds prefer to form dimers with two three-centered bonds, each bond includes three atoms: the two boron atoms and the hydrogen atom between them. These diboranes are, however, very difficult to handle. But Brown and co-workers[1,11] found that dissolving diboranes in tetrahydrofuran (THF) affords a complex that is very easy to handle and highly active toward alkenes.

Hydroboration-oxidative hydroxylation is a reaction that proceeds with syn-stereochemistry to give an anti-Markovnikov product, as well as stereoselectivity to give cis addition.[7,9,10] Brown et al.[10] achieved the selective hydroboration of a terminal alkene in the presence of a ketone or an aldehyde using dicyclohexylborane as the hydroborating agent. Particularly high selectivity is accomplished with organoboranes that have bulky substitutes. Thus, 9-BBN was prepared from diborane and 1,5-cyclooctadiene.

One of the most useful features of 9-BBN is its extremely high regioselectivity in the hydroboration reaction.[5,11-13] The oxidation of alkylboranes with alkaline hydrogen peroxide under mild condition gives alcohols in very good yields, and the stereochemical configuration of the carbon originally bearing the boron is retained in the oxidation step. Seino et al.[14] used 9-BBN to convert a terminal vinyl group on hyperbranched polysiloxysilane (HBPS) to 2-hydroxyethyl in the presence of a platinum catalyst. Eroglu et al.[15] and Ruckenstein and Zhang[16] applied the same approach of using 9-BBN to hydroxylate the pendant vinyl groups of poly(3-hydroxyundec-10-enoate), and poly(3-hydroxypropyl methacrylate)-co-poly(glycidyl methacrylate)-graft-polystyrene, respectively.

2.1.2 Autoxidation reaction

Generally, organoboranes react readily with atmospheric oxygen; the oxygen inserts at the linear alkyl-boron bond to produce peroxyborane (C-O-O-B).[17] The peroxyborane behaves very differently from regular benzoyl peroxides and consequently decomposes even at ambient temperature, producing free radicals.[10,18] Janvikul[19] reported the presence of alkoxyl radicals and not alkyl radicals at room temperature, which means the cleavage must

be at the O-O bond of the boronperoxide. The decomposition of peroxyborane was enhanced by addition of a vinyl monomer, such as methyl methacrylate (MMA). The reaction scheme proposed by Chung et al. is shown in Scheme 2.2.[20]

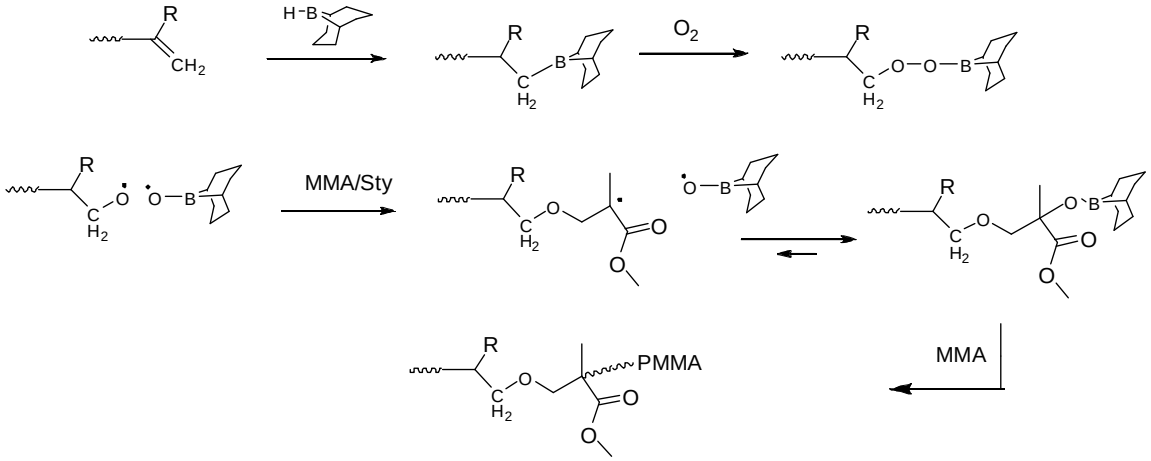

Scheme 2.2: Hydroboration of chain-end unsaturated linear polymer, oxidation, and subsequent free radical chain end extension with MMA.[20]

2.1.2.1 Free radical polymerization by 9-BBN

Oxygen plays a significant role in polymerization reactions, especially those containing trialkylboranes. Oxygen plays roles as initiators or catalysts in the polymerization reaction of vinyl monomers at room temperature.[20-26] The detailed reaction mechanism is described by Chung et al.[20] It is vital to control the amount of O_2 injected into the reaction, so the oxidation reaction occurs at the linear C-B bond attached to the polymer. The oxidized B-C bonds are readily initiated by oxygen at ambient temperature. The ratio of oxygen to the B-C bond should be 0.5:1 in total. The best results are obtained when the O_2 is introduced slowly so that less than 10% O_2 is added hourly; hence, at any time O<<B. An excess of O_2 not only spoils free radical polymerization, but also leads to over-oxidation to boronates and borates, which are poor free radical initiators at room temperature. The decomposition of peroxyborane leads to the alkoxy radical (C-O$^{\bullet}$) and a borinate radical (B-O$^{\bullet}$). The latter is considered a stable radical[22] because of the back-donating of electron density to the empty p-orbital of boron. The alkoxyl radical, on the other hand, produced by homolytic cleavage of peroxyborane, is believed to be very reactive and can therefore be used for the initiation of radical polymerization. Several studies have been carried out using this technique to synthesis polymers and block or graft copolymers. Chung et al.[22] describe the free radical polymerization that initiated by alkyl-9-BBN as a stable radical and used it to synthesize PMMA homopolymers with high molar mass (more than 1 million). Guoqiang et al.[27] used borane terminated isotactic polypropylenes, prepared using metallocene catalysts, to synthesize the block copolymer isotactic polypropylenes-b-poly(methyl methacrylate) (i-PP-b-PMMA). Other block copolymers were synthesized by selectively oxidation of borane functionalized chain ends: polypropylene-b-poly(methyl methacrylate) (PP-b-PMMA),

polypropylene-b-poly(vinyl acetate) (PP-b-PVA), polypropylene-b-polystyrene (PP-b-PS) and polypropylene-co-poly(acrylic acid) (PP-MA).[20,23,27-31] Graft copolymers of polyolefins containing a polyolefin backbone and functionalized polymers in the side chains, via graft from reaction using borane containing polymer, are reported by Chung and Jiang. [29] Butyl rubber and ethylene-propylene rubber were also grafted by selective autoxidation of 9-BBN in the presence of MMA monomer.[24,32] Dong et al.[33] prepared poly(methyl methacrylate)-graft-syndiotactic polystyrene using a metallocene catalyst and borane comonomer. Hong and Chung[34] prepared new telechelic polymers containing two OH groups at the same chain end of PMMA, and poly(trifluoroethyl acrylate) (PTFEA) using trialkyl borane (8-boraindane).

2.2 Living anionic polymerization

Living anionic polymerization was recognized by Ziegler in the early twentieth century.[35] The interest in anionic polymerization is due to the absence of a termination stage, unlike in conventional free radical polymerization. This phenomenon of living polymerization and the value of the living anionic chain end in the synthesis of more complex architectures was described by Szwarc in 1956 [36]. Since then, many scientists have carried out studies on the mechanism and the kinetics[35,37] of the polymerization.

Traditionally, anionic polymerization applies specifically to olefin monomers, but it also includes the opening of double bonds, as well as ring-opening reactions. Sensitivity of the anionic polymerization reaction towards an easily extracted proton limits the range of solvents that are suitable for anionic polymerization. Therefore, a careful choice of solvent, initiator and monomer is necessary to avoid side reactions that result in un-control in molar mass and broad molar mass distribution of the produced polymer. Halogenated solvents, esters, ketones, and alcohols are excluded due to their reactions with the chain polymer active centers. Any solvent containing an easily extracted proton must be avoided. Hydrocarbons and ethers are the solvents most commonly used. Monomers that undergo anionic polymerization are substituted with groups that stabilize the formation of carbanions. Charge delocalization provides the necessary stabilizing force for the monomers (such as styrene).

For the initiation of anionic polymerization, compounds of the most electropositive elements are required. Alkyllithium compounds are the most frequently used anionic initiators since many of them are commercially available and they are soluble in a variety of solvents, especially hydrocarbons and ether. Alkyllithiums are aggregated even in the most dilute solutions or in vapors. The degree of aggregation varies with the nature of alkyl groups and solvent.[38] The aggregation degree decreases with the bulkiness of the alkyl group and increasing polarity of the solvent.[39] The aggregation of initiators in a non-polar medium affects the efficiency of initiation of hydrocarbon monomers. In hydrocarbon solvents, the

initiation of styrene and dienes are slow and incomplete due to high degree of aggregation.[40,41] On the other hand, alkyllithiums are highly reactive and unstable in polar solvents, and hence, the initiation step has to be performed at a low temperature (-78 ^{o}C).[42,43] The reactivity of alkyl lithium is directly linked to the degree of association.[44] Hsieh[45] reported the reactivities of various alkyl lithiums for styrene and diene polymerizations to be as follows:

MeLi> sec-BuLi > i-PrLi > t-BuLi > n-BuLi

Therefore, the selection of an initiator for the polymerization of a particular monomer is very important in order to obtain control of the propagation stage and consequently control in molar mass of produced polymer. Furthermore, the reactivity of the active center or carbanion depends strongly on the size of its counterion.[46]

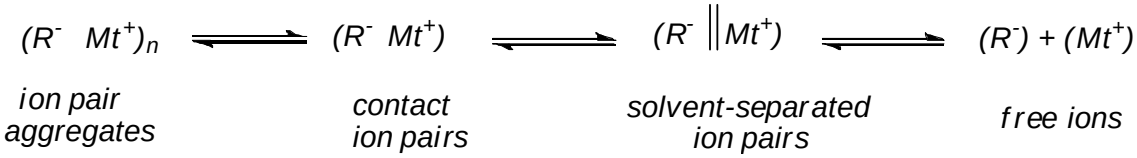

Typically, termination will not occur in the absence of impurities. The coupling and disproportionation terminations for free-radical polymerizations are not possible with anionic polymerizations due to the repulsion of two negatively charged species. Termination involves a proton transfer from another species, such as from a solvent, monomer, polymer, or water.[42] However, there are no inherent termination steps in highly pure systems. Non-terminated polymeric species are referred to as "living" polymers.

Living anionic polymerization is highly versatile for the synthesis of well defined polymers with precisely controlled molecular structure and molecular weight, as well as functionalities.[47,48] The living polymers having at chain ends carbanionic sites, which can either initiate further polymerization or react with various electrophilic compounds, are intentionally added to achieve the desired functionalizations. Another advantage of anionic polymerization is the capability of using difunctional initiators,[49] which can yield linear polymers that have carbanionic sites at both chain ends. These terminal carbanionic sites of living polymers can be reacted with various electrophilic compounds, yielding α-functional polymers, such as esters, nitriles, acid chlorides, anhydrides, epoxides,[50,51] lactones, and benzyl or allyl halogens.[52] The end-groups can also couple, or link reactive groups on, other oligomers or polymers to afford graft crosslink polymers.[53]

These terminating agents are characterized either as non-living (neutralization of active centers) or living (creation of new anionic active centers). The first linking reaction characterized as non-living was used in 1962 by Morton and Ells.[54] Since then, various polymers with branched architecture have been developed. Examples of living terminating

agents that have been used in anionic polymerization are allyl halides: 1,1-diphenylethylene and oxirane. Allyl halides are efficient termination agents for living polymerization reactions, although the reaction is not always quantitative due to side reactions involving the attack of the active center anion at the double bond of the allyl functional group.[55-57] Oxirane and 1,1-diphenylethylene terminating agents are used in living anionic polymerization as end-capping for the anionic polymerization or as adapters to decrease the nucleophilicity of the active center anions, especially when methacryloyl chloride is used as end-capping, to avoid side reactions that involve the polar ester group.[57-59]

Polymer architecture can be achieved by living anionic polymerization due to the living nature of the polymerization; the structure of the synthesized polymer such as in stereochemistry and microstructure, can be controlled.[43,50,52,59-63] PMMA chains end-capped by cyclic anhydrides was reported by Fallais et al.[63]; an ω-epoxide end-group function was prepared by reacting epichlorohydrin with polymeric organolithium.[50,51] Block copolymers can be achieved by introducing different monomers sequentially into the system.[61,64-66] Star, heteroarm star, or branched polymers can be synthesized by terminating the living chain ends with multifunctional linking agents or by using multifunctional initiators.[66-68] A heteroarm star polymer can be prepared by linking several linear chains having different chemical composition to a central core.[50,69,70] The two living polyisoprene PI chains were reacted with methyltrichlorosilane and then coupled with another living chain, polybutadiene (PBd).

The major drawback of living anionic polymerization is its intolerance to most polar functional groups, which puts some limitations when homo- or copolymerization of styrene or dienes with monomers is the content of functional groups. These limitations have been discussed in detail in terms of mechanism and kinetics.[71,72] Nevertheless, acrylates and methacrylates have been co-or/and polymerized via living anionic polymerization.[73-76] Varshney et al.[77] reported using lithium salts as ligands and study the effect on the living anionic polymerization of methyl methacrylate. In addition, Zundel et al.[78] described the synthesis of isotactic methyl methacrylate using anionic polymerization and sec-butyllitium ligated by lithium silanolates, while Peron et al.[79] illustrate a way to prepare syndio-rich PMMA using organoaluminium amide complexes as additives in anionic polymerization. Monomers containing functional groups such as N,N-dialkyl-4-vinylbenzamides and other para-substuted styrene monomers were polymerized using anionic polymerization.[61,62]

2.3 Controlled radical polymerization.

Free radical polymerization is the best known method of polymerization of vinylic monomers. Traditional free radical polymerization suffers from weakness due to its natural mechanism. Radical polymerization is a chain reaction initiated by radicals that then add to monomer, and chains continually grow by the addition of monomer units to the radical chain.

Termination occurs when two propagated chains combine or extract hydrogen from another chain, leaving behind an unsaturated polymer chain.

In the steady state, the initiation step and termination step having similar rates, the concentration of propagating species is low. All chains are essentially dead at any certain time. In addition transfer step at high temperature has higher activation energy than the propagation step leading to dead chains. The molar mass of the chains formed in the early stages of the polymerization is high, but decreases over time due to monomer consumption. In order to overcome the previous limitations, the initiation step must be fast, the chain growth must be instantaneous, and the termination rate must be much slower than propagation. That increases the lifetime of growing chains from ~1 s to about 1 h. To achieve the goals of increasing the lifetime, a new approach in free radical polymerization has been used: living controlled free radical polymerization (CRP) techniques.

Living polymerization processes offer many benefits, for example,

- the ability to control molecular weight and polydispersity,
- to prepare block copolymers as well as functionalized polymers[80] and
- to prepare polymers of complex architecture materials that are not readily synthesized using other methodologies

Achieving an increase of the lifetime of the grown chain eliminates the termination step by trapping the radicals in a reversible process or keeping them in a dormant stay by introducing an activation/deactivation step and establishing equilibrium between propagation and dormant species.

The first of the CRP techniques to emerge was stable free radical polymerization (SFRP), nitroxide mediated polymerization (NMP) systems, reported by workers at Australian Commonwealth Scientific and Research Organization (CSIRO) in Australia,[81] and atom transfer radical polymerization (ATRP), independently developed by Kato et al.[82] and Wang and Matyjaszewski.[83] Both techniques of ATRP and NMP are based on the principle of a reversible activation/deactivation. In conventional systems, steady state is achieved by balancing the rates of initiation and termination. Since the rate of termination must be >1000 times slower than that of propagation in order to grow a sufficiently long chain, initiation must also be very slow.[84] In the new systems, steady state is reached by balancing the rates of activation and deactivation, and the processes are entirely decoupled from the initiation and termination of individual chains.[84,85] Thus, termination is still very slow and initiation much faster. Repeating an activation/deactivation cycle, every living chain slowly grows in an irregular fashion. An advanced strategy has been made to increase the radical polymerization rate of acrylate monomers by using a Lewis acid as a complexation agent.[86] The Lewis acid coordinates to the ester carbonyl group of the acrylate monomer and reduces the electron density in conjugated C=C bond. An increase in the reactivity of the radical

generated and an effect on the stereospecific chain growth has been reviewed by Kamigaito and Satoh.[55] Fukuda et al.[87-89] have reported on the kinetics of living radical polymerization. A typical example of an activation/deactivation agent in NMP is 2,2,6,6-tetramethyl-1-piperidinyloxy (TEMPO). This agent reversibly terminates macroradicals, generating a dormant chain.

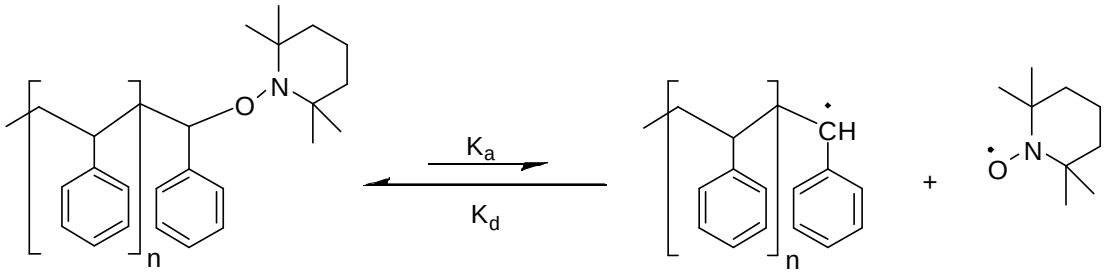

Alkoxyamine (dormant polymer radical) | Polystyrene radical | TEMPO

Scheme 2.3: Nitroxide-mediated polymerization (NMR) using TEMPO (nitroxide) as capping agent.

The equilibrium is shifted toward the dormant species, and as a result the propagating radical concentration is lower than in conventional radical polymerization. The equilibrium between active and dormant chains is sensitive to temperature; high temperatures are necessary to achieve reasonable reaction rates. Several different nitroxides have been investigated for use in bulk or solution polymerization of styrene or a styrene derivative, since these monomers can be polymerized at relatively high temperatures (>100 ^{o}C).

In the case of ATRP, a transition metal (Mt) and complexing ligand (L) are used to generate and deactivate radicals in free radicals polymerizations.

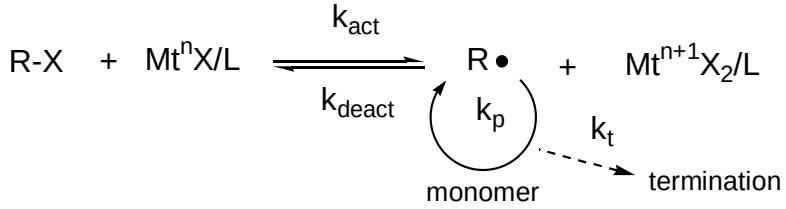

Scheme 2.4: Schematic representation of the ATRP process. Mt represents a transition metal, L represents the ligands complexed to the transition metal, and RX is an alkyl (pseudo)halide.

The key factor in ATRP is using a lower oxidation state metal that abstracts a halogen from an activated alkyl halide, which can then be added across the double bond of an alkene. Therefore, the newly formed radical re-abstracts the halogen from the higher oxidation state metal to form an alkene-alkyl halide species and regenerate the lower oxidation state metal. To achieve control and a living system, trapping of the product radical via transition metal complexes should be faster than the subsequent propagation step, and reactivation of the macroradical should be very slow. ATRP has been used extensively with various metal catalysts (iron, nickel, palladium, ruthenium, molybdenum, chromium, rhenium,

rhodium, and copper). Beside various complexing ligands, amino based (bipyridine, 4,4`-di-(nonyl)-2,2`bipyridine) and phosphorus based, as well as monomers and solvents have been used.[90] The chemistry of metal catalyzed living radical polymerization has been reviewed by Kamigaito et al.[91] and Matyjaszewski and Xia.[85]

Xue et al.[92] reported a living and controlled polymerization reaction of MMA using iron(III) and phosphine-based ligand at different reactions conditions, even in the presence of relatively high concentrations of methanol as a solvent. Subramanian and Dhamodharan[93] described the ATRP of tert-butyl acrylate at ambient temperatures.

Reversible addition-fragmentation chain transfer (RAFT) radical polymerization[94] was also discovered by researchers at CSIRO and reported in the late 1990s.[94,95] At the same time, researchers in France described a technique they called "macromolecular design by interchange of xanthate" (MADIX), based on the principle of addition fragmentation chain transfer. The key factor in this process is a suitable choice of the RAFT agent.

The RAFT agents belong to families of compounds: dithioesters,[95] xanthates,[96] dithiocarbamates,[97] and trithiocarbonates,[98] see Scheme 2.5.

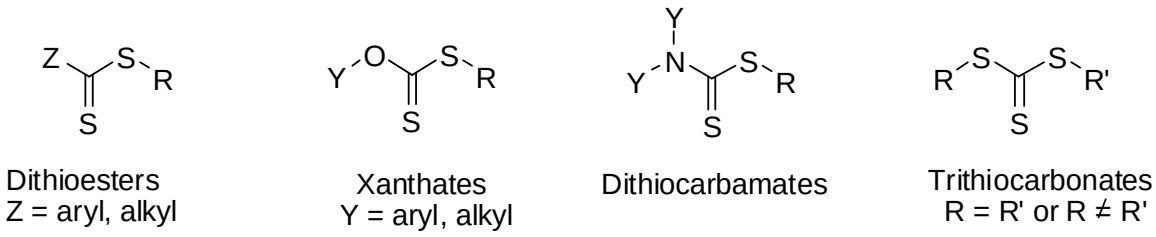

Scheme 2.5: General structures of common RAFT agents.

There are also more specialized species of thiocarbonylthio compounds that have been used in RAFT polymerization, including phosphoryl dithioesters,[99,100] dithiocarbazates,[101] fluorodithioformate,[102] and vinylogous thionothio compounds.[103] The mechanism of these applications will be discussed in Section 2.3.1.

Lately, many techniques have been added to the CRP that include tellurium mediated radical polymerization (TERP),[104,105] which was shown to be more flexible and revealed a higher degree of control, particularly regarding the molecular mass. Organostibene mediated radical polymerization (SBRP) has the ability to polymerize both conjugated and unconjugated monomers. These two techniques were reported by Yamago et al.[106,107] The most recent technique, quinone transfer radical polymerization (QTRP) reported by Caille et al.,[108] has only been confirmed to be efficient for thermally initiated styrene polymerization.

2.3.1 Reversible addition-fragmentation chain transfer polymerization

RAFT is based on one of the oldest polymerization techniques, chain transfer polymerization. The discovery of dithioesters compounds as efficient transfer agents was the major breakthrough in the development of the RAFT process. The simplicity of RAFT arises

from the similarity in experimental conditions used with those of conventional free radical polymerization. It can be carried out in bulk, solution, emulsion or suspension.[109,110] Common initiators such as azo or peroxy can be used. There are no particular limitations on solvent or reaction temperature. It is possible to prepare polymers with wide range of molar mass. Also, RAFT is compatible with a very wide range of monomers, including functional monomers containing acid, acid salt, hydroxyl, or the tertiary amino group.[111-113] To control the free radical polymerization, the system must be initiated while simultaneously avoiding termination reactions before complete conversion. This must be done using a specific additive that blocks the active center while allowing a re-initiation or one that reversibly transforms the growing chain into a dormant species. The active end groups must be preserved to be able to use the end functionalized polymer chains as macro-initiators or as macro-chain transfer agents.

Thiocarbonylthio compounds (S=C(Z)S-R) are used as additives to trap the active center in order to maintain the living nature of a free radical polymerization. The structure is shown below,

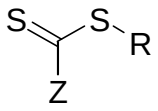

where Z is a group that has influence on the reactivity of the thiocarbonyl group toward free radical addition, and R is a free radical leaving group.[114-116] These two groups have an influence on the effectiveness and transfer coefficients of the RAFT agent, which subsequently affects the produced polymer. Thang and co-worker[114,115] reported on the dependence of RAFT agents on the nature of the Z and R groups. The success of the RAFT process is a result of a high rate of constant chain transfer compared to the rate constant of propagation. The mechanism of RAFT-mediated polymerization is shown in Scheme 2.6.

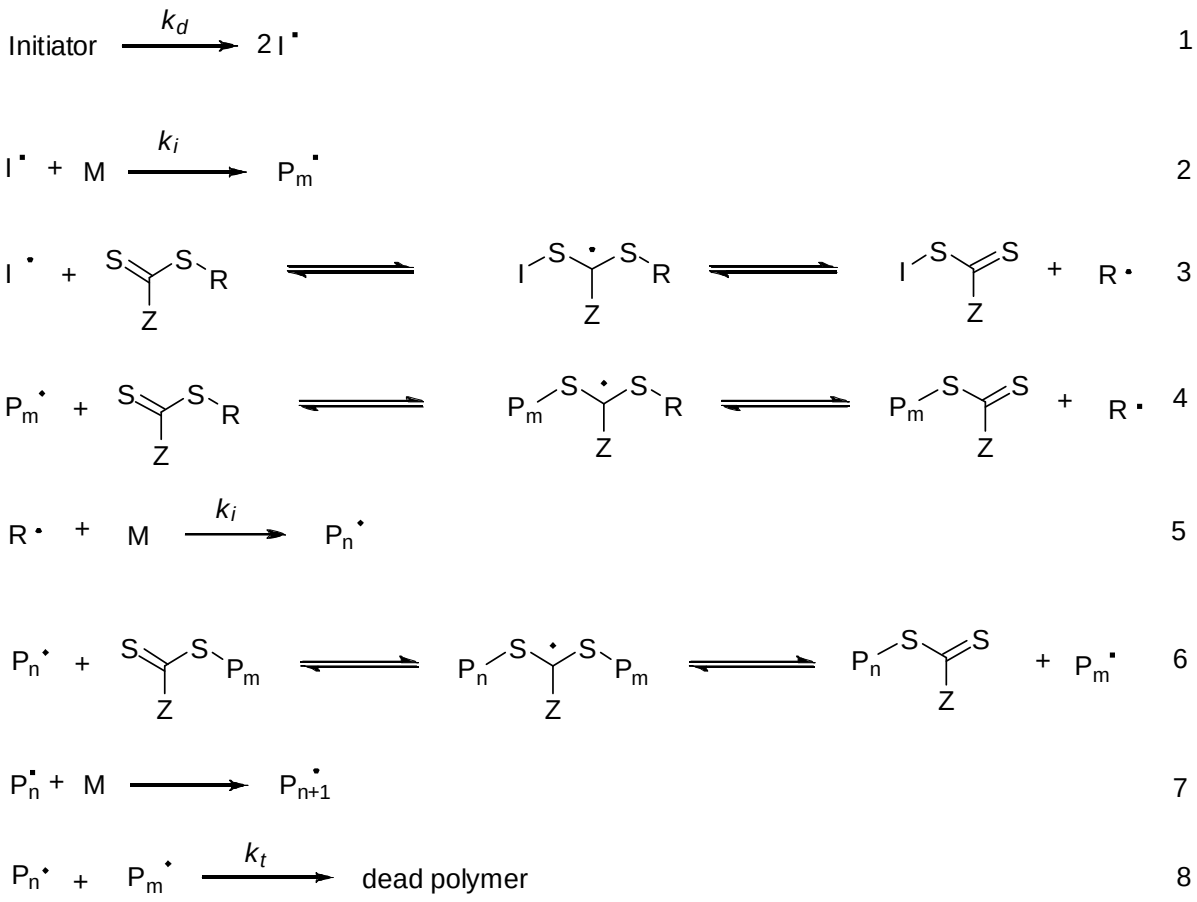

Scheme 2.6: Mechanism of RAFT process based on mechanism proposed by Rizzardo and co-works[117].

In the RAFT mechanism, radicals are formed via a free radical initiator or other source (1). The radicals formed from the initiator either add to the monomer (2) or add directly to the transfer agent (3). Adduct from monomer addition may also add to the transfer agent (4). These steps (3,4) release a leaving group radical. The driving force for fragmentation of the intermediate radical is provided by cleavage of a weak S-R bond and/or formation of a strong C=S bond in the intermediate. This fragmented radical must be able to initiate polymerization of another monomer (5). The rate of addition of radicals to the C=S double bond is strongly influenced by the substituent Z. This rate is higher when Z = aryl, alkyl, and lower when Z = O-alkyl or N,N`-dialkyl. Retardation has been observed when high concentrations of the RAFT agent are used or an inappropriate choice of RAFT agent is made, and in some cases with the use of high k_p monomers, such as vinyl acetate (VAc) and MA, and specific RAFT agents that contain a radical stabilizing Z group, such as a phenyl group. The retardation has been connected to either slow fragmentation of the intermediate radical or termination of the intermediate radical.[118,119]

To overcome retardation, a balance must be achieved between the leaving group ability of R and reinitiation efficiency of R•. The rate constant for reinitiation by R• should be ≥

$k_{p,}$ as in conventional chain transfer. The number of chains in a typical RAFT polymerization should be equivalent to the number of chains produced from the free radical initiator in addition to the number of leaving group radicals provided by the initial transfer agent. Furthermore, the maximum number of terminated chains will not exceed the concentration of the radical initiator. If the fragmentation rate between the incoming radical and the leaving group radical in the initial transfer agent is fast compared with propagation, all radical leaving groups will become initial end groups of the polymer chains. If this fragmentation is slow relative to propagation, not all of the radical leaving groups may form chains. Subsequent transfer and propagation steps 6 and 7 are basically identical, where an active polymer end group adds to the transfer agent at the end of another polymer chain, in that way converting the first chain into a dormant species and the second chain into an active species. Once the RAFT agent has been consumed, chain equilibrium is established between the active and dormant species. Chain termination occurs to a varying extent in the polymerizations depending on the degree of polymerization control (8).

RAFT polymerization has been successfully carried out under different reaction conditions (temperature, pressure, atmosphere, solvent, Lewis acids) and in homogeneous or heterogeneous systems.

One major advantage of RAFT over other living polymerization techniques is its compatibility with protic solvent and other functionalities present in the monomer or the RAFT agent.[120] The RAFT technique can be used to synthesize end functional polymers by incorporating the functionality into the Z or R groups of the RAFT agent.[121-123]

2.4 Multiphase copolymers

Multiphase copolymers, for the purpose of this study, are defined as macromolecules that contain more than one type of monomer unit within the polymer chain.

In these polymers, each polymer molecule consists of two or more segments of simple polymers (random or blocks) joined in certain arrangements. These multiphase copolymers are classified by arrangements of the monomers in the polymer and the arrangements of the blocks. The arrangement of the monomers leads to random or gradient copolymers. Block copolymers with two, three, or more blocks are called diblock, triblock, and multiblock copolymers, respectively. Some arrangements are linear, while others are in star arrangement, in which all of the blocks are connected via one of their ends at a single junction. Scheme 2.7 shows an example of different types of multiphase polymers.

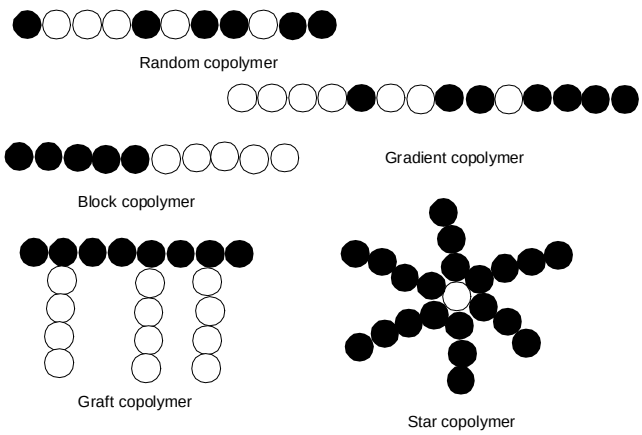

Scheme 2.7: Different type of multiphase polymer structures.

2.4.1 Random and gradient copolymers

Polymers prepared by copolymerizing two or more monomers often have unique properties that cannot be obtained by using mechanical mixtures of homogeneous polymers. In the copolymerization of two different monomers, the monomers are incorporated into the polymer chain at rates determined by their reactivities and concentrations. This leads to a polymer structure in which the monomers are arranged in a random or gradient fashion.[124-127]

Free radical polymerization is the most commonly used technique for the synthesis of random and gradient copolymers. One reason is because it does not suffer from imitated monomer choice as anionic polymerization does, although in some strict conditions of monomer selection and reaction conditions, anionic polymerization and other techniques can be used to prepare copolymers. The Ziegler-Natta polymerization technique was used to prepare random propene/1-decene copolymers, as Tian et al.[128] illustrated. Anionic polymerization was also used to prepare random copolymers and blocks, as Kobayashi et al.[129] reported. Using conventional free radical polymerization random copolymer is achievable.[130-132] Living controlled free radical polymerization was involved intensively in synthesis copolymers random gradient and other structure, Nguyen et al.[133] used RAFT polymerization approach to synthesize random and block copolymers of tert-butyldimethylsilyl methacrylate and MMA. Zhu et al.[134] copolymerized N-vinylcarbazole and vinyl acetate via the RAFT process. RAFT polymerization was also involved in the synthesis of alternative copolymers of PS with maleic anhydride.[135] Matyjaszewski et al.[136,137] used ATRP to prepare gradient copolymers of PS with MA using CuCl/bpy catalyst, and with MMA using CuBr/bpy catalyst. Brar and Puneeta[138] synthesized a PS/PMMA copolymer using ATRP and characterized it with 2D NMR. MMA with n-butyl acrylate (nBA) was also studied using ATRP,[139,140] Yoshida[141] used 4-methoxy-TEMPO to copolymerize PS with a styrene derivative. Fukuda et al.[142] used the TEMPO system to copolymerize PS with polyacrylonitrile (PAN).

2.4.2 Block copolymer

Block copolymers are macromolecules that contain two or more different types of polymer chains, covalently bound together as a block. A block copolymer has advantages over random copolymers and homopolymers in that the blocks retain the physical properties of the original homopolymer although they are joined to each other. Making use of this characteristic, many interesting properties can be achieved. The difference between the block segments brings issues of incompatibility, which is the power drive to a self-assembly structure. In solution, block copolymers act in a fashion similar to small molecule surfactants. If the block is synthesized so that the blocks have different solubilities, the blocks act in a similar way to the hydrophilic and hydrophobic parts of the surfactant.

There are several literature reports on the preparation of block copolymers.[65,143-148] Generally, there are two methods used for the synthesis of block copolymers: a sequence addition of the monomers or the coupling of two functionalized chains with suitable ends.

Living polymerization requires synthesis of well defined block copolymers. Anionic polymerization with a living nature has emerged as the most reliable technique to prepare block copolymers. Hadjichristidis et al.[66,149] reviewed the synthesis of block copolymers and other architectures. Zeng et al.[150] synthesized block copolymers of 2-vinylnaphthalene (2VN) with MMA and tert-butyl acrylate (tBA) using anionic polymerization. Matsumoto et al.[65] prepared block copolymers of 1,1-diethylsilacyclobutane with styrene derivatives and MA derivatives via anionic polymerization. Chong et al.[114] described the role of the free radical leaving group R and synthesis of block copolymers. Garnier and Laschemsky[151] synthesized amphiphilic diblock copolymers using the RAFT technique. Tong and Jerome[152] reported the synthesis of triblock copolymers by transalcoholysis. McMormick and co-workers[153] reported the preparation of AB diblock copolymers in aqueous medium via the RAFT process. Braunecker and Matyjaszewski[90] have presented a comprehensive review on the use of controlled living radical polymerization to synthesize blocks and other structures. Bernaerts and Du Prez[154] successfully synthesized a block copolymer using a dual initiator with the ATRP technique. Kizhakkedathu et al.[155] synthesized a hydrophilic block copolymer by aqueous ATRP.

2.4.3 Graft copolymer

A graft copolymer is comprised of molecules with more than one backbone chain; graft copolymers are nonlinear polymers. A grafted copolymer is characterized by the presence of branch points and by the presence of more than two chain end groups. Grafting of polymers is a common technique by which to modify the chemical and physical properties of polymers.[156] Graft copolymers consist of two different types of polymer, which are usually incompatible or immiscible. The incompatibility between the main chain and the branch

makes graft polymers similar to polymer blends, but in the case of graft polymers, the immiscible phases are joined by covalent bonds. These microphase separations can exhibit remarkable thermal and mechanical properties and applications. Graft polymers can be used as surfactants, compatibilization agents in polymer blends, additives in high-impact materials, adhesives, thermoplastic elastomers,[156] and pigment dispersants.[157] They exhibit enhanced tensile strength, improved metal adhesion, controlled wettability, and surface modification.[158] According to International Union of Pure and Applied Chemistry (IUPAC) nomenclature,[159] the name of the backbone polymer should be given first and the name of the grafts second. For example, in PBd-g-PS, polybutadiene (PBd) is the backbone while PS is the graft.

Free radical polymerization is the oldest method used for the synthesis of graft polymers. It involves radical chain transfer and addition reactions of the polymerizing monomer to the polymer backbone. This process is used to synthesize high-impact polystyrene (HIPS), acrylonitrile-butadiene-styrene (ABS), and other commercial, multiphase polymeric materials. Free radical polymerization, however, usually gives heterogeneous materials that are difficult to characterize.[159]

Ionic polymerization is a "living system" that allows better control over the synthesis of polymers, leading to products with predictable molecular weights and nearly monodisperse distributions of molecular weight.[57,156,160,161] Using this technique, greater control of polymer branch length can be obtained. Three synthetic techniques have been used to obtain graft or comb-polymers: grafting onto, grafting from, and grafting through.

In the “grafting onto” method, the backbone and branches are prepared separately. The backbone has functional groups distributed along the chain, and these functional groups can undergo reaction with the preformed polymer. A reaction takes place after mixing two polymers under suitable experimental conditions. The number of functional groups along the main chain determines the number of branches on the backbone. The molecular weight and polydispersity of the produced polymer can be controlled by using an anionic polymerization mechanism or other controlled polymerization techniques.[47,162] The branching sites can be introduced into the backbone either by post-polymerization reactions or by copolymerization of the main backbone monomer(s) with a suitable co-monomer containing the desired functional group.

In the “grafting from” method, a polymeric substrate is first functionalized to bear a number of accessible reactive groups, then these groups are activated to provide initiating sites, followed by the addition and subsequent polymerization of a monomer, resulting in the formation of branches and the final graft copolymer. The number of branches can be theoretically controlled by the number of active sites generated along the backbone.[47,70]

The “grafting through” approach to the preparation of graft polymers consists of two steps.[47] First, a linear polymer bearing a terminal polymerized end group is prepared; this

species is referred to as a macromonomer. Second, copolymerization of the macromonomer with a suitable comonomer is carried out, generally by radical polymerization. Living polymerization techniques are ideally suited to the preparation of well defined macromonomers, since they allow precise control over the molecular weight and chain-end functionality. Matyjaszewski and co-workers[163] reported the synthesis of graft terpolymers with controlled molecular structure by grafting through technique and ATRP. Lee et al.[164] described the synthesis of graft copolymer PMMA-g-PDMS using macromonomer technique. Hadjichristidis and co-workers[145] reviewed the synthesis and properties of block copolymers having nonlinear architectures, which include star-block copolymers, graft, miktoarm star, and dendritic polymers. By using the macromonomer technique and controlled living polymerization ATRP, Pakula and co-workers[165] synthesized gradient graft copolymers. Chojnowski et al.[166] used living anionic ring-opening polymerization to obtain branched polysiloxanes, while Hadjichristidis and co-workers[66] carried out an anionic polymerization and macromonomer strategy to prepare block-comb/graft copolymers

2.5 Combining various synthesis techniques

It is well known that not all monomers can be polymerized by every available polymerization technique, which limits the possibility of combining various monomers in a block copolymer chain using only one polymerization method. Living and controlled techniques are useful not only in controlling molar mass and the distribution of the molar mass of polymer, but also in synthesizing block and other structures, as well as end functionalized polymers.

These polymerization techniques give several routes for the synthesis of block and other copolymers with well-defined structures: (a) sequential monomer addition, (b) coupling of living chains, and (c) transformation of a growing chain end to a group capable of initiating polymerization of a second monomer.

The latter method is especially well suited for block copolymers prepared from monomers polymerized by two different techniques. The synthesis of block copolymers usually requires efficient controlled and living polymerization. Several papers have reported the synthesis of well defined blocks by combining various techniques using transformation reactions. For example, anionic to cationic,[167,168] anionic polymerization to conventional radical polymerization,[169-172] anionic to stable free radical polymerization (SFRP),[40,147,173-175] and to ATRP,[176] cationic ring opening polymerization to RAFT [177], cationic to anionic,[178] ring opening metahesis polymerization (ROMP) to anionic[179] ROMP to ATRP[180] or anionic,[181] and metallocene catalyzed polymerization or degenerative transfer to anionic, RAFT[182-184] and ATRP.[185] Lopez et al. reviewed a combination of techniques between catalytic olefin polymerization and living controlled polymerization.[186] Examples of these include RAFT to

click chemistry[183], RAFT to the ATRP technique,[187] and ATRP to click chemistry,[188,189] also the combination of chain-growth condensation polymerization and atom transfer radical polymerization,[190] metallocene catalysts, and borane chemistry.[28]

2.5.1 Combination of living anionic polymerization and autoxidation of 9-BBN

In general, block copolymers are synthesized by anionic or coordination polymerization because of the living nature of the polymer chain end. Transformation of a growing chain end to a group capable of initiating another polymerization of a second monomer is critical. Finding a suitable combination of anionic and controlled radical polymerization can bring materials that incorporate some monomers that cannot be polymerized by one of these techniques. In block synthesis, usually the first monomer is polymerized by an anionic technique followed by the conversion of the chain end into functional groups capable of initiating sites for the polymerization of the second monomer via a controlled radical technique. In several articles, Chung et al.[20,23,28,31,32,191-193] introduce a novel method of synthesis of polyolefin block or graft copolymers.

The polyolefins contain boron as an end functional group or side functional group and then this functional site is used to initiate free radical polymerization to produce block or graft copolymers of a polyolefin with other vinyl monomers, such as maleic anhydride, MMA and styrene.

2.5.2 Combination of controlled radical polymerization and autoxidation of 9-BBN.

Several articles have appeared in recent years describing the combination of control/living free radical polymerization with different techniques to create new copolymers. However, there are no reports in the open literature on combining living controlled free radicals with autoxidation of 9-BBN.

2.6 Free volume and glass transition temperature

2.6.1 Glass transition temperature

Due to the massive size of polymer chains, many polymers are unable to form an ordered structure in the solid state and remain glasses or rubbers. The transition from glass to rubber occurs at a temperature called the glass transition temperature (T_g), which is determined not only by the chemical structure, but also by the free volume available for the chains to undergo rotational motion. The T_g is a very important characteristic of amorphous polymers; it is a non-equilibrium property and sensitive to the heating rate and the method used in the measurements. For a particular polymer, T_g may be a function of molar mass,

thermo-mechanical history, tacticity, chemical composition, etc. Accurate measurement of T_g is hence a useful way of characterizing a particular polymer.[194]

The glass transition temperature of a random copolymer containing two monomer species can be expected to be between the glass transitions temperatures of the corresponding homopolymers. The Fox equation would be suitable to predict the T_g of a copolymer.

$$T_{g,c} = \frac{a_1 w_1 T_{g,1} + a_2 w_2 T_{g,2}}{a_1 w_1 + a_2 w_2} \qquad \textbf{Equation 2.1}$$

if the weight fractions of the two components are w_1 and w_2, and a_1 and a_2 depend on the monomer type and would both equal units if the simple rule of mixtures applied.

In some cases of block or gradient and graft copolymers the components could phase separate, then two glass transition temperatures of each phase could be identified.

The glass transition temperature of a particular polymer depends on various parameters, such as molecular weight, blending, crosslink density, tacticity, degree of crystallininty, pressure, mechanical deformation,[195] polymer chain structure, the interaction between the chains, and also the free volume. A number of techniques besides differential scanning calorimetry (DSC) and dynamic mechanical analysis (DMA), have been introduced in recent years to study the glass transitions: neutron scattering,[196] NMR,[197] dynamic light scattering, [198] and computational experiments, including Monte Carlo and molecular dynamic simulation.[199]

2.6.2 Free volume

The concept of free volume, regardless of its qualitative nature, is very useful in explaining many properties and phenomena associated with polymers, such as mobility, viscosity, melt behavior, transport of gases, etc. The free volume theory of materials is based on the idea that molecular motion in the bulk state depends on the presence of holes. In the case of small molecules, when a molecule moves into a hole, the hole exchanges places with the molecule. However, in the case of macromolecules, more than one hole is required before macromolecule segments can move. These holes exist inside a polymer matrix due to the irregular packing of the chains in the amorphous state and the terminal chain ends.[200-202]

The phenomenon of free volume can be observed in a polymer if it is kept at temperatures more or less below its (T_g). It undergoes a slow relaxation process by which the volume gradually decreases, while at the same time the material becomes stiffer and more brittle. This phenomenon can be understood as resulting from a decrease in the free volume. Doolittle proposed an equation to describe the non-Arrhenius dependence of viscosity of liquids on temperature.[201,202] Here the free volume is defined as the difference between the total specific volume and an occupied volume.

$$\ln \eta = \ln A + B\frac{(\upsilon - \upsilon_f)}{\upsilon f} \qquad \textbf{Equation 2.2}$$

where η is the viscosity, ν is the specific volume and ν_f is the free volume.

The linear increase in the free volume with temperature was described by Williams, Landel and Ferry in their equation,[203] the so-called WLF equation:

$$\log a(T) = \log\left[\frac{M(T)}{M(T_g)}\right] \qquad \textbf{Equation 2.3}$$

where T is the time-temperature shift factor, *M* is empirical constants and T_g is the glass transition temperature and the reference temperature to which the master curves are generated by shifting the dynamic mechanical test data at other temperatures. The free volume interpretation of the WLF equation relies on two theories: linearity of the free volume fraction:

$$f(T) = f_g + \alpha_f (T - T_g) \qquad \textbf{Equation 2.4}$$

and

$$B_{f,M} = 1 \qquad \textbf{Equation 2.5}$$

where M is a general parameter; (η viscosity, relaxation time τ, or diffusion coefficient 1/D). T_g is the glass transition temperature or reference temperature, (T) is another temperature, α_f is the free volume fraction expansion coefficient, f (T) is the free volume fraction, f_g is the fraction at T_g, and $B_{f,M}$ represents the coefficients of free volume f and M. [204]

The quantitative measurement of the free volume size and free volume number has become a subject of great interest and importance. A number of techniques have been used to measure free volume. Small angle X-ray scattering and neutron diffraction have been used to determine density fluctuations to deduce free volume size distributions.[44,47] Other techniques used to probe voids and defects in materials, such as scanning tunneling microscopy (STM) and atomic force microscopy (AFM), are both sensitive to angstrom-size holes, but are limited to static holes on the surface, limiting their use in polymers. Scanning electron microscopy (SEM) and transmission electron microscopy (TEM) are more sensitive to static holes at sizes of 10 Å or larger.

Positron annihilation lifetime spectroscopy (PALS) has been established as a powerful tool for characterizing the free volume properties in polymers. Reasons for this include:

- the small size of the positronium probe (1.06 Å) compared to other probes, which offers sensitivity to small holes and free volume of the order of angstrom magnitude

- relatively short lifetime of the o-Ps (typically about 2-4 ns in polymers)
- PALS can probe holes due to molecular motion from 10^{-10}s or longer
- PALS is capable of determining the local hole size and free volume in a polymer without being significantly interfered with by the bulk
- PALS has been developed to be a quantitative probe of free volume in polymers
- PALS gives detailed information on the distribution of free volume hole sizes in the range from 1-10 Å

2.6.2.1 Application of positron annihilation techniques to study polymers

The process of direct transformation of mass into energy is called annihilation, which takes place according to Einstein's equation when matter and anti-matter collide. Anti-matter, by definition, is the matter that has an opposite charge or direction of spin of that of the other matter, while all other physical properties are identical.

The first anti-matter discovered was called a positron or anti-electron; it was revealed in 1933 by Anderson.[200,201] A positron in an electronic medium can pick up an electron and form a neutral atom called a positronium (Ps), which can be formed in most molecular systems. [200-202,205-209] Due to the different combinations of positrons and electrons, there are two states of Ps: the para-Ps from the anti-parallel spin, and the ortho-Ps from the parallel spin combination. Apparently, the electron density inside pores is low compared with the material itself, which makes the lifetime of positrons and positronia a function of the electron density at the site of the particle. A PS atom has a relatively small size (1.06 Å) and can be trapped in a hollow space with dimensions from several angstroms to many tens of nanometers. Eventually, these trapped positronium atoms will bounce from infinite spherical walls of the pore with thermal velocity. During the periods of each bounce, the positron in positronium may be annihilated by pickoff electrons from wall atoms, resulting in two- and three-gamma photons. The lifetimes of p-Ps and o-Ps are very different: the p-Ps has a shorter lifetime than o-Ps, 0.125 ns and 142 ns respectively. As a result of pickoff electrons, the lifetime of o-Ps will be reduced from 142 ns to a few nanoseconds.[201,202]

The bouncing rate decreases with increasing the pore size. Eventually, the pore is so large that the annihilation rate becomes analogous with the self-annihilation rate, and size-dependent changes in the combined annihilation rate are no longer measurable.

The principle of operation of most lifetime spectrometers is to measure the spectrum when positrons are emitted from an isotope source such as ^{22}Na and injected into materials. They lose energy through ionization and excitation. After thermalization, positrons will diffuse in the medium and finally will be annihilated by electrons. A PALS analysis typically gives three lifetime components in polymers: τ_1, attributed to para-positronium self-annihilation; τ_2, attributed to free positron and positron-molecular species annihilation; and τ_3, attributed to

ortho-positronium pick off annihilation. The o-Ps lifetime is related to the free volume size, while the o-Ps intensity contains information about many properties of polymers. [200,202]

The following equation shows the relationships between o-Ps lifetime τ_3 and free-volume radius (R):

$$\tau_3^{-1} = 2\left[1 - \frac{R}{R_o} + \frac{1}{2\pi \sin\left(2\pi \frac{R}{R_o}\right)}\right]\left(ns^{-1}\right) \qquad \textbf{Equation 2.6}$$

where $R_o = R + \Delta R$; ΔR is an empirical parameter, R_o is the infinite spherical potential radius and R is the hole radius.

In addition to determining the hole size of polymers, it is also useful to determine changes in fractional free volume (fv), which is related to the mechanical properties of a polymer. The fv is a result of the average hole size and the hole concentration and can be determined using the following equation[200]:

$$f_v = CI_3\left\langle V_f\left(\tau_3\right)\right\rangle \qquad \textbf{Equation 2.7}$$

where fv is free volume fractions, I_3 is the total fraction of o-Ps formed in the polymer, $\langle v_f\,(\tau_3)\rangle$ (in $Å^3$) is the mean hole volume, and C is an empirical scaling constant.

PALS has been used to examine other properties correlated to free volume in polymers and polymer blends, such as T_g, gas permeation, mechanical properties, and chemical sensitivity. Amorphous polymers exhibit widely different physical and mechanical behaviors, depending on the temperature and structure of the polymer. The T_g for instance, is accompanied by a change in free volume.

A number of studies have been carried out to study this phenomenon using PALS.[209] The diffusion of gases through polymers is determined by the mobility of gas molecules through the polymer matrix. McCulagh et al. [210] showed that there is a correlation between the free volume measured by PALS and the diffusivity of carbon dioxide and oxygen. In a series of polyester copolymers and polycarbonates, they found that the lifetime data (τ_3) are in direct proportion to the gas permeability. PALS was also used to study the miscibility in polymer blends.[200,210]

Chen et al.[211] studied blend systems consisting of PE, PMMA, PC, and PA and found a decrease in o-Ps intensity with time in PE, PMMA, and PC during positron annihilation. They suggested this was due to the formation of free radicals by the positron irradiation.

The influence of structural properties and molar mass of the polymer on the PALS measurement of free volume is obvious. Yu et al.[212] studied the effect of the molar mass of PS samples on the free volume and found that the free volumes below the T_g were not

significantly different in high- and low- molar mass samples, while above the T_g the lower molar mass samples had significantly higher fractional free volume than the high molar mass samples. Another factor that has an effect on free volume, as measured by PALS, besides chain end, is stereoregularity in the chains. Hamielec et al.[213] found an increased lifetime with increased randomness of the chain configuration in a series of polyvinylchloride (PVC) samples. Side chains also have an effect on the lifetime of positrons, which is related to free volume.

Dlubek et al.[214] studied a series of α-polyolefins, from polypropylene to poly-1-eicosene, and found that average hole sizes and o-Ps intensity decreased from polyethylene to polypropylene, followed by a slight increase to poly-1-butene, then a rise in hole size and intensity to poly-1-dodecene, followed by a gradual decrease until poly-1-eicosene. Another application of PALS is to study the structural relaxation of amorphous polymers far below and above their T_g values,[215,216] and investigate the phase separation phenomenon in the multiphase copolymers.[217-219]

2.7 Solid state nuclear magnetic resonance

Solid state NMR (SSNMR) has proven to be a useful tool for studying molecular motions in solid materials. The relaxation measurement of the polymers can detect the microphase structure on the nanometer scale through the process known as spin diffusion. Two useful relaxation times were used, proton spin-lattice relaxation time in the laboratory frame, T_1 (sensitive to motions in the megahertz frequency range) and spin-lattice relaxation in the rotating frame, $T_{1\rho}$ (sensitive to motions in the kilohertz region). These two relaxation times are partially averaged by spin diffusion through the matrix of ^1H nuclei. The individual relaxation times for the component polymers tend to be averaged to a single value. The extent to which the average of relaxation times occurs depends on the degree of mixing and the relaxation times of the individual components.

2.8 Chromatographic analysis

The difficulty in separating copolymers arises mainly from their heterogeneities in composition and molar mass. Most of the reactions used to prepare block and graft copolymers afford products that still contain unreacted and partially reacted starting polymers, or homopolymers.

Liquid chromatography (LC) is currently the most important tool for polymer characterization. It includes a group of techniques, the use of which is based on various mechanisms.

Usually, one single separation technique is not adequate for characterization of complex polymers. Therefore, two or more separation techniques combined in one LC system are required to obtain the required characteristics of complex polymers.

Size exclusion chromatography (SEC), often referred to as gel permeation chromatography (GPC), is one of basic technique used to characterize polymers and copolymers. The separation of polymer molecules is based on the hydrodynamic volume of molecules or their size. While the polymer molecules travel through a column full of pore particles, small molecules might enter these pores, and therefore spend time travelling through the column. On the other hand, larger macromolecules cannot enter the pores, and as a result it takes them a shorter time to travel through the column. A distribution of long and short chains is the result. The molar mass and polydispersity of a polymer sample can be determined either by using a suitable calibration standard (e.g., linear narrow polydispersity polymer) or by using molar mass sensitive detectors (light scattering, viscosity).[220-222] SEC coupled with more than one detector can provide information on the average chemical composition as a function of hydrodynamic volume via the comparison of the response of the respective detector signals as a function of elution volume. In complex polymers with unreacted and partially reacted starting polymers, SEC cannot give the full picture of polymer characterization in terms of chemical composition and its distribution. However, liquid adsorption chromatography (LAC) can be performed in isocratic or gradient (solvent, temperature[223,224]) mode to separate copolymers or polymers according to their chemical composition.[225-228] But, as for SEC, LAC alone is unable to provide information on the molar mass and the distribution of the molar mass. Although with liquid chromatography under critical condition LCCC, which is at the interface between the entropic size exclusion separation and the enthalpy separation liquid adsorption chromatography,[229,230] it is possible, under these conditions of chromatographic analysis, to determine the heterogeneities of the polymer without any influence of the polymer molar mass. Coupling SEC with LCCC is one technique, so it is a called two-dimensional chromatographic separation,[231-234] where in first dimension the polymer elute at critical condition mode, and in second dimension elute in exclusion mode. Special units are used to split the first dimensional into small fraction and then inject it into a second dimension. This technique is highly important in the analysis of complex polymers, due to the capability of the technique to give distributions of molar mass in one dimension and chemical composition or functionality in the second. Pasch et al.[235] applied 2D analysis to determine molecular mass distribution MMD and chemical composition distribution CCD of a variety of polymer samples; PS-b-PMMA, besides analysis of various acrylates and methacrylates copolymers[236] where gradient elution chromatography GEC in the first dimension and SEC at the second dimension succeed in separate a complex copolymers for cosmetic applications. Pasch et al. also characterize a number of graft

copolymers, including Sty and MMA grafted Epoxidized Natural Rubber,[237,238] (with LCCC as the first dimension and SEC as the second one), and PBd-g-PMMA graft[256] (with GEC as the first dimension and SEC as the second). Reversed-phase in first dimension and normal-phase in second dimension were used in 2D analysis by Jandera et al.[239] to analyze (co)oligomers.

2.9 References:

1. Brown, H. C., *Orgnanic Syntheses via Boranes*. John Wiley and Sons: New York, 1975.
2. Xu, Y. J.; Zhang, Y. F.; Li, J. Q. *Chemical Physics Letters* **2006,** 421, 36-41.
3. Nagase, S.; Ray, N. K.; Morokuma, K. *Journal of the American Chemical Society* **1980,** 102, 4536-4537.
4. Balucani, N.; Zhang, F.; Kaiser, R. I. *Chemical Reviews* **2010,** 110, 5107-5127.
5. Brown, H. C.; Liotta, R.; Scouten, C. G. *Journal of the American Chemical Society* **1976,** 98, 5297-5301.
6. Brown, H. C.; Keblys, K. A. *Journal of the American Chemical Society* **1964,** 86, 1795-1801.
7. Ilich, P. P.; Rickertsen, L. S.; Becker, E. *Journal of Chemical Education* **2006,** 83, 1681-1685.
8. Scouten, C. G.; Brown, H. C. *Journal of Organic Chemistry* **1973,** 38, 4092-4094.
9. Hanson, J. R. *Journal of Chemical Research* **2004**, 1-5.
10. Brown, H. C.; Midland, M. M.; Kabalka, G. W. *Journal of the American Chemical Society* **1971,** 93, 1024-1025.
11. Knights, E. F.; Brown, H. C. *Journal of the American Chemical Society* **1968,** 90, 5280-5281.
12. Elschenbroich, C., Organometallic compounds of the boron group (group 13). *Organometallics*, Elschenbroich, C.; Oliveira, J., Eds. Wiley-VCH: Weinheim, 2005; 91-92.
13. Vishwakarma, L. C.; Fry, A. *Journal of Organic Chemistry* **1980,** 45, 5306-5308.
14. Seino, M.; Yokomachi, K.; Hayakawa, T.; Kikuchi, R.; Kakimoto, M.; Horiuchi, S. *Polymer* **2006,** 47, 1946-1952.
15. Eroglu, M. S.; Hazer, B.; Ozturk, T.; Caykara, T. *Journal of Applied Polymer Science* **2005,** 97, 2132-2139.
16. Ruckenstein, E.; Zhang, H. *Journal of Polymer Science: Part A: Polymer Chemistry* **2000,** 38, 1195-1202.
17. Zutty, N.; Welch, F. *Journal of Organic Chemistry* **1960,** 25, 861-863.
18. Mirviss, S. B. *Journal of the American Chemical Society* **1961,** 83, 3051-3056.

19. Janvikul, W. Functionalization of polyolefins via borane/oxygen chemistry: synthesis and reaction mechanism study. PhD thesis. Pennsylvania State University, USA, 1997.

20. Chung, T. C.; Lu, H. L.; Janvikul, W. *Polymer* **1997,** 38, 1495-1502.

21. Masuda, Y.; Hoshi, M.; Numokawa, Y.; Arase, A. *Journal of the Chemical Society, Chemical Communications* **1991**, 1444-1445.

22. Chung, T. C.; Janvikul, W.; Lu, H. L. *Journal of the American Chemical Society* **1996,** 118, 705-706.

23. Lu, B.; Chung, T. C. *Macromolecules* **1998,** 31, 5943-5946.

24. Chung, T. C.; Janvikul, W.; Bernard, R.; Hu, R. *Polymer* **1995,** 36, 3565-3574.

25. Perchyonok, V. T.; Schiesser, C. H. *Tetrahedron Letters* **1998,** 39, 5437-5438.

26. Hansen, R. L.; Hamann, R. R. *Journal of Physical Chemistry* **1963,** 67, 2868-2869.

27. Guoqiang, F.; Dong, J. Y.; Wang, Z.; Chung, T. C. *Journal of Polymer Science: Part A: Polymer Chemistry* **2006,** 44, 539-548.

28. Chung, T. C.; Lu, H. L. *Journal of Molecular Catalysis A: Chemical* **1997,** 115, 115-127.

29. Chung, T. C.; Jiang, G. J. *Macromolecules* **1992,** 25, 4816-4818.

30. Chung, T. C. *Prog. Polym. Sci.* **2002,** 27, 39-85.

31. Chung, T. C.; Rhubright, D.; Jiang, G. J. *Macromolecules* **1993,** 26, 3467-3471.

32. Chung, T. C.; Janvikul, W.; Bernard, R.; Jiang, G. J. *Macromolecules* **1994,** 27, 26-31.

33. Dong, J. Y.; Manias, E.; Chung, T. C. *Macromolecules* **2002,** 35, 3439-3447.

34. Hong, H.; Chung, T. C. *Macromolecules* **2004,** 37, 6260-6263.

35. McGrath, J. E., Preface. *Anionic Polymerization Kinetis Mechanisms and Synthesis*, McGrath, J. E., Ed. American Chemical Society: Washington D.C, 1981; xi.

36. Szwarc, M.; Levy, M.; Milkovich, R. *Journal of the American Chemical Society* **1956,** 78, 2656-2657.

37. Bahsteter, F.; Smid, J.; Szwarc, M. *Journal of the American Chemical Society* **1963,** 85, 3909-3918.

38. Morton, M.; Fetters, L. J.; Pett, R. A.; Meier, J. F. *Macromolecules* **1970,** 3, 327.

39. Baskaran, D.; Muller, A. H. E. *Progress in Polymer Science* **2007,** 32, 173-219.

40. Mahajan, S.; Renker, S.; Simon, P. F. W.; Gutmann, J. S.; Jain, A.; Gruner, S. M.; Fetters, L. J.; Coates, G. W.; Wiesner, U. *Macromolecular Chemistry and Physics* **2003,** 204, 1047-1055.

41. Bywater, S.; Worsfold, D. J. *Journal of Organometallic Chemistry* **1967,** 10, 1-6.

42. Szwarc, M. *Advances in Polymer Science* **1980,** 49, 30-217.

43. Young, R. N.; Quirk, R. P.; Fetters, L. J. *Advances in Polymer Science* **1984,** 56, 3-93.

44. Hofmans, J.; Maeseele, L.; Wang, G.; Janssens, K.; van Beylen, M. *Polymer* **2003,** 44, 4109-4115.

45. Hsieh, H. *Rubber Chemistry and Technology* **1970,** 43, 22.

46. Smid, J.; Beylen, M. V.; Esch, T. E. H. *Progress in Polymer Science* **2006,** 31, 1041-1067.

47. Hadjichristidis, N.; Pitsikalis, M.; Pispas, S.; Iatrou, H. *Journal of Polymer Science: Part A: Polymer Chemistry* **2000,** 38, 3211-3234.

48. Ito, K.; Kawaguchi, S. *Advances in Polymer Science* **1999,** 142, 130-174.

49. Hirao, A.; Haraguchi, N.; Sugiyama, K. *Macromolecules* **1999,** 32, 48-54.

50. Quirk, R. P.; Zhuo, Q. *Macromolecules* **1997,** 30, 1531-1539.

51. Ji, H.; Farmer, B. S.; Nonidez, W. K.; Advincula, R. C.; Smith, G. D.; Kilbey, S. M.; Dadmun, M. D.; Mays, J. W. *Macromolecular Chemistry and Physics* **2007,** 208, 807-814.

52. Grodzinski, J. J. *Journal of Polymer Science: Part A: Polymer Chemistry* **2002,** 40, 2116-2133.

53. Xenidou, M.; Hadjichristids, N. *Macromolecules* **1998,** 31, 5690-5694.

54. Morton, M.; Ells, F. R. *Journal of Polymer Science* **1962,** 61, 25-29.

55. Kamigaito, M.; Satoh, K. *Macromolecules* **2007,** 41, 269-276.

56. Carrot, G.; Hilborn, J.; Knauss, D. M. *Polymer* **1997,** 38, 6401-6407.

57. Rempp, P. F.; Franta, E. *Advances in Polymer Science* **1984,** 58, 1-53.

58. Baskaran, D. *Progress in Polymer Science* **2003,** 28, 521-581.

59. Donkers, E. H.; Willemse, R. X. E.; Klumperman, B. *Journal of Polymer Science: Part A: Polymer Chemistry* **2005,** 43, 2536-2545.

60. Dhara, M. G.; Sivaram, S.; Baskaran, D. *Polymer Bulletin* **2009,** 63, 185-196.

61. Ishizone, T.; Hirao, A.; Nakahama, S. *Macromolecules* **1993,** 26, 6964-6975.

62. Ishizone, T.; Wakabayashi, S.; Hirao, A.; Nakahama, S. *Macromolecules* **1991,** 24, 5015-5022.

63. Fallais, I.; Pantoustier, N.; Devaux, J.; Jerome, C. Z. R. *Polymer* **2000,** 41, 5535-5539.

64. Fontanille, M.; Sigwalt, R. P., *Comprehensive Polymer Science*, Allen, S. G.; Bevington, J. C., Eds. Pergamon: New York, 1989.

65. Matsumoto, K.; Deguchi, M.; Nakano, M.; Yamaoka, H. *Journal of Polymer Science: Part A: Polymer Chemistry* **1998,** 36, 2699-2706.

66. Koutalas, G.; Lohes, D. J.; Hadjichristidis, N. *Journal of Polymer Science: Part A: Polymer Chemistry* **2005,** 43, 4040-4049.

67. Hirao, A.; Matsuo, A.; Morifuji, K.; Takuda, Y.; Hayashi, M. *Polymer for Advanced Technologies* **2001,** 12, 680-686.

68. Bywater, S. *Advances in Polymer Science* **1979,** 30, 89-116.

69. Pennisi, R. W.; Fetters, L. J. *Macromolecules* **1988,** 21, 1094-1099.

70. Hadjichristids, N.; Pitsikalis, M.; Pispas, S.; Latrou, H. *Chemical Reviews* **2001,** 101, 3747-3792.

71. Hatada, K.; Kitayama, T.; Fumikawa, K.; Ohta, K.; Yuki, H., Studies on the anionic polymerization of methyl methacrylate initiated with butyllithium in toluene by using perdeuterated monomer. *Anionic Polymerization Kinetics, Mechanisms, and Synthesis*, McGrath, J. E., Ed. American Chemical Society: Washington, D. C., 1981; 327-341.

72. Zune, C.; Jerome, R. *Progress in Polymer Science* **1999,** 24, 631-664.

73. Castro, N. M. M.; Zhang, M.; Pergushov, D. V.; Muller, A. H. E. *Designed Monomers and Polymers* **2006,** 9, 63-79.

74. Jungling, S.; Gausepohl, H.; Warzelhan, V.; Kee, G. E. M.; Fisher, M. Anionic polymerization of acrylates and methacrylates. US 6,262,213 07/17/2001, 2001.

75. Varshney, S. K.; Jerome, R.; Bayard, P.; Jacobs, C.; Fayt, R.; Teyssie, P. *Macromolecules* **1992,** 25, 4457-4463.

76. Xie, X.; Hogen-Esch, T. E. *Macromolecules* **1996,** 29, 1746-1752.

77. Varshney, S. K.; Hautekeer, J. P.; Fayt, R.; Jerome, R.; Teyssie, P. *Macromolecules* **1990,** 23, 2618-2622.

78. Zundel, T.; Zune, C.; Teyssie, P.; Jerome, R. *Macromolecules* **1998,** 31, 4089-4092.

79. Peron, G. L. N.; Peace, R. J.; Holmes, A. B. *Journal of Materials Chemistry* **2001,** 11, 2915-2918.

80. Jagur-Grodzinski, J. *Reactive & Functional Polymers* **2001,** 49, 1-54.

81. Soloman, D. H.; Rizzardo, E.; Cacioli, E. Polymerization process and polymers produced thereby. 4581429 04/08/1986, 1986.

82. Kato, M.; Kamigaito, M.; Sawamoto, M.; Higashimura, T. *Macromolecules* **1995,** 28, 1721-1723.

83. Wang, J. S.; Matyjaszewski, K. *Journal of the American Chemical Society* **1995,** 117, 5614-5615.

84. Matyjaszewski, K. *Progress in Polymer Science* **2005,** 30, 858-875.

85. Matyjaszewski, K.; Xia, J. *Chemical Reviews* **2001,** 101, 2921-2990.

86. Luo, R.; Sen, A. *Macromolecules* **2007,** 40, 154-156.

87. Fukuda, T.; Terauchi, T.; Goto, A.; Ohno, K.; Tsujii, Y.; Miyamoto, T.; Kobatake, S.; Yamada, B. *Macromolecules* **1996,** 29, 6393-6398.

88. Goto, A.; Fukuda, T. *Progress in Polymer Science* **2004,** 29, 329-385.

89. Fukuda, T. *Journal of Polymer Science: Part A: Polymer Chemistry* **2004,** 42, 4743-4755.

90. Braunecker, W. A.; Matyjaszewski, K. *Progress in Polymer Science* **2007,** 32, 93-146.

91. Kamigaito, M.; Ando, T.; Sawamoto, M. *Chemical Reviews* **2001,** 101, 3689-3746.

92. Xue, Z.; He, D.; Noh, S. K.; Lyoo, W. S. *Macromolecules* **2009,** 42, 2949-2957.

93. Subramanian, S. H.; Dhamodharan, R. *Polymer International* **2008,** 57, 479-487.

94. Chiefari, J.; Chong, Y. K.; Ercole, F.; Krstina, J.; Jeffery, J.; Le, T. P. T. *Macromolecules* **1998,** 31, 5559-5562.

95. Le, T. P.; Moad, G.; Rizzardo, E.; Thang, S. H. Polymerization with living characteristics. 7714075, 05/11/2010, 1998.

96. Lai, J. T.; Shea, R. *Journal of Polymer Science: Part A: Polymer Chemistry* **2006,** 44, 4298-4316.

97. Mayadunne, R. T. A.; Rizzardo, E.; Chiefari, J.; Chong, Y. K.; Moad, G.; Thang, S. H. *Macromolecules* **1999,** 32, 6977-6980.

98. Liu, J.; Hong, C. Y.; Pan, C. Y. *Polymer* **2004,** 45, 4413-4421.

99. Alberti, A.; Benaglia, M.; Laus, M.; Sparnacci, K. *Journal of Organic Chemistry* **2002,** 67, 7911-7914.

100. Laus, M.; Papa, R.; Sparnacci, K.; Alberti, A.; Benaglia, M.; Macciantelli, D. *Macromolecules* **2001,** 34, 7269-7275.

101. Charmot, D.; Chang, H. T.; Huefner, P.; Li, Y. Emulsion living-type free radical polymerization, methods and products of same 20020065380, 09/25/2001, 2002.

102. Coote, M. L.; Henry, D. J. *Macromolecules* **2005,** 38, 1415-1433.

103. Destarac, M.; Gauthier Gillaizeau, I.; Vuong, C. T.; Zard, S. Z. *Macromolecules* **2005,** 39, 912-914.

104. Yamago, S.; Iida, K.; Nakajima, M.; Yoshida, J. *Macromolecules* **2003,** 36, 3793-3796.

105. Yamago, S.; Iida, K.; Yoshida, J. *Journal of the American Chemical Society* **2002,** 124, 13666-13667.

106. Kwak, Y.; Goto, A.; Fukuda, T.; Kobayashi, Y.; Yamago, S. *Macromolecules* **2006,** 39, 4671-4679.

107. Yamago, S.; Ray, B.; Iida, K.; Yoshida, J.-i.; Tada, T.; Yoshizawa, K.; Kwak, Y.; Goto, A.; Fukuda, T. *Journal of the American Chemical Society* **2004,** 126, 13908-13909.

108. Caille, J. R.; Debuigne, A.; Jerome, R. *Macromolecules* **2005,** 38, 27-32.

109. Millard, P. E.; Barner, L.; Stenzel, M. H.; Davis, T. P.; Kowollik, C. B.; Muller, A. H. E. *Macromolecular Rapid Communications* **2006,** 27, 821-828.

110. McLeary, J. B.; Klumperman, B. *Soft Matter* **2006,** 2, 45-53.

111. Bathfield, M.; D'Agosto, F.; Spitz, R.; Charreyre, M.-T.; Delair, T. *Journal of the American Chemical Society* **2006,** 128, 2546-2547.

112. Moad, G.; Chiefari, J.; Chong, B. Y.; Krstina, J.; Mayadunne, R. T. A.; Postma, A.; Rizzardo, E.; Thang, S. H. *Polymer International* **2000,** 49, 993-1001.

113. Szablan, Z.; Toy, A. A.; Davis, T. P.; Hao, X.; Stenzel, M. H.; Barner-Kowollik, C. *Journal of Polymer Science: Part A: Polymer Chemistry* **2004,** 42, 2432-2443.

114. Chong, B. Y. K.; Krstina, J.; Le, T. P. T.; Moad, G.; Postma, A.; Rizzardo, E.; Thang, S. H. *Macromolecules* **2003,** 36, 2256-2272.

115. Chiefari, J.; Mayadunne, R. T. A.; Moad, C. L.; Moad, G.; Rizzardo, E.; Postma, A.; Skidmore, M. A.; Thang, S. H. *Macromolecules* **2003,** 36, 2273-2283.

116. Benaglia, M.; Rizzardo, E.; Alberti, A.; Guerra, M. *Macromolecules* **2005,** 38, 3129-3140.

117. Rizzardo, E.; Chen, M.; Chong, B.; Moad, G.; Skidmore, M.; Thang, S. H. *Macromolecular Symposia* **2007,** 248, 104-116.

118. Brouwer, H. D.; Schellekens, M. A. J.; Klumperman, B.; Monteiro, M. J.; German, A. L. *Journal of Polymer Science: Part A: Polymer Chemistry* **2000,** 38, 3596-3603.

119. Moad, G.; Chong, Y. K.; Postma, A.; Rizzardo, E.; Thang, S. H. *Polymer* **2005,** 46, 8458-8468.

120. Shim, S. E.; Lee, H.; Choe, S. *Macromolecules* **2004,** 37, 5565-5571.

121. Lima, V.; Jiang, X.; Zijp, J. B.; Schoenmakers, P. J.; Klumperman, B.; Linde, R. V. D. *Journal of Polymer Science: Part A: Polymer Chemistry* **2005,** 43, 959-973.

122. Chen, M.; Ghiggino, K. P.; Mau, A. W. H.; Rizzardo, E.; Thang, S. H.; Wilson, G. J. *Chemical Communications* **2002**, 2276-2277.

123. Zhai, G.; Yu, W. H.; Kang, E. T.; Neoh, K. G.; Huang, C. C.; Liaw, D. J. *Industrial and Engineering Chemistry Research* **2004,** 43, 1673-1680.

124. Jiang, R.; Jin, Q.; Li, B.; Ding, D.; Wickham, R. A.; Shi, A.-C. *Macromolecules* **2008,** 41, 5457-5465.

125. Dube, M. A.; Penlidis, A. *Polymer* **1995,** 36, 587-598.

126. Brar, A. S.; Yadav, A. *Journal of Molecular Structure* **2002,** 602-603, 29-39.

127. Ito, T.; Otsu, T. *Journal of Macromolecular Science, Part A Pure and Applied Chemistry* **1969,** 3, 197-203.

128. Tian, X.-z.; Zhu, B.-k.; Jiang, X.; Xu, Y.-y. *Chinese Journal of Polymer Science* **2005,** 23, 627-633.

129. Kobayashi, S.; Kataoka, H.; Ishizone, T.; Kato, T.; Ono, T.; Kobukata, S.; Arimoto, K.; Ogi, H. *Reactive & Functional Polymers* **2009,** 69, 409-415.

130. Nichifor, M.; Zhu, X. X. *Polymer* **2003,** 44, 3053-3060.

131. Nogueira, R. F.; Tavares, M. I. B. *Journal of Applied Polymer Science* **2001,** 81, 261-266.

132. Liu, Y.; Mao, R.; Huglin, M. B.; Holmes, P. A. *Polymer* **1996,** 37, 1437-1441.

133. Nguyen, M. N.; Bressy, C.; Margaillan, A. *Polymer* **2009,** 50, 3086-3094.

134. Zhu, J.; Zhu, X.; Cheng, Z.; Zhang, Z. *Macromolecular Symposia* **2008,** 261, 46-53.

135. Davies, M. C.; Dawkins, J. V.; Hourston, D. J. *Polymer* **2005,** 46, 1739-1753.

136. Matyjaszewski, K.; Ziegler, M. J.; Arehart, S. V.; Greszta, D.; Pakula, T. *Journal of Physical Organic Chemistry* **2000,** 13, 775-786.

137. Min, K.; Li, M.; Matyjaszewski, K. *Journal of Polymer Science: Part A: Polymer Chemistry* **2005,** 43, 3616-3622.

138. A. S. Brar; Puneeta. *Journal of Polymer Science: Part A: Polymer Chemistry* **2006,** 44, 2076-2085.

139. de la Fuente, J. L.; Garcıa, M. F.; Sanz, M. F.; Madruga, E. L. *Macromolecules* **2001,** 34, 5833-5837.

140. Roos, S. G.; Muller, A. H. E.; Matyjaszewski, K. *Macromolecules* **1999,** 32, 8331-8335.

141. Yoshida, E. *Journal of Polymer Science: Part A: Polymer Chemistry* **1996,** 34, 2937-2943.

142. Fukuda, T.; Terauchi, T.; Goto, A.; Tsujii, Y.; Miyamoto, T. *Macromolecules* **1996,** 29, 3050-3052.

143. Davis, K. A.; Matyjaszewski, K. *Advances in Polymer Science* **2002,** 159, 1-156.

144. Hadjichristidis, N.; Pitsikalis, M.; Iatrou, H. *Advances in Polymer Science* **2005,** 189, 1-124.

145. Pitsikalis, M.; Pispas, S.; Mays, J. W.; Hadjichristidis, N. *Advances in Polymer Science* **1998,** 135, 1-129.

146. Liu, G.; Qiao, L.; Guo, A. *Macromolecules* **1996,** 29, 5508-5510.

147. Acar, M. H.; Matyjaszewski, K. *Macromolecular Chemistry and Physics* **1999,** 200, 1094-1100.

148. Urwin, J. R. *Journal of Polymer Science: Part A: Polymer Chemistry* **1958,** 27, 580-581.

149. Hadjichristidis, N.; Iatrou, H.; Pitsikalis, M.; Mays, J. *Progress in Polymer Science* **2006,** 31, 1068-1132.

150. Zeng, F.; Yang, M.; Zhang, J.; Varshney, S. K. *Journal of Polymer Science: Part A: Polymer Chemistry* **2002,** 40, 4387-4397.

151. Garnier, S.; Laschewsky, A. *Macromolecules* **2005,** 38, 7580-7592.

152. Tong, J. D.; Jerome, R. *Polymer* **2000,** 41, 2499-2510.

153. Mitsukami, Y.; Donovan, M. S.; Lowe, A. B.; McCormick, C. L. *Macromolecules* **2001,** 34, 2248-2256.

154. Bernaerts, K. V.; Du Prez, F. E. *Polymer* **2005,** 46, 8469-8482.

155. Kizhakkedathu, J. N.; Kumar, K. R.; Goodman, D.; Brooks, D. E. *Polymer* **2004,** 45, 7471-7489.

156. Garcia, M. F.; Fuente, J. L.; Cerrada, M. L.; Madruga, E. L. *Polymer* **2002,** 43, 3173-3179.

157. Schwartz, A. M. *Chemical and Engineering News* **1978,** 56, 88.

158. Ito, K.; Usami, N.; Yamashita, Y. *Macromolecules* **1980,** 13, 216-221.

159. Costello, C. A.; Schulz, D. N., Copolymers. *Encyclopedia of Chemical Technology*, Knoschwite, J. I.; Grant, M. H., Eds. John Wiley and Sons: New York, 1978; 7, 349.

160. Hirao, A.; Loykulnant, S.; Ishizone, T. *Progress in Polymer Science* **2002,** 27, 1399-1471.

161. Pitsikalis, M.; Pispas, S.; W.Mays, J.; Hadjichristidis, N. *Advances in Polymer Science* **1998,** 135, 1-129.

162. Narayan, R.; Biermann Christopher, J.; Hunt Michael, O.; Horn David, P., Cellulose Graft Copolymers for Potential Adhesive Applications. *Adhesives from Renewable Resources*, Hemingway, R. W.; Conncr, A. H., Eds. American Chemical Society: Washington, DC, 1989; 337-354.

163. Lutz, J. E.; Jahed, N.; Matyjaszewski, K. *Journal of Polymer Science: Part A: Polymer Chemistry* **2004,** 42, 1939-1952.

164. Lee, Y.; Akiba, I.; Akiyama, S. *Journal of Applied Polymer Science* **2002,** 86, 1736-1740.

165. Neugebauer, D.; Zhang, Y.; Pakula, T. *Journal of Polymer Science: Part A: Polymer Chemistry* **2006,** 44, 1347-1356.

166. Chojnowski, J.; Cypryk, M.; Fortuniak, W.; Scibiorek, M.; Rozga-Wijas, K. *Macromolecules* **2003,** 36, 3890-3897.

167. Alexander, V. L.; Joseph, P. K. *Journal of Polymer Science: Part A: Polymer Chemistry* **1993,** 31, 2825-2834.

168. Liu, Q.; Wilson, G. R.; Davis, R. M.; Riffle, J. S. *Polymer* **1993,** 34, 3030-3036.

169. Perrier, S.; Davis, T. P.; Carmichael, A. J.; Haddleton, D. M. *Chemical Communications* **2002**, 2226-2227.

170. Ramakrishnan, A.; Dhamodharan, R. *Journal of Macromolecular Science Part A: Pure and Applied Chemistry* **2000,** 37, 621-631.

171. Tsoukatos, T.; Pispas, S.; Hadjichristidis, N. *Macromolecules* **2000,** 33, 9504-9511.

172. Kobatake, S.; Harwood, H. J.; Quirk, R. P.; Priddy, D. B. *Macromolecules* **1998,** 31, 3735-3739.

173. Korczagin, I.; Hempenius, M. A.; Vancso, G. J. *Macromolecules* **2004,** 37, 1686-1690.

174. Grubbs, R. B. *Macromolecular Chemistry and Physics* **2005,** 206, 625-627.

175. Pyun, J.; Jia, S.; Kowalewski, T.; Matyjaszewski, K. *Macromolecular Chemistry and Physics* **2004,** 205, 411-417.

176. Wang, W. P.; You, Y. Z.; Hong, C. Y.; Xu, J.; Pan, C. Y. *Polymer* **2005,** 46, 9489-9494.

177. Martinez-Castro, N. M.; Zhang, M.; Pergushov, D. V.; Muller, A. H. E. *Designed Monomers and Polymers* **2006,** 9, 63-79.

178. Myers, S. B.; Register, R. A. *Macromolecules* **2008,** 41, 5283-5288.

179. Mecerreyes, D.; Atthoff, B.; Boduch, K. A.; Trollsas, M.; Hedrick, J. L. *Macromolecules* **1999,** 32, 5175-5182.

180. Cheng, C.; Yang, N.-L. *Macromolecular Rapid Communications* **2005,** 26, 1395-1399.

181. Kawahara, N.; Kojoh, S. I.; Matsuo, S.; Kaneko, H.; Matsugi, T.; Saito, J.; Kashiwa, N. *Polymer Bulletin* **2006,** 57, 805-812.

182. Chung, T. C.; Lu, H. L.; Ding, R. D. *Macromolecules* **1997,** 30, 1272-1278.

183. Kaneyoshi, H.; Inoue, Y.; Matyjaszewski, K. *Macromolecules* **2005,** 38, 5425-5435.

184. Schellekens, M. A. J.; Klumperman, B. *Polymer Reviews* **2000,** 40:2, 167-192.

185. Lopez, R. G.; D'Agosto, F.; Boisson, C. *Progress in Polymer Science* **2007,** 32, 419-454.

186. Godoy Lopez, R.; D'Agosto, F.; Boisson, C. *Progress in Polymer Science* **2007,** 32, 419-454.

187. Venkatesh, R.; Yajjou, L.; Koning, C. E.; Klumperman, B. *Macromolecular Chemistry and Physics* **2004,** 205, 2161-2168.

188. Ranjan, R.; Brittain, W. J. *Macromolecules* **2007,** 40, 6217-6223.

189. Lutz, J. F.; Borner, H. G.; Weichenhan, K. *Macromolecules* **2006,** 39, 6376-6383.

190. Huang, C. F.; Yokoyama, A.; Yokozawa, T. *Journal of Polymer Science: Part A: Polymer Chemistry* **2010,** 48, 2948-2954.

191. Lu, B.; Chung, T. C. *Macromolecules* **1999,** 32, 2525-2533.

192. Chung, T. C.; Xu, G.; Lu, Y.; Hu, Y. *Macromolecules* **2001,** 34, 8040-8050.

193. Chung, T. C. *Progress in Polymer Science* **2002,** 27, 39-85.

194. Campbell, D.; Pethrick, R. A.; White, J. R., *Polymer Characterization: Physical Techniques*. Stanley Thornes: Cheltenham, 2000; p 362-399.

195. Ngai, K. L., *The glass transition and the glassy state*. third ed.; Cambridge university: Cambridge, 2004.

196. Hansen, J. P.; Levesque, D.; Zinn-Justin, J., *Liquids Freezing and Glass Trasition*. North-Holland Amsterdam, 1991.

197. Rohr, K. S.; Spiess, H. W., *Multidimensional Solid State NMR and Polymers*. Academic press: London, 1994.

198. Pecora, R., *Dynamic Light Scattering*. Academic press: New York, 1986.

199. Binder, K., *Monte Carlo and Molecular Dynamics Simulation in Polymer Science*. Oxford university press: Oxford, 1995.

200. Mallon, P. E., Application to Polymers. *Principles and Applications of Positron and Positronium Chemistry*, First ed.; Jean, Y. C.; Mallon, P. E.; Schrader, D., Eds. World Scientific: Singapore, 2003; 253.

201. Brandt, W.; Berko, S.; Walker, W. W. *Physical Review* **1960,** 120, 1289–1295.

202. Prochazka, I. *Materials Structure* **2001,** 8, 55-60.

203. Bueche, F., *Physical Properties of Polymers*. Robert E. Krieger: New York, 1979.

204. Bartos, J.; Kristiakova, K.; Sausa, O.; Kristiak, J. *Polymer* **1996,** 37, 3397-3403.

205. Brandt, W.; Spirn, I. *Physical Review* **1966,** 142, 231–237.

206. Hristov, H. A.; Bolan, B.; Yee, A. F.; Xie, L.; Gidley, D. W. *Macromolecules* **1996,** 29, 8507–8516.

207. Dlubek, G.; Fretwell, H. M.; Alam, M. A. *Macromolecules* **2000,** 33, 187–192.

208. Dlubek, G.; Supej, M.; Bondarenko, V.; Pionteck, J.; Pompe, G.; Krause-Rehberg, R.; Emri, I. *Journal of Polymer Science: Part B: Polymer Physics* **2003,** 41, 3077-3088.

209. Hill, A. J.; Weinhold, S.; Stack, G. M.; Tant, M. R. *European Polymer Journal* **1996,** 32, 843-849.

210. McCulagh, C. M.; Yu, Z.; Jamieson, A. M.; Blackwell, J.; McGervey, J. D. *Macromolecules* **1995,** 28, 6100-6107.

211. Chen, Z. Q.; Uedono, A.; Suzuki, T.; He, J. S. *Journal of Radioanalytical and Nuclear Chemistry* **2003,** 255, 291-294.

212. Yu, Z.; Yahsi, U.; McGervey, J.; Jamieson, A. M.; Simha, R. *Journal of Polymer Science: Part B: Polymer Physics* **1994,** 32, 2637-2644.

213. Hamielec, A. E.; Eldrup, M.; Mogensen, O. *Journal of Macromolecular Science Polymer Reviews* **1973,** 9, 305-337.

214. Dlubek, G.; Bamford, D.; Rodriguez-gonzalez, A.; Bornemann, S.; Stejny, J.; Schade, B.; Alam, M. A.; Arnold, M. *Journal of Polymer Science: Part B: Polymer Physics* **2002,** 40, 434–453.

215. Uedono, A.; Kawano, T.; Tanicawa, S.; Ban, M.; Kyoto, M.; T, U. *Journal of Polymer Science: Part B: Polymer Physics* **1996,** 34, 2145-2151.

216. Cangialosi, D.; Wübbenhorst, M.; Schut, H.; van Veen, A.; Picken, S. J. *Materials Science Forum* **2004,** 445-446, 271-273.

217. Fang, J.; Tanaka, K.; Kita, H.; Okamoto, K.-I.; Ito, Y. *Journal of Polymer Science: Part B: Polymer Physics* **2000,** 38, 1123-1132.

218. Consolati, G.; Levi, M.; Turri, S. *Polymer* **2001,** 42, 9723-9728.

219. Xu, J.; Zhang, X.; Chen, H.; Chen, B.; Zhang, Q. *Spectroscopy Letters* **2007,** 40, 139-147.

220. Wen, J.; Arakawa, T.; Philo, J. S. *Analytical Biochemistry* **1996,** 240, 155-166.

221. Mourey, T. H. *International Journal of Polymer Analysis and Characterization* **2004,** 9, 97-135.

222. Trathnigg, B., Size-exclusion chromatography of polymers. *Encyclopedia of Analytical Chemistry*, Meyers, R. A., Ed. John Wiley and Sons: Chichester, 2000; 8008-8034.

223. Chang, T.; Lee, H. C.; Lee, W.; Park, S.; Ko, C. *Macromolecular Chemistry and Physics* **1999,** 200, 2188-2204.

224. Albrecht, A.; Brull, R.; Macko, T.; Pasch, H. *Macromolecules* **2007,** 40, 5545-5551.

225. Trathnigg, B. *Progress in Polymer Science* **1995,** 20, 615-650.

226. Philipsen, H. J. A.; Klumperman, B.; German, A. L. *Journal of Chromatography A* **1996,** 746, 211-224.

227. Fitzpatrick, F.; Edam, R.; Schoenmakers, P. *Journal of Chromatography A* **2003,** 988, 53-67.

228. Mori, S. *Journal of Chromatography* **1990,** 507, 473-479.

229. Berek, D. *Progress in Polymer Science* **2000,** 25, 873-908.

230. Bruna, Y.; Aldenb, P. *Journal of Chromatography A* **2002,** 966, 25-40.

231. van Horst, A.; Schoenmakers, P. J. *Journal of Chromatography A* **2003,** 1000, 693-709.

232. Dugo, P.; Cacciola, F.; Kummb, T.; Dugo, G.; Mondello, L. *Journal of Chromatography A* **2008,** 1184, 353-368.

233. Im, K.; Park, H.-W.; Kim, Y.; Chung, B.; Ree, M.; Chang, T. *Analytical Chemistry* **2007,** 79, 1067-1072.

234. Weidner, S.; Falkenhagen, J.; Krueger, R. P.; Just, U. *Analytical Chemistry* **2007,** 79, 4814-4819.

235. Pasch, H.; Mequanint, K.; Adrian, J. *e-Polymers* **2002,** 5, 1-19.

236. Raust, J. A.; Brull, A.; Moireb, C.; Farcet, C.; Pasch, H. *Journal of Chromatography A* **2008,** 1203, 207-216.

237. Graef, S. M.; van Zyl, A. J. P.; Sanderson, R. D.; Klumperman, B.; Pasch, H. *Journal of Applied Polymer Science* **2003,** 88, 2530-2538.

238. Siewing, A.; Lahn, B.; Braun, D.; Pasch, H. *Journal of Polymer Science: Part A: Polymer Chemistry* **2003,** 41, 3143-3148.

239. Jandera, P.; Fischer, J.; Lahovska, H.; Novotna, K.; Cesla, P.; Kolarova, L. *Journal of Chromatography A* **2006,** 1119, 3-10.

CHAPTER 3

SYNTHESIS AND CHARACTERIZATION OF PS-b-PMMA

The synthesis of the block copolymer PS-b-PMMA, prepared via a combination of living anionic polymerization with autoxidation of the borane-terminated polymer adducts, and their characterizations are described in this chapter.

3.1 Introduction

Block copolymers generally have characteristic properties that effectively differ from those of their own block segments, and the properties may be a hybrid of those of the individual homopolymers. Much attention has been given to the synthesis and characterization of block copolymers and their properties.[1-4] Living polymerizations, free radical and anionic, are the most common synthetic routes used to prepare block polymers. This is due to the living nature of the polymerization and the wide range of monomers that can be used. Anionic polymerization was the first recognized technique used to prepare block copolymers. It offers the opportunity to prepare polymers with well defined structures. Various polymer properties can be controlled, such as molar mass, molecular mass distribution, stereochemistry, and chain-end functionality.

The synthesis of block copolymers with different monomer functionalities and polarities is not simple, due to the limited suitability of monomers and strict conditions required.[5,6] A combination of different techniques together with anionic polymerization offers an alternative strategy for the preparation of block copolymers. Kobatake et al.[7] synthesized the block copolymer polybutadiene-block-polystyrene by combining anionic polymerization with NMP. Acar and Matyjaszewski[8] synthesized block copolymers by combining anionic polymerization with ATRP; they transformed the carbanion end group to 2-bromoisobutyl and then used it to initiate the ATRP polymerization. Korczagin et al.[9] synthesized a block copolymer of ferrocenylsilane-b-methacrylates using anionic polymerization and ATRP. Mahajan et al.[10] prepared an amphiphilic diblock copolymer made of polyethylene oxide and polyhexyl methacrylate by combining anionic polymerization with ATRP.

9-BBN hydroboration agents are used extensively to hydroboronate polymer chains. This is followed by autoxidation, by oxygen or hydroxylation, to incorporate functional groups into the polymer chain (manly OH groups).[11-19] The hydroboration of allyl terminated macromonomers followed by selective autoxidation by oxygen results in stable polymeric radicals that are capable of generating the free radical

polymerization of vinyl monomers. These borane-terminated macromonomers have been shown to be very useful intermediates for the preparation of block copolymers with different polarities.[11,12,15-17,20]

The characterization of block copolymers has also attracted much attention among researchers, particularly the chemical composition, thermal behavior, dielectric properties, solubility, self-assembly, and mechanical properties.

Several very useful chromatographic techniques have been developed to characterize polymers and copolymers.[21-25] The determination of chemical composition distribution (CCD) is one of the most fundamental items in the characterization of copolymers.

High-performance liquid chromatography (HPLC) has been used to determine the CCD of copolymers.[26-28] Liquid chromatography at critical conditions (LCCC) is a separation mode in which the condition of macromolecules on porous media is governed by the exactly balanced forces of entropic exclusion to enthalpic interactions. The result is that a polymer elutes independently of molar mass; it only elutes according to chemical differences. This makes LCCC ideally suited for the study of the CCDs of copolymers, especially block copolymers.

For block copolymers, critical conditions are established for one of the blocks by using homopolymer standards. The phase system is generally chosen such that the conditions allow for the block segment of interest to elute in exclusion mode. According to theory, the block at its critical condition becomes chromatographically “invisible” and elutes at the same time regardless of the block length.[21] There are many reports on the use of this technique to characterize blends, blocks and graft copolymers, and which confirm that the elution of the blocks occurs according to the chemical composition of the block of interest.[22,24,29-36] The use of two-dimensional liquid chromatography (2D LC) is the best way to obtain more information on molecular heterogeneity. Usually the separation developed in the first dimension is based on chemical composition, using interaction chromatography, and in the second dimension the separation is based on the hydrodynamic volume, using SEC. A number of applications of coupling two techniques have been described, such as gradient HPLC-SEC and LCCC-SEC.[23,25,37]

A combination of anionic polymerization and the autoxidation of a borane adduct was used to prepare block copolymers. The synthesis of a well controlled polymer via anionic polymerization was carried out. The polymerization reaction was terminated with an allylchlorodimethylsilane terminating agent to produce the polymers with unsaturated chain ends. There were several reasons for the selection of this terminating agent. Firstly, the chlorosilane (-SiCl) group does not undergo side

reactions, and it gives a more efficient and quantitative termination of a living anionic system. Also, the allyl end function group is less hindered and can undergo a hydroboration reaction via 9-BBN. PS of three different chain lengths were prepared (Section 3.2.2). The effect of the chain length on the block formation via autoxidation of the borane-terminated polymer was considered. The probability of the formation of homopolymer during the block formation reaction was also considered. Chung et al.[11,38] have suggested that the formation of the block and graft copolymer using hydroboration-autoxidation reaction is a result of the alkoxy radical and not the boronate radical that forms during the homolytic cleavage of peroxborane. In their case, they used polyolefins polymers, and the analysis of the produced polymers was limited to the use of high temperature SEC, FTIR, and NMR. In this case, it is not possible to tell if the polymer is a block or simply a blend. Thus, the possibilities of forming homopolymer via free 9-BBN during the hydroboration-autoxidation reaction or as a result of the boronate radical has not been adequately studied. Consequently, using this system for the synthesis of PS-b-PMMA copolymer in combination with various chromatographic techniques allows a detailed study to be done to understand the role of free 9-BBN and the boronate radical in producing the homopolymer. Characterization of PS-b-PMMA copolymer was carried out using chromatographic techniques, including LCCC and 2D LC analysis, to study the chemical composition of the copolymers thus prepared.

3.2 Experimental

3.2.1 Materials

The following reagents were used as received: methanol (Acros, 99.8%), n-butyllithium (Aldrich, 15% in hexane), acetonitrile (ACN; Sigma-Aldrich, HPLC grade), methyl ethyl ketone (MEK; Sigma-Aldrich, HPLC grade), cyclohexane (Sigma-Aldrich, HPLC grade), 1-decene (Acros Organics, 95%), 0.5 M 9-BBN (Sigma-Aldrich in THF solution), allylchlorodimethylsilane (Sigma-Aldrich), deuterated chloroform as NMR solvent ($CDCl_3$; Cambridge Isotope Laboratories), PS and PMMA standards (Polymer Laboratories), and oxygen gas (Afrox). The oxygen gas was transferred from a pressure-equalized vessel at atmospheric pressure and was therefore assumed to be at atmospheric pressure.

Styrene (Plascon Research) was purified prior to use by distillation under reduced pressure to remove the inhibitor and any impurities. The monomer was first washed with a 0.3 M potassium hydroxide solution to remove the hydroquinone inhibitor and then distilled under reduced pressure and low heat (about 35 °C) to avoid self-polymerization of the monomer. The distilled fraction was collected and

dried over anhydrous magnesium sulphate (Merck) to ensure a completely dry monomer. The styrene monomer was stored at -8 °C prior to use.

Toluene (Analytical Reagent, 99.9%) and THF (Sigma-Aldrich, 99.9%) were purified prior to use by distilling over small pieces of sodium metal (SaarChem) and benzophenone (Fluka, 99%)[23,25,37] under an argon atmosphere for several hours. A deep blue-green color, attributed to the formation of the benzophenone ketyl radical, indicated when the solvent was dry and ready for use. (THF used in experiments was considered dry and O_2 free.)

3.2.2 Synthesis of the styrene macromonomer

The following procedure was used to prepare PS. Freshly distilled Sty (4.2 g, 40 mmol) and toluene (10 mL) were introduced into a dry 100 mL round-bottom flask equipped with a magnetic stirrer bar and rubber septum under an argon atmosphere. Then n-butyllithium (0.69 mmol) initiator was slowly added until the characteristic color of the styryl anion (reddish) appeared, indicating the initiation of the polymerization reaction. The reaction was allowed to proceed for 50 min at 30 °C, with stirring, before the polystyryllithium solution was terminated by introducing, via a syringe, allylchlorodimethylsilane as the terminating agent (equivalent number of moles as n-BuLi) into the reaction mixture. The addition of allylchlorodimethylsilane resulted in the reaction mixture's losing its color (a good indicator of termination of the polymerization reaction). The macromonomer was then precipitated in methanol, collected by filtration, and dried in a vacuum at room temperature overnight to constant weight. The product was characterized by ^{1}H-NMR and SEC.

3.2.3 Hydroboration reaction

3.2.3.1 Hydroboration and oxidation of 1-decene to 1-decanol

The following procedure was used for the hydroboration-hydroxylation of 1-decene. An oven-dried round-bottom flask containing a magnetic stirrer was charged with 9-BBN (0.92 g, 7.5 mmol). THF (1.5 volumes) was added and the solution cooled to 0 °C. 1-Decene (15 mmol) was added over 5 min, and the reaction allowed to proceed at room temperature for 2 h, with stirring. The reaction mixture was then cooled to 10 °C, and NaOH solution (3 M, 9 mL) and hydrogen peroxide (30 wt % in water, 3 mL) were added. This reaction mixture was then heated to 50 °C and stirred for 2 h. After cooling to room temperature, diethyl ether (20 mL) was added. The organic phase was washed with water (20 mL) and then with brine (20 mL). It was then filtered and dried over magnesium sulfate. The crude product was passed

through a silica gel column using diethyl ether (150 mL) as eluent. The ratio of the regioisomers 1- and 2-decanol was determined by ^{1}H-NMR.

3.2.3.2 Synthesis of 9-decyl-poly(methylmethacrylate)

A 100 mL round-bottom flask was charged with 9-decyl-9-borabicyclo[3.3.1]nonane (1.5 mmol) under an argon atmosphere. MMA (2 g, 20 mmol) was added, and the polymerization was initiated by injecting O_2 gas (0.156 mL) directly into the solution, using a microsyringe. Further quantities of O_2 (0.156 mL) were added three-hourly to the reaction mixture, while stirring, until a total amount of 1.24 mL O_2 was introduced over a period of 24 h. The oxygen gas was transferred from a pressure-equalized vessel at atmospheric pressure, and it was therefore assumed to be at atmospheric pressure. The number of moles added was calculated using the standard gas equation. The homopolymer PMMA was precipitated in methanol and vacuum dried overnight.

3.2.3.3 Selective autoxidation free radical polymerization of MMA initiated via 9-BBN

An oven-dried 100 mL round-bottom flask with magnetic stirrer bar was charged with freshly distilled MMA (5 g, 50 mmol) monomer, THF (3 mL), and 9-BBN (0.41 g, 3 mmol) under an argon atmosphere. Polymerization was initiated by injecting 36 µL dry O_2 three hourly, over a period of 54 h. The polymer was precipitated in methanol and dried in a vacuum oven.

3.2.3.4 Hydroboration and autoxidation of allyl functional polymer.

PS with an unsaturated chain end (1.0 g) was placed in a 100 mL round-bottom flask with magnetic stirrer bar, and a solution of THF (30 mL) in an argon atmosphere was added. The polymer was hydroborated by the addition of 9-BBN solution in THF (3.0 mL, 0.5 M). The polymer solution was stirred at 55 °C for 2 h.

Borane-terminated polystyrene (0.5 g) was placed in a solution of 3 g dry uninhibited MMA (3 g, 30 mmol) with THF (10 mL) in a sealed round-bottom flask. The reaction was initiated by injecting O_2 gas directly into the solution. O_2 gas (0.44 mL) was added over a period of 24 h. The mole ratios were calculated using the standard gas equation. After stirring the mixture at room temperature for 2 h, the reaction was terminated by addition of methanol (10 mL). The polymer product was isolated by filtration and then dried in a vacuum oven.

3.2.4 Extraction of unreacted PS homopolymer

Attempt to extricate unreacted PS from the block copolymer PS-b-PMMA was carried out using a heptane/cyclohexane mixture as solvent to the PS homopolymer and nonsolvent to the block and PMMA.

3.3 Characterization

3.3.1 Size-exclusion chromatography (SEC)

The SEC instrument used in this study was comprised of the following units: a Waters 1515 isocratic HPLC pump; Waters 717 plus auto sampler; Waters 2487 dual λ absorbance detector, and Waters 2414 refractive index (RI) detector at 30 °C. Data processing was performed using Breeze Version 3.30 SPA (Waters) software. A set of two columns was used: PLgel (Polymer Laboratories) 5 μm Mixed-C (300×7.5mm) columns connected in series with a PLgel 5 μm guard column (50×7.5mm). The columns were kept at a constant temperature of 30 °C. THF (HPLC grade solvent; 0.125% BHT stabilized) was used as mobile phase at a flow rate of 1 mL/min. Samples were dissolved in the stabilized THF at a concentration of 5 mg/mL, and 100 μL injection volumes were used. The system was calibrated using PS Easivial Standards from Polymer Laboratories (10 standards, ranging from 580 $g.mol^{-1}$ to 3,000,000 $g.mol^{-1}$).

3.3.2 Liquid chromatography under critical conditions (LCCC)

Experiments were carried out on a conventional liquid chromatograph. The columns used were symmetry 300 C18 and Nucleosil 120 C18. The column oven temperature was set at 30 °C. The detectors used were a Waters 486 tunable absorbance UV detector, at a wavelength of 254 nm, and a Polymer Laboratories PL-EMD960 evaporative light scattering detector (ELSD). The settings were the following: nebuliser at 80 °C and evaporator at 90 °C, with a N_2 carrier gas flow rate 1 SLM (standard liters per minute). ACN-THF was used as eluent, at a flow rate of 0.5 mL/min.

3.3.3 Two-dimensional liquid chromatography

For the first dimension, the same setup was used as described for the LCCC analysis of blocks copolymers (see section 3.4.2). The flow rate was set at 0.05 mL/min in the first dimension. Sample fractions from the first dimension were collected in an eight-port valve system (VICI Valco EHC8W), which consisted of two loops, each having a sample capacity of 100 μL.

The second dimension comprised a Waters 510 pump delivering a flow rate of 4 mL/min. The column used was a Polymer Standards Service SDV (styrene divinylbenzene) column (pore size 5 μm, dimensions 300×8 mm). The same detectors were used for the analysis of the block copolymers at the critical point. Calibration in the second dimension was done with PS standards.

Sample fractions collected in the first dimension were automatically injected into the second dimension. Data acquisition and processing were automatically performed by the Polymer Standards Service software, WINGPC 7.

3.3.4 Nuclear magnetic resonance (NMR) spectroscopy

Proton NMR spectra were recorded in $CDCl_3$, using a Varian Unity Inova 400 MHz NMR instrument and a Varian VXR 300 MHz NMR instrument.

3.4 Results and discussion

3.4.1 Hydroboration-hydroxylation of 1-decene to 1-decanol

The hydroboration-hydroxylation reaction of 1-decene occurs according to anti-Markovnikov addition, were a water molecule adds across a double bond.[39] However, some Markovnikov addition may take place.[40] The model compound 1-decene was used to study the yield percentage of hydroboration-hydroxylation of the terminal double bond and the efficacy of the hydroboration of unsaturated end function groups. The hydroboration reaction was carried out according to a procedure reported in the literature.[41] ^{1}H-NMR data show that the hydroboration and oxidation of 1-decene was successful; the yield was 91.66 mol%, which does, however, mean that not all the 1-decene underwent hydroboration. This will later affect the block and graft formation reactions when the system is applied on PS macromonomers. ^{1}H-NMR analysis of the reaction mixture also confirmed the presence of isomers as byproducts, as illustrated in Figure 3.1. Unreacted 1-decene was confirmed by the presence of the vinyl double bond in the region δ 5.5-6 ppm, and it was 3.8 mol%.

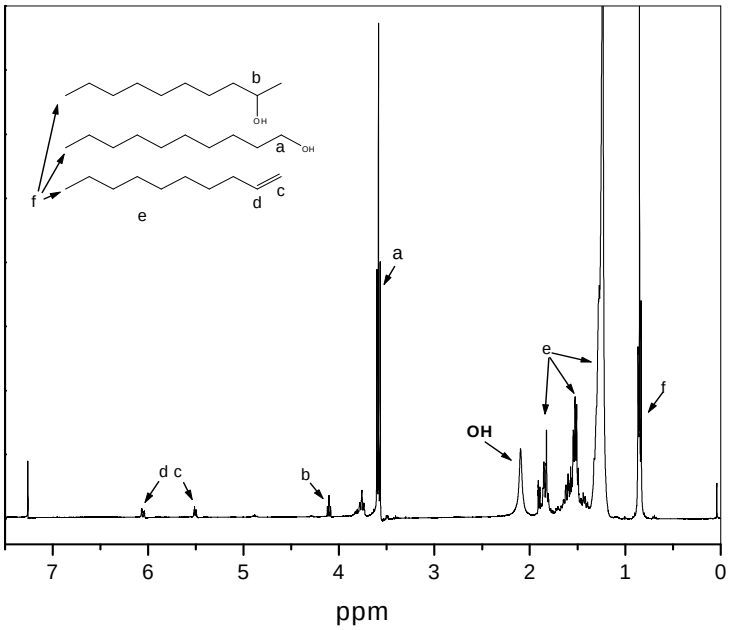

Figure 3.1: ^{1}H-NMR spectrum of the product of the reaction of 1-decene with 9-BBN. (Solvent: $CDCl_3$)

3.4.2 Optimizing the hydroboration-autoxidation reaction using methyl methacrylate monomer

Optimization of the hydroboration reaction, and subsequently the autoxidation reaction, were carried out according to a procedure described by Janvikul.[42] Two types of reactions are involved. The first reaction involves an α-terminated olefin chain and 9-decyl-9-borabicyclo[3.3.1]nonane as macroinitiator. In the second reaction, the 9-BBN initiates polymerization in the presence of the MMA monomer. Monomer conversion versus polymerization time and the M_n are shown in Figure 3.2. A high M_n was obtained at low conversion (5%). The maximum conversion achieved was 40%, and the PDI increased with conversion, reaching 2. This indicates that a 9-BBN-terminated polymer can initiate the polymerization of other monomers and that free 9-BBN in solution is also capable of initiating polymerization and could lead to the formation of homopolymer during the preparation of blocks or graft copolymers.

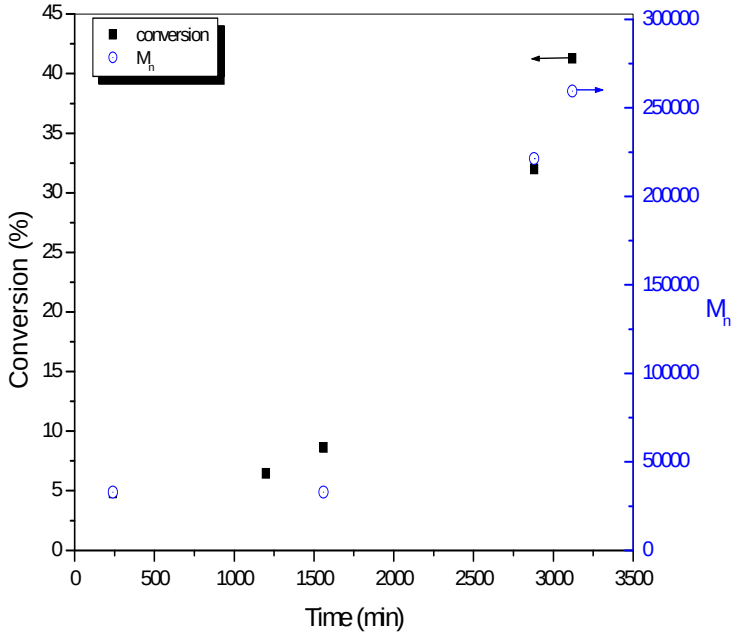

Figure 3.2: Conversion vs. time, and M_n, of autoxidation polymerization of MMA with 9-BBN.

3.4.3 Synthesis of styrene macromonomers

Styrene macromonomers were synthesized using the anionic polymerization technique in order to obtain products with narrow polydispersity and controlled molecular weight, according to the relationship:

$$M_{n\ (g/mol)} = (\text{styrene}_{\ (g)}) / (\text{BuLi}_{\ (mol)})$$

A general procedure for the preparation of styrene macromonomers terminated with allylchlorodimethylsilane is shown in Scheme 3.1.

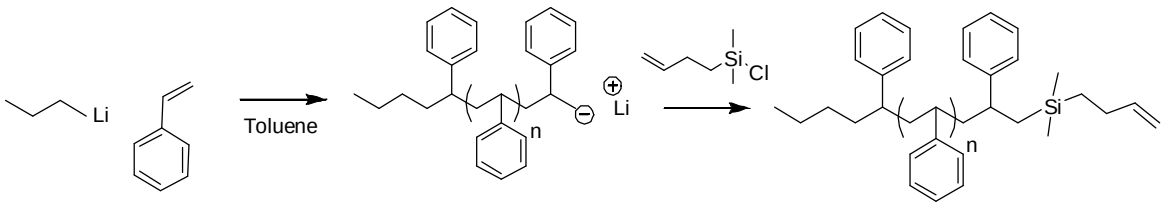

Scheme 3.1: Anionic polymerization of styrene in toluene, using n-BuLi as initiator, terminated via allylchlorodimethylsilane.

^{1}H-NMR spectra of the styrene macromonomers showed that the allyl functional groups of the terminating agent were present in the polymer after precipitation in methanol. Unreacted terminating agent was removed under vacuum. A ^{1}H-NMR spectrum of a styrene macromonomer terminated with an allyl group is shown in Figure 3.3 The peaks at δ 4.5-5.0 ppm and 5.5-5.8 ppm, corresponding to the allyl functional group, proved that the synthesis was successful.

The termination efficiency was calculated from the ratio of the methyl groups (CH_3) at δ 0.5-0.8 ppm of n-BuLi and the methylene group (CH_2) at δ 5-6 ppm of the allyl group in the ^{1}H-NMR spectra of macromonomers. Results revealed that not all the chains were terminated by the terminating agents. This had an effect on the hydroboration reaction and further copolymerization reactions. Termination efficiencies of 80% were obtained.

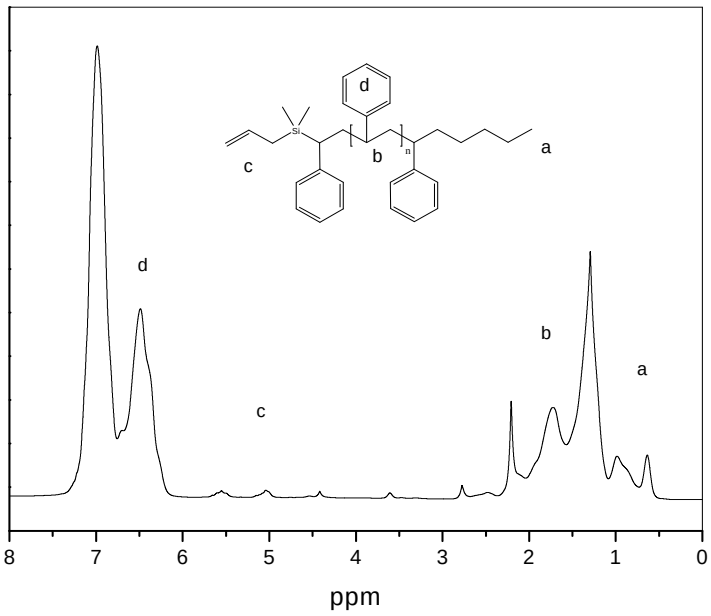

Figure 3.3: ^{1}H-NMR of PS macromonomer end-capped with allyldimethylsilane, showing the allyl functional end group to be used in further reactions (solvent: $CDCl_3$).

Table 3.1 shows the composition and characteristics of the products of the anionic polymerization of styrene macromonomer terminated by allyl functional groups (three different reactions PS_{allyl}). Equal molar amounts of terminating agent and initiator were used in these reactions. The values for termination efficiency illustrate that 20% of the styrene chains had died before the termination took place. High termination efficiency was nonetheless achieved.

Table 3.1: Compositions and characteristics, M_n, M_w, and PDI, of the styrene macromonomers terminated by an allyl functional group

	Sty (mmol)	BuLi (mmol)	M_n (g/mol)	M_w (g/mol)	PDI	Termination efficiency (%)*
$PS_{allyl}1$	96	2.2	3900	5200	1.3	~80
$PS_{allyl}2$	96	1.8	4800	5900	1.2	~80
$PS_{allyl}3$	48	0.5	9400	11400	1.2	~80

*determined by ^{1}H-NMR

3.4.4 Copolymerization reaction via hydroboration-autoxidation

The copolymerization of styrene macromonomers with MMA monomer to form block structures was performed by exposing a boron-terminated styrene macromonomer to oxygen.

The reaction mechanism of the hydroboration and subsequent autoxidation of styrene macromonomer is presented in Scheme 3.2. This scheme is based on that proposed by Chung and Lu[16] for the homolytic decomposing of peroxborane and the generation of the alkoxy radical and boronate radical. Accordingly, the formation of the block or the graft copolymers is the responsibility of the alkoxy radical (II) that is formed during the homolytic cleavage of peroxyborane (I), and not the boronate radical (III), which they claim is stable and does not initiate radical polymerization. Since they used the hydroboration-autoxidation reaction with polyolefins, the analysis of the produced polymers was limited to the use of high temperature SEC, FTIR and NMR, which cannot tell if the polymer is a block or simply a blend. Thus, the possibility of forming homopolymer via free 9-BBN during the hydroboration-autoxidation reaction of a polyolefin is not fully explored. Consequently, it was considered to be important to study and understand the role of free 9-BBN and the boronate radical in producing homopolymer using the PS-block-PMMA copolymer system and various chromatographic techniques to study the produced polymers.

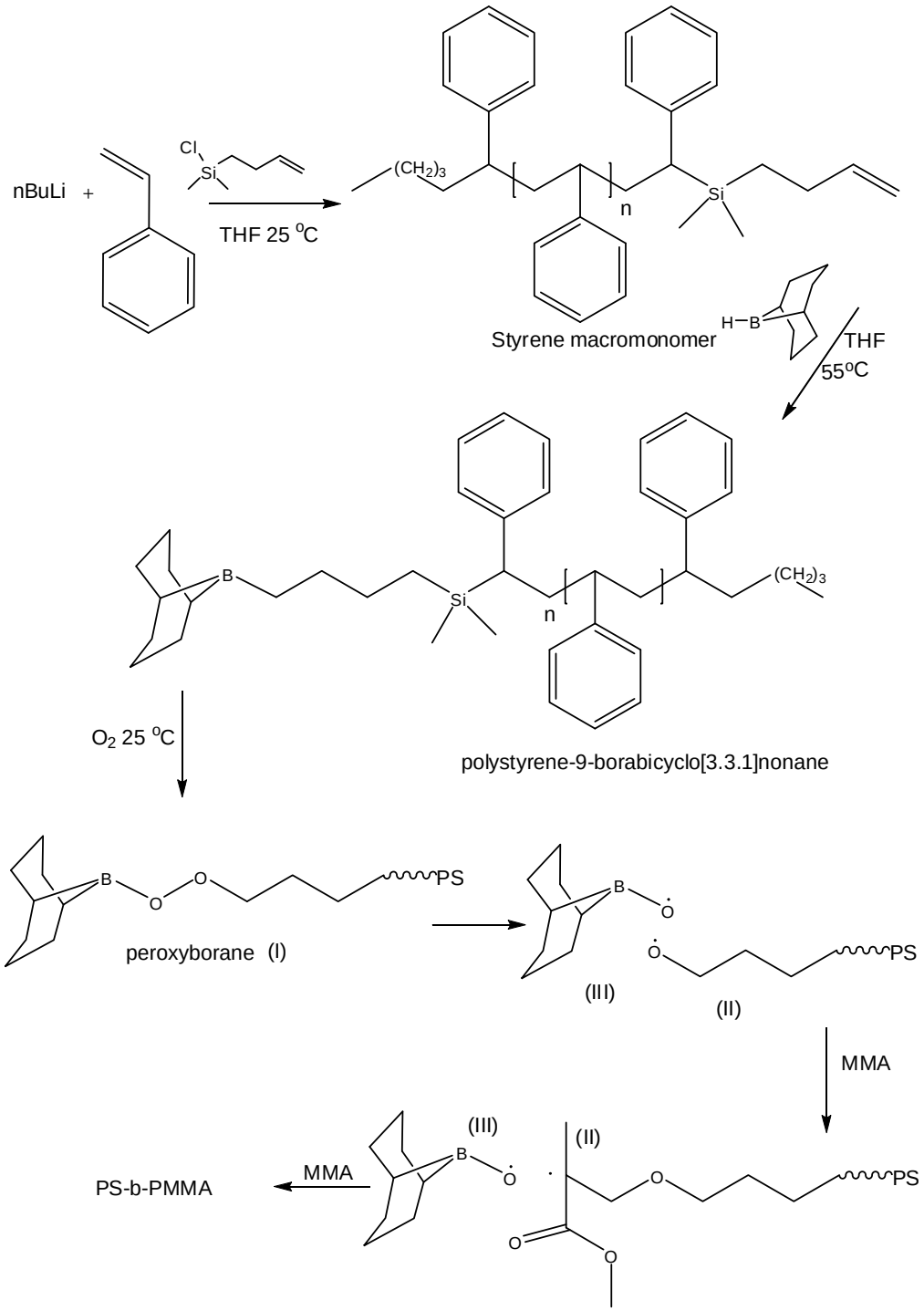

Scheme 3.2: Hydroboration and subsequent autoxidation of styrene macromonomer based on scheme by Chung et al.[16]

Three styrene macromonomers with different styrene lengths ($PS_{allyl}1$, $PS_{allyl}2$, and $PS_{allyl}3$), as mentioned in Table 3.1, were used to determine the effect of the styrene segment length on the polymerization and the role of the boronate radical in initiating homopolymerization. A predetermined quantity of 9-BBN (number of moles) equal to the number of moles of the allyl end functional group was added to the styrene macromonomer to ensure that all 9-BBN underwent hydroboration and that

no free 9-BBN was left in the solution before the MMA monomer was added. However, results obtained for the hydroboration of 1-decene showed that about 8% of 9-BBN did not undergo hydroboration.

The results reported in this chapter are those for the $PS_{allyl}2$ macromonomer and its reaction with MMA monomer, unless otherwise stated.

Figure 3.4 shows the SEC chromatograms of $PS_{allyl}2$ for the copolymerization of PS-b-PMMA via 9-BBN. There is a shift in the average molar mass from a low molar mass towards a high molar mass as the reaction proceeds. Some unreacted styrene or unfunctionalized macromonomer is left even after 24 h. This was also observed in the copolymerization reactions of $PS_{allyl}1$ and $PS_{allyl}3$, as shown in Figure 3.5.

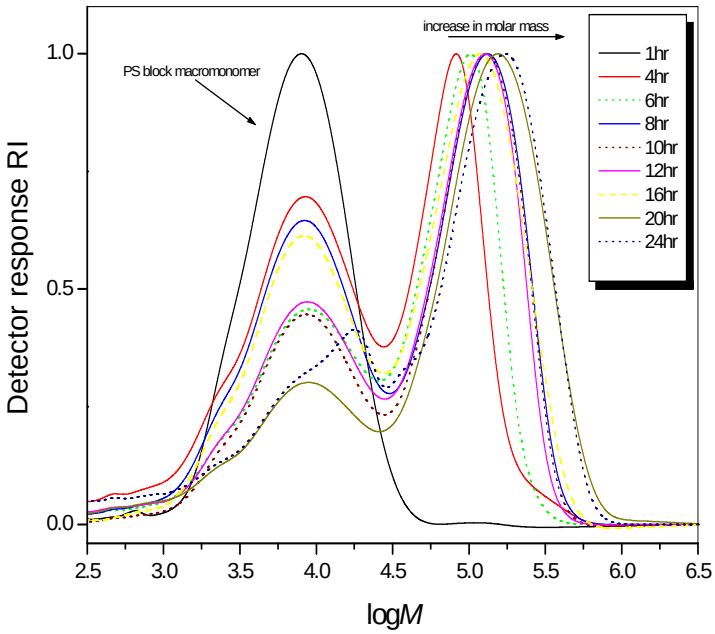

Figure 3.4: SEC traces of conversion reaction of block formation PS_{ally2}-b-PMMA showing molar mass distributions with increasing conversion.

The block length of the styrene macromonomer does not have any effect on the chain extension polymerization reaction, as can be seen in Figure 3.5. The block length of the first segment does not have any effect on the polymerization via the hydroboration-autoxidation reaction.

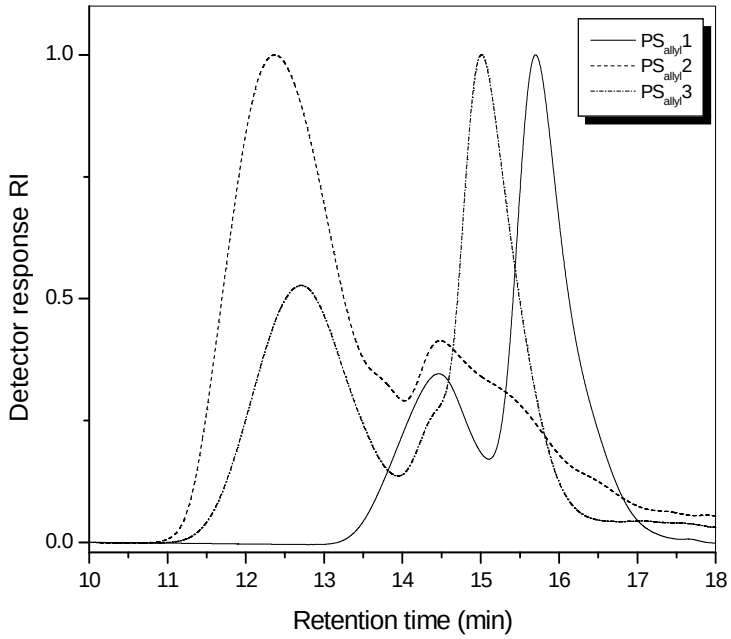

Figure 3.5: SEC traces of the product of the three copolymerization reactions to yield: $PS_{allyl}1$, $PS_{allyl}2$, and $PS_{allyl}3$.

Figure 3.6 shows the monomer conversion versus time for the block copolymer reaction. The conversion increased with time, and the molar mass of the copolymer increased (M_w of the second peak in Figure 3.4). After 24 h, the highest conversion achieved was about 65%.

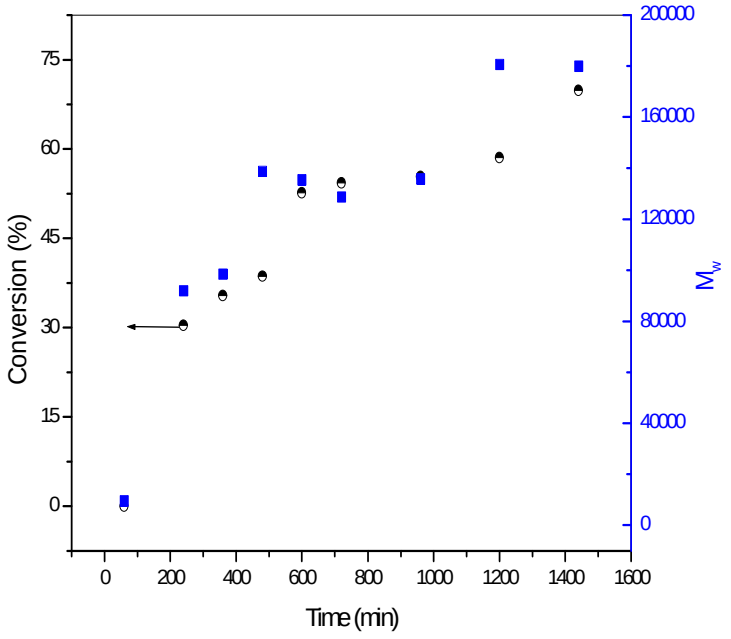

Figure 3.6: Monomer conversion versus time for the block copolymer reaction of PS_{ally2}-b-PMMA via hydroboration-autoxidation.

An attempt to extract unreacted PS from the reaction mixture was considered. A solution mixture of heptane/cyclohexane was used as solvent for PS and

nonsolvent for block copolymer PS-b-PMMA and PMMA homopolymer. The results were not conclusive due to co-precipitation of PS macromonomers with the block, as shown in Figure 3.7. A shoulder at high retention time is seen with RI and UV response. This indicated the presence of PS homopolymer that co-precipitated with the block copolymer PS-b-PMMA.

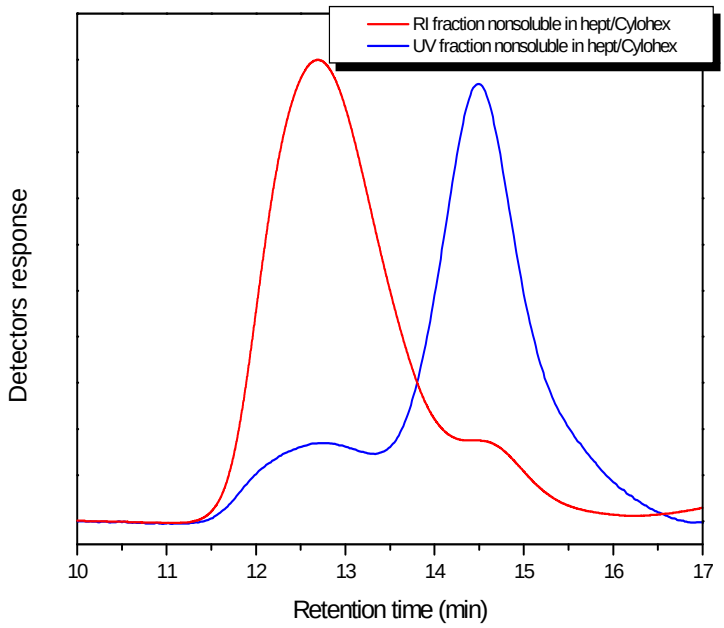

Figure 3.7 SEC traces of PS_{ally2}-b-PMMA after solvent extraction (heptane/Cyclohexane).

Due to the air sensitivity of the borane-terminated styrene macromonomer, the ^{1}H-NMR analysis also proved very difficult to carry out. However, after the copolymerization and block formation reaction, ^{1}H-NMR analyses were carried out on the reaction mixture. The results show that 2.8% of styrene macromonomer are unfunctionalized and are therefore not able to initiate block formation. This inevitably meant that some free 9-BBN is present in the reaction solution, which may initiate homopolymerization.

3.4.5 Chromatographic analysis at the critical point of adsorption of styrene

In order to separate the block from their homopolymers and determine the chemical composition of the block copolymers, chromatographic analyses were carried out on the samples at the critical point of adsorption of styrene. According to literature, mixtures of THF-ACN as mobile phases are well suited for establishing critical conditions of styrene. [29,32,43,44] When using a set of non-polar C18 stationary phases (300, 100 μm), PS will elute at critical conditions, whereas PMMA will elute in the SEC mode.

The composition at which the critical point was determined was a 51.7-48.3 ACN-THF mobile phase mixture. Figure 3.8 shows three modes of separation in the liquid chromatography of polystyrene.

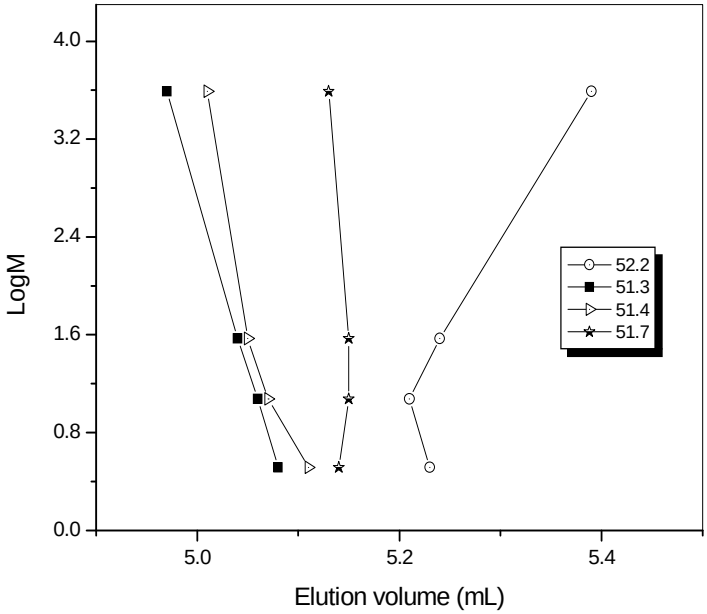

Figure 3.8: Molar mass versus elution volume of narrow PS standards using ACN/THF as eluent, in different ratios: 52.2, 51.7, 51.4, and 51.3 vol%. Experimental: columns symmetry C18 5 micro and Nucleosil C18. of ACN. Sample solvent was 50/50 eluent. Flow rate of 0.5mL/min, injection volume 20 mL, and polymer concentration was 5.0 mg/mL. The critical condition was at elution mixture 51.7.

Figure 3.9 shows the separation of the block copolymer PS-b-PMMA from unreacted PS macromonomer under the critical conditions for PS. The block copolymer and MMA homopolymer elute in SEC mode, as explained earlier (Section 3.1.2). The large molecules elute first, followed by the small ones, and then the unreacted styrene macromonomer elutes at the critical point of styrene. There is a very weak UV detector response for the first elution peak, indicating that at least some block formation has occurred. The weak response is reflective of the fact that the styrene block only has a molar mass of 6,000 g/mol, while the block molar mass is 120,000 g/mol (20 times higher than the PS macromonomer). In addition to this, the block copolymer co-elutes with any homo-PMMA that forms as a result of initiation by the borinate radical or free 9-BBN in solution.

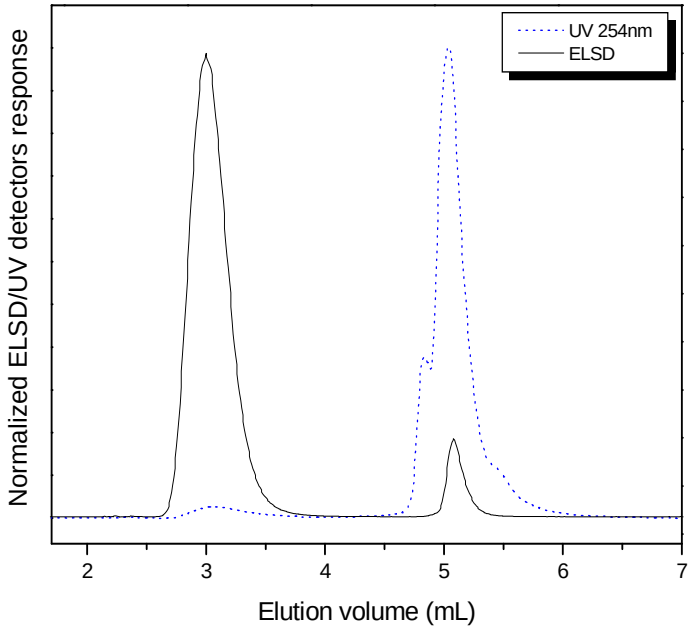

Figure 3.9: Separation to the block copolymer PS-b-PMMA under the critical conditions for styrene.

Figure 3.10 shows the contour plots of the online 2D-LC separation of the block copolymer. The separation is accomplished in two different directions of molecular heterogeneity: in one direction the separation occurs according to chemical composition, while in the other it is according to the molar mass or hydrodynamic volume. Good separation between the styrene macromonomer and block copolymer is obtained using the LCCC of PS in the first dimension (presented on y-axis) and SEC in the second dimension (presented on the x-axis).

The molar mass calibration in the second dimension was carried out using PMMA calibration standards. Thus, the molar mass of the block can be calculated based on that calibration. Furthermore, the relative amounts of the components can be determined. The elution of the block copolymer PS-b-PMMA is dependent on the chain length of PMMA, with a broader area indicating different chemical composition of the block. The higher molar mass copolymer elutes first, followed by the lower molar mass polymer. The styrene macromonomer elutes in a relatively narrow area, and no chemical composition distribution is seen (as expected).

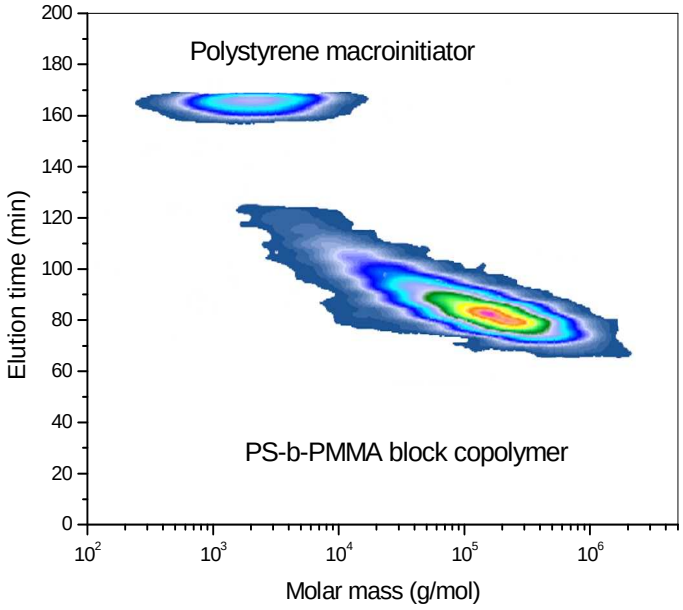

Figure 3.10: 2D-LC contour plots of the block copolymer PS_{ally2}-b-PMMA showing separation of the block copolymer and the unreacted styrene macromonomer. First dimension: critical conditions for PS, flow rate 0.05 mL/min; second dimension: SEC, flow rate 4 mL/min. (Experimental conditions as described in the text.)

The molar mass of the second peak in the 2D analysis was determined using PMMA calibration standards, and hence the molar mass of the block could be calculated based on that calibration. Table 3.2 tabulates these results.

Table 3.2: 2D data of M_n and M_w of the block copolymers, obtained using PMMA calibration standards

	M_n (g/mol)	M_w (g/mol)		M_n (g/mol) *10^2	M_w (g/mol) *10^2
$PS_{allyl}1$	2900	4400	PS-b-PMMA	220	350
$PS_{allyl}2$	4700	7600	PS-b-PMMA	140	220
$PS_{allyl}3$	9100	11400	PS-b-PMMA	160	260

3.4.6 Chromatographic analysis at the critical point of adsorption of methyl methacrylate

As mentioned above, there is a strong indication that PMMA homopolymerization has occurred. Analysis under the critical conditions of PS does not allow for determination of the presence of the PMMA homopolymer, since the PMMA homopolymer and the block copolymer may co-elute. Therefore, determination of the critical point of PMMA was also carried out in order to determine the amount of the PMMA homopolymer formed during the hydroboration-autoxidation reaction. Figure 3.11 shows the three modes of LC separation obtained according to the method developed by Pasch.[35,45] MEK-cyclohexane was used as a mobile phase, and the polar stationary phase was Nucleosil Si 300. The critical point was obtained

at composition MEK 77/ cyclohexane 23; the PMMA homopolymer eluted at the critical point and the PS block, and PS homopolymer eluted in the SEC mode.

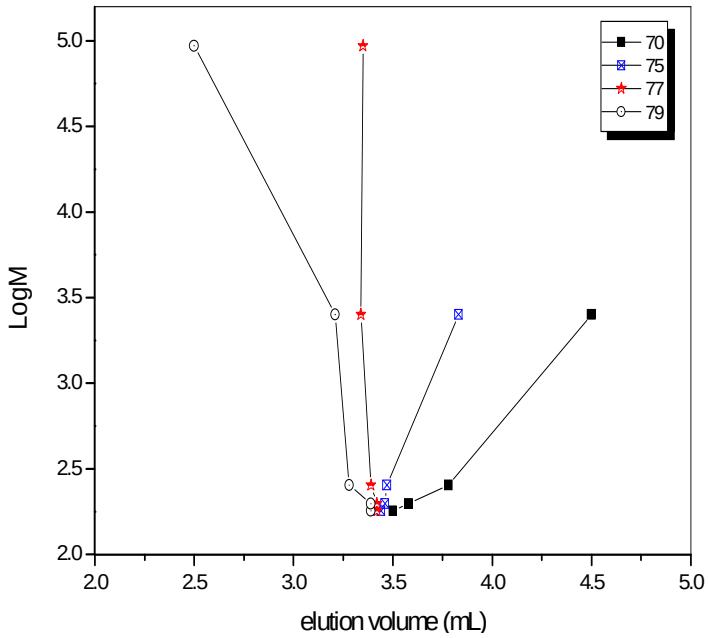

Figure 3.11: Molar mass versus elution volume of narrow PMMA standards using MEK/Cyclohexane as eluent, in different ratios: 70, 75, 77 and 79 vol% of MEK. [Exp: column Nucleosil Si 300. Sample solvent was 70/30 eluent. Flow rate of 0.5mL/min, injection volume 20 mL, and polymer concentration was 2.0 mg/mL. The critical condition was at elution mixture 77].

Figure 3.12 illustrates the separation of the block copolymer PS-b-PMMA and PS homopolymer from PMMA homopolymer under critical conditions for PMMA. A significant amount of the PMMA homopolymer was obtained, which is a result of the mechanism of the hydroboration-autoxidation reaction and presence of free 9-BBN.

The amount of the PMMA homopolymer formed was estimated from the SEC traces by deconvolution through multiple peak fitting, assuming a Lorentzian line shape, using the software package Origin 7.0. The percentage area of the PMMA homopolymer represented by narrow sharp peak at elution volume 3.38 mL was 17.53%.

The presence of PMMA homopolymer in the reaction mixture indicates that the 9-BBN does not completely react with the allyl functional groups (as observed in the hydroboration reaction of 1-decene). This free 9-BBN initiates free radical polymerization of PMMA, and this is the mostly likely means of homoploymer formation.

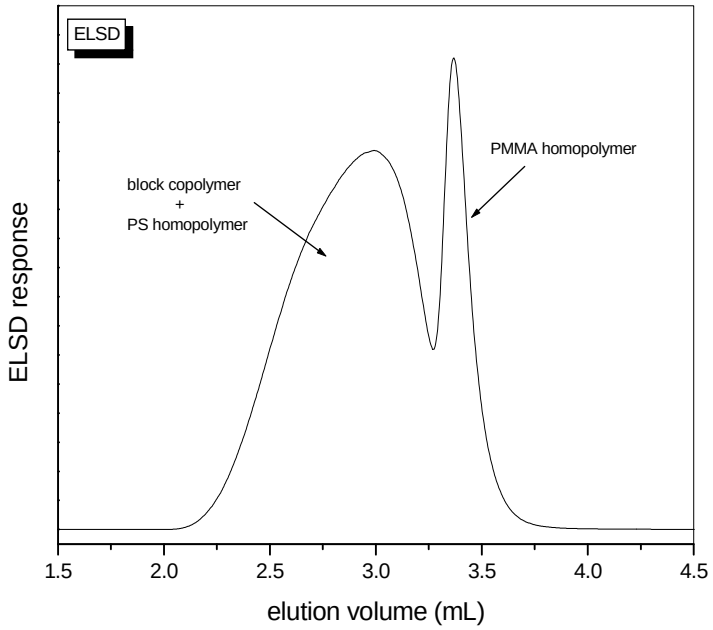

Figure 3.12: Example of separation of the block copolymer PS_{ally2}-b-PMMA under the critical conditions for MMA.

3.5 Conclusions

A combination of anionic polymerization and the autoxidation of a borane adduct was achieved to prepare block copolymers PS-b-PMMA. The results show there is no effect by the chain length of the first segment on the block formation. LCCC analysis of styrene and MMA showed a significant amount of PMMA homopolymer was formed during the polymerization via selective oxidation of borane-terminated PS. This was attributed to the presence of free 9-BBN and the activity of the boronate radical. The results presented in this chapter indicate that in the subsequent use of the hydroboration technique for the synthesis of the graft copolymers, it can be expected that significant homopolymerization will occur during the grafting step due to either the incomplete reaction of the 9-BBN with the vinyl reactive sites or by initiation of boronate radical, which up to now has been proposed as not reactive enough to initiate homopolymerization.

3.6 References:

1. Nakashima, K.; Bahadur, P. *Advances in Colloid and Interface Science* **2006,** 123-126, 75-96.
2. Erhardt, R.; Zhang, M.; Boker, A.; Zettl, H.; Abetz, C.; Frederik, P.; Krausch, G.; Abetz, V.; Muller, A. H. E. *Journal of the American Chemical Society* **2003,** 125, 3260-3267.
3. Ullal, C. K.; Schmidt, R.; Hell, S. W.; Egner, A. *Nano Letters* **2009,** 9, 2497-2500.
4. Hadjichristidis, N.; Pispas, S. *Advances in Polymer Science* **2006,** 200, 37-55.
5. Baskaran, D.; Muller, A. H. E. *Progress in Polymer Science* **2007,** 32, 173-219.
6. Smid, J.; Beylen, M. V.; Esch, T. E. H. *Progress in Polymer Science* **2006,** 31, 1041-1067.
7. Kobatake, S.; Harwood, H. J.; Quirk, R. P.; Priddy, D. B. *Macromolecules* **1998,** 31, 3735-3739.
8. Acar, M. H.; Matyjaszewski, K. *Macromolecular Chemistry and Physics* **1999,** 200, 1094-1100.
9. Korczagin, I.; Hempenius, M. A.; Vancso, G. J. *Macromolecules* **2004,** 37, 1686-1690.
10. Mahajan, S.; Renker, S.; Simon, P. F. W.; Gutmann, J. S.; Jain, A.; Gruner, S. M.; Fetters, L. J.; Coates, G. W.; Wiesner, U. *Macromolecular Chemistry and Physics* **2003,** 204, 1047-1055.
11. Chung, T. C.; Lu, H. L.; Janvikul, W. *Polymer* **1997,** 38, 1495-1502.
12. Chung, T. C.; Janvikul, W.; Bernard, R.; Jiang, G. J. *Macromolecules* **1994,** 27, 26-31.
13. Naga, N.; Tsuchiya, G.; Toyota, A. *Polymer* **2006,** 47, 520-526.
14. Eroglu, M. S.; Hazer, B.; Ozturk, T.; Caykara, T. *Journal of Applied Polymer Science* **2005,** 97, 2132-2139.
15. Chung, T. C.; Janvikul, W.; Bernard, R.; Hu, R. *Polymer* **1995,** 36, 3565-3574.
16. Chung, T. C.; Lu, H. L. *Journal of Molecular Catalysis A: Chemical* **1997,** 115, 115-127.
17. Chung, T. C.; Rhubright, D.; Jiang, G. J. *Macromolecules* **1993,** 26, 3467-3471.
18. Lu, B.; Chung, T. C. *Macromolecules* **1999,** 32, 2525-2533.
19. Lu, B.; Chung, T. C. *Macromolecules* **1998,** 31, 5943-5946.
20. Guoqiang, F.; Dong, J. Y.; Wang, Z.; Chung, T. C. *Journal of Polymer Science: Part A: Polymer Chemistry* **2006,** 44, 539-548.

21. Pasch, H.; Trathnigg, B., *HPLC of Polymers*. Springer: New York, 1998.

22. Macko, T.; Hunkeler, D.; Berek, D. *Macromolecules* **2002,** 35, 1797-1804.

23. Pasch, H.; Mequanint, K.; Adrian, J. *e-Polymers* **2002,** 5, 1-19.

24. Olesik, S. V. *Analytical and Bioanalytical Chemistry* **2004,** 378, 43-45.

25. Raust, J. A.; Brull, A.; Moireb, C.; Farcet, C.; Pasch, H. *Journal of Chromatography A* **2008,** 1203, 207-216.

26. Sato, H.; Mitstani, K.; Shimizu, I.; Tanaka, Y. *Journal of Chromatography* **1988,** 447, 387-391.

27. Sato, H.; Takeuchi, H.; Tanaka, Y. *Macromolecules* **1986,** 19, 2613-2617.

28. Kawai, E.; Shimoyama, K.; Ogino, K.; Sato, H. *Journal of Chromatography A* **2003,** 991, 197-203.

29. Macko, T.; Hunkeler, D. *Advances in Polymer Science* **2003,** 163, 61-136.

30. Zimina, T. M.; Kever, J. J.; Melenevskaya, E. Y.; Fell, A. F. *Journal of Chromatography* **1992,** 593, 233-241.

31. Falkenhagen, J.; Weidner, S. *Analytical Chemistry* **2009,** 81, 282-287.

32. Pasch, H.; Rode, K. *Polymer* **1998,** 39, 6377-6383.

33. Pasch, H.; Rode, K. *Macromolecular Chemistry and Physics* **1996,** 197, 2691-2701.

34. Pasch, H.; Rode, K.; Chaumien, N. *Polymer* **1996,** 37, 4079-4083.

35. Pasch, H. *Polymer* **1993,** 34, 4095-4099.

36. Im, K.; Park, H. W.; Kim, Y.; Ahn, S.; Chang, T.; Lee, K.; Lee, H. J.; Ziebarth, J.; Wang, Y. *Macromolecules* **2008,** 41, 3375-3383.

37. Siewing, A.; Lahn, B.; Braun, D.; Pasch, H. *Journal of Polymer Science: Part A: Polymer Chemistry* **2003,** 41, 3143-3148.

38. Chung, T. C.; Janvikul, W.; Lu, H. L. *Journal of the American Chemical Society* **1996,** 118, 705-706.

39. Daley, R. F.; Daley, S. J., Electrophilic addition to unsaturated carbons. *Organic Chemistry*, 2005; Chapter 14, 727-731.

40. Knights, E. F.; Brown, H. C. *Journal of the American Chemical Society* **1968,** 90, 5281.

41. Sigma-Aldrich Technical Bulletin LA 218. http://www.sigmaaldrich.com/etc/medialib/docs/Aldrich/Bulletin/al_techbull_al218.Par.0001.File.tmp/al_techbull_al218.pdf (22-7-2010),

42. Janvikul, W. Functionalization of polyolefins via borane/oxygen chemistry: synthesis and reaction mechanism study. PhD thesis. Pennsylvania State University, USA, 1997.

43. Phlllpsen, H. J. A.; Klumperman, B.; Herk, A. M. v.; German, A. L. *Journal of Chromatography A* **1996,** 727, 13-25.

44. Lee, H. C.; Chang, T. *Macromolecules* **1996,** 29, 7294-7296.

45. Pasch, H.; Brinkmann, C.; Gallot, Y. *Polymer* **1993,** 34, 4100-4104.

CHAPTER 4

A NEW APPROACH TO THE PREPARATION OF GRAFT COPOLYMERS BY A COMBINATION OF RAFT AND THE BORANE APPROACH

This chapter discusses the synthesis and characterization of graft copolymers prepared via combining living free radical polymerization RAFT with autoxidation of the borane side chain polymer adducts.

4.1 Introduction

Polymerization of monomers containing two double bonds of different reactivities may result in regioselective reactions.[1-4] Due to this difference in reactivity, the chain-growth reaction occurs preferentially at the more favorable reactive vinyl double bond to form the primary chain, leaving the allyl group as a pendant group. Regardless of the low reactivity of the allyl group, some allyl functional groups are still able to react with propagating free radicals, leading to the formation of branch points. Consequentially, branch polymerization will commence, which eventually leads to gelation.

Syntheses of homo/copolymers contenting an allyl group as a side chain has been addressed by many scientists. Matsumoto et al.[5-9] carried out studies on the free radical polymerization of allyl methacrylate under different reaction conditions and found that a delayed in the gelation reaction was caused by the steric effect of long chain alkyl methacrylates in the copolymerization. Paris and De la Fuente[10-14] studied gel formation in the homo/copolymerization of allyl methacrylate under different conditions, using living free radical polymerization, mainly ATRP. They found that an increase in initiator concentration increases the process of gel formation. They also found that a decrease in the polymerization temperature advances the gelation process. Zhang and Ruckenstein[15] prepared an allyl methacrylate polymer via a living anionic polymerization technique and found that (1,1-diphenylhexyl) lithium and living oligomers of methyl methacrylate and tert-butyl methacrylate are suitable initiators, in temperature range -30 to -60 ^{o}C, in the presence of LiCl, for living polymerization. Chain transfer agents[5] and RAFT[16] have been studied in terms of gelation formation and the synthesis of hyperbranched polymers.

Yu et al.[17] investigated the gelation behaviors of allyl methacrylate in the presence of an increasing amount of RAFT agent and found that the gel point is significantly postponed with an increase in the amount of RAFT agent used.

In the present study, a combination of living free radical polymerization (RAFT) and the hydroboration-autoxidation of a borane adduct was used to prepare graft copolymers using the "grafting from" technique. The synthesis of a well-controlled polymer via RAFT techniques was carried out to produce the polymer backbone. The selected polymer must have a functional group capable of undergoing a hydroboration-autoxidation reaction. Copolymerization of styrene, MMA, or BA with AM gives the opportunity to introduce an allyl functional group into the main chain. Consequently, graft formation using the hydroboration-autoxidation reaction of borane adducts was carried out.

RAFT-mediated AM polymerization was carried out in solution. Kinetic studies of the homopolymerization of AM and the possibility of cross-linking reaction's taking place was considered.

RAFT-mediated copolymerization of styrene, MMA, and BA with AM was carried out. The focus will be on the copolymerization of AM with styrene and the consequent graft reaction via the hydroboration-autoxidation reaction in the presence of MMA.

Kinetic study of the copolymerization of styrene and AM was carried out for three different comonomer contents, 5, 10 and 20% AM.

The possibility of homopolymer formation during the copolymerization via hydroboration-autoxidation of the copolymer was also considered.

Characterization of the graft copolymers (PS-co-AM)-g-PMMA were carried out using chromatographic techniques and NMR.

4.2 Experimental

4.2.1 Materials

The following reagents were used as received: methanol (Sigma-Aldrich, 99.8%), tetrahydrofuran (THF Sigma-Aldrich, HPLC grade), acetonitrile (ACN; Sigma-Aldrich, HPLC grade), n-heptane (Sigma-Aldrich, HPLC grade), 0.5 M 9-BBN (Sigma-Aldrich in THF solution), deuterated chloroform as NMR solvent ($CDCl_3$; Cambridge Isotope Laboratories), 2,2`-Azobis (isobutyronitrile) (AIBN) (Riedel de Haen, 99%), recrystallized from ethanol prior to use.

Diethyl ether (Merck, 98%), hydrochloric acid (HCl Merck, 32%), bromobenzene (Fluka, 98%), carbon disulfide (CS_2 Merck, 99.5%), carbon tetrachloride (CCl_4 LabChem, 99.5%), dimethyl sulfoxide (DMSO Sigma-Aldrich) magnesium sulphate (Merck), absolute ethanol (Sigma-Aldrich), dichloromethane (Sigma-Aldrich), chloroform (Sigma-Aldrich, 99%), n-hexane (Sigma-Aldrich 99%), PS and PMMA

standards (Polymer Laboratories), and oxygen gas (Afrox) were used. The oxygen gas was transferred from a pressure-equalized vessel at atmospheric pressure and was therefore assumed to be at atmospheric pressure.

The monomers, styrene, MMA, and BA (Plascon Research) and allyl methacrylate (AM Sigma-Aldrich) were purified to remove the inhibitors and any impurities. The monomer was first washed with 0.3 M potassium hydroxide solution to remove the hydroquinone inhibitor and then distilled under reduced pressure and low heat (about 35 °C) to avoid self-polymerization of the monomer. The distilled fraction was collected and dried over anhydrous magnesium sulphate (Merck) to ensure a completely dry monomer.

Toluene (Analytical Reagent, 99.9%) and THF (Sigma-Aldrich, 99.9%) were purified prior to use by distilling over small pieces of sodium metal (SaarChem) and benzophenone (Fluka, 99%)[18-20] under an argon atmosphere for several hours. A deep blue-green color, attributed to the formation of the benzophenone ketyl radical, indicated when the solvent was dry and ready for use. (THF used in experiments was considered dry and O_2 free.)

4.2.2 Synthesis of 2-cyanoprop-2-yl dithiobenzoate

The method used for the synthesis of RAFT is based on the method described by McLeary.[21] Magnesium turnings (1 g, 40 mmol) with crystals of iodine as catalyst and THF (~10 mL) were placed in a 250 mL three-necked round bottom flask, fitted with two dropping funnels, containing bromobenzene (6.28 g, 40 mmol) in one and THF (30 mL) in the other. A few drops of bromobenzene were added from the dropping funnel into the flask. The content of the reaction flask was then heated gently, with stirring, until the reaction commenced as indicated by the disappearance of the yellow color of the iodine and the appearance of a clear white solution. A few drops of THF and the remainder of the total volume of bromobenzene were added from the dripping funnels. The reaction was allowed to proceed at room temperature for 10 min. Anhydrous carbon disulfide (3.05 g, 40 mmol) was added drop-wise over a period of 15 min. The mixture was diluted by the addition of cold water 250 mL and three times diethyl ether 100 mL. Then 33% fuming hydrochloric acid (0.2 M, 200 mL) was added. The organic extract was washed with water and dried over anhydrous magnesium sulphate.

The prepared benzenecarbodithioc acid was reacted with DMSO (6.25 g, 80 mmol) and a crystal of iodine as catalytic reagent in absolute ethanol (100 mL). The reaction mixture turned pink when crystals formed. The crystals were placed in 250

mL three-necked round bottom flask. To this was added AIBN (20 mmol) dissolved in ethyl acetate (100 mL). The reaction mixture was refluxed under nitrogen gas for 24 h. The solvent was removed under vacuum. The resulting product was dissolved in dichloromethane, and purified by column chromatography on silica gel, using chloroform: n-hexane (1:10) as eluent.

^{1}H NMR ($CDCl_3$) δ: 1.95 (s, 6H, 2xCH_3), 7.38 (dd, 2H, meta-ArH), 7.57 (dd, 1H, para-ArH) and 7.92 (d, 2H, ortho-ArH). ^{13}C NMR ($CDCl_3$) δ: 26.5 (CH3), 41.7 (C(CN)), 120.0 (CN), 126.6, 128.5, 132.9, 144.5 (ArC) and 227 (C=S).

4.2.3 RAFT-mediated allyl methacrylate polymerizations

Solution polymerization was carried out using AM, toluene, and AIBN as monomer, solvent, and initiator, respectively, and RAFT agent (CPDB). In a typical experiment, a 100 mL round bottom flask was charged with AM (40 mmol), CPDB (0.05 mmol), AIBN (0.005 mmol), and toluene (10 mL). A magnetic stirrer bar was placed in the flask, and the homogeneous solution was purged with dry argon at room temperature for 15 min in order to remove the oxygen from the system. The polymerization was carried out at 70 ^{o}C and was run for 24 h. The conversion was determined gravimetrically.

4.2.4 RAFT-mediated copolymerization of styrene and allyl methacrylate

Solution polymerizations were carried out at 70 ^{o}C in toluene solution, (50% v/v), with a constant monomer/initiator concentration ratio of (800:0.1). A 100 mL round bottom flask was charged with AM (15.3 mmol), styrene (76 mmol), AIBN (0.0114 mmol) and CPDB (0.114 mmol) and toluene (10 mL). The concentration of the various compounds used for all the experiments are listed in Table 4.1. The homogeneous solution was purged with argon for 15 min to remove the oxygen from the system.

Table 4.1 shows that the AM mol % in the copolymers is greater than that in the feed. This is a result of the difference in the reactivity ratios between the styrene and AM monomers.[22-24]

Table 4.1: Compositions and characteristics of PS-co-AM prepared via free radical polymerization in the presence of RAFT agent CPDB

Sty (mmol)	AM (mmol)	CTA (mmol) *10^{-2}	AIBN (mmol) *10^{-3}	AM mol % in feed	M_n (g/mol)	M_w (g/mol)	PDI	AM mol % copolymer (^{1}H-NMR)
76	3.8	9.9	9.9	5	14000	17500	1.2	5.3
76	7.6	10.4	10.4	10	12500	15700	1.2	13.3
76	15.3	11.4	11.4	20	14900	19000	1.2	34.3

4.2.5 RAFT-mediated copolymerization of methyl methacrylate and allyl methacrylate

All copolymerizations were carried out at 70 ^oC in toluene solution, (50% v/v), and with a constant monomer/initiator concentration ratio of 100:0.1, degassed monomers AM (40 mmol) and MMA (3.9 mmol), and toluene 10 mL, (previously bubbled with dry argon for at least 15 min) AIBN (4.9X10^{-5} mmol), and (CPDB) (4.9X10^{-4} mmol) were all added to a dry Pyrex tube. Next, the polymerization mixtures were carefully degassed by bubbling dry argon during 10 min. The ampoules were immediately placed in a thermostatic oil bath. The composition of the produced copolymer is shown in the Table 4.2.

Table 4.2: Compositions and characteristics of PMMA-co-AM prepared via free radical polymerization in presence of RAFT agent CPDB

MMA (mmol)	AM (mmol)	CTA (mmol) *10^{-4}	AIBN (mmol) *10^{-5}	AM mol % in feed	M_n (g/mol)	M_w (g/mol)	PDI	AM mol % copolymer (^{1}H-NMR)
47.5	1.97	4.9	4.9	5	6600	7600	1.1	4.2
45	3.95	4.9	4.9	10	5700	7100	1.2	9.8
40	3.90	4.9	4.9	20	6400	7800	1.2	19.8

4.2.6 RAFT-mediated copolymerization of butyl acrylate and allyl methacrylate

All copolymerizations were carried out at 70 ^oC in toluene solution, (50% v/v), with a constant monomer/initiator concentration ratio of 100:0.1, degassed monomers AM (31.2 mmol) and BA (3.9 mmol), and toluene 10 mL, (previously bubbled with dry argon for at least 15 min) AIBN (3.89X10^{-5} mmol), and (CPDB) (3.89X10^{-4} mmol) were all added to a dry Pyrex tube. Next, the polymerization mixtures were carefully degassed by bubbling dry argon during 10 min. The ampoules were immediately placed in a thermostatic oil bath. The composition of the produced copolymer is shown in the Table 4.3.

Table 4.3: Compositions and characteristics of PBA-co-AM prepared via free radical polymerization in presence of RAFT agent CPDB

BA (mmol)	AM (mmol)	CTA (mmol) *10^{-4}	AIBN (mmol) *10^{-5}	AM mol % in feed	M_n (g/mol)	M_w (g/mol)	PDI	AM mol % copolymer (^{1}H-NMR)
37	1.97	3.89	3.89	5	6600	8300	1.2	9.1
35.1	3.95	3.89	3.89	10	7500	10000	1.3	13.0
31.2	3.9	3.89	3.89	20	6100	8500	1.3	39.4

4.2.7 Functionalization and autoxidation of the copolymer by 9-BBN

Functionalization of the copolymer PS-co-AM and then subsequent copolymerization via 9-BBN was carried out according to the following process: 0.5 g PS-co-AM copolymer was placed in 100 mL round bottom flask containing THF (20 mL). The polymer was hydroborated by the addition of 9-BBN solution (0.0035 mmol) in THF. The polymer solution was stirred at 50 ℃ for 16 h. A functionalized PS-co-AM copolymer was then obtained. Dry uninhibited MMA (39.6 mmol) and THF 10 mL was added in all cases. The reaction was initiated by injecting O_2 gas directly into the solution. Total volume of 0.1 mL dry O_2 gas was injected over a period of 24 h. The O_2 gas was transferred from a pressure-equalized vessel at atmospheric pressure and was therefore assume to be at atmospheric pressure. The moles added were calculated using the standard gas equation.

The reaction mixture was stirred at room temperature for 24 h and then terminated by the addition of methanol. The crude polymer products were isolated by filtration and dried in a vacuum oven.

4.3 Characterization

4.3.1 Size exclusion chromatography

The SEC instrument used was comprised of the following units: Waters 1515 isocratic HPLC pump; Waters 717 plus Autosampler; Waters 2487 Dual λ Absorbance detector; Waters 2414 Refractive index (RI) detector at 30^o C. Data processing was performed using Breeze Version 3.30 SPA (Waters) software. A set of two PLgel (Polymer Laboratories) and a 5 μm Mixed-C (300×7.5 mm) columns connected in series along with a PLgel 5 μm guard column (50×7.5mm) was used. The columns were kept at a constant temperature of 30^o C. THF Chromasolve HPLC grade solvent (0.125% BHT stabilized) was used as mobile phase at a flow rate of 1 mL/min. Samples were dissolved in the stabilized THF at a concentration of 5

mg/mL, and 100 μL injection volumes were used. The system was calibrated using Polymer Laboratories Easivial PS Standards (10 Standards ranging from 580 $g.mol^{-1}$ to 3 000 000 $g.mol^{-1}$).

4.3.2 Gradient chromatography

Separations were achieved on a chromatographic system used for gradient HPLC analyses. It comprised a Waters 2690 Separations Module (Alliance) system comprising a degasser, a solvent mixing chamber, a pump, and an auto sampler. An evaporative light scattering detector, Polymer Laboratories PL-EMD960 (ELSD), was used and the Waters SAT/IN module. The ELSD was operated at 80° C with an N_2 carrier gas flow rate of 1 SLM (standard liters per minute). For data collection and processing, the software package WinGPC-Software v. 7.0 (Polymer Standards Service, Mainz, Germany) was used. Symmetry C18 column (particle size 5 μm, pore size 100 Å, and column dimensions 150 X 3.9 mm i.d.) was used for the separation of (PS-co-AM)-g-PMMA, and a Nucleosil 100 column (particle size 5 μm) was used for the separation of (PMMA-co-AM)-g-PBA. The flow rate was set at 1 mL/min for one-dimensional LC. THF and ACN (HPLC grade) were the solvents used in the mobile phase to the (PS-co-AM)-g-PMMA system and flow rate in (PMMA-co-AM)-g-PBA system was 0.5 mL/min, (THF) and n-heptane. Table 4.4 and 4.5 show the gradient profiles used for the reversed phase separation setups.

Table 4.4: Gradient profile for reversed phase separation of the (PS-co-AM)-g-PMMA

Time (min)	**0**	**2**	**12**	**14**	**15**	**16**
THF (%)	0	0	100	100	0	0

Table 4.5: Gradient profile for reversed phase separation of the (PMMA-co-AM)-g-BA

Time (min)	**0**	**1**	**11**	**17**	**20**	**23**
THF (%)	0	0	100	100	0	0

4.3.3 Nuclear magnetic resonance (NMR) spectroscopy

Proton NMR spectra were recorded in $CDCl_3$, using a Varian Unity Inova 400 MHz NMR instrument and a Varian VXR 300 MHz NMR instrument.

4.4 Results and Discussion

4.4.1 RAFT-mediated AM polymerizations

The homopolymerization of AM in free radical polymerization leads to cross-linked polymer even in the early stages of the polymerization.[5] Controlled polymerization techniques, living anionic polymerization,[15] and ATRP[11] have been used to prepare

soluble AM polymers, but at low conversions. Lin et al.[16] reported the preparation of the homopolymer AM via benzyl dithiobenzoate (BDB), but with low yield.

In this study, homopolymerization of AM in solution and the presence of the CPDB RAFT agent was carried out to study the effect of similar conditions of the reaction on the gel formation and how far the reaction can progress without cross-linking. The polymerization was carried out in toluene to obtain high polymer conversion because bulk polymerization or the use of polar solvents does not favor high conversions. Homopolymerization of AM in toluene (50% v/v) was carried out at 70 ^{o} C. The total monomer conversion versus M_n is presented in Figure 4.1 There was a linear increase in the molecular mass with conversion, followed by an increase in the polydispersity.

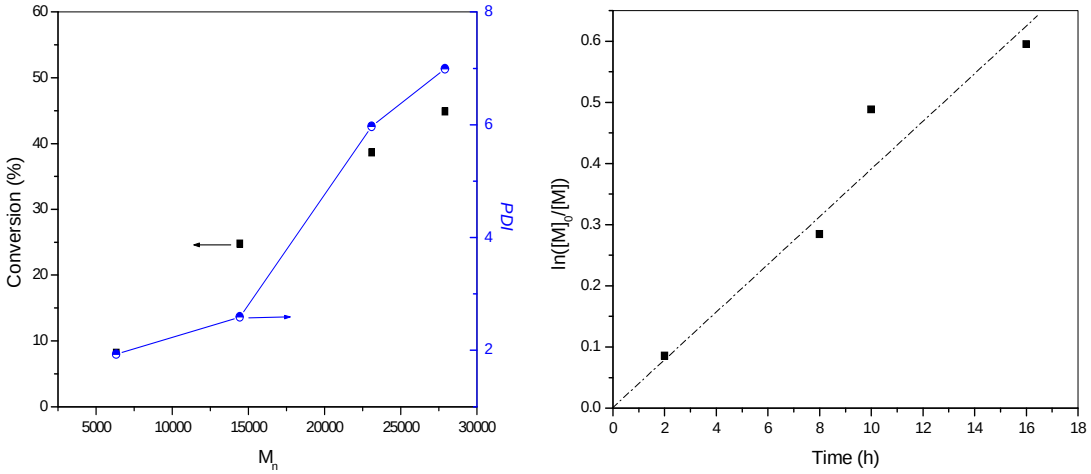

Figure 4.1: Conversion versus M_n and kinetic plot of the polymerization of AM in the presence of CPDB.

In the early stages, the molecular mass distribution is mono-modal. This is attributed to the regular chain growth reaction; an active radical is added to the methacrylyl group.[5] As the reaction proceeds, the dependence of M_n on conversion is no longer linear. This is consistent with the observation that molecular mass distributions become multimodal, which is an indication of the branching reaction that takes place, as will be discussed later. Table 4.6 shows the M_n and M_w of the PAM homopolymer at different stages of the reaction. There is an increase in the molar mass with an increase in the reaction time, followed by an increase in the PDI.

Table 4.6: SEC data of soluble fraction of PAM homopolymer

	M_n (g/mol)	M_w (g/mol)	PDI
PAM 2 h	6300	12200	1.9
PAM 8 h	14400	37400	2.5
PAM 10 h	23000	138000	5.9
PAM 16 h	27900	195300	6.9

Figure 4.2 shows the SEC traces of the PAM homopolymer at different reaction times. The mono-modal nature of the curves is lost at high conversions, as a result of a chain branching reaction taking place during the polymerization at later stages.[5,25] In the initial stages of the reaction, the monomer is present in large quantity, and the active radicals added much faster to a methacrylyl double bond than to a pendant allyl double bond due to the high reactivity of the methacrylate bond.[25] As the reaction proceeds, the monomer is consumed and the probability of attack at the pendant double bonds of the allyl group by the active radical increases. The branching reaction now takes place, leading to highly branched polymer or cross-linked polymer.

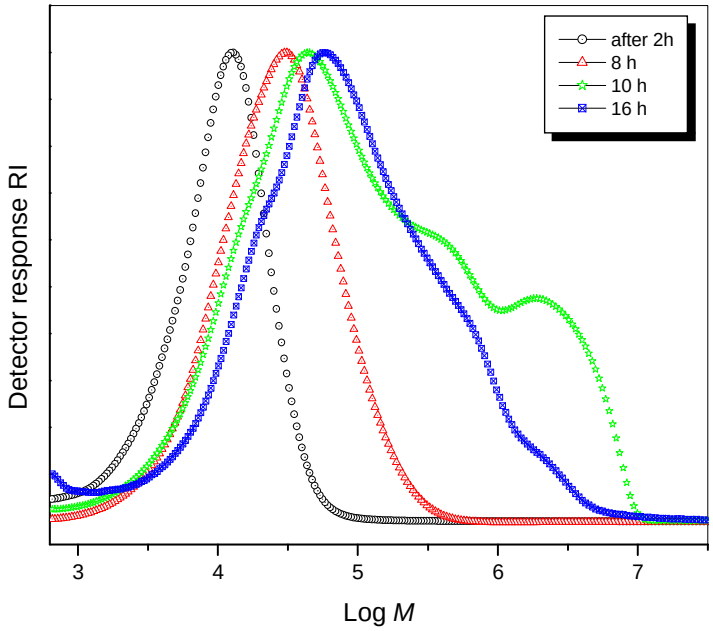

Figure 4.2: SEC of the RAFT mediated radical polymerization of PAM homopolymer as a function of reaction time. [Exp: the temperature was 70^{o} C, the polymerization condition was as follows: [M]/[CPDB]/[AIBN] = 800:1:0.1].

The individual chains within the distribution will have different lengths, and, consequently, this will be reflected in a broadening of the molar mass distribution. Cross-linking takes place when no more monomer or pendant double bonds are available.[5,26-28] Although the reactivity of the growing polymer radical toward the pendant allyl group of the pre-polymer is low, resulting in the formation of cross-linked polymer with low cross-link density,[5,25] the branching reaction takes place at 24% conversion, as indicted by a broadening of the SEC curve. This result is similar to the results obtained by Paris and de la Fuente[11] using the ATRP technique. However, the cross-linking reaction and gel were obtained at higher conversions above 45%.

4.4.2 RAFT-mediated copolymerization of PS-co-AM

The copolymerization of styrene with AM using a CPDB RAFT agent was performed in order to obtain a well controlled polymer with a narrow molar mass distribution as well as a number of pendent groups in terms of the distribution of the allyl functionality. Unlike in the previous section, the inclusion of the styrene monomers would be expected to lead to a higher molar mass and a decreased probability of cross-link formation (or at least a delay). Kinetic and conversion studies were carried out for 5, 10, and 20% AM copolymer of styrene and AM. Samples were removed from oil baths at different time intervals, and each sample was analyzed using SEC and NMR. The SECs of copolymers at different degrees of conversion are shown in Figure 4.3. There is an increase in the molar mass with conversion. The SEC curves remained mono-modal with low polydispersity, indicating the controlled and living nature of the polymerization process. Some tailing was observed at low molar mass, which causes the molar mass distribution to be broad. According to the literature,[29] this is mainly due to the radical-radical termination among the short chains. At high conversion, a broadening of the molar mass distribution is obtained in the cases of 5, 10, and 20% AM as a result of the branching reaction's taking place, and it is observed as a shoulder on the high molar mass side of the peak.

Figure 4.4 shows conversion and kinetic plots of the copolymerization reactions. The there is a nearly linear relationship between molar mass and conversion. M_n increases with monomer conversion, which indicates that there is a constant number of growing chains during the polymerization. In addition, the progress of polydispersity with conversion demonstrates the living character of the polymerization. The polydispersity remains constant during the polymerization of the range of the 25% conversion, providing evidence that most of the chains are capped with RAFT. Hence control over the molar mass was achieved at low conversion (below 20%) in all cases. The polydispersity of the 20% AM increases as the polymerization reaches higher conversions (from 25% conversion).

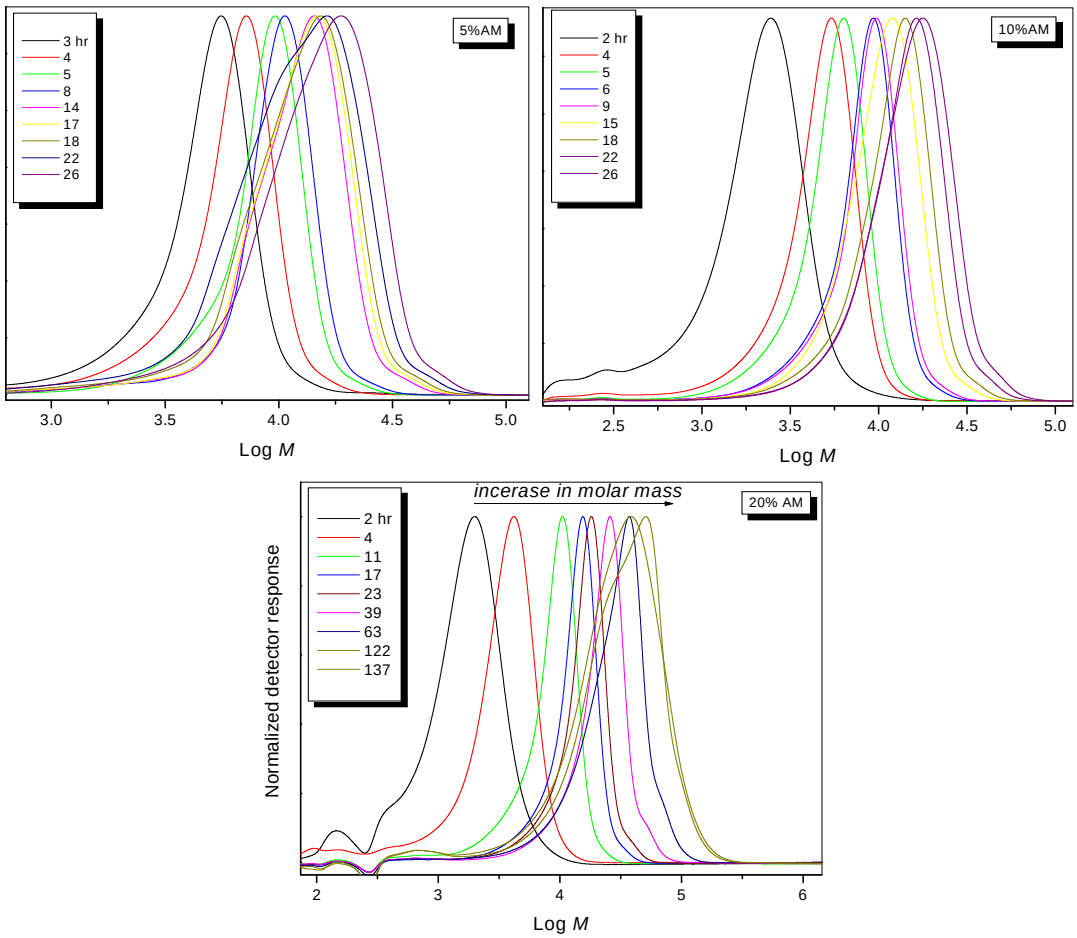

Figure 4.3: Molar mass distributions curves of the RAFT mediated radical copolymerization of (PS-co-AM as function of time.[Exp: the temperature was 70 ^{o}C, the copolymerization condition was as follows: [M]/[CPDB]/[AIBN] = 800:1:0.1].

This indicates that the branching reaction is the dominant reaction at the higher conversion when there is a high AM concentration. This is also clearly seen in the relationship between ln[M_0]/[M] and time, where there is deviation from a first-order reaction at longer reaction times for all the copolymers, which confirms the observations of the SEC traces.

NMR spectroscopy analysis of the copolymers has been predominantly useful in the determination of the chain structure of the copolymers. The sequence distribution and chemical composition distribution as determined form NMR are given later. Figure 4.5 shows the ^{1}H-NMR spectra of three produced copolymers PS-co-AM (5, 10, 20% AM). The presence of allyl groups in the copolymers is clearly seen (peaks a, b, d, allyl, ethoxy and methyl groups respectively) in the Figure 4.5. All signals are very broad, especially the O-CH_2 signal peak (b), which covers a chemical shift range of 1 ppm.

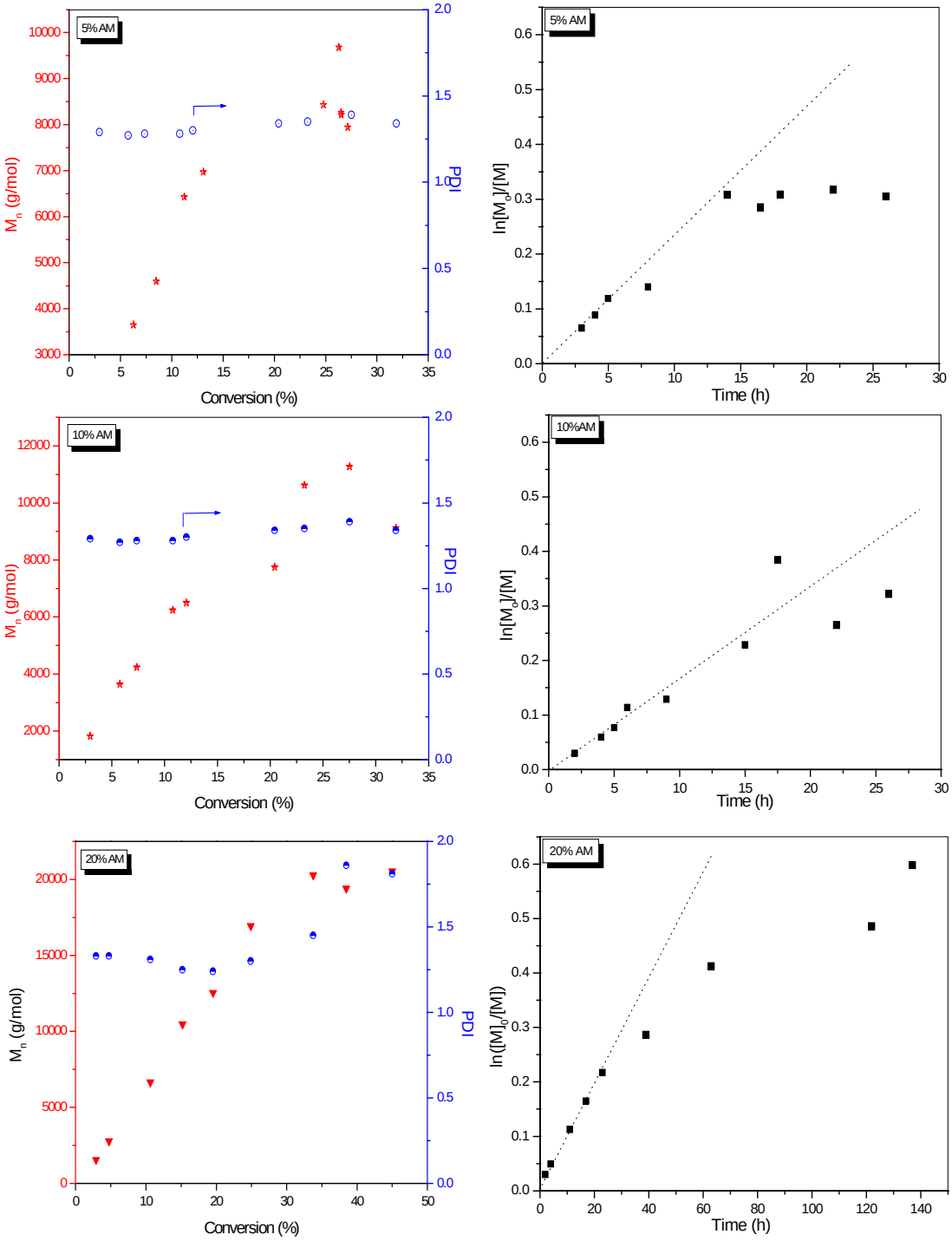

Figure 4.4: Conversion and kinetic plots of the copolymerization of PS-co-AM 5, 10 and 20% AM in the presence of CPDB.

In addition to the atacticity, the broadness of all the NMR signals is attributed to the monomer sequence in the copolymers due to the difference in the reactivity of the monomers.[24] This results in gradient copolymers; the AM monomer is inserted more frequently then the styrene monomer in the early stages of the reaction.

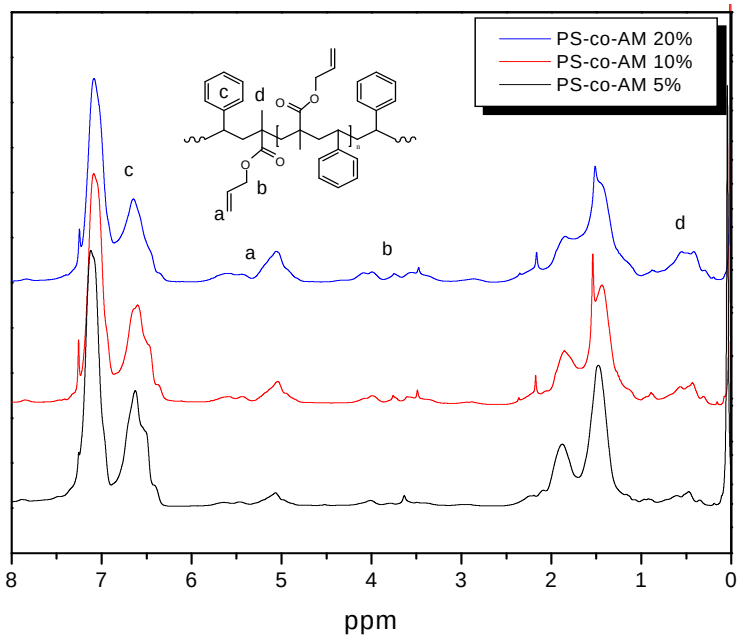

Figure 4.5: ^{1}H-NMR spectra in $CDCl_3$ of PS-co-AM copolymers (5, 10, and 20 mol% AM) in the feed obtained from RAFT mediated polymerization at 70^{o} C before the gelation reaction take place at 25% conversion.

Figure 4.6 shows the integral ratio of the allyl groups of copolymers PS-co-AM (20% AM), compared to the aromatic protons of the styrene units in the 20% AM copolymer as a function of conversion. The ^{1}H-NMR spectra of the conversion reactions of each sample show that, with increasing conversion in the copolymerization, there is a decrease in the AM fraction in the copolymer. This observation is in agreement with the finding of Paris and de la Fuente[23] when they used the ATRP system on PBA-co-AM. This result can be explained by: i) the favored incorporation of the AM monomer in the early stages of the polymerization, or ii) a higher probability of a reaction at the pendant allyl group with increasing conversion. The mole fraction of AM in the copolymer was found to be 5.3, 13.3 and 34.3% (calculated by NMR) at 25 conversion, as illustrated in Table 4.7.

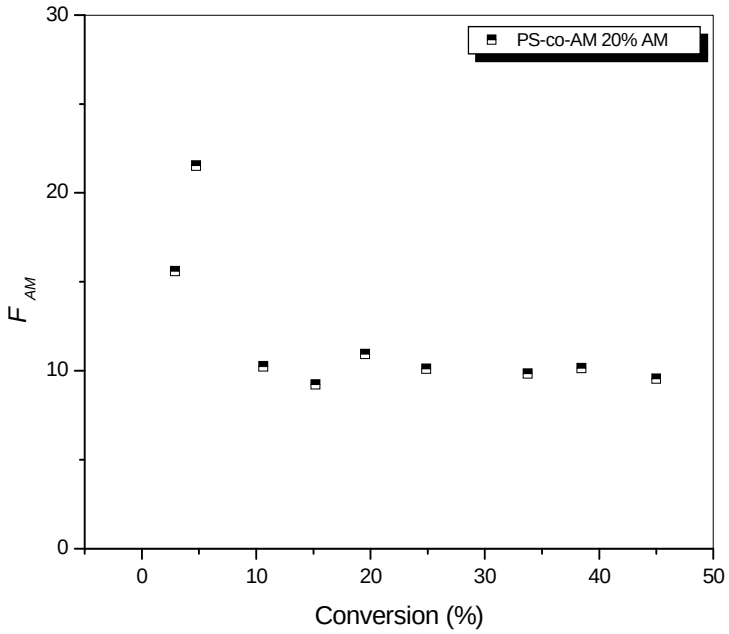

Figure 4.6: Copolymer composition (F_{AM}) obtained from ^{1}H-NMR, as a function of conversion for the 20% AM PS-co-AM copolymer.

Table 4.7: Copolymer composition data obtained from ^{1}H-NMR of the (PS-co-AM) copolymer at 20% conversion.

	AM monomer mole % in feed (f_{AM})	AM mole fraction in copolymer (F_{AM})
PS-co-AM	5	5.3
	10	13.3
	20	34.3

Figure 4.7 shows the complete assignment of the ^{13}C-NMR spectra of copolymer PS-co-AM (5, 10 and 20%) and shows distinctive signals of the AM comonomer. The carbonyl carbon signal of the AM unit is assigned to the region around δ 175.7-176.6 ppm. The α-methyl carbon of the AM unit signal is found around δ 16.6-19.7 ppm. A more detailed analysis of the region was used to determine the relative stereochemical configuration of the copolymers obtained.

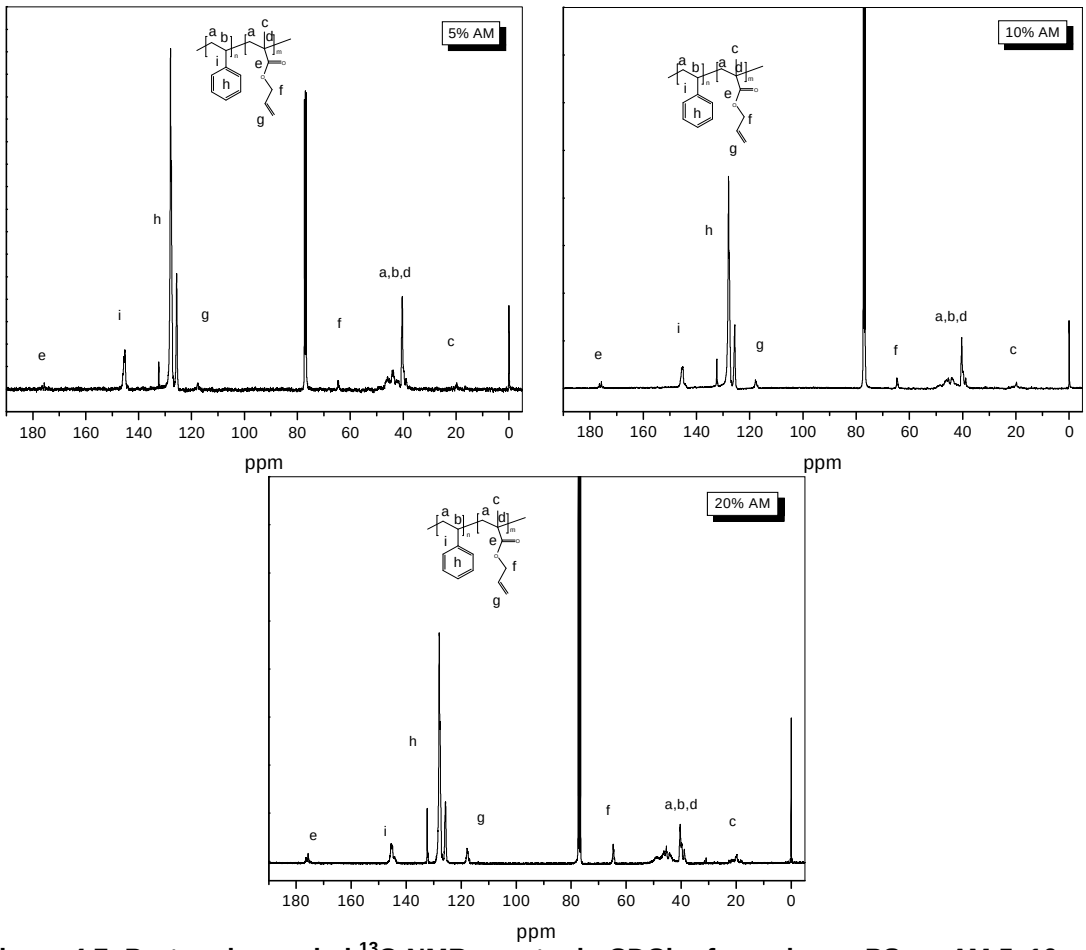

Figure 4.7: Proton decoupled ^{13}C-NMR spectra in $CDCl_3$ of copolymer PS-co-AM 5, 10 and 20% AM in the feed obtained from RAFT mediated polymerization at 70^{o} C before the gelation reaction take place at 25% conversion.

The protons decoupled ^{13}C-NMR spectra can be used to determine the relative composition and configurational distributions in the copolymers. Figure 4.8 shows an expansion of the α-methyl region of AM, which is the most sensitive to configuration differences for the PS-co-AM copolymers and the PAM homopolymer. The relative stereochemical configuration of the copolymer AM centered triads was considered for complete description of the monomer sequence distribution. The assignment of the signals is based on the assumption made by Puneeta[30] for PS-co-PMMA copolymers. So the MmMmM, MmMrM, and MrMrM refer to the isotactic, heterotactic, and syndiotactic triad configurations, respectively, of the PAM homopolymer. Figure 4.8 shows that a significant amount of the syndiotactic triad sequence is found for the PAM homopolymer. The SrMrS, and MmMmS, configurations are for the copolymer PS-co-AM, where M refers to a centered AM monomer unit, S the styrene unit, and m and r symbolizes meso and racemic diads, as described by Moad and Solomon.[31]

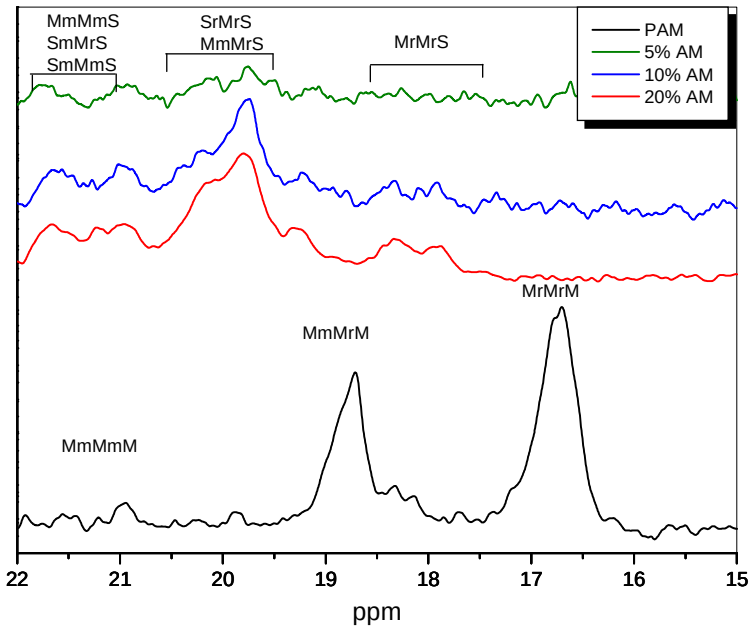

Figure 4.8: Proton decoupled ^{13}C-NMR spectra of PAM and corresponding copolymers PS-co-AM (5, 10, and 20% AM) at 25% conversion.

The stereochemical configurations are summarized in Table 4.8 for three copolymers, 5, 10, and 20% AM. It should, of course, be noted that the peak integrations are difficult due to the low signal-to-noise ratio in this part of the spectra. Nevertheless, an integration of these regions gives an indication of the relative amounts of the different compositional and tacticity sequences. The relative fraction of SrMrS/MmMrS sequence is the main fraction present in the copolymers. This is followed by MmMmM and (mmMmS/SmMrS/SmMmS) fractions. A small fraction of MrMrS triad is obtained in the 10 and 20% AM. Much of the copolymer tacticity is heterotactic, with some syndiotactic configuration in terms of AM cantered triads, which is similar to the configuration of the PS-co-MMA copolymer prepared by ATRP.[30] From the data in Table 4.8, the sequence comonomer distribution in the copolymer MmMmM increases with an increase in the comonomer feed. This is to be expected not only from a probability point of view, but also due to the larger incorporation of the AM units in the early stages of the reaction due to the reactive ration difference of the two monomers. Despite this, the SrMrS and MmMrS constitute the major sequences present in the three copolymers, which would indicate the allyl groups are distributed throughout the chain.

Table 4.8: Experimentally observed (^{13}C-NMR) α-methyl resonances of AM centered sequences for various PS-co-AM copolymers prepared by RAFT-mediated polymerization with different monomer feed compositions

AM monomer mol % in feed f_{AM}	AM mole fraction in copolymer F_{AM}	MrMrM	MrMrS	MmMrM	SrMrS MmMrS	MmMmM	MmMmS SmMrS SmMmS
5	5.3	-	-	-	0.8	0.1	0.1
10	13.3	-	0.1	-	0.6	0.2	0.1
20	34.3	-	0.1	-	0.6	0.2	0.1

The copolymerization of styrene and AM in solution in the presence of RAFT agent CPDB does not show any gel formation at conversions less than 45%. The reactions are first-order until the reactions reach 25% conversion, after which branching reactions commence, as indicated in the SEC traces by the broadening of the curve.

4.4.2.1 Hydroboration and autoxidation

The hydroboration reaction of copolymers of PS-co-AM was used to produce the graft copolymer using the "grafting from" technique. The hydroboration was carried out by adding 9-BBN onto the copolymer in an O_2 free solution of THF. Due to the good solubility of the borane reagents and borane containing polymers, the hydroboration reactions were expected to be very similar to those of small organic compounds or block as described in the previous chapter Section 3.5.4.

It should be mentioned here that the addition of 9-BBN (Lewis acids) to the reaction mixture to form hydroboration-autoxidation adduct destroys the CPDB RAFT agent attached to the end of the polymer chains. The evidence for this is the observed color change of the polymerization mixtures from pink to orange. This observation is similar to the observations of Chong et al.[32] and Lutz et al.[33] when they used scandium triflate as Lewis acid with cumyl dithiobenzoate (CDB) RAFT agent to control free radical polymerization of MMA. As a result of this observation, it is expected that the graft reaction occurs as result of hydroboration of allyl function group, and there is no role of RAFT in the grafting reaction.

Figure 4.9 shows the SEC traces of the synthesized graft copolymers. Bimodal distribution curves are obtained; the peak at higher retention time corresponds to the copolymer PS-co-AM backbone. The second peak corresponds to graft copolymer and homopolymer of PMMA. UV response at 254 nm is related to the styrene ring, and at the first peak there is a strong response of the UV, as expected.

A UV response is also seen for the lower retention time peak, which corresponds to the graft copolymer and PMMA homopolymer. Since the grafting reaction is via MMA, which does not have a UV response at this wave length, it can be concluded from the SEC traces that at least some of the polymer chains were successfully grafted. As expected, the 20% Am copolymer produces the higher amount of the graft copolymer.

HPLC gradient chromatography was carried out to separate the complex mixture of graft copolymers and corresponding homopolymers. For the separation to be complete, the polarity of the polymer species has been taken into consideration. In the present case, PMMA is more polar than the graft copolymer (PS-co-AM)-g-PMMA and PS-co-AM. When using a reversed phase column, elution should follow an order of decreasing polarity. Therefore, the PMMA should elute first, followed by graft copolymer and then the PS-co-AM. Solvent compositions of ACN and THF were used on the Symmetry C18 column.[20] ACN is a good solvent for the PMMA homopolymer, and THF is a good solvent for the PS-co-AM copolymers.

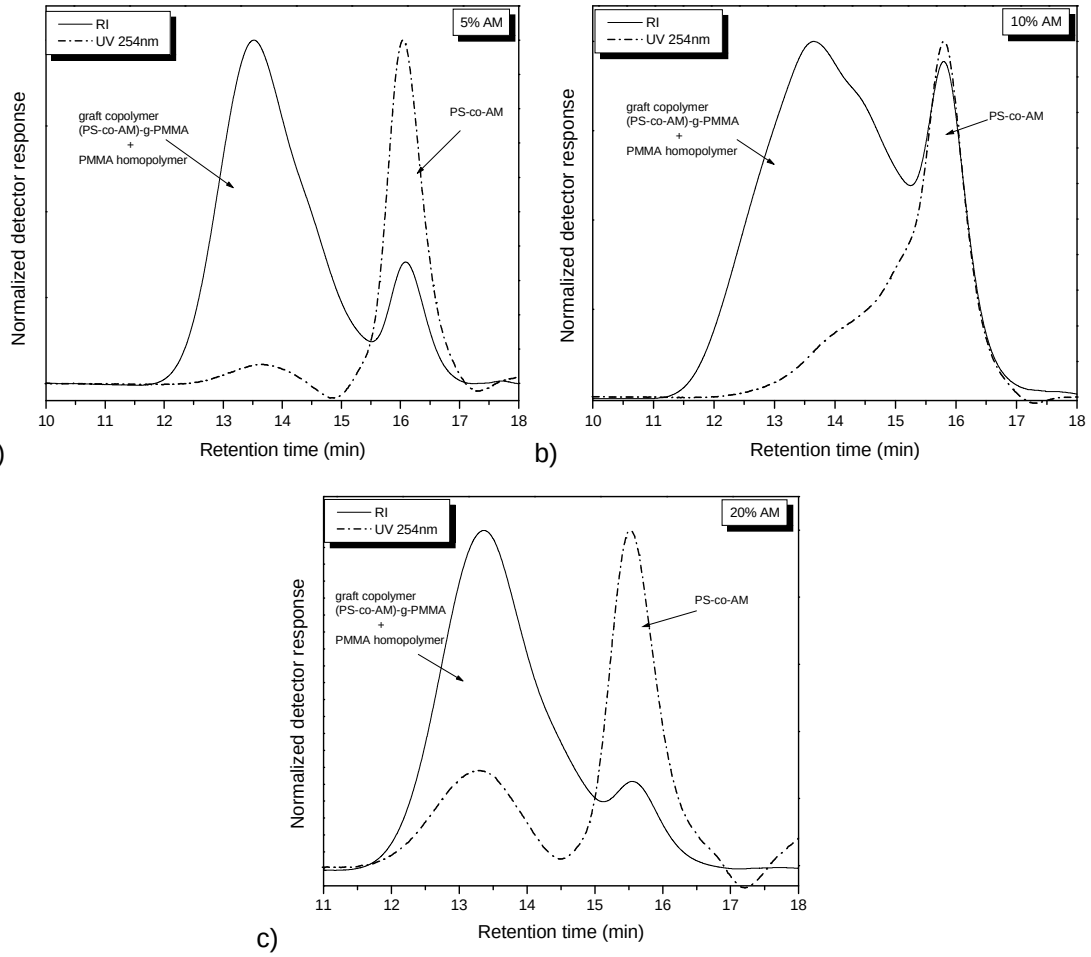

Figure 4.9: SEC elution of the borane autoxidation radical copolymerization of (PS-co-AM)-g-PMMA, a) 5% AM b) 10% AM, and c) 20% AM.

The gradient elution profile used was as follows: 100% (v/v) ACN was eluted for 2 min then changed linearly to 100% (v/v) THF. The chromatographic separation of graft copolymers is shown in Figure 4.10. Good separation into three fractions was obtained. The assignment of the peaks was carried out by comparison with the chromatographic behavior of PMMA and PS-co-AM. Between the two peak signals of PMMA at low retention time and the PS-co-AM peak at higher retention time, a third peak related to the graft copolymers was obtained. The HPLC gradient chromatography results confirm the graft formation. In all the graft copolymers, tailing is observed, ELSD detector signal toward the fraction rich in PS-co-AM backbone. This is the result of some of the backbone chain's only having a few PMMA branches. Since the separation is carried out according to the chemical composition of the copolymer the polymer eluting in the tail is richer in PS-co-AM than the main peak. The tailing occurs due to the difficulty in insertion of the monomer at high comonomer content due to steric hindrance around the grafting site.

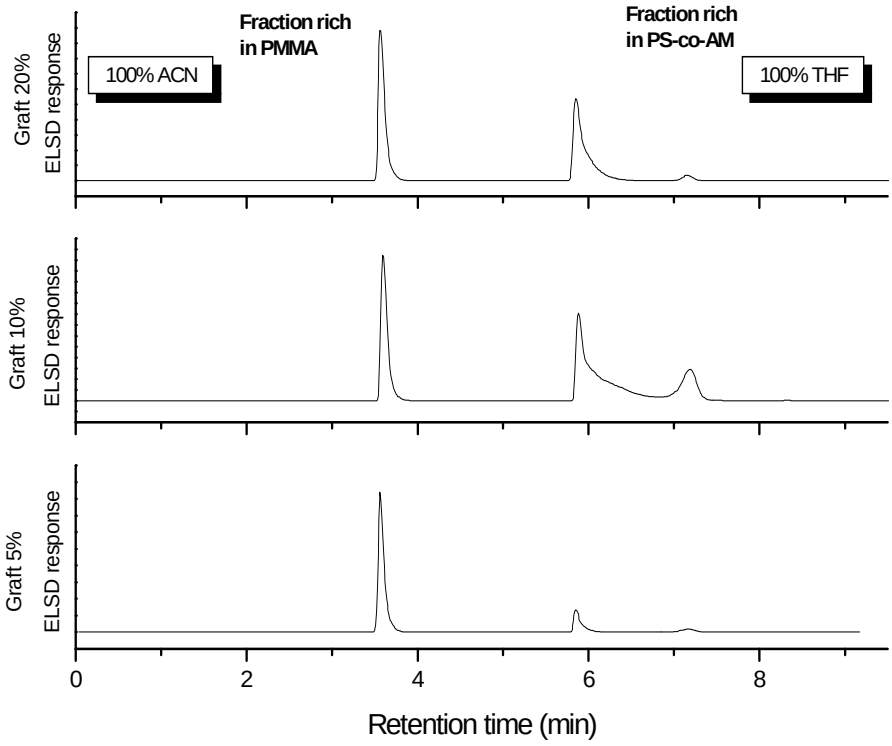

Figure 4.10: Gradient HPLC separation of the grafts copolymers,[Exp: stationary phase: Silce 300, mobile phase: 100% ACN for 2 min then 10 min linear gradient ACN-THF 100 to 0% ACN, flow rate: 1 mL/min, detection: ELSD].

It is also clear that a significant amount of PMMA homopolymer is formed. This is consistent with the results from the previous chapter and will be discussed later. An estimation of the grafting efficiency can be evaluated by comparing the

relative peak intensities of the ELSD response to the different components of the grafting products

The relative areas of the peaks of PMMA homopolymer, PS-co-AM copolymer, and graft copolymer were calculated, and the results are shown in Table 4.9 The result indicates that up to 79% of the reaction mixture obtained is PMMA homopolymer. There are a number of possibilities to explain the PMMA homopolymer formation. Firstly, it is possibly a result of branch formation in the copolymer backbone PS-co-AM, which is evident in the Figure 4.4 where a deviation from a first order reaction is seen. Any branching reaction will consume the allyl side groups. This will result in the presence of free 9-BBN in solution. In the case of branching, the active sites will undergo hydroboration. However, the branching point will result in steric hindrance, and the internal active site will be very difficult to hydroborate, especially when the reaction proceeds and the branches grow. Secondly, there may not be 100% conversion of the allyl sites to the boronated adducts due to the steric hindrance of the neighboring allyl site. This is evidenced by the higher reactivity ratio of the AM group's resulting in an uneven distribution of the groups along the polymer chain and is discussed below. Lastly, the PMMA homopolymerization may be the result of initiation by the boronate radical, as is observed in the block copolymerization.

Table 4.9: Estimation of component amounts for graft copolymers as determined by gradient HPLC analysis

	Relative area (%)		
	PMMA	(PS-co-AM)-g-PMMA	PS-co-AM
Graft 5%	79	16	4
Graft 10%	32	50	18
Graft 20%	49	47	3

In order to determine the efficiency of the conversion and subsequent initiation efficiency of the ally side chains, ^{1}H-NMR was done on the unfractionated graft polymers. Figure 4.11 shows an example of the ^{1}H-NMR spectra of the un-fractionated 20% AM graft copolymer. It is clear from the figure that not all the allyl functional groups are converted, and a number are still present in addition to the signals of the O-CH_3 of MMA and the aromatic ring of styrene. This confirms that not all the allyl functional groups of the copolymer are converted and initiate graft formation.

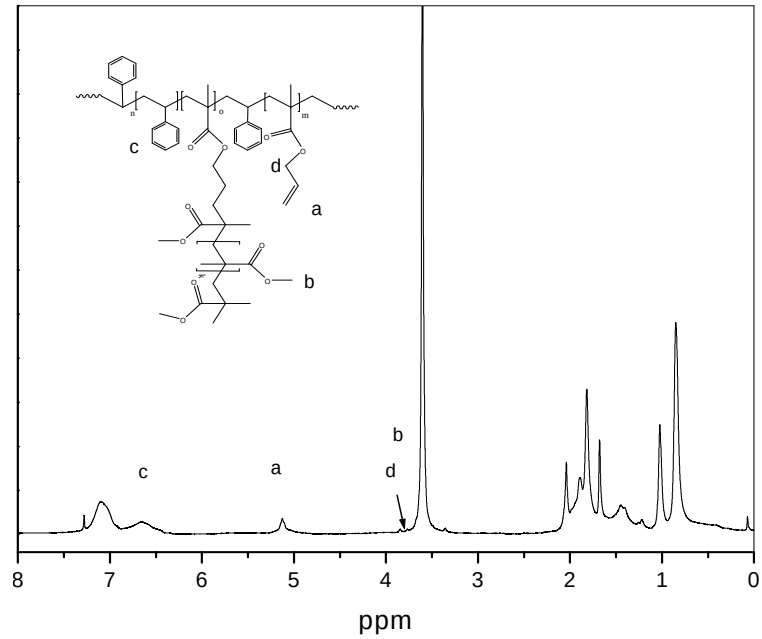

Figure 4.11: ^{1}H-NMR in $CDCl_3$ the graft copolymers (PS-co-AM)-g-PMMA 20% AM shows the presence of the allyl functional group in the graft copolymer.

The ^{1}H-NMR spectra were used to determine the amount of the unconverted ally side groups. Integration of the peaks (a, b, c) in Figure 4.11 can give the mol fraction of the unreacted allyl groups. The percentage of grafting can also be predicted. The data are illustrated in the Table 4.10 The 5% AM copolymer shows a very low amount of unreacted ally groups. About 94% of these groups are converted and at least potentially can act as initiating points for grafting. The higher content of AM copolymers shows a lesser degree of conversion of the allyl groups. The results mean that in the 5% AM copolymer, 94% of the active site are hydroborated and undergo autoxidation and at least one MMA monomer is inserted. In the 10% and 20% AM, the amount of hydroboration-autoxidation was relatively low in comparison to the 5% AM copolymer.

Table 4.10: Grafting efficiency via hydroboration reaction for the 5, 10, and 20% AM copolymers

AM mol fraction in copolymer	Unreacted allyl function group in the graft copolymer*	Percentage conversion of the allyl groups (%)
5.3	0.3	94
13.3	3.6	73
34.3	5.0	85

* calculated by ^{1}H-NMR

As mentioned above, significant amounts of PMMA homopolymer were produced during the reaction. One of the reasons is the incomplete hydroboration reaction of all allyl function groups, which led to the presence of free 9-BBN. The free 9-BBN is responsible for the formation of homopolymer PMMA. The larger number of active sites in the 10% and 20% AM, however, leads to an increased probability of the graft formation.

^{1}H-NMR analysis of the fractionated graft copolymers collected from HPLC was also done. Table 4.11 shows the NMR analysis of the isolated graft copolymer from a retention time of 5 to 6.5 min during the HPLC analysis. NMR analysis shows that there is more MMA in the copolymer with 10% AM comonomer content. In other words, the PMMA segment in the graft copolymer is longer than that in the case of graft copolymers 5% and 20% AM.

Table 4.11: ^{1}H-NMR analysis of the collect graft copolymer from HPLC

	mol% styrene	mol% MMA
5%AM	88	12
10%AM	70	30
20%AM	87	13

4.4.3 RAFT-mediated copolymerization of PMMA-co-AM

The copolymerization of MMA with AM via CPDB was performed to investigate the possibility of forming gel-free PMMA-co-AM with well controlled molar mass and narrow molar mass distribution, as well as a number of pendent group incorporated in the polymer chain. These could then be used to initiate the grafting reaction in the second step. Once again a series of copolymers with 5, 10, and 20% AM in the feed were synthesized. Kinetic studies and conversion study were only carried out for 20% AM copolymer of MMA and AM.

Figure 4.12 shows the SEC analysis of the 20% AM copolymer at different reaction times. The figure shows a nearly linear relationship between molar mass and conversion. The SEC peak remained mono-modal with a low polydispersity, indicating the controlled and living nature of the polymerization process. A tailing at low molar mass appeared which caused the molar mass distribution to be broad. The literature explains this as being due mostly to the radical-radical termination among short chains.

At high conversion, a broadening of the molar mass distribution is obtained as a result of the branching reaction's taking place and is observed as a shoulder on the high molar mass side of the peak.

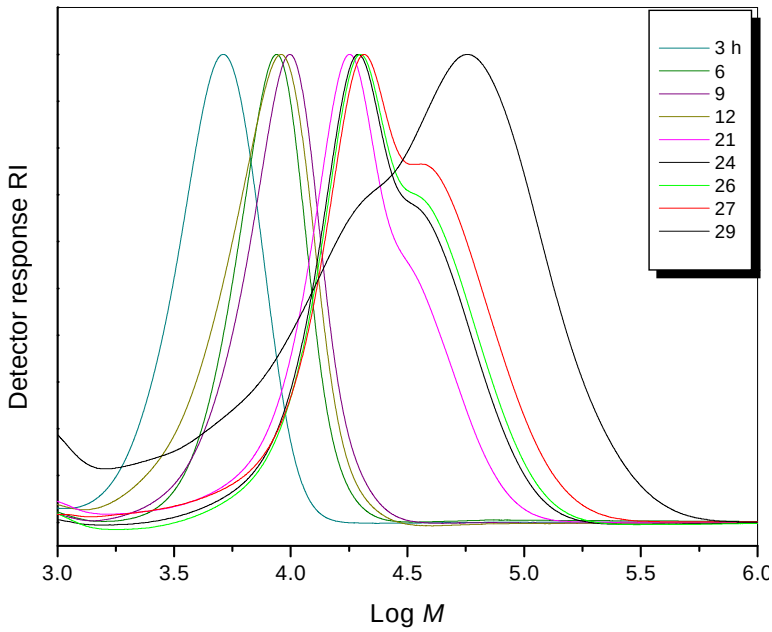

Figure 4.12: Molar mass distributions of the RAFT mediated radical copolymerization of PMMA-co-AM (20% AM). [Exp: the temperature was 70° C, the copolymerization condition was as follows: [M]/[CPDB]/[AIBN] = 800:1:0.1].

Figure 4.13 shows a conversion and kinetic plot of the copolymerization in the presence of CPDB. It can be seen that M_n increases with monomer conversion. This gives evidence that there is a constant number of growing chains during the polymerization. In addition, the polydispersity slightly increases with the conversion that demonstrates the living characteristic of the polymerizations. It increases during the polymerization, which is evidence that the most of the chains are capped with CPDB, so a control over the molar mass was achieved at low conversion 20%. The branching reaction is the dominant reaction at higher conversions when there is a high AM concentration. That is also clearly seen in the relationship between $\ln[M_0]/[M]$ and time, where there is deviation from first-order reaction at higher conversion and confirms the appearance of the high molar mass peak in the SEC traces.

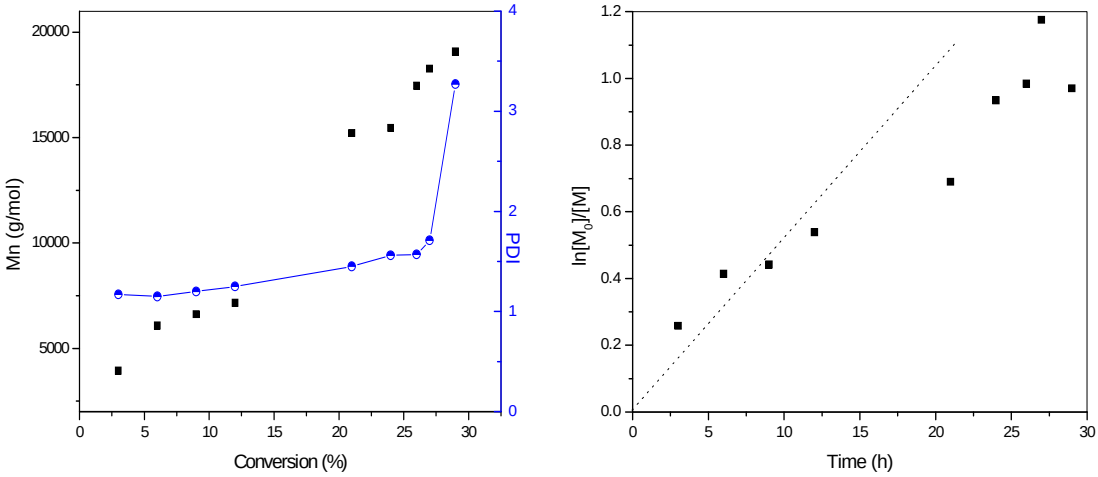

Figure 4.13: Conversion and kinetic plot of copolymerization of PMMA-co-AM in the presence of CPDB.

Figure 4.14 shows the ^{1}H-NMR of the copolymers PMMA-co-AM with different feed ratios of 5, 10, and 20% AM at 15% conversion: distinctive signals of the allyl group at δ 5.2 - 6.0 ppm as well as the O-CH_2 of the AM comonomer at δ 4.5 ppm and O-CH_3 signal of the MMA at δ 3.6 ppm. By comparing the signal of the O-CH_2 in the copolymers, an increase in the intensity with an increase in the feed composition of the AM comonomer is seen.

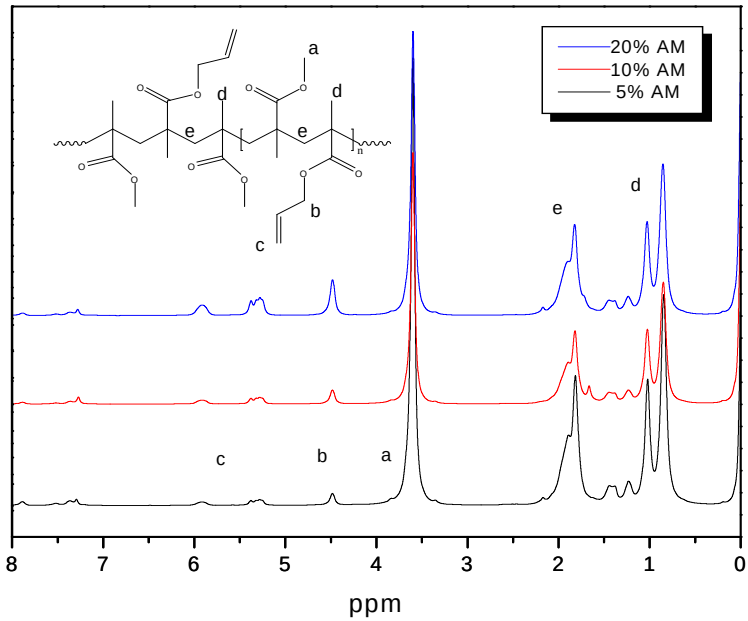

Figure 4.14: ^{1}H-NMR spectra in $CDCl_3$ of PMMA-co-AM copolymers (5, 10, and 20 mol% AM) at 15% conversion shows the assignment of the functional group of each copolymer.

From the ^{1}H-NMR analysis, the integration of signals (a, b), illustrated in Figure 4.14, the copolymer composition was determined and listed in the Table 4.12

Unlike the case for the PS-co-AM copolymers, the copolymer composition closely matches the feed composition due to the relatively close value of the reactivity ration.

Table 4.12: Copolymer composition at 15% conversion obtained from ^{1}H-NMR of the PMMA-co-AM copolymer

	AM mole fraction in feed (f_{AM})	AM mole fraction in copolymer (F_{AM})
PMMA-co-AM	5	4.30
	10	9.50
	20	18.36

4.4.3.1 Hydroboration and autoxidation of copolymer PMMA-co-AM

The hydroboration-autoxidation reaction of the PMMA-co-AM (20% AM) copolymer was used to produce the graft copolymer via the “grafting from” technique. The PMMA-co-AM (20% AM) copolymer is shown as an example of the grafting reaction and would be applicable to the other copolymers with different compositions. Butyl acrylate (BA) was used as a grafting monomer in this case. Initially, styrene was investigated, but the grafting reaction with styrene was very slow and insufficient. The hydroboration reaction was carried out by adding 9-BBN onto the copolymer in an O_2-free solution of THF. The graft reaction initiated when a certain amount of O_2 gas was injected directly into the solution at room temperature in the presence of BA (the amount of BA in the solution is (39.6 mmol)) for 24 h. Details of the procedure as well as the characteristics of the PMMA-co-AM copolymers can be found in Section 4.2.5

Figure 4.15 shows the SEC result of the grafting reaction of the 20% AM copolymer. Once again, a bimodal curve is observed. The peak at a low retention time corresponds to the BA homopolymer and graft copolymer, and the second peak is the copolymer ungrafted PMMA-co-AM copolymer.

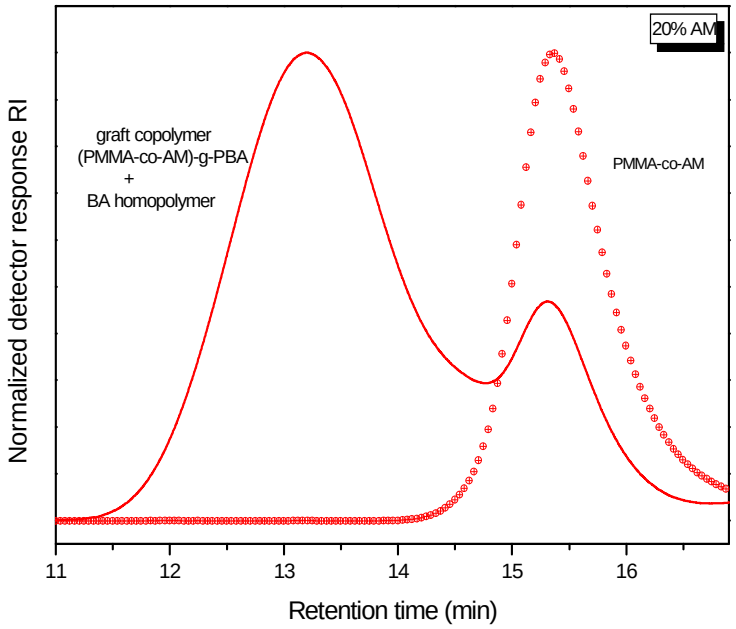

Figure 4.15: SEC elution of the borane autoxidation radical copolymerization of (PMMA-co-AM)-g-PBA.

^{1}H-NMR spectroscopy of the graft copolymer is shown in Figure 4.16. The signals of the O-CH_2 of AM at δ 4.5 ppm and BA at δ 4.0 ppm and signal peak of the O-CH_3 of MMA at δ 3.6 ppm are presented. As was the case previously, the allyl functional group signal is also observed, which indicates that not all the allyl functional groups of the copolymer are successfully used as grafting points. From the integration of the peaks, 7% of the allyl functional group remains ungrafted.

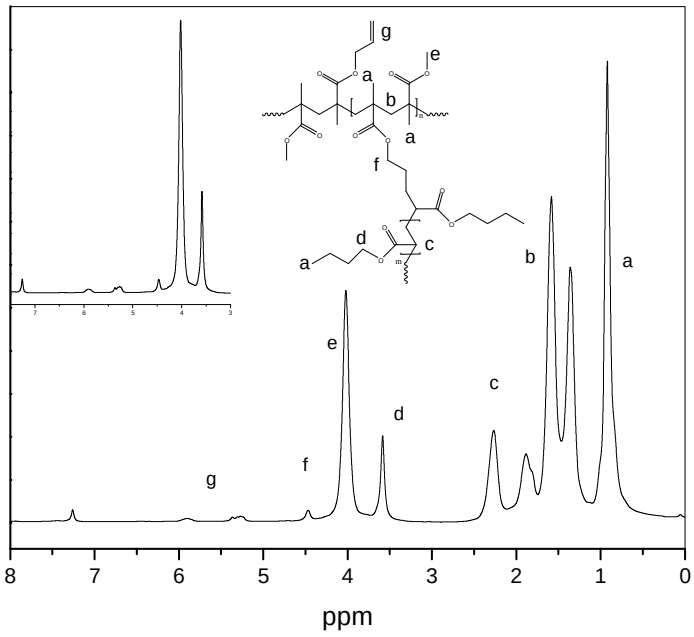

Figure 4.16: ^{1}H-NMR in $CDCl_3$ the graft copolymers (PMMA-co-AM)-g-PBA show the assignment of the signal of each component.

HPLC gradient chromatography was carried out in order to separate graft copolymer and corresponding homopolymers. For the separation to be complete, the polarity of the polymer species has been taken into consideration. In the present case, PMMA-co-AM is more polar than the graft copolymer (PMMA-co-AM)-g-PBA and PBA. When using a normal phase column, elution should follow an order of increasing polarity. The gradient starts with a non-solvent, and subsequently the solvating power of the eluent is increased by the gradient. Therefore, the PBA should elute first, followed by graft copolymer, and then the PMMA-co-AM copolymer. The solvents used were an n-heptane-THF mixture, and a Silica 100 column was used. The gradient profile was set as follows: 100% (v/v) n-heptane was eluted for 1 min to precipitate all polymers, then the composition was changed linearly in a period of 10 min toward 100% (v/v) THF, which is a good solvent to the copolymer. Good separation into three fractions was obtained, as shown in Figure 4.17.

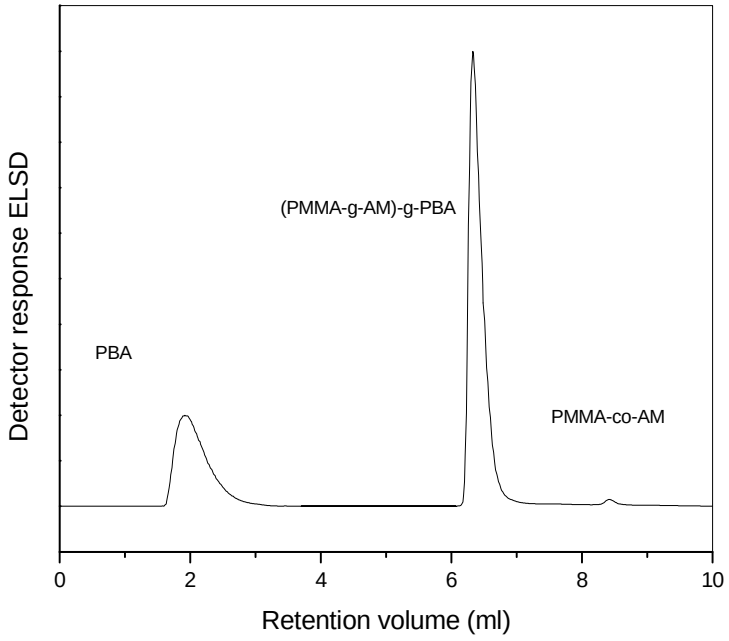

Figure 4.17: Gradient HPLC separation of the corresponding homopolymers BA and (MMA-co-AM) the graft copolymer, stationary phase: Silice100, mobile phase: 100% n-Hept for 1 min then 10 min linear gradient n-hept-THF 100 to 0% n-hept, flow rate: 0.5 mL/min, detection: ELSD.

The assignment of the peaks was carried out by comparison with the chromatographic behavior of PBA and PMMA-co-AM. Between the two peaks for the PBA and PMMA-co-AM a peak attributed to the graft copolymer was obtained. The HPLC gradient chromatography results confirm the formation of the graft copolymer. A significant amount of PBA homopolymer was obtained from the reaction.

The relative peak areas of the BA homopolymer, PMMA-co-AM copolymer, and graft copolymer were calculated, and the results are shown in Table 4.13. The results indicate that the amount of the homopolymer PBA is lower than the grafting reaction involved PMMA monomer and PS-co-AM. This is as a result of a backbiting reaction of the propagating secondary BA radical and self-termination of BA monomer when it polymerized at low temperature.[34]

Table 4.13: Estimate of component amounts for graft copolymers as determined by gradient analysis

	Relative area (%)		
	PBA	**(PMMA-co-AM)-g-PBA**	**PMMA-co-AM**
Graft 20%	**31**	**67**	**2**

4.4.4 RAFT-mediated copolymerization of PBA-co-AM

RAFT-mediated copolymerizations of PBA-co-AM were preformed with different comonomer content in an effort to synthesize the gel-free copolymer. However, the prepared PBA-co-AM copolymers have low T_gs, which made the separation of the BA monomer from the synthesized copolymer difficult. The presence of the BA monomer with the copolymer during the hydroboration reaction will have an effect on the hydroboration, and no further graft reaction was applied. Nevertheless, SEC traces of the three copolymers and ^{1}H-NMR were able to show the ability of CPDB of synthesized gel-free copolymer and calculate the comonomer composition in the feed.

Figure 4.18 shows the normalized SEC traces of three copolymers, PBA-co-AM 5, 10, and 20% AM. The responses of the RI show a monodisperse curve for all the copolymers prepared after a 12-h reaction time.

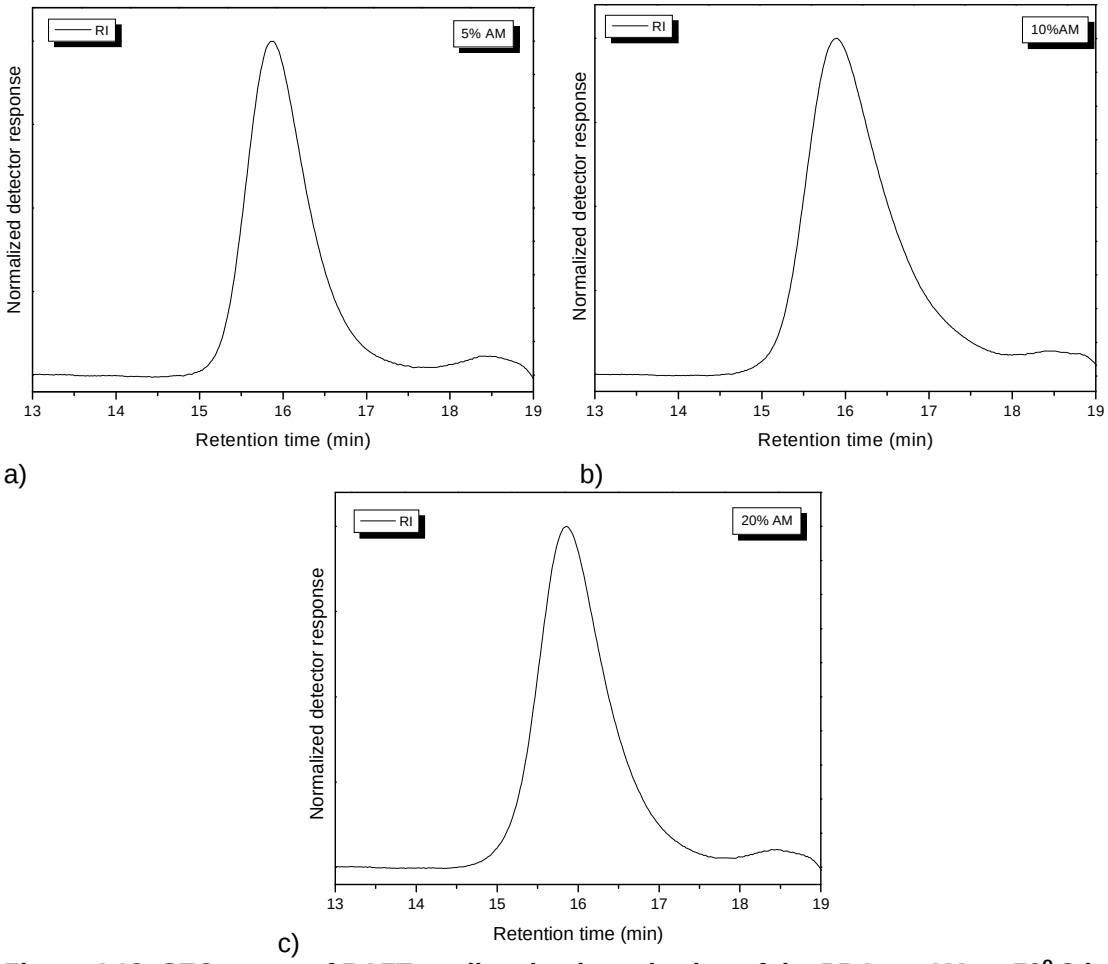

Figure 4.18: SEC traces of RAFT mediated polymerization of the PBA-co-AM, at 70^{o} C in tolune solution, a) 5, b) 10, and c) 20% AM.

Figure 4.19 shows the ^{1}H-NMR of the copolymers PBA-co-AM with different feed ratios 5, 10, and 20% AM after 12 h of reaction: distinctive signals of the allyl group at δ 5.2 - 6.0 ppm as well as the O-CH_2 of the AM comonomer at δ 4.5 ppm and O-CH_2 of the BA at δ 4 ppm. The evidence of BA monomer presence in the copolymers is seen in the O-CH_2 signal of the BA small signal at δ 4.1 ppm. By comparing the signal of the O-CH_2 in the copolymers, an increase in the intensity with increase in the feed is seen.

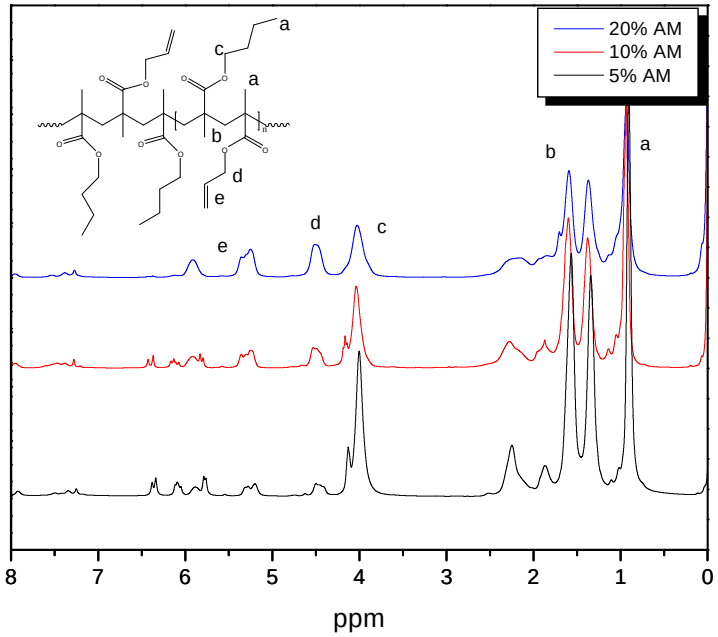

Figure 4.19: ^{1}H-NMR spectra in $CDCl_3$ of PBA-co-AM copolymers (5, 10, and 20 mol% AM).

From the ^{1}H-NMR, the integration of these signals gives the copolymer composition, which is listed in the Table 4.14. The difference in the mole fractions of AM in the copolymers on the mole fraction in the feed is due to the difference in the reactivity between the BA and AM.[23]

Table 4.14: Copolymer composition data of the PBA-co-AM copolymer (at high conversion)

	AM mole fraction in feed (f_{AM})	AM mole fraction in copolymer (F_{AM})
PBA-co-AM	5	9.1
	10	13.0
	20	39.4

4.5 Conclusions

The combination of living free radical polymerization RAFT and hydroboration-autoxidation of a borane adduct was successfully carried out to prepare graft copolymers. The choice of RAFT-mediated copolymerization of AM and styrene, MMA and BA in an effort to synthesize polymer backbone containing unsaturated allyl function group were successful.

Gel-free homopolymer MA was successfully carried out in solution in the presence of CPDB to conversion up to 45%.

Linear increase in the M_n with conversion followed by an increase in PDI is observed.

Broadening in the SEC curve is detected at 24% conversion as a result of the chain branching reaction.

The RAFT agent CPDB was demonstrated to be an appropriate chain-transfer agent to inhibit cross-linking and obtain polymers with moderate-to-high conversions.

Copolymerization of styrene, MMA, and BA with AM in different feed compositions were successfully carried out in solution in the presence of CPDB with relatively high conversion 45%, and no gel formation was observed. All the reactions show significant branching reaction at 20% conversion, indicted by the broadening in the SEC curves.

NMR analysis of the 20% AM PS-co-AM as a function of conversion illustrate that with an increase in the conversion of the copolymer there is a decrease in the AM fraction in the copolymer, which results in the formation of a gradient copolymer.

In the PS-co-AM copolymer, the majority sequence of comonomer distribution is SrMrS/MmMrS as obtained from the protons decouple ^{13}C-NMR. In both copolymers PS-co-AM and PBA-co-AM, the comonomer content obtained was higher than the feed ratios of 5, 10, 20% AM due to the monomer reactivity ratio difference.

Graft reaction of the copolymers PS-co-AM with MMA and PMMA-co-AM with BA via hydroboration-autoxidation reaction of 9-BBN were successfully done. However, gradient HPLC shows that a significant amount of homopolymer was produced during the grafting reaction due to the presence of free 9-BBN, which is a result of incomplete hydroboration of the allyl functional group. The incomplete conversion during the hydroboration is a result of the branching reactions that consumes some of the allyl group and makes the graft reaction more difficult in terms of bulkiness of the backbone.

Using the hydroboration reaction of the allyl function copolymer in the presence of the BA monomer at low temperature, gave a low yield of homopolymer PBA as a result of backbiting of the propagating secondary BA radical and self-termination of BA monomer.

4.6 References:

1. Guoqiang, F.; Dong, J. Y.; Wang, Z.; Chung, T. C. *Journal of Polymer Science: Part A: Polymer Chemistry* **2006,** 44, 539-548.
2. Chung, T. C.; Lu, H. L.; Janvikul, W. *Polymer* **1997,** 38, 1495-1502.
3. Lu, B.; Chung, T. C. *Macromolecules* **1999,** 32, 2525-2533.
4. Wang, X.-s.; Luo, N.; Ying, S.-k. *Polymer* **1999,** 40, 4515-4520.
5. Matsumoto, A.; Asai, S.; Aota, H. *Macromolecular Chemistry and Physics* **2000,** 201, 2735-2741.
6. Matsumoto, A.; Kawasaki, N.; Shimatani, T. *Macromolecules* **2000,** 33, 1646-1650.
7. Matsumoto, A.; Asai, S.; Shimizu, S.; Aota, H. *European Polymer Journal* **2002,** 38, 863-868.
8. Matsumoto, A.; Fujihashi, M.; Aota, H. *European Polymer Journal* **2003,** 39, 2023-2027.
9. Matsumoto, A.; Kodama, K.; Aota, H.; Capek, I. *European Polymer Journal* **1999,** 35, 1509-1517.
10. Paris, R.; de la Fuente, J. L. *Journal of Polymer Science: Part A: Polymer Chemistry* **2005,** 43, 6247-6261.
11. Paris, R.; de la Fuente, J. L. *Journal of Polymer Science: Part A: Polymer Chemistry* **2005,** 43, 2395-2406.
12. Rodrigo, P.; de la Fuente, J. L. *Journal of Polymer Science: Part A: Polymer Chemistry* **2006,** 44, 5304-5315.
13. Paris, R.; de la Fuente, J. L. *Journal of Polymer Science: Part A: Polymer Chemistry* **2007,** 45, 3538-3549.
14. Paris, R.; de la Fuente, J. L. *European Polymer Journal* **2008,** 44, 1403-1413.
15. Zhang, H.; Ruckenstein, E. *Journal of Polymer Science Part A: Polymer Chemistry* **1997,** 35, 2901-2906.
16. Lin, Y.; Liu, X.; Li, X.; Zhan, J.; Li, Y. *Journal of Polymer Science: Part A: Polymer Chemistry* **2007,** 45, 26-40.
17. Yu, Q.; Xu, S.; Zhang, H.; Ding, Y.; Zhu, S. *Polymer* **2009,** 50, 3488-3494.
18. Siewing, A.; Lahn, B.; Braun, D.; Pasch, H. *Journal of Polymer Science: Part A: Polymer Chemistry* **2003,** 41, 3143-3148.
19. Pasch, H.; Mequanint, K.; Adrian, J. *e-Polymers* **2002,** 5, 1-19.

20. Raust, J. A.; Brull, A.; Moireb, C.; Farcet, C.; Pasch, H. *Journal of Chromatography A* **2008,** 1203, 207-216.

21. McLeary, J. B. Reversible addition fragmentation transfer polymerization in heterogeneous aqueous media. PhD thesis, University of Stellenbosch, Stellenbosch, 2004.

22. Catalgil-Giz, H.; Uyanik, N.; Erbil, C. *Polymer* **1992,** 33, 655-656.

23. Paris, R.; de la Fuente, J. L. *Reactive & Functional Polymers* **2007,** 67, 264-273.

24. Liu, Y.; Mao, R.; Huglin, M. B.; Holmes, P. A. *Polymer* **1996,** 37, 1437-1441.

25. Zhang, Z.; Zhu, J.; Cheng, Z.; Zhu, X. *Polymer* **2007,** 48, 4393-4400.

26. Heatley, F.; Lovell, P. A.; McDonald, J. *European Polymer Journal* **1993,** 29, 255-268.

27. Quinn, J. F.; Chaplin, R. P.; Davis, T. P. *Journal of Polymer Science: Part A: Polymer Chemistry* **2002,** 40, 2956-2966.

28. Nagelsdiek, R.; Mennicken, M.; Maier, B.; Keul, H.; Hocker, H. *Macromolecules* **2004,** 37, 8923-8932.

29. Moad, G.; Chiefari, J.; Chong, B. Y.; Krstina, J.; Mayadunne, R. T. A.; Postma, A.; Rizzardo, E.; Thang, S. H. *Polymer International* **2000,** 49, 993-1001.

30. Puneeta, A. S. B. *Journal of Polymer Science: Part A: Polymer Chemistry* **2006,** 44, 2076-2085.

31. Moad, G.; Solomon, D., *The Chemistry of Radical Polymerization* 2nd ed.; Elsevier Amsterdam 2006.

32. Chong, Y. K.; Moad, G.; Rizzardo, E.; Skidmore, M. A.; Thang, S. H. *Macromolecules* **2007,** 40, 9262-9271.

33. Lutz, J. F.; Jakubowski, W.; Matyjaszewski, K. *Macromolecular Rapid Communications* **2004,** 25, 486-492.

34. Wang, W.; Nikitin, A. N.; Hutchinson, R. A. *Macromlecular Rapid Communications* **2009,** 30, 2022-2027.

CHAPTER 5

GRAFTED EPDM RUBBER

The synthesis and characterization of the EPDM-g-PS graft copolymers are described in this chapter. EPDM-g-PS was prepared in a two-step reaction, hydroxylation and esterification reaction, followed by living free radical RAFT polymerization.

5.1 Introduction

Ethylene-propylene rubbers (EPRs) are some of the most widely used and studied synthetic polymers due to their heat and oxidation resistance. In general, there are three different commercial polymerization processes used for the preparation of EPRs: solution, slurry (suspension), and gas-phase. The ethylene and propylene monomers combine to form a chemically saturated and stable polymer backbone, which provides excellent properties. The non-conjugated diene monomer, 5-ethylidene-2-norbornene (ENB), and dicyclopentadiene (DCPD), can be terpolymerised in a controlled manner to maintain a saturated backbone and place the unsaturated in a side chain, which makes it available for vulcanization or modification.[1-3] The terpolymers are referred to as EPDM (or ethylene-propylene-diene, with M referring to monomer). The EPDM polymer repeating unit containing ENB is illustrated in Scheme 5.1.

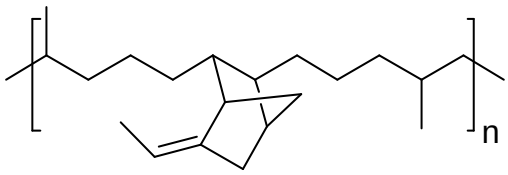

Scheme 5.1: Structure of EPDM containing ENB.

Ethylene-propylene-diene rubber (EPDM) has excellent resistance to heat, oxidation, ozone, and weather aging. However, their interaction with a wide range of materials and their compatibility with thermoplastics polymers limit their application. In order to overcome this limitation and improve their compatibility with polar thermoplastics, functionalization of the backbone or copolymerization with polar monomer had led to dramatic increases in the interaction between the rubber and blend polymers and enhancing the compatibility of the rubber.[4,5] Such copolymers could then be used as compatibilizers for polymer blends and composites.

Several methods have been used to prepare EPR graft polymers. The most frequently used procedure is melt-free radical grafting,[6] where the main graft

monomers are maleic anhydride,[6-8] maleic acid, dibutyl maleate, and acrylic acid.[9] Ruggeri et al.[10] studied the free radical functionalization reactions of atactic and isotactic PP with several unsaturated compounds, such as α-methylstyrene, diethyl fumarate, and diethyl maleate. Graft copolymers of glycidyl methacrylate (GMA) onto PE, PP and EP copolymers have been prepared by means of a melt-free radical polymerization process initiated by peroxides.[11-15] Radiation-initiated grafting reactions of vinyl monomers from EPDM rubber have been studied.[16-18] Grafting polymerization of EPDM via 9-BBN in presence of MMA and styrene monomer was also investigated by Baleg.[19] Grafting polymerization in solution has also been investigated.[14,20,21]

Grafting polymerization using a living polymerization approach affords well-defined polymers with controlled molar mass, low polydispersity, and controlled chain-end functionality. The polymerization of styrene onto a butadiene rubber via TEMPO has been studied.[22] The ATRP technique has been used to graft MMA onto brominated EPDM.[23]

To the best of my knowledge, no study has yet been carried on the graft copolymerization of EPDM using RAFT in a grafting from approach. However, Joo et al.[24] studied the grafting reaction of EPDM with PS via the grafting onto approach where they synthesized PS by the RAFT technique using trithiocarbonates as RAFT agent followed by grafting to EPDM in presence of a radical generator. On the other hand RAFT approach has been used to graft monomers on solid surfaces i.e. silica nanoparticles,[25,26] silicon wafers,[27,28] carbon nontubes,[29,30] multi-walled carbon nanotubes,[31] and cellulose.[32,33]

The approach used in this study involves two steps. Step 1: hydroboration/ hydroxylation and esterification reactions were used to produce the multifunctional RAFT macroinitiator EPDM-DIBTC. Step 2: the grafting by living free radical RAFT polymerization was performed. The immobilization of the RAFT agent onto the rubber chain can be done in one of the two ways, either via the Z-group, in cases where the chain transfer agent (CTA) is attached to the backbone via the stabilizing Z group, or via the R-group, in cases where the CTA is attached to the backbone via the leaving and reinitiating R group. Both methods have advantages and limitations.[34,35]

The difference between these two methods is as follows. In the R approach, the leaving group of the RAFT agent is attached to the backbone. After initiation, the radical is located on the backbone of the rubber; therefore, the polymer branches grow from the rubber chain and are always attached to the rubber backbone. The trithiocarbonate moieties are mainly located at the end of the polymer branches. In the Z-group approach, the leaving group of the RAFT agent is never on the

backbone, and therefore the polymer branches grow away from the backbone, and hence the trithiocarbonate moieties are located between the backbone and the branches.

In the R-group approach, the termination reaction could lead to intermolecular or intramolecular cross-links. In the Z-group approach, the restriction is the bulkiness of the chain, which will limit the access of the growing macroradical to the propagating radicals, thus reducing their transfer activity.[35,36]

Here the aim is to prepare EPDM containing the RAFT agent via the hydroboration-hydroxylation route. This will be used to prepare the EPDM-g-PS graft copolymer via the R-group approach. Two specific studies were carried out:

(1) The polymerization of the EPDM-DIBTC with styrene monomer

(2) Free DIBTC added to the EPDM-g-PS polymerization solution to study its effect on the cross-linking reaction

5.2 Experimental

5.2.1 Materials

EPDM rubber (5.6 mol% of double bonds, ExxonMobil), 9-BBN (Sigma-Aldrich), methanol 99.9% (Sigma-Aldrich), hydrogen peroxide (Analytical Reagents 30 wt% aqueous solution), sodium hydroxide pellets (Merck), i-Octane (2,2,4-tri-methylpentane) (Sigma-Aldrich, HPLC grade), THF (Sigma-Aldrich, HPLC grade), 1-dodecanethiol (Riedel de Haen), acetone (Sigma-Aldrich), Aliquot 336 (Acros), carbon disulfide (Aldrich, 99%), chloroform (Sigma-Aldrich), hydrochloric acid HCl (ACE, 32%), thionyl chloride (Merck, 99%), Sodium sulphate (Na_2SO_4) (98% Analytical Reagents), AIBN (Riedel de Haen, 99%), 2-propanol (Sigma-Aldrich), ethanol (Sigma-Aldrich), sodium hydroxide (Analytical Reagents), anhydrous dichloromethane (Sigma-Aldrich).

5.2.2 Hydroboration and hydroxylation of EPDM

EPDM rubber (1 g, 5.6 mol% double bond content) was dissolved in THF (50 mL) at 40 ^{o}C under an argon atmosphere. Hydroboration was carried out by adding 9-BBN (1.23 mmol) into the THF solution. The reaction was run for 16 h at 70 ° C to ensure complete hydroboration of the internal double bonds of EPDM.

This was immediately followed by the hydroxylation reaction. The following were then added to the above mixture, with vigorous stirring: ethanol (4 mL), 6 M sodium hydroxide (2 mL), and then hydrogen peroxide (4 mL). Ethanol, sodium hydroxide and hydrogen peroxide were deoxygenated by passing a stream of argon

through them before their addition to the solution of hydroborated polymer. The temperature of the stirred solution was increased to 66 °C and stirring was continued for 6 h. The EPDM-OH polymer product was then recovered by precipitation in methanol and drying under vacuum.

A schematic representation of the hydroboration and hydroxylation reactions is shown in Scheme 5.2.

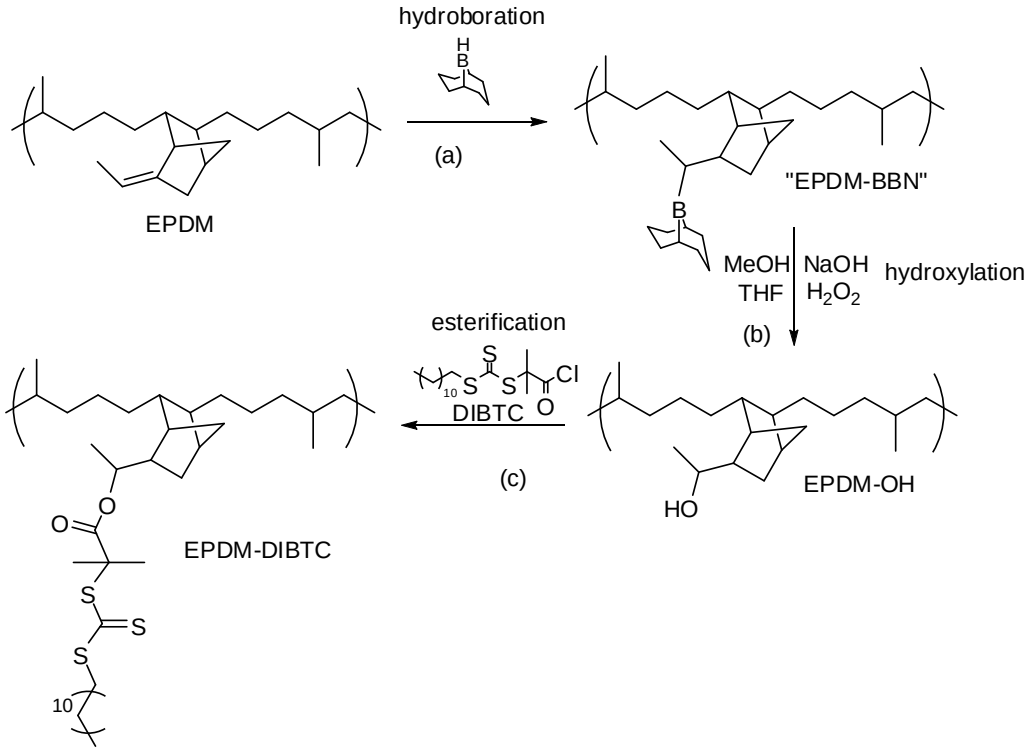

Scheme 5.2: Hydroboration and hydroxylation of EPDM followed by immobilization of DIBTC RAFT agent.

5.2.3 Synthesis of S-1-dodecyl-S'-(isobutyric acid) trithiocarbonate (DIBTC)

The synthesis of DIBTC was carried out according to the method of Lai et al.[37] 1-Dodecanethiol (0.40 mol), acetone (3.31 mol), and Aliquot 336 (0.016 mol) were mixed in a jacketed reactor cooled to 10 ℃ under a nitrogen atmosphere. Sodium hydroxide solution (50%; 0.42 mol) was then added over 20 min. The reaction was stirred for an additional 15 min before carbon disulfide (0.40 mol) in acetone (0.69 mol) was added over 20 min, during which time the color turned red. Ten minutes later, chloroform (0.60 mol) was added in one portion, followed by the drop-wise addition of sodium hydroxide solution (50%; 2 mol) over 30 min. The reaction was stirred overnight. Then water (600 mL) was added, followed by concentrated HCl (100 mL) to acidify the aqueous solution. The reaction mixture was vigorously purged with nitrogen to remove the acetone. The solid was collected on a

Buchner funnel and then stirred in 2-propanol (1 L). The undissolved solid was then filtered off and identified by NMR as S,S'-bis (1-dodecyl)trithiocarbonate. The 2-propanol solution was concentrated to dryness, and the resulting solid was recrystallized from hexanes to afford a yellow crystalline solid DIBTC (92.5 g).
^{1}H-NMR ($CDCl_3$): 0.88 (t, 3H), 1.21-1.44 (m, 20H), 1.72 (s, 6H), 3.28 (t, 2H), 10.19 (s, 1H).

5.2.3.1 Synthesis of DIBTC with acid chloride functionality (DIBTC-Cl)

The reaction was carried out according to the Donkers method[38] under an argon atmosphere. DIBTC (5.5 mmol) was dissolved in anhydrous dichloromethane (10 mL) in an oven-dried, argon-purged flask. The flask was immersed in a cold 2-propanol bath until the reaction mixture solidified. Thionyl chloride (27.5 mmol) was added drop-wise to the cold reaction mixture. The mixture was then allowed to warm to room temperature, while being stirred. Gas development (HCl and SO_2) was observed as the reaction mixture became warmer. After reaching room temperature, the flask was placed in a water bath at 30 °C for 3 h. On completion of the reaction, the solvent and excess thionyl chloride was removed under vacuum overnight. The product was used directly for further reactions without any purification or characterization. The reason for this was to avoid any unwanted side reactions.

5.2.4 Esterification of EPDM-OH with DIBTC-Cl

EPDM-OH (1.4 g) and pyridine (2.6 mmol) were dissolved in dry THF (20 mL). DIBTC-Cl (2.62 mmol) in THF (5 mL) was added drop-wise at room temperature, while being stirred. The reaction was allowed to run overnight at room temperature. The solvent was then evaporated off and the product was redissolved in THF, and then extracted with brine (three times) and water (three times). The organic layer was dried over Na_2SO_4. After removal of the solvent, the polymer was dried in vacuum. The two-step esterification reaction of EPDM-OH with DIBTC yielded the macromolecular RAFT agent (EPDM-DIBTC) with polymeric leaving groups as shown in Scheme 5.2. c) IR: 3439, 2923, 2850, 1704, 1464, 1267, 1070, 813 cm^{-1}.

5.2.4.1 Reaction conditions optimization

Various reactions conditions were used in the two-step reaction (hydroxylation and esterification) to prepare EPDM-DIBTC in order to achieve high hydroxylation and esterification conversions. See Table 5.1.

The following conditions were varied: 9-BBN, NaOH and H_2O_2; reaction temperature (60 and 75 °C), reaction time; and type of solvent, polar and non-polar solvent (THF and toluene).

The highest conversion of the double bonds of EPDM into hydroxyl groups was 43%, achieved when using the reaction conditions described in paragraph 5.2.2.

Different esterification reaction conditions were also tested. First, a direct reaction between the acid functional group of DIBTC-Cl and EPDM-OH rubber in the presence of N,N'-dicyclohexylcarbodiimide (DCC) and 4-(dimethylamino)pyridine (DMAP) was carried out. An esterification reaction via DIBTC with EPDM-OH was also carried out. The best result for the conversion of the -OH group to the ester was achieved with the acid chloride approach. Table 5.1 shows the different reaction conditions (reagents and quantities) that were used.

Table 5.1: Hydroxylation and esterification reactions conditions

EPDM (g)	9-BBN (mmol)	EtOH (mL)	NaOH (mmol)	H_2O_2 (mL)
1.0	1.2	4.0	12.0	4.0
1.2	0.3	4.0	12.0	4.0
1.1	7.2	0.5	9.6	1.6
1.7	20.0	---	9.0	3.0
1.9	7.5	---	27.0	3.0

EPDM-OH (g)	Pyridine (mmol)	DIBTC-Cl (mmol)	DIBTC (mmol)	DMAP (g)	DCC (g)
1.4	2.6	2.6	---	---	---
1.0	2.6	0.3	---	---	---
0.2	---	---	0.05	0.08	0.06

5.2.5 RAFT-mediated copolymerization of EPDM-DIBTC

The general procedure used for RAFT-mediated copolymerization was as follows: AIBN initiator (0.077 mmol), macroinitiator EPDM-DIBTC (0.11 g), and styrene monomer (0.019 mol) were added to toluene (10 mL) in a 50 mL round-bottom flask, equipped with a stirrer The solution was degassed by purging it with argon for 45 min, and then it was kept under an argon atmosphere. The flask plus contents was then immersed in a preheated oil bath at 70 °C for 24 h, the polymerization terminated by adding methanol. The products were then precipitated in methanol and then filtered and dried in vacuum at room temperature. A schematic representation of the RAFT-mediated copolymerization of EPDM-DIBTC is shown in Scheme 5.3.

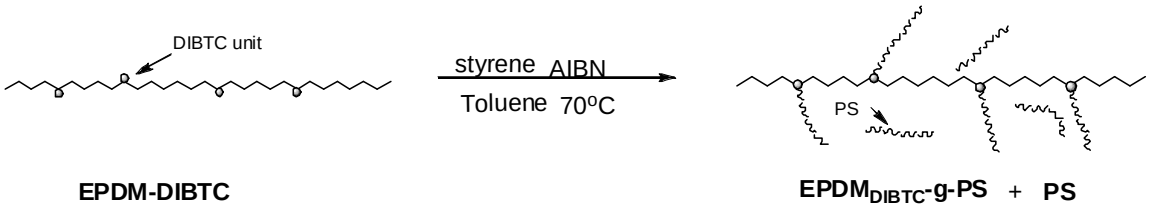

EPDM-DIBTC **$EPDM_{DIBTC}$-g-PS** + **PS**

Scheme 5.3: RAFT-mediated copolymerization of EPDM-DIBTC.

5.2.5.1 RAFT mediated copolymerization of EPDM-DIBTC in the presence of free DIBTC in solution

The reaction procedure to this reaction is similar to the previous reaction except the presence of free DIBTC in the solution. This approach was used to ensure the living nature of the radical segment when it emerges in solution during the polymerization, beside the effect of free RAFT on the gel formation and grafting efficiency. The procedure as follows: AIBN initiator (0.077 mmol), macromolecular RAFT agent EPDM-DIBTC (0.11 g), and styrene monomer (0.019 mol) and DIBTC (0.07 mmol) were added to toluene (10 mL) in a 50 mL round-bottom flask, equipped with a stirrer The solution was degassed by purging it with argon for 45 min, and then it was kept under an argon atmosphere. The flask plus contents was then immersed in a preheated oil bath at 70 °C for 24 h, the polymerization terminated by adding methanol. The products were then precipitated in methanol and then filtered and dried in vacuum at room temperature.

5.2.6 Soxhlet extraction of insoluble polymer fractions from its homopolymer

After the synthesis of the EPDM-g-PS graft copolymers, the mixture of products was separated into its respective components using the Soxhlet extraction method. Soxhlet extractions were carried out with n-hexane, acetone, and THF, as shown in Scheme 5.4.

The separated polymers fractions, PS homopolymer, EPDM, and graft copolymer, were precipitated in methanol, dried, and characterized. The remaining material was considered to be cross-linked polymer. The mass of insoluble material was determined gravimetrically.

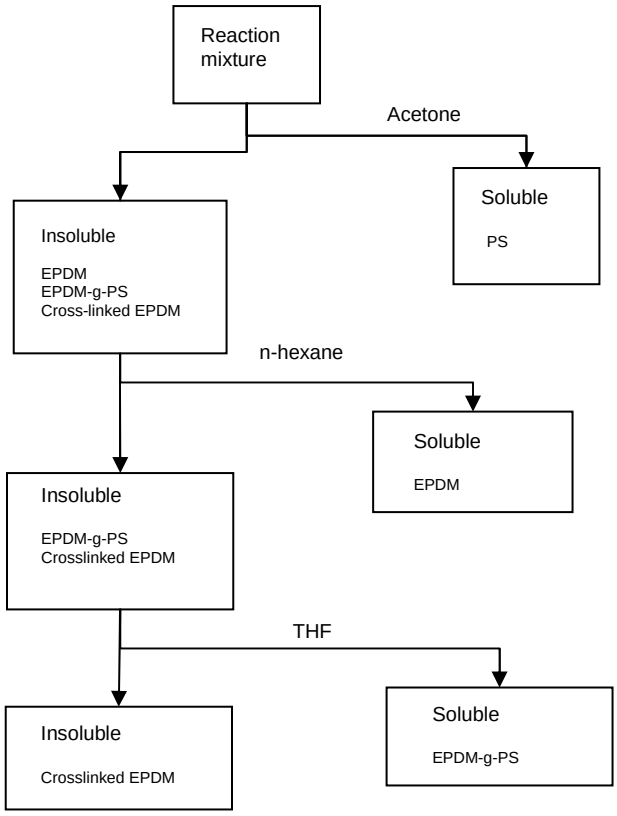

Scheme 5.4: Schematic representation of the extraction process used for the EPDM-g-PS.

5.3 Characterization

5.3.1 IR

IR spectra of the EPDM rubber and EPDM-g-PS were obtained using a Perkin-Elmer Paragon 1000 FT-IR in the range of 4000-500 cm^{-1}, with a resolution of 4 cm^{-1}. Samples were prepared as thin films cast from toluene solution.

5.3.2 SEC

Molar mass and molar mass distributions were determined using size exclusion chromatography (SEC). The instrument was comprised of the following units: Waters 1515 isocratic HPLC pump; Waters 717 plus autosampler; Waters 2487 dual λ absorbance detector; Waters 2414 refractive index (RI) detector, at 30 °C. Data processing was performed using Breeze Version 3.30 SPA (Waters) software. A set of two columns, Plgel (Polymer Laboratories) 5μm Mixed-C (300×7.5 mm) columns, connected in series along with a Plgel 5 μm guard column (50×7.5 mm), was used. The columns were kept at a constant temperature of 30° C. THF

Chromasolve HPLC grade solvent (0.125% BHT stabilized) was used as mobile phase, at a flow rate of 1 mL/min. Samples were dissolved in the stabilized THF at a concentration of 5 mg/ml, and 100 µL injection volumes were used. The system was calibrated using Polymer Laboratories Easivial PS Standards (10 standards ranging from 580 $g.mol^{-1}$ to 3 000 000 $g.mol^{-1}$).

5.3.3 NMR

^{1}H-NMR analyses were performed on a Varian 400 MHz spectrometer. Samples were dissolved in deuterated chloroform (with internal standard TMS).

5.3.4 HPLC

Separations were achieved on a chromatographic system used for gradient HPLC analyses. It comprised a Waters 2690 Separations Module (Alliance) system, comprising a degasser, a solvent mixing chamber, a pump, and an autosampler, and an evaporative light scattering detector (ELSD) Polymer Laboratories PL-EMD960 (ELSD) was used. The ELSD was operated at 80 °C, with an N_2 carrier gas flow rate of 1 SLM (standard liters per min). For data collection and processing, the software package WinGPC-Software v. 7.0 (Polymer Standards Service, PSS; Mainz, Germany) was used. Separation was carried out according to the chemical composition of the different polymer species by gradient HPLC, THF/i-octene mobile phases, and cyano-modified silica gel (Nucleosil CN) as a stationary phase, column temperature 40 °C injection volume 5 µL flow rate 1.0 mL/min.

The stepwise gradient used for the separation of the EPDM-g-PS composition commenced at 90 vol% i-octene and ended at 100 vol% THF.

5.4 Results and discussion

5.4.1 Immobilization of DIBTC onto EPDM rubber

Figure 5.1 shows an ^{1}H-NMR spectrum of the pure EPDM rubber in deuterated chloroform. Characteristic signals of the ethylene-propylene repeat unit as well as vinyl signals of the norbornene group are observed. Integration of the signals of the double bond at δ 5.3-4.9 ppm and the remaining signals of the polymer at δ 2.8-0.2 ppm reveals that the mol percentage of the norbornene in the EPDM was 5.6 mol%.

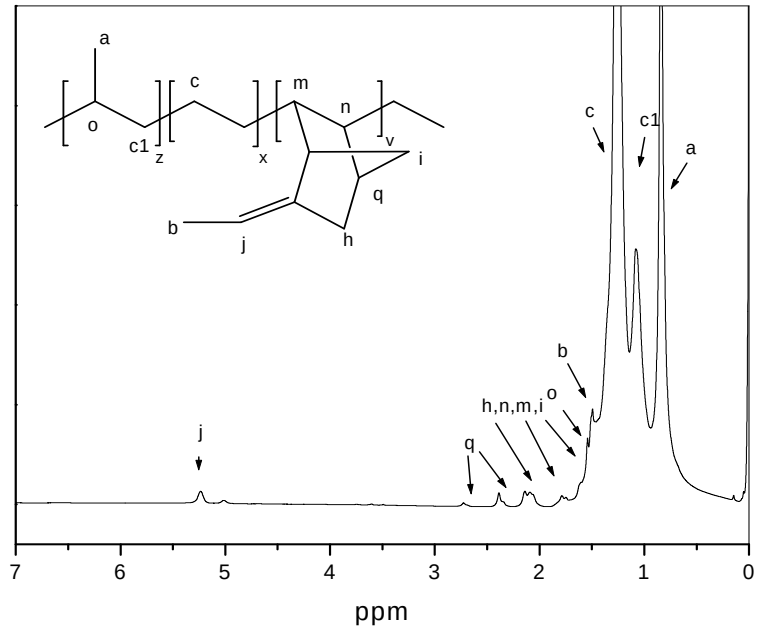

Figure 5.1: Typical example of ^{1}H-NMR spectrum of EPDM rubber ($CDCl_3$).

5.4.1.1 Hydroboration and hydroxylation of EPDM

Immobilization of the RAFT group onto the EPDM chains involves a two-step process. The step involves the introduction of a hydroxyl group onto the EPDM chains via a hydroboration-hydroxylation reaction. Secondly, the RAFT agent is attached using an esterification reaction with the DIBTC-Cl. The hydroxylation reaction of EPDM was carried out using 9-BBN in THF solution, followed by the hydroxylation reaction of the product. Figure 5.2 shows an example of the ^{1}H-NMR spectra of the EPDM-OH and corresponding EPDM. The signal of the hydroxyl group is observed at δ 4.7 ppm, which overlaps with the signal at δ 5 ppm, which is associated with the double bond, indicating that not all the double bonds are hydroborated. In addition to the hydroxyl group, a signal at 3.6 ppm appears that is associated with the CH adjacent to the hydroxyl group. In the spectra shown in Figure 5.2, 43% of the double bonds had been converted into hydroxyl groups.

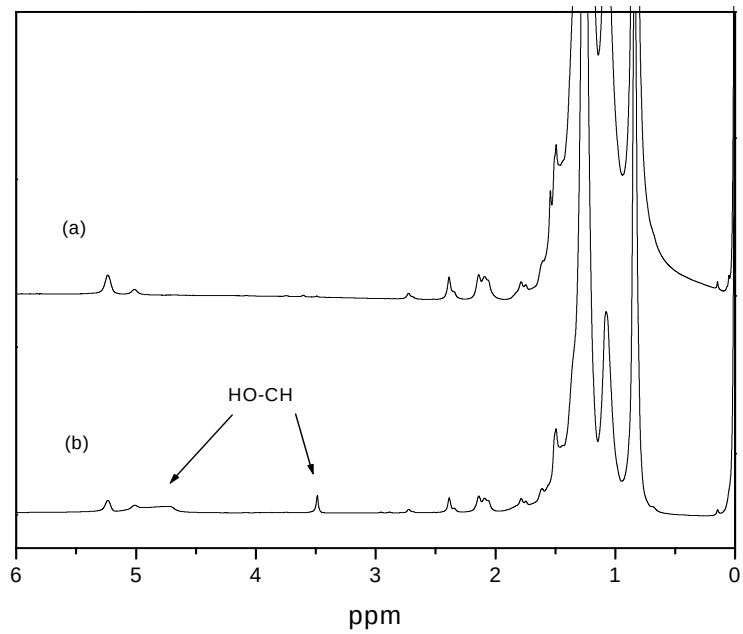

Figure 5.2: ^{1}H-NMR spectra of EPDM (a) and EPDM-OH (b) ($CDCl_3$).

Figure 5.3 shows the FTIR spectra of EPDM-OH and pure EPDM. Strong absorption peaks for the C-H of the ethylene-propylene units in the backbone were observed at 2800-3000 cm^{-1}. The broad absorption peak at 3400 cm^{-1} was assigned to the stretching vibrations of the hydroxyl (-OH) groups. The IR results confirmed that the hydroxylation reaction had taken place.

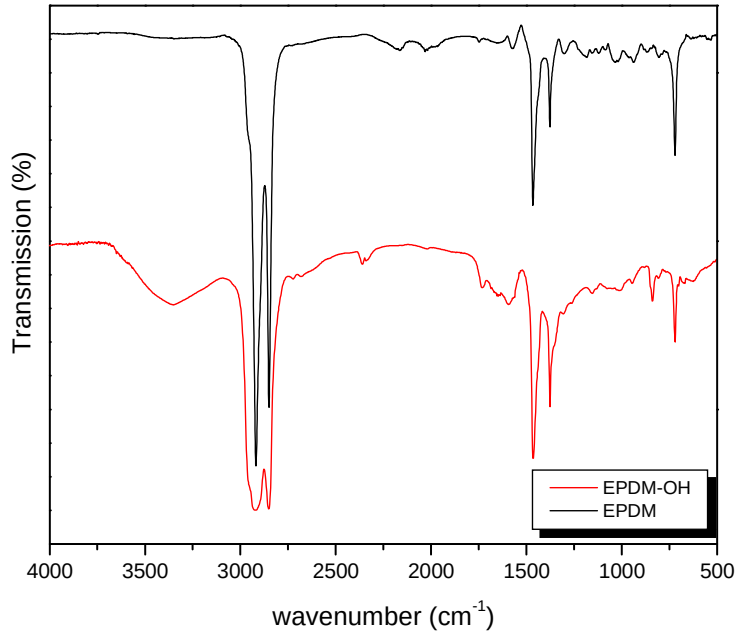

Figure 5.3: FTIR spectra of thin films of EPDM and EPDM-OH.

5.4.1.2 Esterification of EPDM-OH with DIBTC-Cl

The EPDM-OH was subsequently used in the esterification reaction with the DIBTC-Cl. The esterification reaction was confirmed by NMR and FTIR. ^{1}H-NMR

spectrum of EPDM-DIBTC is shown in Figure 5.4. The signals of the RAFT agent overlap with the EPDM signals. The small triplet signal of the methylene adjacent to sulfur (S-CH_2) at δ 3.2 ppm was used to determine the amount of the RAFT agent attached to the EPDM chain. Results of integration of the signals of S-CH_2 relative to –O-CH- revealed that 50 mol% of the -OH groups were esterified. The reason for this result is the bulkiness of the DIBTC-Cl and the bulkiness of the backbone EPDM rubber.

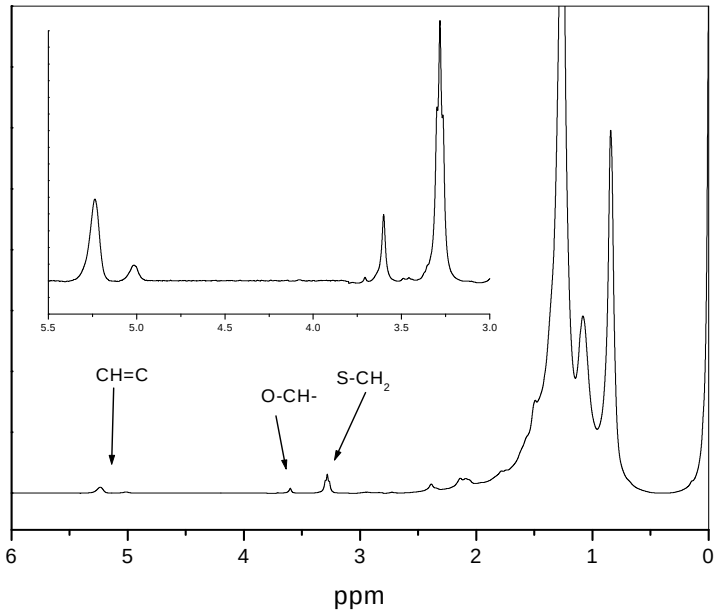

Figure 5.4: ^{1}H-NMR spectrum of EPDM-DIBTC ($CDCl_3$).

Figure 5.5 shows FTIR spectra of a thin film of EPDM, EPDM-DIBTC and KBr disc DIBTC. The characteristic peaks of DIBTC, present in the EPDM-DIBTC spectrum, appeared at 813 cm^{-1} (C-S stretching vibration) and at 1070-1154 cm^{-1} (stretching of C=S).[26,29,30,33,39-41] This confirmed that the DIBTC had been attached to the EPDM chain. As seen in the NMR spectra, there were indications that not all the -OH groups were converted to the thiol-ester group during the esterification reaction, where the O-CH- signal has shifted downfield as indication of “ether” formation. A broad absorption band at 3400 cm^{-1} (stretching vibration of hydroxyl groups -OH) was still observed.

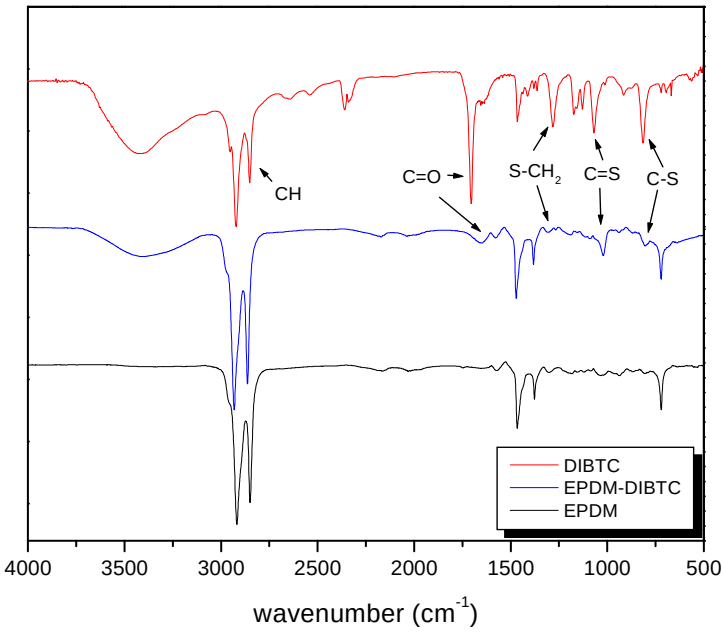

Figure 5.5: FTIR spectra of a thin film of EPDM, a KBr disc DIBTC, and a thin film of EPDM-DIBTC.

5.4.2 RAFT-mediated copolymerization of EPDM-DIBTC in solution

Solution polymerization of styrene monomer onto EPDM was carried out at 70 °C in toluene, using AIBN as the initiator (see Section 5.2.5). At the start of the polymerization, it is most likely that the radical initiated from the decomposition of the AIBN will react with the styrene in solution, and then some of these radicals will transfer to the trithiocarbonate on the EPDM rubber, since the DIBTC is immobilized at the R group isobutyrate. There are four possible steps in which the reaction will proceed:

- initiation of RAFT grafting polymerization from the EPDM chain
- transfer of the radical to a neighboring RAFT molecule on the same EPDM chain
- transfer of the radical to a neighboring RAFT molecule on another EPDM chain
- transfer of the radical to styrene in solution.

All four are illustrated in Scheme 5.5.

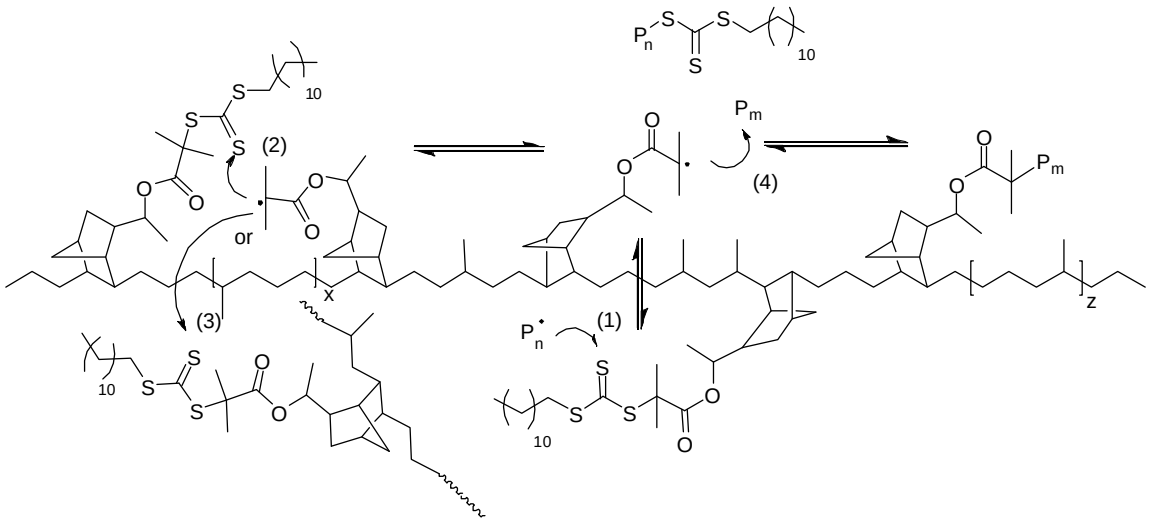

Scheme 5.5: Illustration of the four steps in the initiation and RAFT-mediated polymerization of EPDM-DIBTC.

It is shown later in Section 5.4.3 with gradient elution chromatography that after the grafting reactions, there is, in fact, a mixture of products after grafting reaction that include ungrafted rubber, the graft copolymer EPDM-g-PS, and PS homopolymer. The analysis presented in this section is for the extracted materials, unless otherwise stated. Figure 5.6 shows the FTIR spectra of the graft copolymer EPDM-g-PS and pure EPDM. The appearance of the following absorption peaks indicates the presence of PS at 3000 cm^{-1} (CH_2 stretching of PS) and at 694-755 and 1595 cm^{-1} (aromatic groups).

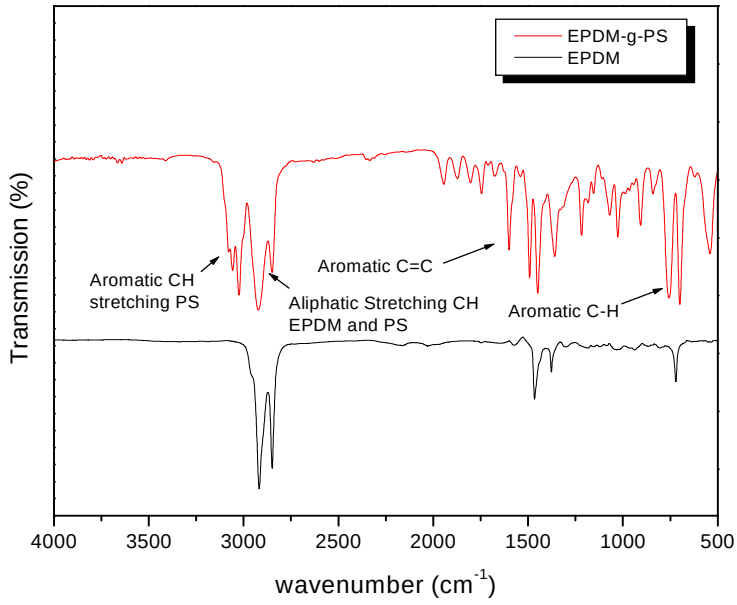

Figure 5.6: FTIR spectra of thin films of EPDM, and EPDM-g-PS.

Figure 5.7 shows SEC traces of the graft copolymer EPDM-g-PS and the PS homopolymer (after extraction). The PS homopolymer had PDI 1.51 and M_n 17000 g/mol. while EPDM-g-PS had PDI 6.58. The UV response at 254 nm is in agreement with the RI: Sty is attached to the EPDM backbone.

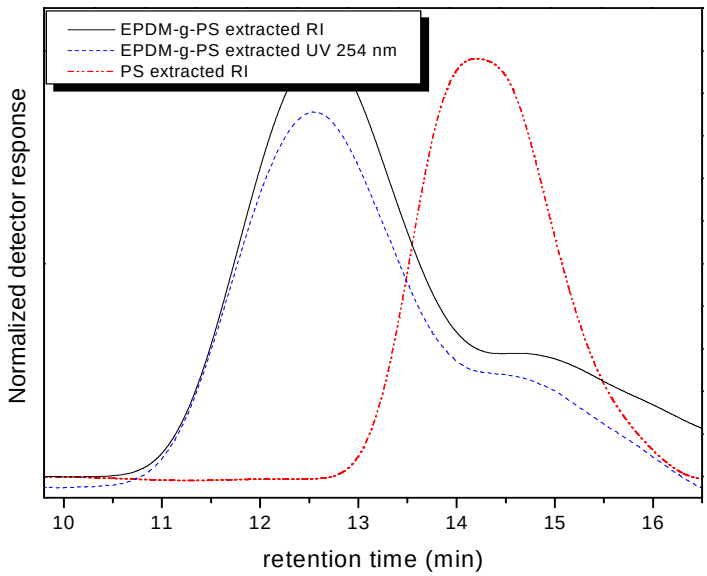

Figure 5.7: SEC traces of RAFT-mediated copolymerization of EPDM-g-PS.

The amounts of the graft copolymer and cross-linked polymer were determined gravimetrically after extraction (Section 5.2.6). The following results were obtained: 67 wt% of the product was graft copolymer, 8 wt% was cross-linked, 23 wt% was PS homopolymer, and 1.3 wt% was EPDM, 80% of the EPDM was grafted.

Figure 5.8 shows ^{1}H-NMR spectra of extracted EPDM and EPDM-g-PS graft copolymer. Integration of the signals at δ 0.8 ppm and δ 6.7 ppm, which correspond to the methyl group (CH_3) of the EPDM and the aromatic group of the styrene, respectively in the spectrum of the EPDM-g-PS, revealed that the amount of the PS in the graft was 86.5% mol. The average number of the styrene units per graft was calculated to be approximately 20 units. This was determined by taking the ratio of the signal of the methylene group adjacent to the sulfur (S-CH_2) at δ 3.5 ppm and the signal at δ 6.5-7.0 ppm corresponding to the aromatic group of the styrene. In the magnified inset in the spectrum of the extracted EPDM, from δ 3-7.5 ppm signals of S-CH, OH, CH=C and a signal of aromatic ring are seen. The presence of these signals in the extracted EPDM means that styrene is attached (few units) onto the EPDM rubber extracted with the EPDM. The integration of these signals shows that 0.26% of the S-CH is ungrafted, which means almost all the DIBTC on the EPDM has successfully grafted.

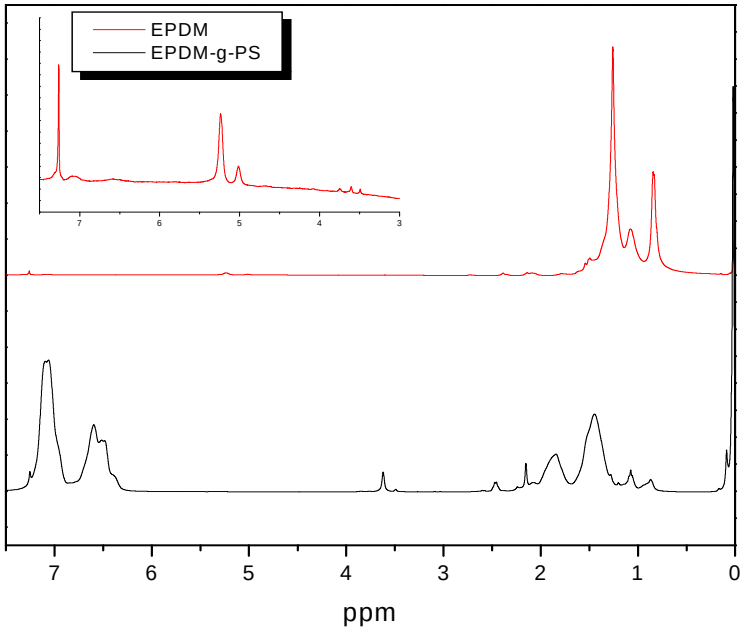

Figure 5.8: ^{1}H-NMR spectra of extracted EPDM and EPDM-g-PS graft copolymer ($CDCl_3$).

The polymerization most likely will start in solution with styrene monomer, which will react rapidly, forming PS homopolymer. There is also a high probability that at least some of the formed polystyrene radicals will attack the unfunctionalized double bonds of the EPDM, resulting in “uncontrolled grafting chains.”

5.4.2.1 RAFT-mediated copolymerization of EPDM-DIBTC in the presence of free DIBTC in solution

In the study above, the RAFT group DIBTC is attached to the main polymer chain. The free radicals for initiation are produced in solution in the presence of the styrene monomers. Scheme 5.5 shows the possible transfer reactions that lead to initiation of the grafting chain. In this Section, the effects of the presence of “free” RAFT agent are considered. In this case, nearly all of the styrene chains initiated will be “end-capped” with the DIBTC.

Solution polymerization of styrene monomer onto the EPDM-DIBTC chains was carried out in toluene with AIBN at 70 °C and the presence of free DIBTC in solution. This approach was used to ensure the living nature of the radical segment when it emerges in solution during the polymerization. In addition the effect of free RAFT on the gel formation and grafting efficiency is determined.

Figure 5.9 shows the SEC traces of the graft copolymer EPDM-g-PS and PS homopolymer (after extraction). The fraction that is soluble in acetone (mainly PS homopolymer) is the fraction that polymerized in solution. This fraction has a very narrow polydispersity PDI 1.19 and M_n 20 000 g/mol. This is indicative of the fraction that the homopolymerization in this case is in fact controlled by the presence of the

free RAFT agent. The fraction extracted by THF (graft copolymer) shows a relatively broad peak with a polydispersity PDI 1.78. There is tailing toward low retention time (high molar mass) in the graft copolymer trace. This indicates that some of the Sty monomer is grafted onto long EPDM chains, due to the steric hindrance effect and presence of free DIBTC in solution, which reduce the probability of monomer insertion to the backbone. The UV response at 254 nm appears to be slightly broader than the RI signal, and it shifts toward low retention time and the RI signal.

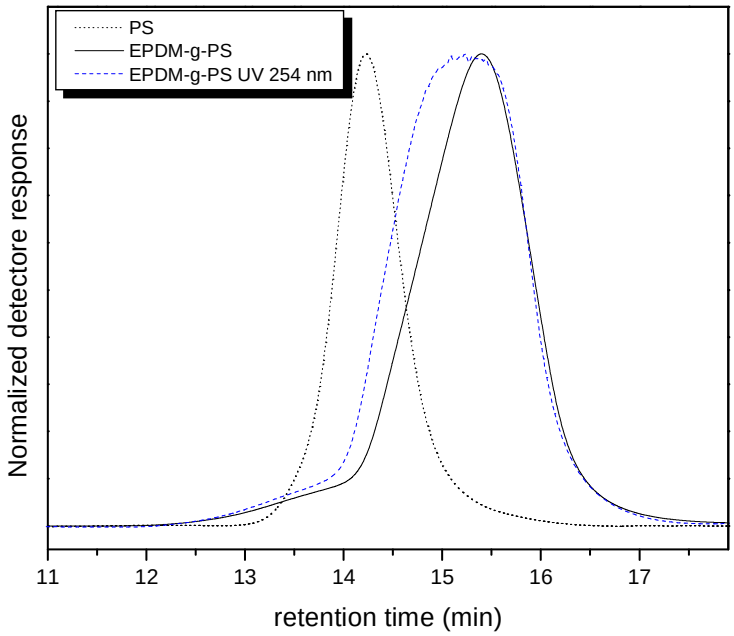

Figure 5.9: SEC traces of RAFT-mediated copolymerization of EPDM-DIBTC in presence of free DIBTC in solution.

The amount of the graft copolymer obtained and cross-linked polymer were gravimetrically determined after the extraction procedure; 2 wt% of the product was graft copolymer, 3 wt% was cross-linked, the majority of the product was PS homopolymer and 0.4 wt% EPDM; 84% of the EPDM was grafted.

Figure 5.10 shows ^{1}H-NMR analysis of the extracted copolymer, the fraction soluble in n-hexane, which is pure EPDM rubber, while the fraction soluble in THF is graft copolymer. Integration of the signals at δ 0.8 ppm and δ6.7 ppm correspond respectively to the methyl group (CH_3) of the EPDM, and the aromatic group of the styrene shows that the amount of the PS in the graft is 78.4% mol.

The average number of the styrene units per graft was calculated to be approximately 40 units. This was determined by taking the ratio of the signal of the methylene group adjacent to the sulfur (S-CH_2) at δ 3.2 ppm and the signal at δ 6.5-7.0 ppm corresponding to the aromatic group of the styrene. The extracted EPDM

still contained some of the functional EPDM-OH and EPDM-DIBTC. The integration of these signals shows that 1.93% of the S-CH is ungrafted, which means almost all the DIBTC on the EPDM is grafted. The amount of ungrafted DIBTC in this case is much higher than in the absence of free DIBTC. This is a result of the presence of free DIBTC, which reduces the radical flux in solution and keeps the radical much longer in solution. This results in most of the reactive sites in the main chain undergoing grafting.

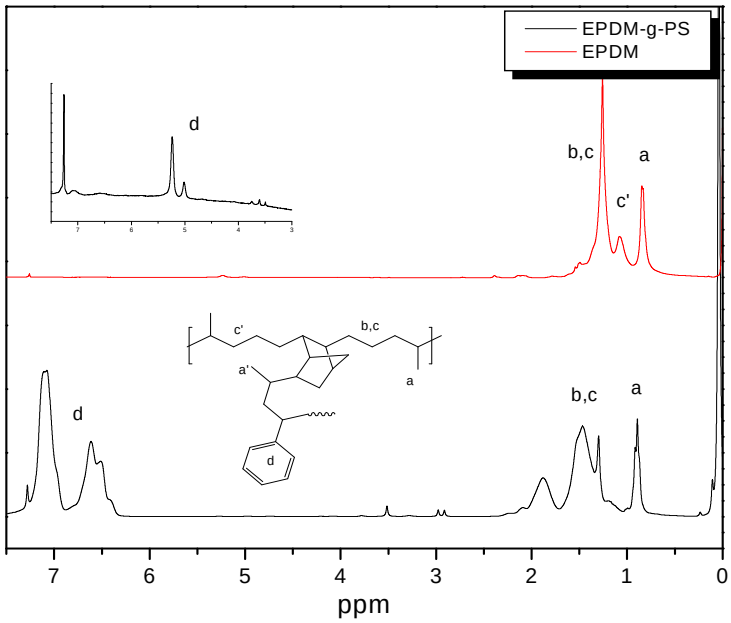

Figure 5.10: ^{1}H-NMR of extracted EPDM and EPDM-g-PS graft copolymer.

In this approach, using free RAFT in solution turns out to produce mostly PS homopolymer, with very narrow polydispersity, with a relatively small amount of the graft as determined using ^{1}H-NMR analysis. In addition to the amount of graft, the ^{1}H-NMR analysis shows also that 78% mol of the graft is PS, and the average number of the styrene units pre-graft is approximately 40 units, in contrast to the approach where the polymerization run without free DIBTC in solution and the amount of EPDM-g-PS graft copolymer is 86% mol, and the average number of styrene units pre graft is approximately 20 units.

5.4.3 HPLC gradient analysis

As has been shown in the previous sections, in all cases the grafting reactions lead to a mixture of ungrafted rubber, graft copolymer, and styrene homopolymer. It was also possible to isolate the various materials using the extraction procedure presented in Section 5.26. This process is, however, very long and tedious, so a gradient elution method was developed to allow for a quick and

similar analysis of the grafting efficiency. Figure 5.11 shows the gradient HPLC analysis of (a) pure EPDM and (b) PS standard (experimental conditions given in the table caption below.) The pure EPDM elutes at a retention time of 2 min, and the PS standard elutes at a retention time 7.6 min. These elution times were used to identify the eluted component of the graft copolymers.

HPLC gradient separation was used to separate the graft copolymer of EPDM-g-PS from the homopolymers EPDM and PS. The gradient profile used for the separation is shown in Table 5.2.

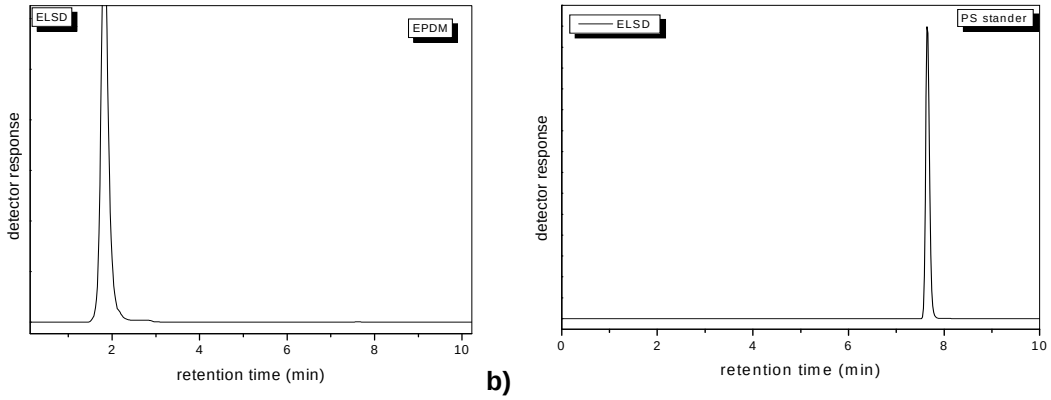

Figure 5.11: Gradient HPLC separation of the homopolymers a) EPDM and b) PS. [Exp: stationary phase, CN 100 Å; mobile phase, 90% i-oct for 2 min then 10 min linear gradient i-oct-THF 100-0% flow rate, 1 mL/min, detection: ELSD.]

Table 5.2: Gradient profile of THF used for the reversed phase separation of EPDM-g-PS

Time (min)	2	12	14	16
THF	10	100	100	10

Figure 5.12 shows the gradient analysis of the EPDM-g-PS for the grafting reaction discussed in section 5.4.2 (grafting in the absence of “free RAFT agent.”) It can be seen that, under the condition described above, there is a very good separation of the polymers into three fractions. The three elution peaks visible are assigned to EPDM, EPDM-g-PS, and PS, respectively. EPDM is lower in polarity than PS, which means the less polar component EPDM consequently eluted first, followed by the graft copolymer EPDM, and then PS homopolymer. As discussed earlier, there is a significant amount of graft copolymer formed.

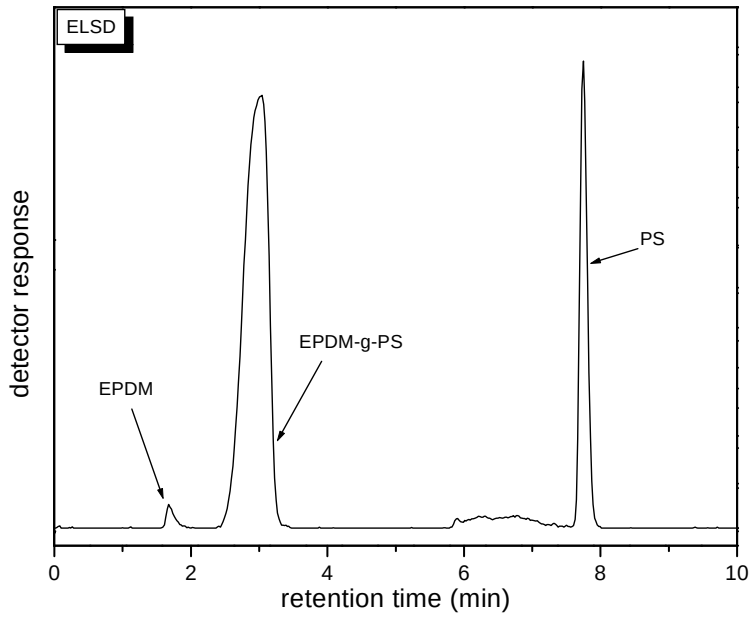

Figure 5.12: Gradient HPLC separation of the EPDM-g-PS grafts from the EPDM-DIBTC and PS.
[Exp: stationary phase, CN 100 Å; mobile phase, 90% i-oct for 2 min then 10 min linear gradient i-oct-THF 100-0% flow rate, 1 mL/min, detection: ELSD.]

Figure 5.13 shows the HPLC gradient of the reaction mixture of EPDM-DIBTC in the presence of free DIBTC in solution with styrene monomer. Once again, the three fractions are seen.

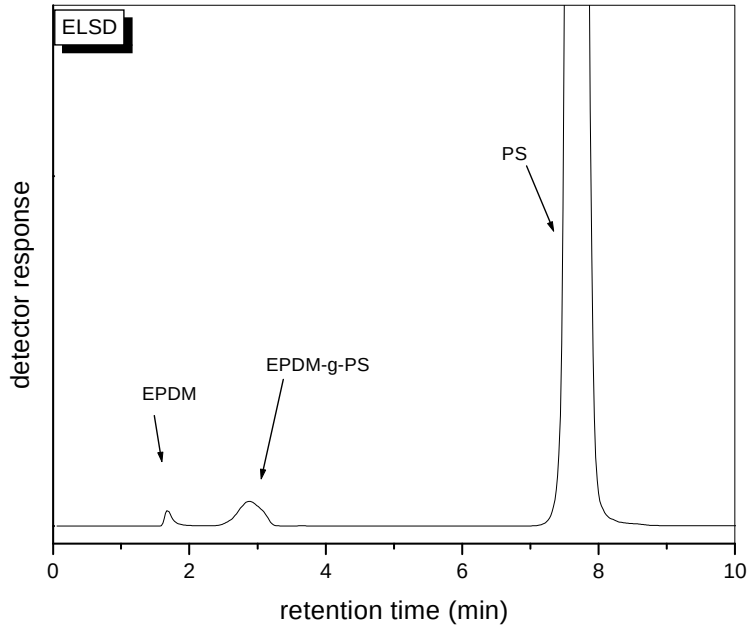

Figure 5.13: Gradient HPLC separation of the EPDM-g-PS grafts from the EPDM-DIBTC and PS in presence of free DIBTC in solution
[Exp: stationary phase, CN 100 Å; mobile phase, 90% i-oct for 2 min then 10 min linear gradient i-oct-THF 100-0% flow rate, 1 mL/min, detection: ELSD.]

The gradient elution analysis visually shows the difference in the relative amount of the different products formed. In the case of the grafting in the presence of

the free RAFT agent, there is a much larger relative amount of PS homopolymer formed, while in the case of the grafting reaction without free DIBTC, the amount of PS homopolymer is relatively less. Although the reaction conditions of the two reactions were the same, in the case of grafting reaction without free DIBTC, the conversion of styrene monomer to polymer was not high, due to uncontrolled reaction in solution and rapid termination.

The gradient HPLC analysis can be used to estimate the relative amount of the materials based on the peak areas of the different components. These relative peak areas for the two different systems are shown in Table 5.3.

In the absence of the free DIBTC, the amount of the EPDM-g-PS graft copolymer is higher than the EPDM-g-PS graft copolymer in the presence of free DIBTC as well as an increase the amount of PS. This can be explained by fact that the free radical initiating in solution via AIBN, and in the presence of the styrene monomer and free DIBTC the polymerization starts off forming PS homopolymer. With time, the macro-chain radical attaches to the EPDM backbone, forming the graft. Since the DIBTC moiety is attached to the EPDM chain, the R• leaving group will return to the solution to continue the living free radical reaction, forming another PS homopolymer. It should also be mentioned here that the reaction carried in the presence of free DIBTC resulted in a very low yield of cross-linked polymer compared to the reaction carried in the absence of free DIBTC. This is explained by the dramatic decrease in the instantaneous radical flux' dramatically decreasing the probability of the cross-linking reaction. Table 5.3 shows the relative peak areas of the different components for the two different grafting reactions.

Table 5.3: Relative peak areas of EPDM-g-PS and cross-linked material in the reaction mixture calculated from gradient HPLC

		EPDM	EPDM-g-PS	PS	Wt (%) cross-linked
mol fraction	EPDM-g-PS	0.013	0.67	0.23	~0.08
	EPDM-g-PS+ free DIBTC	$4.7*10^{-3}$	0.02	0.94	~0.03

The results of the HPLC showed the effect of the presence of free DIBTC on the resulting graft copolymerization. In the case of the free DIBTC in the solution, the amount of the EPDM-g-PS graft produced was less than the EPDM-g-PS graft produced with no DIBTC in the solution. The presence of free DIBTC in solution encourages the radical to stay in solution.

5.5 Conclusions

The preparation of EPDM-g-PS via RAFT process as a novel approach was successfully carried out. The approach was achieved by immobilizing the DIBTC RAFT agent onto the rubber chain EPDM through the R-group.

The immobilization of the DIBTC onto the EPDM was carried out via a two-step reaction: hydroboration-hydroxylation reactions of 9-BBN and then esterification reaction with DIBTC-Cl.

Two specific studies were carried out:

(1) The polymerization of the EPDM-DIBTC with styrene monomer was studied.

(2) Free DIBTC was added to the EPDM-g-PS polymerization solution.

HPLC and NMR analysis of the graft copolymers EPDM-g-PS for the two grafting reactions shows that the polymerization proceeded and graft copolymers were obtained.

However, the polymerization of the EPDM-g-PS in the absence of free DIBTC produced a graft copolymer with shorter styrene side chains and a higher branching density compared to the polymerization of the EPDM-g-PS in the presence of free DIBTC in solution. The PS homopolymer yielded from the reaction in the absence of free RAFT agent was low as a result of rapid radical-radical termination in solution since the initiation step occurred in solution, and it is most likely that the styrene monomer will polymerized rapidly, leading to termination and short polymers. In addition, there is also the probability of the propagated radical's transferring to the EPDM unfunctionalized double bond formed graft copolymer through a “grafting onto” process.

In contrast, the polymerization carried in the presence of free DIBTC showed that much longer styrene branches are formed, since the polymerization reaction initiation in solution in the presence of free DIBTC will ensure the living nature of the propagating polymer. This results in longer styrene branches. The presence of free DIBTC also increases the life time of the propagated radical, and as a result more PS homopolymer was produced. The reaction carried out in the presence of free DIBTC resulted in a very low yield of cross-linked polymer compared to the reaction carried in the absence of free DIBTC.

5.6 References

1. Lee, J. K.; Hong, S. J.; Liu, X.; Yoon, S. H. *Macromolecular Research* **2004,** 12, 478-483.

2. Ghosh, P., Rubbers-Materials and Processing Technology. *Polymer Science and Technology Plastics, Rubbers, Blends and Composites*, Ghosh, P., Ed. Tata McGraw-Hill: New Delhi, 2002; 415-555.

3. Duin, M. v.; Leemans, L.; Neilen, M. *Polymer* **1999,** 40, 1001-1009.

4. Lourenco, E.; Felisberti, M. I. *Journal of Applied Polymer Science* **2007,** 105, 986-996.

5. Fang, Z.; Guo, Z.; Zha, L. *Macromolecular Materials and Engineering* **2004,** 289, 743-748.

6. Grigoryeva, O. P.; Karger-kocsis, J. *European Polymer Journal* **2000,** 36, 1419-1429.

7. Zhang, H.; Datta, R. N.; Talma, A. G.; Noordermeer, J. W. M. *European Polymer Journal* **2010,** 46, 754-766.

8. Nakason, C.; Kaesaman, A.; Supasanthitikul, P. *Polymer Testing* **2004,** 23, 35-41.

9. Kennedy, J. E.; Devine, D. M.; Lyons, J. G.; Geever, L. M.; Higginbotham, C. L. *Journal of Materials Science* **2009,** 44, 889-896.

10. Ruggeri, G.; Aglietto, M.; Petragnani, A.; Clardelli, F. *European Polymer Journal* **1983,** 19, 863-866.

11. Cartier, H.; Hu, G.-H. *Journal of Polymer Science: Part A: Polymer Chemistry* **1998,** 36, 1053-1063.

12. Zhang, X.; Yin, Z.; Li, L.; Yin, J. *Journal of Applied Polymer Science* **1996,** 61, 2253-2257.

13. Pticek, A.; Hrnjak-Murgic, Z.; Jelencic, J. *eXPRESS Polymer Letters* **2007,** 1, 173-179.

14. Zeng, Z.; Wang, L.; Cai, T.; Zeng, X. *Journal of Applied Polymer Science* **2004,** 94, 416-423.

15. Shenc, J.; Hu, J. *Journal of Applied Polymer Science* **1996,** 60, 1499-1503.

16. Katbab, A. A.; Ataee, M. *Journal of Applied Polymer Science* **1998,** 69, 25-31.

17. Haldar, S. K.; Singha, N. K. *Journal of Applied Polymer Science* **2006,** 101, 1340-1346.

18. Chmela, S.; Teissedre, G.; Lacoste, J. *Macromolecules* **1996,** 29, 3055-3059.

19. Baleg, A.-A. Synthesis and Characterization of Graft and Block Copolymers using Hydroboration. Master, Stellenbosch, Stellenbosch, 2006.

20. Qu, X.; Shang, S.; Liu, G.; Zhang, L. *Journal of Applied Polymer Science* **2002,** 86, 428-432.

21. Fu, J.; Wang, L.; Zhang, A. *Polymer Bulletin* **2008,** 60, 405-416.

22. Abbasian, M.; Namazi, H.; Entezami, A. A. *Polymers for Advanced Technologies* **2004,** 15, 606-611.

23. Wang, X.-s.; Luo, N.; Ying, S.-k. *Polymer* **1999,** 40, 4515-4520.

24. Joo, S.-i.; Bae, S.-k.; Hong, S. C.; Cho, H.-c.; Lee, S.-h.; Kim, Y.-g. *Macromolecular Research* **2010,** 18, 927-934.

25. Liu, C. H.; Pan, C. Y. *Polymer* **2007,** 48, 3679-3685.

26. Li, C.; Han, J.; Ryu, C. Y.; Benicewicz, B. C. *Macromolecules* **2006,** 39, 3175-3183.

27. Stenzel, M. H.; Zhang, L.; Huck, W. T. S. *Macromolecular Rapid Communications* **2006,** 27, 1121-1126.

28. Li, D.; Luo, Y.; Li, B. G.; Zhu, S. *Journal of Polymer Science: Part A: Polymer Chemistry* **2008,** 46, 970-978.

29. Wang, G. J.; Huang, S. Z.; Wang, Y.; Liu, L.; Qiu, J.; Li, Y. *Polymer* **2007,** 48, 728-733.

30. Pei, X.; Hao, J.; Liu, W. *Journal of Physical Chemistry C* **2007,** 111, 2947-2952.

31. Hong, C. Y.; You, Y. Z.; Pan, C. Y. *Polymer* **2006,** 47, 4300-4309.

32. Hernandez-Guerrero, M.; Davis, T. P.; Barner-Kowollik, C.; Stenzel, M. H. *European Polymer Journal* **2005,** 41, 2264-2277.

33. Roy, D.; Guthrie, J. T.; Perrier, S. *Macromolecules* **2005,** 38, 10363-10372.

34. Perrier, S.; Takolpuckdee, P. *Journal of Polymer Science: Part A: Polymer Chemistry* **2005,** 43, 5347-5393.

35. Favier, A.; Charreyre, M.-T. *Macromolecular Rapid Communications* **2006,** 27, 653-692.

36. Zhao, Y.; Perrier, S. *Macromolecules* **2006,** 39, 8603-8608.

37. Lai, J. T.; Filla, D.; Shea, R. *Macromolecules* **2002,** 35, 6754-6756.

38. Donkers, E. H. D. Block copolymers with polar and non-polar blocks combination of living anionic polymerization and RAFT-mediated polymerization. PhD thesis, Eindhoven University, 2006.

39. Liu, J.; Hong, C. Y.; Pan, C. Y. *Polymer* **2004,** 45, 4413-4421.

40. Zheng, Q.; Pan, C. Y. *European Polymer Journal* **2006,** 42, 807-814.

41. Farmer, S. C.; Patten, T. E. *Journal of Polymer Science: Part A: Polymer Chemistry* **2002,** 40, 555-563.

CHAPTER 6

MICROPHASE STRUCTURE OF MULTIPHASE POLYMER VIA POSITRON ANNIHILATION LIFETIME TECHNIQUE AND SOLID STATE NMR

6.1 Introduction

The variety in the structure and nature of multiphase polymer unit sequences, along with that of their homopolymer, provide opportunity for tailoring the properties of copolymers and producing special and advanced materials. In this chapter, the analysis of selected copolymers using positron annihilation lifetime spectroscopy (PALS) is presented. The PALS data are correlated to the results of solid state NMR spectroscopy (SSNMR).

The PALS technique uses the unique probe of ortho-positronium (o-Ps) to probe the free volume properties of polymer materials directly. The techniques is based on the fact that the lifetime of the o-Ps atoms localized within the free volume holes can be directly correlated with the free volume hole size, and in theory the yield of relative intensity (I_3) of o-Ps can be correlated to the "hole concentration." While the analysis and interpretation of PALS data on homogeneous amorphous polymers are clear, the situation is less clear in more complex polymer morphologies, such as semi-crystalline materials, or, as in this case, multiphase materials. This is because of the way the raw positron lifetime data need to be analyzed in order to extract the free volume information.

The typical PALS spectra in a homogeneous amorphous polymers give three lifetime components: τ_1 is attributed to para-positronium self-annihilation, τ_2 is attributed to free positron and positron-molecular species annihilation, and τ_3 is attributed to ortho-positronium pickoff annihilation. Ortho-positronium (o-Ps) pickoff annihilation is a quenching process during which the positron (localized in free volume cavities) is annihilated with an electron (of opposite spin) from the surrounding cavity wall. The o-Ps lifetime is related to the free volume size, while the o-Ps intensity contains information about number of "holes" in polymers. PALS results have correlated to other properties related to the free volume in polymers, such as glass transition temperature (T_g),[1] gas permeation,[2-4] and miscibility of polymers blends.[5]

Solid state NMR, on other hand, is a powerful technique to study the structure and dynamics of polymers. It is especially useful in the characterization of multiphase copolymers since it can detect the microphase structure on the nanometer scale through the process known as spin diffusion. By measuring NMR spin-lattice relaxation times, one can probe molecular motions of polymeric materials at different time-scales. In this respect, proton relaxation measurements have been popular because they have relatively high sensitivity, require no sample enrichment, and are technically modest, which makes it a useful tool to

study polymer chain microstructure and changes in molecular dynamics that occur upon chain modification.

Here two different graft copolymers produced using different synthesis technquies will be examined. The first series of graft copolymers studied were made by the combination of RAFT polymerization techniques and hydroboration and then autoxdiation of trialkylboranes in the presence of a suitable monomer, as described in Chapter 4. The second series was synthesis via grafting through polymerization techniques.[6]

As has already been discussed,[7,8] these graft copolymers are expected to phase segregate in the solid state due to the incompatibility of the backbone and graft segments. Phase segregation in block copolymers is well understood,[9-11] but the morphologies of graft materials are less clear with respect to chemical composition. Detection of the phase segregation point as a function of the graft composition can often be a very difficult point to detect with conventional techniques, such as DSC. Generally, it would be expected that at very low graft contents, the materials would have more or less homogenous phase morphology, and phase segregation would occur at higher graft contents.

6.2 Experimental

The samples studied in the first part of this chapter were prepared as described in Chapter 4 sections 4.2.4 and 4.2.7. Small discs about 2 mm thick were pressed at 120 ^{o}C and allowed to cool slowly to room temperature. The same samples were used in PALS analysis and SS-NMR to ensure a uniform thermal history for the two analyses. The second series of graft copolymers studied were synthesized via a grafting through technique, using a functional styrene macromonomer and MMA monomer in a conventional free radical polymerization reaction. The details of the synthesis procedures are described in reference.[6] The PALS result of the later graft copolymers series has also been presented previously.[6]

6.2.1 Positron annihilation lifetime spectroscopy

A positron source, radioactive ^{22}Na in the form of NaCl in aqueous solution, was deposited and sandwiched between two thin foils (0.5 μm Ni), which was in turn sandwiched between two pieces of polymer sample. The sample was placed between two detectors. The detectors were placed at 180^{o} to each other, as shown in Figure 6.1.

The principle of the operation of lifetime spectrometers is to measure the spectrum of time between the start signals, generated by detecting the rapid gamma rays following the release of positrons, and stop signals from one of the annihilation gamma photons.

PALS measurements were performed using a fast-fast coincidence system with a time resolution of 240.34 ps full width of half maximum (FWHM) and a total of 1024 channel. The duration of each measurement was 120 min, during which time 1x10^{6} counts were collected.

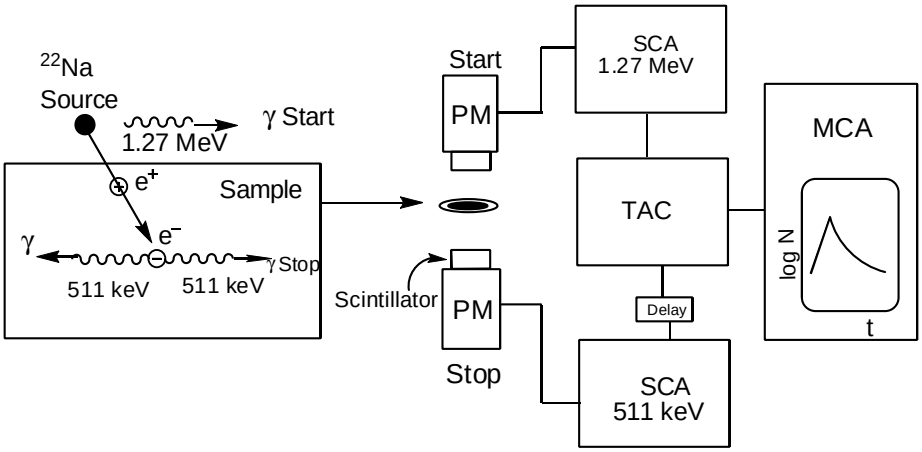

Figure 6.1: Standard positron lifetime set-up: PM TUBE, photomultiplier tube, CF DIFF DISC, constant fraction differential discriminator, DELAY, delay box fixed length of 50 Ω cable, TAC, time-to-amplitude converter, MCA, multichannel analyzer.[12]

6.2.2 Positron lifetime data analysis

Figure 6.2 shows the lifetime interval spectrum of the graft copolymer (PS-co-AM)-g-PMMA, representing the N coincidence time distribution that comes from the positron and positronium annihilation processes. Each spectrum with a total count of approximately $1x10^6$ counts was obtained at room temperature and was composed of three exponential decay functions corresponding to the three mechanisms of positron annihilation. The lifetime spectra were resolved for the graft copolymers into three decay components using the PATFIT program. The component with the longest mean lifetime τ_3 is that for *o*-Ps annihilation, which is sensitive to free volume in the sample. τ_1 is associated with *p*-Ps, quick annihilation; τ_2 is the annihilation of free positron Ps. The τ_3 and I_3 intensity, which corresponded to the size and number of free volumes holes, respectively, were plotted as a function of the macromonomer content, as will be shown later.

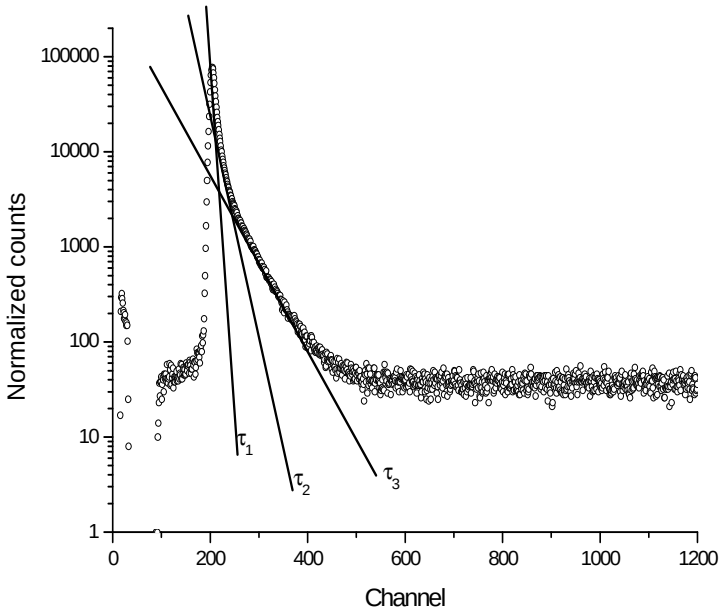

Figure 6.2: A typical positron lifetime spectra PALS of synthesized graft copolymer (PS-co-AM)-g-PMMA with three different decays decomposing Ps lifetimes fitted using PATFIT.

6.2.3 Solid State NMR

The SS-NMR experiments were performed on a Varian VNMRS 500 MHz two-channel spectrometer using 6 mm zirconia rotors and a 6 mm Chemagnetics^{TM} T3 HX probe. All cross-polarization (CP) spectra were recorded at ambient temperature with proton decoupling, a 3.5 μs 90° pulse, and a recycle delay of 5 s. The power parameters were optimized for the Hartmann-Hahn match. The contact time for cross-polarization was 1 ms. The free induction decay was 780 points, Fourier transformed with 1560 points and 0.5 Hz line broadening. Magic-angle-spinning (MAS) was performed at 7 kHz, and adamantane was used as an external chemical shift standard with the downfield peak set at 38.3 ppm. Proton spin-lattice relaxation times in the rotating frame, $T_{1\rho}(^1H)$, associated with the respective carbon signals of certain structural units, were determined using a variable contact time (VCT) experiment. It was measured by means of the dependencies of the respective carbon signal intensities on the contact time, where the contact time was varied from 20 to 8500 μsec with an array dimension of 25.

6.3 Results and discussion

6.3.1 Microstructure of (PS-co-AM)-g-PMMA

6.3.1.1 PALS of (PS-co-AM)-g-PMMA

All the lifetime spectra of the samples were analyzed using a three-component unconstrained fit. In all cases, this fit was determined to be better than a four-component fit. Table 6.1 shows the annihilation lifetime of the o-Ps (τ_3) and the corresponding intensity (I_3),

which is indicative of the relative number of o-Ps annihilation. The radius of the free volume (R) holes, the volume of the holes (fv), as well as the free volume fraction (*f*fv) determined from the positron lifetime parameters are listed in Table 6.1.

Data in Table 6.1 show that the PMMA homopolymer has a higher *f*fv of 3.05% than that of the PS-co-AM polymers used in the graft backbones. Data also show that PMMA grafted copolymers show larger fv sizes as well as larger *f*fv than the corresponding graft backbone polymers. This is generally to be expected, as the relatively bulky side chains are grown from the main backbone chain of the polymer. This can be explained as being the result of the introduction of much more end chain into polymer in the case of the graft copolymers compared to linear polymers.

Within the grafts series, one can see the unexpected decrease in the *f*fv for 20% graft copolymer compared to 10 and 5% graft copolymers. When looking at the positron data, it is seen that, although the R are similar in the copolymer series, the difference in *f*fv is a result of the decrease in the I_3 intensity. In chapter 4, the analysis of these copolymers by HPLC and NMR showed that the 10% graft copolymer has a higher amount of PMMA, and consequently also a much larger graft length, than the 20% graft polymer, In addition, the mol% of PMMA in the graft copolymer is much higher in comparison with other two grafts. The decrease in the mol% PMMA in 20% graft is a result of a steric hindrance effect, as described in chapter 4.

Table 6.1: Positron data of PS-co-AM and (PS-co-AM)-g-PMMA copolymers, lifetime (τ_3) relative intensity (I_3) radius of free volume hole (R) free volume (fv) fractional free volume (*f*fv)

Sample	τ_3	$\Delta\tau_3$	I_3	ΔI_3	R(Å)	ΔR(Å)	fv(Å^3)	Δfv(Å^3)	*f*fv(%)	Δ*f*fv(%)
Graft 5%	1.92	0.010	25.12	1.87	2.79	0.008	90.98	0.82	4.11	0.34
Graft 10%	1.99	0.009	26.81	0.13	2.85	0.006	97.25	0.70	4.69	0.05
Graft 20%	1.89	0.009	24.12	0.14	2.75	0.007	87.49	0.73	3.79	0.05
PS-co-AM 5%	1.83	0.024	11.47	0.20	2.70	0.021	82.68	1.92	1.70	0.07
PS-co-AM 10%	1.86	0.022	12.49	0.21	2.72	0.019	84.69	1.77	1.90	0.07
PS-co-AM 20%	1.83	0.022	13.99	0.24	2.69	0.018	82.31	1.71	2.07	0.07
PMMA	1.88	0.015	19.55	0.20	2.74	0.012	86.92	1.16	3.05	0.07

Figure 6.3 shows the *o*-Ps lifetime τ_3 plotted against the graft percent and copolymer content of the backbone. Both the backbone and the graft show similar features of an increase and then a decrease in the τ_3 at different compositions. However, the graft copolymers have longer τ_3 values than backbone copolymer.

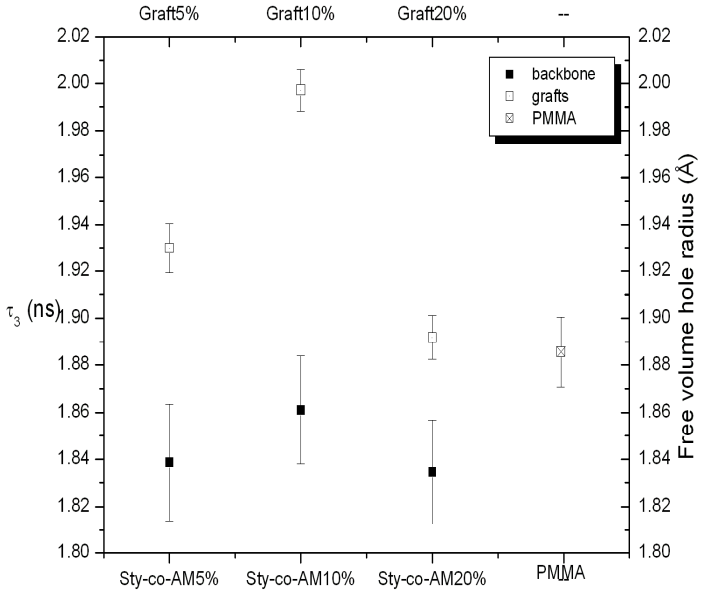

Figure 6.3: *o*-Ps lifetime τ_3 in PS-co-AM (5, 10, and 20%) copolymer and the graft copolymers as a function of comonomer composition and graft composition.

The relative intensity of the *o*-Ps lifetime (number of free volume) component is also plotted versus the graft percent and copolymer content of the backbone, as shown in Figure 6.4. The relative intensity I_3 was found to increase continuously with an increase in the comonomer content for the backbone copolymer, as shown in Figure 6.4, while in the case of the graft copolymer, the relative intensity I_3 value was found to be much higher than the backbone copolymers. However, there is an increase in the value of I_3 from the graft 5% to graft 10% followed by a decrease in the I_3 for the 20% graft copolymer.

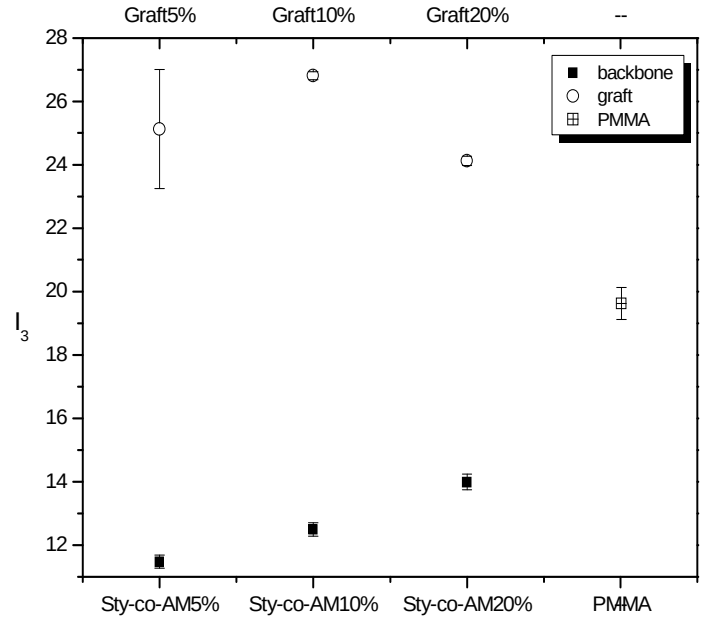

Figure 6.4: *o*-Ps intensity I_3 in PS-co-AM (5, 10, and 20%) copolymer graft copolymers as a functions of comonomer composition and graft composition.

Position lifetime results obtained when using the three-components fitting of the amorphous graft copolymers do not give any induction of phase separation. In other words, the positron data could not be resolved into four components where two distinct o-Ps lifetimes (τ_3 and τ_4) could be observed, one for each phase in the copolymer. This is partially due to the difficulties in fitting a four-component analysis to the positron lifetime raw data, but may also be a result of there being little difference in the measured free volume proprieties between each of the phases. This highlights the limitation of PALS analysis in complex multiphase morphologies. DSC measurement for the detection of two T_gs that would indicate phase separation proved to be difficult and inconclusive. In order to investigate any potential phase separation in the polymer, SSNMR was employed to investigate the microstructure on the nanometer scale of the graft copolymer.

6.3.1.2 SSNMR of (PS-co-AM)-g-PMMA

Microstructure of the graft copolymer on the nanometer scale was investigated through the process known as spin diffusion, which is one of the useful relaxation times obtained from SS-NMR. The spin occurs due to the magnetic pulse applied to the sample after being averaged by spin diffusion through the matrix of ^{1}H nuclei. The spin diffusion proceeds until relaxation occurs at a particular structural unit. In this way, the individual relaxation times for the component polymers tend to be averaged to a single value. The extent to which the averaging of relaxation times occurs depends on the degree of mixing and the relaxation times of the individual components.

Figure 6.5 shows the ^{13}C CP/MAS NMR spectrum of graft copolymer (PS-co-AM)-g-PMMA. The peak assignments were done based on work by Ming et al.[13] and Gandhi et al.[11] for PS-b-PMMA. The peak at 17 ppm is assigned to α-CH_3, the 40 ppm is assigned to $CHCH_2$, the 45 ppm is assigned to q-C, 52 ppm is assigned to O-CH_3, the 128 ppm is assigned to Aromatic, and 167 ppm is assigned to C=O group of the MMA units.

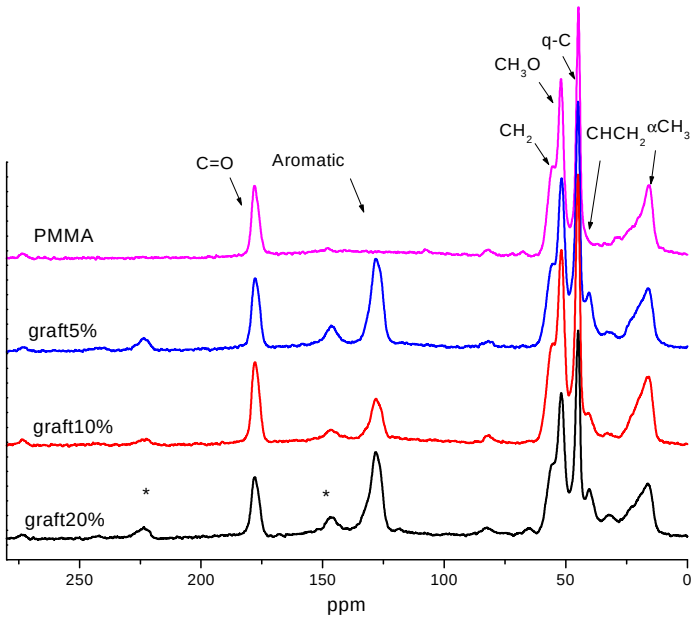

Figure 6.5: ^{13}C CP/MAS spectrum of graft copolymer (PS-co-AM)-g-PMMA and PMMA homopolymer (*) peaks indicate spinning side bands.

All the peak areas were determined by deconvolution through multiple peak fitting, assuming a Lorentzian line shape, using the software package Origin 7.0. The following equation shows the carbon signal intensity dependence on the contact time:

$$I = 1/\alpha \exp(-t/T_{1\rho}(^1H)) \qquad \textbf{Equation 6.1}$$

where

$$\alpha = 1-(T_{CH}/T_{1\rho}) \qquad \textbf{Equation 6. 2}$$

The $T_{1\rho}$ values for the various structural units were determined by fitting an exponential decay function to the decay phase of the VCT data:

$$I = I_{max} \exp(-t/T_{1\rho}(^1H) \qquad \textbf{Equation 6.3}$$

Figure 6.6 illustrates the fitting procedure where the initial points on the curve were masked and only the decay was used in the determination of $T_{1\rho}$.

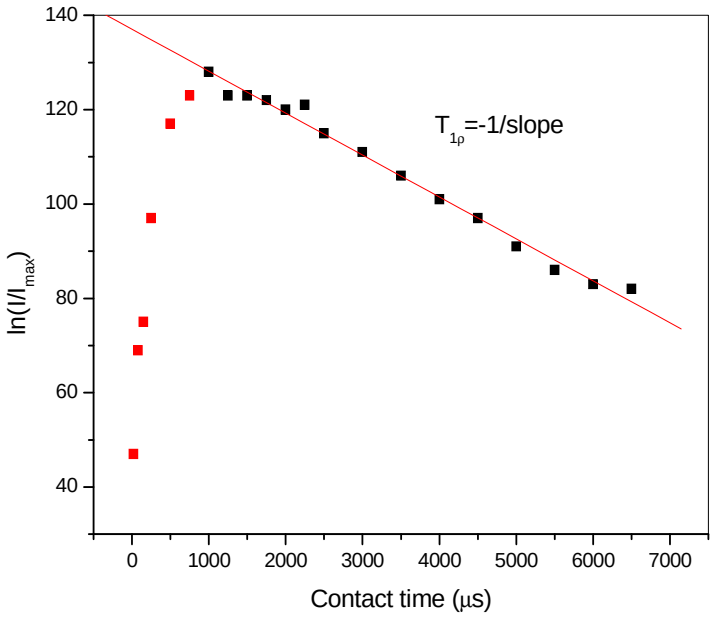

Figure 6.6: Values of $\ln(I/I_{max})$ versus contact time for graft copolymer (PS-co-AM)-g-PMMA, the $T_{1\rho}$ values determined from the negative inverse of the slope of the decay part of the curve.

The final $T_{1\rho}$ values collected for the various structural units in the backbone copolymer and graft copolymers are listed in Table 6.2. The peak position CH_3O and q-C are associated to MMA and $CHCH_2$ associated to styrene. The $T_{1\rho}$ values of the PS and AM components in the backbone copolymers obtained from the individual chemical positions are averaged, meaning that the spin diffusion process between the PS and AM is efficient and the two segments in the copolymer are completely miscible on the time scale of $T_{1\rho}$. This is what would be expected for a random distribution of the AM units along the polymer chain.

In the case of the graft copolymers, the $T_{1\rho}$ values obtained from the individual chemical positions are noticeably different. The $T_{1\rho}$ values of the PS and PMMA components in the graft copolymer are visibly different, not only from each other, but also from the corresponding homopolymer, meaning that the spin diffusion process between PS and PMMA is not efficient enough to average out the $T_{1\rho}$ values. Thus, on the time scale of $T_{1\rho}$ over which spin diffuses occurs, the two segments are not completely miscible, but at best are only partially mixed. This indicates that these segments occur in different regions and is an indication of a multiphase morphology (again based on the time scale of the spin diffusion process).[14]

Table 6.2: $T_{1\rho}$ data obtained from the VCT experiment of the backbone copolymer and graft copolymers

Peak position	Graft 20%	Graft 10%	Graft 5%	PS-co-AM 5%	PS-co-AM 10%	PS-co-AM 20%	PMMA
	$T_{1\rho}$ (s)	$T_{1\rho}$(s)	$T_{1\rho}$(s)	$T_{1\rho}$(s)	$T_{1\rho}$(s)	$T_{1\rho}$(s)	$T_{1\rho}$(s)
CH_3O	8.8	9.9	8.8	---	---	---	7.3
q-C	10.5	10.5	10.0	8.4	8.6	8.7	5.8
$CHCH_2$	6.8	3.5	7.1	8.5	8.5	8.7	---

6.3.1.3 Thermal analysis of (PS-co-AM)

As mentioned previously, the DSC analysis of the graft copolymers proved inconclusive with regards to the determination of the T_gs. The T_gs of the PS-co-AM copolymers, however, were easily observable when measured with DSC. Figure 6.7 shows a decrease in the T_g of the copolymer with an increase in the comonomer content, a result of introducing low T_g comonomer into the styrene backbone.

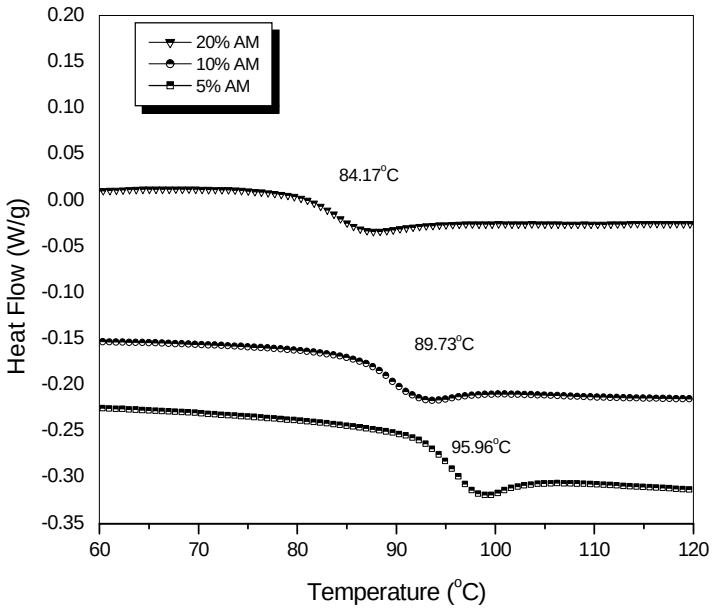

Figure 6.7: DSC curves of the PS-co-AM with different comonomer content (5, 10, 20 AM%), the heat rate 10° C/min.

DSC measurements of the copolymer backbones are summarized in Table 6.3. All the PS-co-AM copolymers show a single T_g. The decrease in the T_g with an increase in the comomoner content is due to low T_g of the AM units (the allylmethacrylate homopolymer has a Tg of about ± 0 °C). The decrease in the T_g is associated with an increase in *f*fv of the copolymers. In graft copolymers 5, 10, and 20% AM, the observation of the T_g was challenging due to similarity in the T_g of the backbone with graft copolymers.

Table 6.3: Glass transition temperatures and free volume fraction of PS-co-AM copolymer with different comonomer content 5, 10, and 20%AM

Copolymer	T_g (°C)	*f*fv(%)	Δ*f*fv(%)
PS-co-AM 5%	95.9	1.70	0.07
PS-co-AM 10%	89.7	1.90	0.07
PS-co-AM 20%	84.1	2.07	0.07

The discussion above clearly shows the advantage of combining PALS data with SSNMR data in so far as the NMR data can confirm phase separation even when PALS data cannot be resolved into multiple o-Ps components and the thermal analysis is inconclusive.

6.3.2 Microstructure of PMMA-g-PS

In order to investigate this further, a second series of graft copolymers was studied with PALS and SSNMR techniques. This second series of graft copolymers was synthesized via a conventional "grafting through" approach. The synthesis and detailed analysis of these copolymers has been reported before,[6] and only a brief summary of the copolymers studied is given here. It should be noted that, in this copolymers series, the PS component forms the branch of the polymer, while the PMMA forms the main chain, unlike in the previous series studied.

In this copolymer series, the graft chain lengths are well controlled since the macromonomer is synthesized via living anionic techniques. The living anionic polymerization of the styrene monomer allows for the synthesis of macromonomers of controlled length, but in addition the living nature of the polymerization also allows for the more or less quantitative termination of the chains with specific functionality. In this case, the polymerization is terminated with *p*-vinyl benzyl chloride, thus producing a vinyl functional macromonomer. Copolymerization of styrene macromonomers with MMA is used to form graft structures. The styrene macromonomer has a molar mass of 3700 g/mol, which correlates to roughly 36 styrene units per graft chain. Different feed compositions of macromonomer to monomer (50, 30, 20, 10, and 5 wt %) were used. It has been reported previously that the copolymer composition closely matches the copolymerization feed ratios, and for the sake of simplicity, the various copolymers will be identified by the weight percentage PS in the polymerization feed.[6] This produces a systematic series of graft copolymers with an increasing number of graft chain lengths. The copolymerization reaction was carried out in freshly distilled and dried toluene at 70 °C for 24h. AIBN was used (1 w %) as the initiator. Table 6.4 illustrates the formulation and characterization of graft copolymer with different macromonomer content. The yield was determined gravimetrically after extraction of the unreacted macromonomer.

Table 6.4: Formulation and characterization of graft copolymers, number average molar mass and weight average molar mass of the graft copolymers obtained via SEC, and chemical compositions of graft copolymers PMMA-g-PS_{VB} determined using ^{1}H-NMR

Sample code*	Macromonomer (g)	Monomer (g) (MMA)	AIBN (g)	Graft copolymer (10^4)		PDI	Chemical composition#		T_{g1}	T_{g2}
				M_n	M_w		PS aromatic ring	MMA ester group		
$G_{50}V1$	2.1	2.1	0.020	4.5	7.1	1.5	65	35	90	100
$G_{30}V2$	1.2	2.9	0.030	2.5	2.9	1.6	26	74	88	99
$G_{20}V3$	0.8	3.3	0.002	2.9	3.9	1.3	7	93	85	---
$G_{10}V4$	0.2	1.8	0.002	4.1	6.6	1.6	5	95	84	---
G_5V5	0.1	1.9	0.002	4.1	6.7	1.6	2	98	82	---

* Where G stands for graft, the subscript number represents the percent of macromonomer in the polymerization feed and V represents the type of terminating macromonomer (vinyl benzene terminated polystyrene 3700 g/mol).
# determined using the ^{1}H-NMR

The result of the free volume measurement using position lifetimes and their correlation with macromonomers content has also been presented previously.[6] However, the results of SS-NMR of the graft copolymers and correlation of their results with position lifetime analysis have not been reported before.

6.3.2.1 PALS of PMMA-g-PS

A summary of the positron results is presented in Table 6.5. It can be seen that the PMMA homopolymer has a *f*fv of 4.25%. The data for the Sty macromonomer is also shown, but it should be noted that this value is high since the sample consists of relatively very short PS chains and consequently a high free volume. The *f*fv of the graft copolymers decreases from the 50% to 5% graft. This is an indication that high macromonomer content graft polymer has a higher *f*fv than the other copolymers, as would be expected. However, a closer look at the positron data shows that the o-Ps lifetime τ_3 has a more complex relationship with the macromonomer content.

Table 6.5: Positron data, lifetime (τ_3) relative intensity (I_3) radius of free volume hole (R) free volume (fv) fractional free volume (*f*fv)

Macromonomer content	τ_3 (ns)	$\Delta\tau_3$ (ns)	I_3 (%)	ΔI_3 (%)	R(Å)	ΔR(Å)	fv(Å^3)	Δfv(Å^3)	Ffv (%)	Δffv (%)
PS	2.10	0.011	32.64	0.27	2.95	0.008	107.9	0.83	6.34	0.10
50 V	2.05	0.012	29.68	0.32	2.90	0.009	102.6	0.95	5.48	0.11
30 V	1.98	0.008	27.70	0.18	2.48	0.006	96.5	0.68	4.84	0.06
20 V	2.02	0.018	26.29	058	2.87	0.013	99.5	1.41	4.71	0.17
10 V	2.07	0.026	20.49	0.64	2.92	0.019	104.6	2.07	3.85	0.19
5 V	2.25	0.035	9.54	0.29	3.07	0.023	122.0	2.79	2.09	0.11
PMMA	1.83	0.006	28.61	5.59	2.70	0.005	82.6	0.46	4.25	0.85

Figure 6.8 shows the relationship between the o-Ps lifetime τ_3 and macromonomer content in the graft copolymers. The results show an initial decrease in the o-Ps lifetime with an increase in the macromonomer content, but this decrease stops at 30% macromonomer content, where it starts to rise again for the very high graft content copolymers.

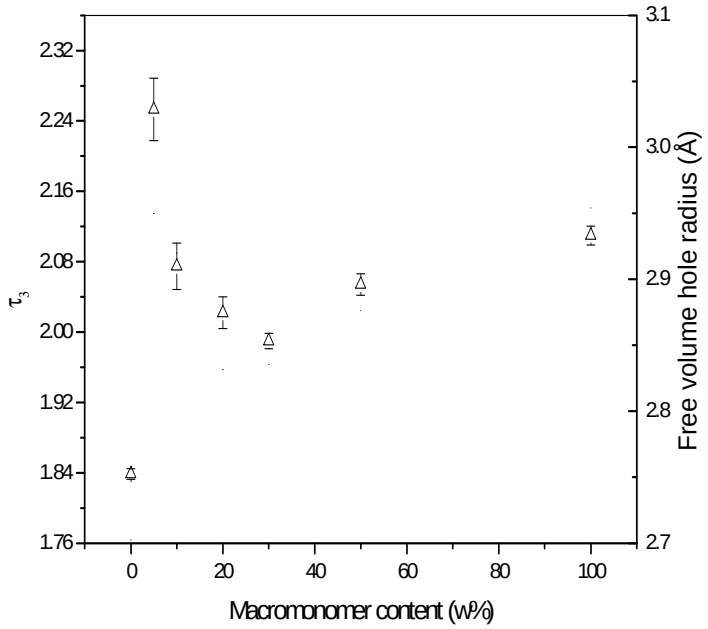

Figure 6.8: *o*-Ps lifetime τ_3 in graft copolymer PMMA-g-PS_{VB} as function of macromonomer content (wt %) and radius of free volume holes.

The relative intensity of the *o*-Ps lifetime (I_3) (number of free volume) component is also plotted versus macromonomer content. The relative intensity I_3 was found to increase continuously with an increase the macromonomer content, as shown in Figure 6.9. It is this general increase that is responsible for the increase in the overall fractional free volume, since this value is calculated from a combination of the hole volume (determined for the o-Ps lifetime τ_3 and the intensity value I_3 using equation 2.7). Essentially, this means that the free volume increases with an increased macromonomer content due to the increase in the number of chain ends in the graft molecule. The anomalous variation on the τ_3 free volume hole size with macromonomer content is not as clear.

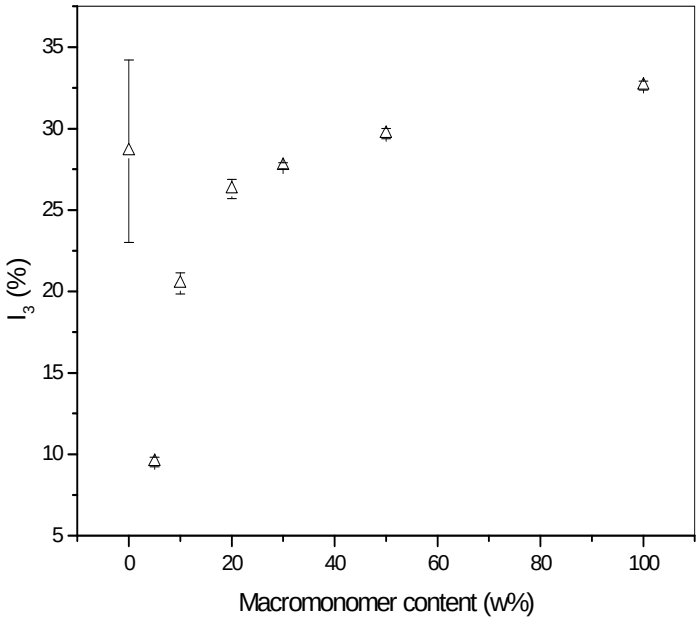

Figure 6.9: *o*-Ps intensity I_3 in graft copolymer PMMA-g-PS_{VB} as function of macromonomer content (wt %).

Once again, the positron data are best fitted across the entire graft copolymer series with a three-component fit. Once again, this would indicate that only one distinct o-Ps is resolved. This is confirmed in the hole distribution analysis that did not show a bimodal distribution. Interestingly, in the series two T_gs could be detected via DSC. Figure 6.10 shows the relationships between the glass transition temperature and free volume of grafts copolymer. Generally, incorporation of Sty macromonomers in the PMMA chain leads to plasticization of the polymer. This is observed as a lowering of T_g and an increase in the mean size of local free volume fv at room temperature, obtained from the *o*-Ps lifetime τ_3. T_g decreases and the free volume hole size increases with the initial inclusion of the macromonomer (relative to PMMA homopolymer). Figure 6.10 also shows the decreased τ_3 values with the increasing T_g. The two highest T_g points in the figure do not fit this trend. It should be noted that the number in the figures at these points represent the values of a second detected T_g in these samples. Despite the detection of the two T_gs, the positron data suggest only one hole size distribution. It does, however, show an inflection point in the case where two T_gs are detected.

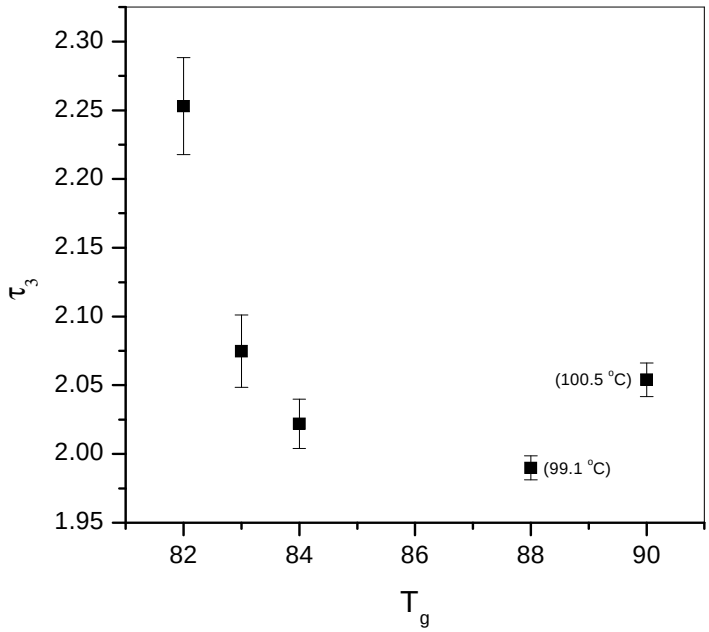

Figure 6.10: Relationship between T_g with o-Ps lifetime τ_3 of PMMA-g-PS_{VB}. (Note: values indicated in brackets are for second detected T_g.)

6.3.2.2 SSNMR of PMMA-g-PS

SSNMR is used further to investigate in detail the microstructure of the graft copolymer and correlate the resulting data with positron measurements.

Figure 6.11 shows the ^{13}C CP/MAS NMR spectrum of graft copolymer PMMA-g-PS. In a similar way as in Figure 6.5, the peak assignments were done according to the publication by Ming Li et al.[13] and Gandhi et al.[11] On PS-b-PMMA, the peak at 17 ppm is assigned to α-CH_3, 40 ppm is assigned to $CHCH_2$, 45 ppm is assigned to q-C, 52 ppm is assigned to O-CH_3, 128 ppm is assigned to Aromatic and 167 ppm is assigned to C=O. The peaks marked with an asterisk are spinning side bands.

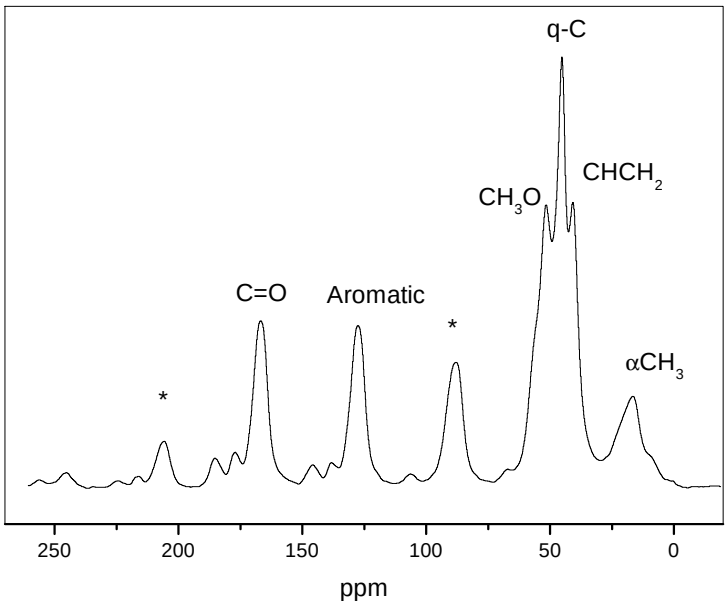

Figure 6.11: ^{13}C CPMAS spectrum of graft copolymer PMMA-g-PS$_{VB}$.

As explained previously in section 6.3.1.2, all peak areas were determined by deconvolution through multiple peak fitting, assuming a Lorentzian line shape.

The $T_{1\rho}$ values for the various structural units were determined by fitting an exponential decay function to the decay phase of the VCT data.

The final $T_{1\rho}$ values collected for the various structural units in the graft copolymer are listed in Table 6.6 The $T_{1\rho}$ values obtained from individual chemical positions are obviously different in the graft copolymer. Furthermore, the $T_{1\rho}$ values of the PS and PMMA components in the graft copolymer are quite different, not only from each other, but also from the corresponding homopolymer, meaning that the spin-diffusion process between PS and PMMA is not efficient enough to average out the $T_{1\rho}$ values. Thus, on the time-scale of $T_{1\rho}$ over which spin diffuses, the two segments are not completely but partially mixed.

Table 6.6: $T_{1\rho}$ data obtained from the VCT experiment of homopolymers PS and PMMA and graft copolymers PMMA-g-PS

	$T_{1\rho}$ ($CHCH_2$) ms	$T_{1\rho}$ (q-C) ms	$T_{1\rho}$ (OCH_3) ms
PS	44.8	-	-
50%	139	100	67.0
30%	7.8	14.5	40.4
20%	6.4	30.0	6.8
10%	18.8	34.4	10.2
5%	108.6	112.6	117.6
PMMA	-	236	40

Figure 6.12 shows the relationship between T_g, free volume τ_3, and $T_{1\rho}$ with macromonomer content. The $CHCH_2$ unit represents the styrene, and q-C and OCH_3

represent the structural units associated with the MMA in the graft copolymers. $T_{1\rho}$ and τ_3 show the same trend with macromonomer content, whereby the initial decrease with increasing macromonomer content is followed by an increase at around 30-50%. The apparent decrease in ^1H $T_{1\rho}$ from PMMA homopolymer to 30% macromonomer incorporation can be ascribed to the pi-stacking that can occur between neighboring styrene units, thereby limiting the mobility of the OCH_3 group of the PMMA, which manifests in a lower ^1H $T_{1\rho}$. It has generally been accepted that if the component polymers in a blend exhibit a common ^1H $T_{1\rho}$, then the blend is homogeneous on a scale of a few nanometers.[15] When comparing the ^1H $T_{1\rho}$ values for the protonated carbons for styrene and methyl methacrylate, they are similar below 30% and significantly different above 30%. This indicates that phase separation occurs above 30% incorporation of the macromonomer and explains the sudden increase in ^1H $T_{1\rho}$ above 30%. This small-scale heterogeneity within the system (5-30nm) can easily be missed by other analytical techniques.

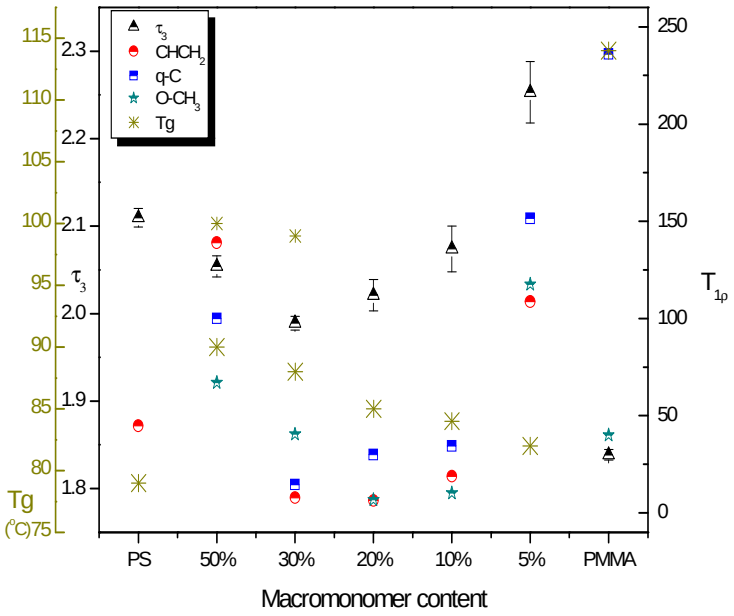

Figure 6.12: Relationship between macromonomer contents with T_g, τ_3, and $T_{1\rho}$ of the graft copolymers PMMA-g-PS_{VB}.

The spatial scale over which the spin diffusion takes place in the time $T_{1\rho}$ can be estimated from the following equation for the maximum spin diffusive path length:

$$L = (6*D*(T_{1\rho}))^{0.5} \qquad \textbf{Equation 6.4}$$

Where L is the maximum linear scale over which spin diffusion is quite effective, to the diffusion coefficient, D, which is assumed to be $5*10^{-12}$ cm^2/s.[14] The spin diffusion obtained using $T_{1\rho}$ often reflects the minimum size of the microdomain. The data listed taken from the largest $T_{1\rho}$ value of the copolymers component are summarized in the Table 6.7. The result shows that, in the first graft series, the minimum domain size is much bigger than in the second series. This is reflective of the fact that in the first series, phase separation must occur for all the graft copolymers.

Table 6.7: Microphase structure of the graft copolymer (PS-co-AM)-g-PMMA and PMMA-g-PS_{VB}

	Minimum domain size(nm)based on $T_{1\rho}$ (OCH_3)
graft 20%AM	162
graft 10% AM	172
graft 5% AM	162
Second series	
graft 50%	14
graft 30%	11
graft 20%	4
graft 10%	5
graft 5%	18
PMMA	11

6.4 Conclusion

PALS results of the graft copolymers (PS-co-AM)-g-PMMA with a three-component fitting do not show any induction of phase separation. This is partially due to the difficulties in fitting a four-component analysis to the positron lifetime raw data and the very closely matching free volume parameters in the two phases. Phase separation was clearly observed by using SSNMR and using spin-lattice relaxation time in rotating frame $T_{1\rho}$, where the spin diffusion process between the (PS-co-AM) and PMMA is not average on the time scale of $T_{1\rho}$, over which spin diffuses, the two segments are not completely miscible.

In the graft series where the branches where controlled via anionic polymerization techniques, the phase separation was observed as the branch number was increased. SS-NMR was also able to observe this phenomenon where the $T_{1\rho}$ data was not averaged for the high by branched polymer. In this series, once again only a three-component positron lifetime analysis was detected. The τ_3 values did, however, show an inflection point at the 30% macromonomer content. This is very well correlated to the phase separation point in the copolymer. The initial inclusion of the grafting chains has a plasticization effect, detected by the decreased T_g and τ_3 values.

6.5 References:

1. Dlubek, G.; Bamford, D.; Rodriguez-gonzalez, A.; Bornemann, S.; Stejny, J.; Schade, B.; Alam, M. A.; Arnold, M. *Journal of Polymer Science: Part B: Polymer Physics* **2002,** 40, 434-453.

2. Hill, A. J.; Weinhold, S.; Stack, G. M.; Tant, M. R. *European Polymer Journal* **1996,** 32, 843-849.

3. McCulagh, C. M.; Yu, Z.; Jamieson, A. M.; Blackwell, J.; McGervey, J. D. *Macromolecules* **1995,** 28, 6100-6107.

4. Hong, X.; Jean, Y. C.; Yang, H.; Jordan, S. S.; Koros, W. J. *Macromolecules* **1996,** 29, 7859-7864.

5. Wastlund, C.; Berndtsson, H.; Maurer, F. H. J. *Macromolecules* **1998,** 31, 3322-3327.

6. Elhrari, W. K. Synthesis and characterization of comb-polymers of controlled structure. MSc thesis, University of Stellenbosch, Stellenbosch, 2006.

7. Rabeony, M.; Peiffer, D. G.; Behal, S. K.; Disko, M.; Dozier, W. D.; Thiyagarajan, P.; Lin, M. Y. *Journal of the Chemical Society, Faraday Transactions* **1995,** 91, 2855-2861.

8. Xenidou, M.; Beyer, F. L.; Hadjichristidis, N.; Gido, S. P.; Tan, N. B. *Macromolecules* **1998,** 31, 7659-7667.

9. Rosati, D.; Perrin, M.; Navard, P.; Harabagiu, V.; Pinteala, M.; Simionescu, B. C. *Macromolecules* **1998,** 31, 4301-4308.

10. Lynd, N. A.; Meuler, A. J.; Hillmyer, M. A. *Progress in Polymer Science* **2008,** 33, 875-893.

11. Gandhi, S.; Melian, C.; Demco, D. E.; Brar, A. S.; Blumich, B. *Macromolecular Chemistry and Physics* **2008,** 209, 1576-1585.

12. Coleman, P. G., Experimental Techniques in Positron Spectroscopy. *Principles and applications of positron and positrnium chemistry*, Jean, Y. C.; Mallon, P. E.; Schrader, D., Eds. World Scientific Publishing: Singapore, 2003.

13. Ming, L.; Li, C.; Zhang, B.; Huang, W.; Men, A.; He, B. *European Polymer Journal* **1998,** 34, 515-521.

14. Li, M.; Li, C.; Zhang, B.; Huang, W.; Men, A.; He, B. *European Polymer Journal* **1998,** 34, 515-521.

15. Wagler, T.; Rinaldi, P. L.; Han, C. D.; Chun, H. *Macromolecules* **2000,** 33, 1778-1789.

CHAPTER 7

CONCLUSIONS

The use of 9-BBN in polymerization reactions to produce non-polyolefin's multiphase copolymer has been successfully illustrated. The combination of hydroboration-autoxidation with living anionic polymerization to produce block copolymers of PS-b-PMMA was successful. The combination hydroboration-autoxidation with living free radical polymerization (namely the RAFT) technique was successfully carried out to prepare graft copolymers (PS-co-AM)-g-PMMA and (PMMA-co-AM)-g-PBA. EPDM-g-PS was made using the 9-BBN in a hydroboration-hydroxylation reaction of EPDM rubber chains followed by conversion to a multifunctional RAFT macroinitiator, which allowed for a grafting reaction via living free radical polymerization. A study of the microphase structure of selected synthesized graft copolymers as well as a series of graft copolymers synthesized via a "grafting through" technique has also been done using PALS and SS-NMR techniques.

7.1 Combination of hydroboration and living anionic polymerization to produce block-copolymers

The combination of living anionic polymerization with borane chemistry was successfully achieved. The process involved transformation of the carbanion end to an allyl end group via an end capping reaction of the living anionic polymerization using an allylchlorodimethylsilane terminating agent. The allyl end groups were converted to the polystyrene-9-borabicyclo[3.3.1]nonane using 9-BBN. This was followed by a hydroboration-autoxidation reaction initiated by injecting oxygen gas into the reaction mixture.

The use of the hydroboration reaction allowed the polymerization to proceed at room temperature, which is a novel approach in block copolymer synthesis.

Incomplete hydroboration of the unsaturated functional group was observed in the model study of the hydroboration of 1-decene. This observation has implications for the hydroboration of the Sty macromonomer. It is clear that in this method for block copolymer synthesis it is not possible to prevent the formation of significant amounts of PMMA homopolymer during the autoxidation polymerization reaction. This is due to the difficulty of balancing the mole ratio of 9-BBN to the unsaturated functional group and presence of free 9-BBN as a result of the incomplete conversion of the allyl end groups to the initiating species. Nevertheless, block copolymer was obtained and confirmed via chromatographic analysis, namely LCCC.

7.2 Combination of hydroboration and living free RAFT radical polymerization for the production of graft copolymers

Synthesis of allyl methacrylate copolymers via the RAFT polymerization technique was achieved as a first example of the preparation of gel-free copolymers at high conversion. This approach allows the synthesis of copolymers containing unsaturated functional groups as pendant groups along the main polymer chain with controlled molar mass and low polydispersity. Three copolymers, PS-co-AM, PMMA-co-AM, and PBA-co-AM, were synthesized each with different comonomers content. The difference in the reactivity ratios between the monomers was expressed in the difference of the mole fraction of the allyl methacrylate in the copolymer from the mole fraction in the feed. The presence of the RAFT agent suppresses the formation of the gel during the polymerization reaction. Although a limitation that cannot be avoided when using RAFT agent is the formation of at least some gel, which consumes the unsaturated allyl group and inevitably leads to a broader molar mass distribution.

The hydroboration-autoxidation of the PS-co-AM copolymer through the allyl side chain was successfully carried out in the presence of MMA monomer. Using the hydroboration reaction of the allyl function copolymer in the presence of the BA monomer at low temperature gave a low yield of homopolymer PBA as a result of the backbiting of the propagating secondary BA radical and self-termination of BA monomer. In all the grafting reactions involving 9-BBN, a significant amount of homopolymer was produced, and it is not possible to prevent this due to the presence of free 9-BBN that results from the incomplete hydroboration of the allyl functional group due to the branching reaction that consumes some of the allyl group and makes the graft reaction more difficult in terms of bulkiness of the backbone. The use of the RAFT technique and synthesis of allyl methacrylate copolymers containing unsaturated function group as pendent side groups at high conversion open the door to their uses in other grafting techniques where the allyl groups present either reactive sites for initiation of grafting or for “grafting onto” points.

7.3 Synthesis and characterization of the EPDM-g-PS

The first example of the syntheses of EPDM-g-PS graft copolymer using a RAFT approach has also been shown. The technique involves a three-step reaction. Firstly, a hydroboration-hydroxylation reaction is done to convert the double bond of the norbornene into hydroxyl groups. This is followed by an esterification reaction with DIBTC-Cl to produce the multifunctional RAFT polymer. The DIBTC was immobilized to the EPDM rubber by the “R-leaving group.” The use of this approach ensures the presence of the radical on the rubber backbone, and, therefore, the polymer branches grow from the rubber chain in a grafting “grafting from” reaction. These chains are always attached to the rubber chain, and

the trithiocarbonate moieties are always located at the end of the growing polymer branches. In contrast, if the "Z approach" is used, the trithiocarbonate moieties are always located on the backbone, and the radical grows away from the backbone, but can also react with the backbone chain in a "grafting onto" process. The possibility of the formation of homopolymer of the polymer side chains in the latter approach is considerably higher than in the former approach.

Two specific studies were carried out to determine the optimum process for the maximization of grafting and limitation of homopolymerization during the grafting reaction.

- The polymerization of the EPDM-DIBTC with Sty monomer
- Free DIBTC added to the EPDM-g-PS polymerization solution

The results of these studies were distinctively different. Both polymerizations resulted in PS homopolymer and EPDM-g-PS formation as well as ungrafted EPDM rubber. The ratio between the different products is, however, very different. In the first approach, more graft copolymer was synthesized, and the number of Sty units in the side chains was estimated to be 20 units per graft. In second approach, however, the amount of the graft copolymer was less, and the number of Sty units in the side chains is much higher. The dissimilarity in the result is a consequence of the different techniques, the grafting from and grafting onto approaches. In the later approach, the polymer radical grows in the solution and then attaches onto the rubber chain. This process suffers of huge radical diffusion and steric hindrance. In the grafting from approach, the polymer branch grows from the main chain, which means the monomers will diffuse more easily than the macro radical.

7.4 Microphase structure

This study presents the first example of the use of $T_{1\rho}$ relaxation times from SS-NMR to detect the phase segregation limit as a function of chemical composition (graft content) in a PMMA and PS graft copolymers (or for any graft copolymer). This approach has the advantage that the phase segregation limit can be detected at relatively low comonomer content. It is extremely difficult to detect the phase segregation with other techniques due to the very closely matching T_gs and electron densities of the two phases. It has also been shown for the first time that the data obtained from SS-NMR can complement data from the PALS technique. It is shown how the apparent anomaly in the variation of the free volume parameters can be explained by the onset of the phase segregation limit at a certain copolymer composition. The variation in the chemical composition of the graft copolymers allows us to study the phase separation of the graft material as a function of the chemical composition of the graft copolymers.

A PALS result of the graft copolymers (PS-co-AM)-g-PMMA with a three component fitting does not show any induction of phase separation. This is partially due to the difficulties

in fitting a four-component analysis to the positron lifetime raw data and the very closely matching free volume parameters in the two phases. Phase separation was clearly observed by using SS-NMR, which detects the phase separation at a very small scale using spin-lattice relaxation time in rotating frame $T_{1\rho}$, where the spin diffusion process between the (PS-co-AM) and PMMA is not average on the time scale of $T_{1\rho}$ over which spin diffuses indicating that the two segments are not completely miscible.

In the graft series where the branches where controlled via anionic polymerization techniques, the phase separation was observed as the branch number was increased. SS-NMR was also able to observe this phenomenon where the $T_{1\rho}$ data are not averaged at high branch polymer.

7.5 Recommendation

It has been shown in this study that the hydroboration-autoxidation and hydroboration-hydroxylation reactions can be used to synthesize multiphase copolymer. The hydroboration-autoxidation opens the door to more sophisticated techniques in the synthesis of complex copolymers at room temperature. However, the technique also has severe limitations. Primarily, the limitations relate to the unavoidable formation of significant amounts of homopolymer in the autoxidation polymerization step. From a practical point of view, this inevitably requires the use of separation techniques to isolate the graft copolymer. It has also been shown that allyl methacrylate copolymers with unsaturated double bond as pendent groups along the main polymer chain can be made to relatively high conversions via the RAFT technique. The production of these graft precursors offers the opportunity for alternative strategies for the synthesis of graft copolymers by using the unsaturated double bond. This can be done in two ways. Firstly, the unsaturated group can act as a reactive site for a “grafting onto” reaction. One possible strategy would be to use these unsaturated groups as grafting onto sites by using preformed silane function side chains and a platinum catalyzed hydrosilylation reaction, which are known to produce very high reaction efficiencies. It would, for example, be relatively easy to produce silane functional preformed styrene side chains by terminating a living anionic polymerization of styrene with a chlorodimethylsilane agent.

The second approach would be to use the unsaturated groups as points along the chain that can be converted into polymerization initiation sites (in a way similar to the EPDM grafting presented in this study). One option is to convert these functional sites to ATRP initiation sites to produce the multifunctional macroinitiator using a α-haloester group or hydrosilylation reaction. The ATRP approach has the advantage that limited homopolymerization of the monomers occurs during the “grafting from” step, unlike in the case of the present study where significant homopolymerization occurs.

A number of studies have been done on the phase separation of block copolymers and the use of solid state NMR techniques to study this phase segregation. The current study has shown, however, that the technique can also be applied to graft copolymers, which show much more morphological “richness” in terms of heterogeneity and chemical composition. It has also been shown that the SS-NMR technique and PALS technique can be complementary. This opens up the possibilities for further studies were the techniques are used in combination. Each of the two techniques provides unique measures of fundamental properties of the multiphase polymer materials on an atomic scale. The combination of solid state molecular dynamics and free volume properties offers the possibility for a deeper understanding of these factors in complex polymer morphologies.